The role of neutrophil elastase in the pathogenesis of pulmonary fibrosis

Felix Chua

A thesis submitted to the University of London for the degree of PhD

Centre for Respiratory Research
Royal Free and University College London Medical School
Rayne Institute
5 University Street
London WC1E 6JJ

ProQuest LLC
789 East Eisenhower Parkway
P.O. Box 1346
Ann Arbor, MI 48106-1346

ACKNOWLEDGEMENTS

I thank Professor Geoffrey Laurent, for welcoming me to the lab and for agreeing to be my joint supervisor. He gave me innumerable opportunities and impressed upon me the importance of always remembering the bigger picture. His advice has been impartial, sometimes personal and always helpful. I thank Dr. Sarah Dunsmore, my other supervisor, without whom neutrophil proteinases would still be an alien concept to me. She taught me (often by example) that there are many different approaches to sizing up and solving a problem, and often the best one is not necessarily the most apparent. Her comments on the written word themselves constitute a course in critical thought upon which I will always draw.

I am grateful to Dr. Jurgen Roes for his collaboration and for supplying the neutrophil elastase-deficient mice used in these studies. Drs. Robin McAnulty, Geoffrey Bellingan, Rachel Chambers and Mike Hill provided many insightful discussions over a variety of beverages. The Laurent Lab experience would have been a poorer one without social and scientific contributions from Keith Abayasiriwardana, Gisli Jenkins, Rebecca Hodges, David Howell, Gisela Lindahl, Natasha Papafili, Danielle Copeman, Alistair Reinhardt and Mike Wood. Mr. Steve Bottoms provided incomparable histology advice and expertise. Dr. Patricia Garcia helped with many difficult *in vitro* problems; her philosophical and extraordinary knowledge of protein biology is refreshing.

I acknowledge a Research Training Fellowship from the Wellcome Trust and additional support from the British Lung Foundation (BLF). The Lancet, the British Thoracic Society, the BLF and the University College London Graduate School provided travel fellowships to conferences abroad.

Although I have inevitably missed out names, other people have been involved in criticising, analysing and evangelising my work, and I am grateful to them. During the course of my research, my uncle Eddie passed away. He was important in my life, and I dedicate this thesis to him. Finally, I want to thank my wife Joyce. She has been an unflinching source of inspiration, happiness and haute cuisine all these years. She has also organised all our holidays whilst holding down a full-time job, allowing me to concentrate selfishly on my work. Had I written this last sentence myself, I couldn't have put it any better.

ABSTRACT

Pulmonary fibrosis is the clinico-pathological outcome of excessive lung extracellular matrix accumulation. Although it may complicate a variety of lung diseases, the circumstances that lead to the development of pulmonary fibrosis remain poorly understood. In particular, many regulatory events controlling the inception and progression of pulmonary fibrosis remain unclear. Neutrophil elastase is a potent serine proteinase historically associated with alveolar destruction in pulmonary emphysema. However, elevated levels of neutrophil elastase have been reported in fibrotic lung disease, and pharmacological inhibition of its activity in animal models is associated with attenuated fibrotic lung damage. These observations have led to the hypothesis that excessive neutrophil elastase activity may be important to the pathogenesis of pulmonary fibrosis. In the present studies, the potential to ameliorate pulmonary fibrosis was investigated by subjecting neutrophil elastase null ($NE^{-/-}$) mice to bleomycin treatment. Instillation of 0.05U bleomycin into these animals failed to increase lung collagen content or to induce the formation of fibrotic lung lesions. This protective effect lasted for at least 60 days following bleomycin administration. Neutrophil elastase deficiency itself was not associated with reduced severity of bleomycin-induced early lung injury or lung neutrophil influx. However, quantities of active transforming growth factor-beta (TGF-β) were significantly decreased in the lungs of bleomycin-treated $NE^{-/-}$ mice. This finding correlated with increased lung tissue reserves of activatable TGF-β which indicates an abnormality at the level of stored latent TGF-β.

The initial section of this dissertation will detail the phenotypic characteristics of bleomycin-treated neutrophil elastase null mice. Temporal changes in collagen accumulation, lung histology and indices of lung injury will be presented in subsequent chapters. The final section will contain a thorough analysis of TGF-β production, localisation and activation in the lungs of bleomycin-treated $NE^{-/-}$ mice. Here, the hitherto unreported observation that pulmonary TGF-β activation is inhibited *in vivo* in the absence of neutrophil elastase will be presented. In light of these data, a novel proteolytic role for neutrophil elastase in generating active TGF-β within the repairing lung extracellular matrix will be discussed. These findings support the hypothesis that neutrophil elastase increases TGF-β activity in the repairing lung by mobilising preformed latent TGF-β stored in the extracellular matrix. Conversion of this pool of activatable TGF-β allows an augmented fibrotic response to be focused at sites of lung connective tissue repair.

CONTENTS

LIST OF FIGURES & TABLES

TEXT NARRATIVE

Figures

Tables

RESULTS

Figures

CHAPTER ONE

INTRODUCTION

Overview

One distinctive and adverse outcome of pulmonary injury is the abnormal accumulation of lung extracellular matrix. Excessive matrix deposition disrupts normal lung anatomy and predisposes to progressive, and often irreversible, physiological disturbance. Tissue damage due to uncontrolled proteolytic activity may initiate the aberrant extracellular matrix turnover that characterises fibrosis in the lung. Neutrophil elastase is a potent degradative enzyme that has been implicated in the development of destructive lung diseases, such as pulmonary emphysema. However, a number of experimental and clinical studies have indicated that its activity may also be relevant to lung fibrosis. Nonetheless, the molecular mechanisms by which neutrophil elastase contributes to the pathogenesis of pulmonary fibrosis remain unclear.

This thesis will contain evidence to show that neutrophil elastase plays a novel role in promoting pulmonary fibrosis in the bleomycin model. Qualitative and quantitative assessments will be used to characterise lung inflammation, injury and fibrosis in bleomycin-treated neutrophil elastase null mice. Data will be presented to demonstrate that neutrophil elastase can modulate transforming growth factor-β activity at sites of damaged lung matrix. Based on these observations, a molecular model for the fibrogenic activity of neutrophil elastase will be proposed. The relevance of these findings in a mouse model to the pathogenesis of pulmonary fibrosis in humans will be discussed.

1.1 Normal lung anatomy and physiology

The lung is the sole respiratory organ in mammals. It is comprised of a branching system of airways that gradually diminish in caliber and lead to a large attenuated surface area for gas exchange. This process takes place distal to the terminal bronchioles, within the alveolar acini that begin as respiratory bronchioles but quickly terminate in air sacs lined by simple epithelium. This unique interface between the body and the environment presents a total surface area of approximately 75 m^2 for gas diffusion with only a minimal barrier of approximately 0.5 μm between the airspace and the microvasculature.

The principal function of the lung is to facilitate the movement and extraction of oxygen from ambient air into the bloodstream and to allow excess carbon dioxide from the blood to be expelled. In the acini, diffusion is the primary mechanism responsible for this exchange of gases, and it occurs according to *Fick's law of diffusion*. According to this principle, the rate of gas diffusion is proportional to the available surface area and diffusion coefficient (a function of the solubility of each gas) and is inversely proportional to the thickness of the exchange barrier. This equation thus underscores the importance of a large, unencumbered and single-cell thin alveolar surface for efficient gas exchange. Consequently, any alteration to the lung architecture can affect oxygenation of the blood. For instance, connective tissue over-deposition in the pulmonary interstitium increases the distance oxygen molecules have to traverse, and thus decreases the efficiency of gas exchange.

1.1.i Characteristics of the normal pulmonary extracellular matrix (ECM)

Structure, function and location of ECM components

Extracellular matrices are specialised structures that determine the physical and mechanical properties of an organ. In the lung, cartilage provides tensile strength to the trachea and large airways. Basement membranes found underneath the airway and alveolar epithelia regulate the diffusion of gases and the differentiation of cells that make up the gas exchange machinery. The alveolar basement membrane is composed mainly of type IV collagen, fibronectin, laminin and entactin (Dunsmore and Rannels, 1996). The pulmonary interstitium provides the intrinsic recoil of the lung and its ECM is composed predominantly of fibrillar collagens, elastic fibres and proteoglycans produced by tissue fibroblasts.

Signal transduction processes in the pulmonary ECM

Far from being biologically inert, the pulmonary ECM interacts dynamically with its surrounding cells, vascular and neural structures. These interactions are bi-directional. The pulmonary ECM exerts important influences on cell morphology, behaviour and homing; in return, the intracellular cytoskeleton can exert forces that orientate and direct different matrix macromolecules. These communications are vital for a range of biological processes that are epitomised by efficient gas exchange. Cell surface receptors belonging to the integrin family form

the most important group of transmembrane linkers and signal transducers that regulate cell-matrix communication. The structure and functional diversity of integrin molecules are based on the pairing abilities of the individual alpha and beta subunits. Key to the molecular interactions between integrin receptors and their respective ligands is the recognition of the Arg-Gly-Asp (RGD) sequence, known to be present in the extracellular matrix components fibronectin, vitronectin, collagen, fibrinogen, and von Willebrand factor (Cheresh, 1991). In the lung, the largest number of integrins belong to the β1 integrin subfamily (Roman, 1996). Within this group, β1 integrins very late antigen (VLA)-4 and VLA-5 act as fibronectin receptors on cells, while αvβ3 and αvβ5 are vitronectin receptors. α1β1 and α2β1 (also known as VLA-2) are collagen-binding receptors found primarily on fibroblasts. Increasingly, the importance of abnormal integrin signalling has been implicated in pathological conditions such as tumour invasion, and metastasis, as well as fibrotic matrix scarring in a variety of disease states.

1.1.ii Individual matrix components

Collagens are the most abundant proteins of the pulmonary ECM. Approximately 11% of total adult lung protein (Bradley et al., 1974) and 60 - 70% of ECM protein content (Raghu et al., 1985) is attributed to collagen. All collagens contain a characteristic right-handed triple helix, formed by three tightly binding polypeptide α-chains. The helical regions of these chains are composed of repeating Gly-X-Y triplets, with approximately every third X being proline and every third Y hydroxyproline. The ring structure of these amino acids help stabilise the helical conformation in each chain. Glycine residues are located in the central helical portion of the superhelix, and peptide bonds are located deep within the structure. Thus, the helical portion of the molecule is resistant to proteolytic degradation (Chambers and Laurent, 1997).

In the normal lung, collagen fibres are found mostly along conducting airways, interstitial septae and blood vessel walls. Fibrillar collagens (types I, II, III, V and XI) form strong intra- and intermolecular covalent bonds that impart structural integrity and tensile strength to the entire lung (Yamanuchi and Mechanic, 1988). Although all five fibrillar types are found in the pulmonary ECM, almost 90% of interstitial collagens are composed of types I and III and are present in a ratio of 2:1 (Kirk et al., 1984). Type II collagen has a restricted distribution, and is found mainly within tracheal and bronchial walls (Dunsmore and Rannels, 1996). Non-fibrillar types IV and V are network-forming collagens that form essential components of basement

membranes all over the lung, with type IV predominating both in quantity and distribution in mature basal laminae (Dunsmore and Rannels, 1996). Type VII collagen molecules dimerise into specialised structures called anchoring fibrils that help attach the basement membrane to the underlying connective tissue. Types IX and XII collagens, also known as FACIT (fibril-associated with interrupted triple helices), decorate the surface of mature fibrillar collagens but their functions are incompletely understood.

In contrast to collagen fibres that are the main determinants of the expansile properties of the lung, elastic fibres provide the resiliency for restoring shape and volume known as pulmonary elastic recoil. Elastin accounts for 20 - 30% of the weight of the lung ECM and contains regions of extreme hydrophobicity interspersed with unique cross-linking domains. It is synthesised as a 70-kDa soluble precursor (tropoelastin) that is rapidly cross-linked and polymerised into a random network of elastin molecules (Rosenbloom, 1987). Its cross-linking domains, desmosine and isodesmosine, represent condensation products formed by the interaction of lysyl residues on at least two tropoelastin molecules. Mature elastic fibres also contain a proportionately smaller amount of 10 -12 nm microfibrillar components that are intrinsically associated with elastin in a complex three-dimensional manner.

Proteoglycans are a distinct group of complex macromolecules containing a core protein linked to variable numbers of glycosaminoglycan polysaccharide side-chains (Ruoslahti, 1988). Aggregating proteoglycans regulate ECM hydration, and contribute to compressive and hypersteric properties of connective tissue. In addition, certain proteoglycans such as decorin and betaglycan can also sequester growth factors in the ECM (Andres et al., 1989). Other members of the family such as perlecan, versican and biglycan are emerging as important molecules with novel functions in cell-matrix adhesion and communication. Heparan sulfate, chondroitin sulfate and dermatan sulfate are the major proteoglycans found in the alveolus.

1.1.iii ECM turnover under homeostatic conditions

Synthesis

Production of the pulmonary ECM is a complex tightly regulated process that is controlled by a balance of stimulatory and inhibitory molecular signals. During lung development

or repair, the proportions of individual matrix proteins may fluctuate to reflect dynamic changes in ECM turnover. Maximal rates of collagen synthesis occur during the perinatal period. However, lung collagens are continuously synthesised and degraded, with net deposition evident throughout most of adulthood. In mature rats and rabbits, as much as 10% of the total collagen pool may be degraded and replaced daily (Laurent, 1982; McAnulty and Laurent, 1987).

In contrast, elastin is substantially more resistant to proteolysis. The half-life of elastin under healthy conditions is extremely long. Thus, loss of elastic fibres may be more detrimental to the alveolar wall than the loss of collagens. The available evidence suggests that the most intense period of elastogenesis is undertaken by myofibroblasts late in foetal development and during the early post-natal period (Shapiro et al., 1991). Glycoslylated non-collagenous ECM components, such as proteoglycans, have higher rates of turnover with half-lives that range from hours to weeks (Hascall and Hascall, 1991). Some ECM components, such as fibronectin, form provisional matrices that are laid down during organogenesis or repair. Although the precise details of their turnover are unclear, these proteins utilise specialised mechanisms that facilitate their dynamic incorporation into and removal from the mature ECM.

Degradation

Extracellular degradation of the pulmonary ECM is mediated principally by the matrix metalloproteinases (MMPs) with some contribution from serine proteinases such as plasmin, urokinase and tissue plasminogen activators (Dunsmore and Rannels, 1996). The degradation of helical collagen into characteristic ¼ and ¾ fragments is accomplished by at least three different collagenases: interstitial collagenase (MMP-1), neutrophil collagenase (MMP-8) and collagenase-3 (MMP-13) (Gross and Nagai, 1965; Hirose et al., 1993; Mitchell et al., 1995). The resultant products are susceptible to further degradation by the same collagenases or other gelatinolytic enzymes, such as gelatinase A (MMP-2), gelatinase B (MMP-9), neutrophil elastase and plasmin at neutral pH, and cathepsins B and L at acidic pH (Kafienah et al., 1998). MMP activity is controlled by a group of tissue inhibitors of metalloproteinases (TIMPs), and collagen turnover is therefore subject to MMP-TIMP counter-regulation (Dunsmore and Rannels, 1996).

1.2 Neutrophil elastase

1.2.i Historical perspectives

Leukoprotease activity was first described early in the 20th century but human neutrophil elastase (EC 3.4.21.37, IUBMB) was only identified relatively recently (Janoff and Scherer, 1968). In this seminal paper, the enzymatic properties of serum-derived pancreas-secreted elastase (PPE) were found to differ from those of elastase purified from polymorphonuclear granulocytes (neutrophils). Even so, most early studies concentrated on defining the structure and function of pancreatic elastase and the amino acid sequence of this enzyme was reported (Shotton and Hartley, 1973) fourteen years prior to that of neutrophil elastase (Sinha et al., 1987).

A principal factor that promoted early interest in neutrophil elastase as a pathogenic molecule was the pioneering observations of Laurell and Eriksson in 1963 which described the greatly increased predisposition of individuals with α_1-AT deficiency towards premature and severe pulmonary emphysema. In the forty years since then, the pathogenesis of this devastating condition has been linked to the production of abnormal forms of α_1-AT that have an increased tendency to polymerise and sequester within hepatocytes. Thus, uncontrolled elastastolytic activity in the alveolar lining fluid may be the unavoidable result of deficient levels of circulating α_1-AT (Mahadeva and Lomas, 1998).

1.2.ii Structural chemistry, expression and biological functions

Neutrophil elastase is a 29 kDa serine proteinase belonging to the chymotrypsin superfamily. It is secreted as a single chain 220-amino acid glycoprotein (Salvesen et al., 1987) with an amino acid sequence containing 30 - 40% sequence homology to many other elastinolytic and non-elastinolytic serine proteinases (Takahashi et al., 1988). Its tertiary structure is similar to that of other chymotrypsin-like serine proteinases, comprising of two interacting anti-parallel β-barrel cylindrical domains and a small proportion of helices (Navia et al., 1989). The two domains form a crevice which contains the catalytic site and is stabilised by four disulfide bridges. The substrate-binding site straddles this crevice and includes part of the two domains.

Neutrophil elastase exists in several isoforms that differ in their degree of glycosylation (Bieth, 1998). All isoforms possess identical catalytic properties and have an optimal working pH that is close to neutrality (Bode et al., 1989). In humans, expression of the neutrophil elastase gene (ELA2, chromosome 19p) occurs within a narrow period during promyelocytic differentiation. The enzyme is stored in its active form within cytoplasmic azurophilic granules (Zimmer et al., 1992). Circulating neutrophils lack the capacity for further synthesis of elastase as evidenced by the absence of mRNA transcripts in these cells (Takahashi et al., 1988). Monocytes contain low levels of neutrophil elastase (about 5 - 6%). Upon differentiation into macrophages, an elastinolytic macrophage metalloproteinase replaces neutrophil elastase (Bieth, 1986).

Intracellular neutrophil elastase is a key effector molecule of the innate immune system, with potent antimicrobial activity against gram-negative bacteria (Belaaouaj et al, 1998; Weinrauch et al., 2002), spirochaetes (Garcia et al., 1998) and fungi (Tkalcevic et al, 2000). Its ability to degrade the outer membrane protein A (OmpA) molecule on *Klebsiella pneumoniae* has been proposed to explain its lethal effects on this particular pathogen (Belaaouaj et al., 2000).

In contrast to its intracellular role, the main targets of extracellular neutrophil elastase activity appear to be components of the ECM, a variety of cell surface ligands, soluble proteins and a number of important adhesion molecules (Starcher, 1986; Bieth, 1998). In general, neutrophil elastase is capable of digesting virtually every connective tissue component, including several types of collagen, fibronectin, proteoglycans, heparin and cross-linked fibrin (Travis, 1988). The biological roles of neutrophil elastase also include acting as a secretagogue for cytokines (Bedard et al., 1993), glycosaminoglycans (Sommerhoff et al., 1990) and mucin (Voynow et al., 1999) in addition to acting as a modulator of inflammation (reviewed in Lee and Downey, 2001).

1.2.iii Substrate specificity

Neutrophil elastase has an extensive substrate range (Table 1.1). Unlike most other proteinases, it is able to solubilise elastic fibres, a key component of the lung ECM with important functions in elastic recoil and structural integrity. The insolubility of elastin is partly due to its high content of non-polar amino acids such as alanine (26%) and valine (13%), residues to which human neutrophil elastase shows P1 specificity (Bieth, 1986). In addition, elastase can also cleave various types of collagen (Gadher et al., 1988; Kittelberger et al., 1992), fibronectin, laminin (Heck

et al., 1990) and proteoglycans (Janusz and Doherty, 1991). Moreover, neutrophil elastase can inactivate certain substrates without cleaving them, most notably members of the coagulation cascade such as clotting factor V (Allen and Tracey, 1995), fibrinogen and thrombin (Brower et al., 1987).

TABLE 1.1 PROTEOLYTIC SUBSTRATES OF NEUTROPHIL ELASTASE

ECM COMPONENTS	***SOLUBLE PROTEINS***	***CELL SURFACE MOLECULES***
Elastin and elastic fibres	Coagulation system factors	Leukocytes
Collagen (types II, III, IV, VI, VIII, IX, X)	Complement factors	*CD11b/18(Mac-1)*
Fibrillin microfibrils	Fibrinogen	*CD14*
Fibrin (cross-linked)	Immunoglobulins	*CD43*
Fibronectin	Proenzymes	*ICAM-1*
Laminin	*pro-Collagenase*	Tissue resident cells
Proteoglycans	*pro-Cathepsin B*	*ICAM-1*
Bubepidermal BP-180	Tenascin	Endothelial cells
Latent TGF-β binding protein-1	Tumour necrosis factor-alpha	*VE-cadherin*
	Proteinase Inhibitors	*Heparan sulfate*
	α_1-proteinase inhibitor	Platelets
	α_2-macroglobulin	*IIb/IIIa fibrinogen receptor*
	α_2-plasmin inhibitor	Human immuno-deficiency virus
	Antithrombin III	*gp120 coat protein*
	Complement C1 inactivator	Gram-negative bacteria
	Plasminogen activator inhibitor 1	*Outer membrane protein (Omp) A*
	Metalloproteinases	
	MMP-9	
	Tissue Inhibitor of MMP	
	TIMP-1	
	Surfactant protein D	

1.2.iv Mechanism of proteolytic action

Neutrophil elastase contains a primary catalytic site (S_1) and a number of extended substrate-binding sites to accommodate substrates of varying chain lengths (Lestienne and Bieth, 1980). The primary catalytic triad of His^{57}-Asp^{102}-Ser^{195} residues (in chymotrypsin numbering order) form a potent charge-relay system for initiating peptide bond attack (Travis, 1988; Bode et al., 1989). As a result of electron transfer from the carboxyl group of Asp^{102} to the oxygen of Ser^{195}, the γ-oxygen on Ser^{195} is transformed into a powerful nucleophile that targets the carbonyl atom in the engaged substrate. During proteolysis, the initial formation of a reversible Michaelis complex between the enzyme and its substrate is followed by cleavage of the peptide bond and formation of an acyl-enzyme intermediate. Deacylation of this covalent molecule yields a hydrolysed carboxyl-moiety product and a regenerated enzyme (Powers and Harper, 1986).

Neutrophil elastase has a particular propensity for hydrolysing non-bulky amino acids such as valine at the substrate P1 position, with alanine, methionine and leucine residues being less reactive (Del Mar, 1980). Porcine pancreatic elastase differs from neutrophil elastase in its higher affinity for substrates containing alanine residues. This affinity may explain why it hydrolyses elastin, containing a high proportion of alanyl residues, much faster than neutrophil elastase (Reilly, 1980).

1.2.v Tissue locations

Soluble neutrophil elastase is usually quantified according to its catalytic activity in the presence of exogenously added substrate. In this manner, increased neutrophil elastase activity has been measured in BAL fluid in a number of pathological states, including emphysema (Wewers, 1989), cystic fibrosis (Meyer et al., 1991), the acute respiratory distress syndrome (Gando et al., 1997) and pulmonary fibrosis (Yamanouchi et al., 1998). Although there is a wealth of knowledge about the biochemistry and enzyme kinetics of neutrophil elastase in free solution, the presence of high-affinity extracellular inhibitors can make it difficult to identify this serine proteinase in its pure enzymatic form *in situ*. Its predominant intracellular location and transient extracellular existence also complicate histological identification of the enzyme outside the neutrophil.

Even so, catalytically active neutrophil elastase has been localised to the plasma membrane of mature neutrophils following release from intracellular stores (Owen et al., 1995). The ability of neutrophil proteinases to sequester in the immediate pericellular environment is believed to be an adaptive mechanism whereby their catalytic activities may be preserved despite the presence of extracellular inhibitors. It has been estimated that at any one time, as much as 12% of stored human neutrophil elastase may be expressed on the cell surface by a charge-dependent mechanism following neutrophil priming by either TNF-α or activation by IL-8 (Owen et al., 1997). The quantity of such cell-bound neutrophil elastase is approximately six-fold greater than the amount released into the extracellular environment.

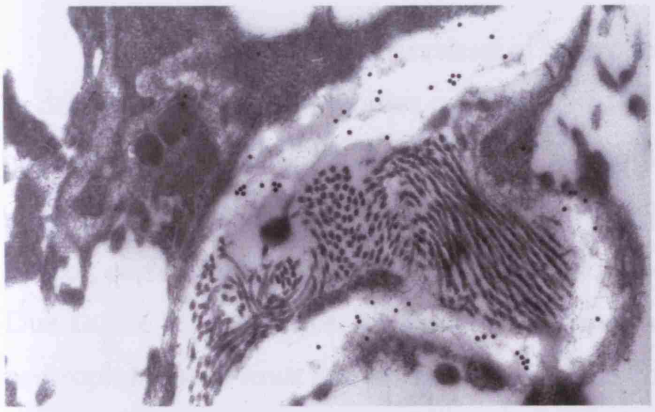

Reproduced from Cavarra et al., 1999

Figure 1.1 Extracellular localisation of neutrophil elastase in lung matrix

Colloidal particles of immunogold-labeled neutrophil elastase particles are present in the alveolar wall, surrounding bundles of damaged elastic fibres (original magnification x 34 000).

Although the amount of neutrophil elastase extruded extracellularly appears to be small (in the order of 1 x 10^6 molecules/cell), it is in this form that most of its proteolytic activity is directed at the lung extracellular matrix. Most demonstrations of extracellular matrix-bound neutrophil elastase have utilised immunogold-labeling techniques. In human lungs exposed with neutrophil elastase *in vitro*, prominent immunogold positivity may be evident in damaged elastic fibres of varying sizes (Morris et al., 1993). Likewise, immunoreactive neutrophil elastase released into the matrix of murine lungs has been identified in areas of ECM breakdown within the alveolar wall following neutrophil degranulation induced by N-formyl-L-methionyl-leucyl-L-phenylalanine (fMLP) instillation (Cavarra et al., 1999).

More recently, Brinkmann and colleagues have shown that activated neutrophils can secrete discrete webs of extracellular fibres that contain DNA, histones and granule proteinases such asneutrophil elastase and cathepsin G (Brinkmann et al., 2004). These so-called neutrophil extracellular traps (NETs) are dispersed to trap bacteria that are then digested by the activity of neutrophil elastase protected within them. Not only is this an efficient way of maintaining the relevance of neutrophil-derived enzymes outside the confines of the neutrophil, it may also focus the activity of neutrophil elastase in targeting the extracellular matrix during tissue remodelling.

1.2.vi Proteinase inhibition: a key strategy for regulating neutrophil elastase activity

Inadvertent extracellular release of neutrophil elastase occurs during neutrophil necrosis or degranulation. Such responses can be stimulated *in vitro* with agents that prime or activate neutrophils such as TNF-α, LPS, C5a, phorbol esters and *N*-formyl-methionyl-leucyl-phenylalanine (fMLP) (Senior and Campbell, 1983; Baggiolini and Dewald, 1984; Wright, 1988). *In vivo*, chemical and microbial toxins are the commonest triggers of neutrophil degranulation. Due to the high turnover of neutrophils, studies have estimated that around 250 mg of neutrophil elastase must be eliminated from the circulation daily which necessitates the presence of a large anti-proteinase screen (Travis et al., 1991). The immense variety of neutrophil elastase activities in the extracellular space obliges tight and efficient regulation by specialised antagonists. In the lung, neutrophil elastase activity is controlled by several antiproteinases, namely alpha-1-proteinase inhibitor (α1-PI, *synonymous with alpha-1-antitrypsin or α1-AT*), SLPI and to a lesser extent, elafin. These naturally occurring compounds interfere with the neutrophil elastase catalytic site to disrupt its enzymatic activity.

α1-PI, a highly polymorphic 52 kDa glycopeptide belonging to the serpin (serine protease inhibitor) superfamily, is the primary circulating and tissue-based inhibitor of neutrophil elastase. It is synthesised principally by liver hepatocytes, and to a lesser extent, peripheral blood monocytes and alveolar macrophages (Perlmutter et al., 1985; Venembre et al., 1994). The normal gene product of the α1-AT gene is a 394-amino-acid acute phase protein whose concentration may rise up to four or five-fold in response to systemic inflammation or injury. Although best known as the principal inhibitor of neutrophil elastase, the anti-proteinase spectrum of α1-PI is broad and includes trypsin, cathepsin G and proteinase 3 (Lomas and Parfrey, 2004). In the alveolus, α1-PI contributes to over 90% of the neutrophil elastase

inhibitory activity with a concentration of approximately 10 – 15% of normal serum levels, or between 2 and 5 μM of anti-proteinase activity (Wewers et al., 1988; Crystal, 1990). During intense lung inflammation, the alveolar spaces become flooded with increased amounts of α1-AT, and levels in the epithelial lining may exceed 10 μM. α1-PI potently (K_i 3.3 x 10^{-14} M) and rapidly (K_{assoc} 6.5 x 10^7 M) neutralises neutrophil elastase activity by forming an irreversible 1 : 1 molar complex with the solubilised serine proteinase (Bernstein et al., 1994). These inactive complexes are then recognised by hepatic receptors and cleared from the circulation. Despite its potency, the large size of α1-PI renders it ineffective against neutrophil elastase that is bound to components of the extracellular matrix including elastin (Bruch and Bieth, 1986). Abnormalities in the α1-PI gene are associated with gross reductions in circulating concentrations of α1-PI and intracellular aggregation of the polymerized α1-PI protein within liver cells (Lomas et al., 1992). Consequently, patients with these genetic defects are predisposed to early hepatocellular failure and a particularly severe form of pulmonary emphysema (Mahadeva and Lomas, 1998).

SLPI ('mucus proteinase inhibitor') and elafin ('elastase-specific inhibitor') are low-molecular weight proteins belonging to the antileukoprotease (ALP) family (Hiemstra, 2002). Both are found primarily in tracheo-bronchial and lung secretions. In addition, glandular epithelial cells, alveolar macrophages and neutrophils also secrete SLPI; elafin is detectable in sputum and the skin (Sallenave, 2001).

SLPI is an 11.7 kDa cationic, non-glycosylated potent inhibitor of neutrophil elastase (K_i 3.3 x 10^{-10} M), cathepsin G and trypsin but not of proteinase 3 (Tetley, 2000). It can also inhibit chymotrypsin and mast cell tryptase. The SLPI molecule comprises two homologous cysteine-rich domains (supporting eight disulfide bridges), with the C-terminal domain containing elastase binding and inhibitory activity (Grutter et al., 1988). In the lung, SLPI is produced predominantly by Clara and goblet cells of the surface epithelium and to a lesser extent by serous cells lining submucosal glands. Unlike α_1-PI, it is a reversible inhibitor of neutrophil elastase but like its larger counterpart, it is unable to inhibit elastase that is bound to elastin.

In contrast, elafin is a specific inhibitor of neutrophil elastase containing a four-disulfide core protein that belongs to the recently described trappin family (Schalkwijk et al., 1999). Also known as skin-derived antileukoproteinase (SKALP), it bears structural similarities to SLPI and has similar patterns of expression (Pfundt et al., 1996). However, unlike SLPI, elafin is able to

inhibit proteinase 3 activity. Its particularly small size enables elafin to access pericellular sites that exclude SLPI and α_1-PI.

More recently, a number of studies have shown that α_1-PI, SLPI and elafin may exert their anti-inflammatory effects beyond simple antagonism of neutrophil elastase activity. In the bleomycin model of lung injury and fibrosis, α_1-PI attenuates the degree of lung damage without affecting neutrophil numbers or levels of measured elastase (Nagai et al., 1992). Elastase:α_1-PI complexes can also stimulate production of α_1-PI by macrophages (Joslin et al., 1991). SLPI can inhibit the pro-inflammatory activity of bacterial lipopolysaccharide (Jin et al., 1997). In addition, an antimicrobial 'defensin-like' role for both SLPI and elafin has recently been described, a property that may contribute to their protective effects in the lungs (Hiemstra et al., 1996; Simpson et al., 1999).

1.2.vii Evasion of the antiproteinase screen

Neutrophils contain an estimated 1.11 ± 0.11 (SD) pg of neutrophil elastase (Campbell et al., 1989) which is packaged into approximately 400 azurophilic granules per cell (Damiano et al., 1988). Analysis by quantum proteolysis has calculated that each of these specialised granules contains approximately 67,000 molecules of neutrophil elastase. This estimation equates to a mean intra-granular elastase concentration of 5 mM in each neutrophil (Liou and Campbell, 1995). Once released, soluble neutrophil elastase is completely inactivated when its extracellular concentration falls by two orders of magnitude relative to the concentration of surrounding proteinase inhibitors (Liou and Campbell, 1995). In a normal extracellular environment replete with antiproteinases, the obligate catalytic activity of extruded neutrophil elastase will persist for milliseconds before being quenched by pericellular inhibitors. Therefore, successful antiproteinase evasion in the extracellular milieu is critical for unimpeded neutrophil elastase activity.

Massive neutrophil degranulation leading to swamping of the antiproteinase screen is one means by which immediate inhibition of extracellular elastase activity can be limited. This occurs in acute inflammatory states such as overwhelming sepsis or massive tissue injury. In addition, neutrophil-derived oxidative intermediates can rapidly inactivate α_1-PI, SLPI and elafin by

directly oxidising a key methionine residue in their substrate-binding sites (Bernstein et al., 1994). This mechanism is believed to operate in the lungs of chronic smokers and to contribute to the widespread neutrophil-mediated tissue damage encountered in their lungs.

Mounting evidence also suggests that neutrophil elastase can exist in shielded pericellular microenvironments where its catalytic activity is protected from inhibition (Takeyama et al., 1998). In the lungs and other organs, this phenomenon may explain why substantial tissue breakdown can occur despite an apparently low intensity of inflammation. Furthermore, neutrophil elastase that is bound to insoluble elastin is relatively resistant to neutralisation by most endogenous antiproteinases (Morrison et al., 1990). Finally, MMP-9 has recently been shown to digest and inactivate α_1-PI, a mechanism that would decrease tissue anti-elastase capacity and enhance neutrophil elastase activity at sites of extracellular tissue damage (Liu et al., 2000).

1.2.viii Neutrophil elastase - extracellular matrix interactions

Neutrophil elastase is a prime example of a matrix-modifying enzyme whose actions are dependent on the context in which it finds itself. Due to its varied substrate range, neutrophil elastase activity can induce cytokine secretion, degrade clotting factors and activate a number of cell surface receptors that regulate inflammation and host defences. However, its unrestrained degradative activity on matrix constituents forms the pathological basis for diseases such as pulmonary emphysema, chronic bronchitis and cystic fibrosis. Outside the lungs, neutrophil elastase-mediated proteolysis of murine BP180, a hemidesmosome protein located at the dermal-epidermal junction of intact skin, has been shown to induce skin blistering that is analogous to human bullous pemphigoid (Liu et al., 2000).

Several lines of evidence indicate that the crosstalk between infiltrating immune cells and the surrounding matrix during tissue injury profoundly influence the migratory capacity and target-organ functions of these cells. Inhibition of neutrophil elastase has been shown to reduce neutrophil adhesion to extracellular matrix-coated surfaces *in vitro* and to endothelial cells *ex vivo* (Carney et al., 1998). Neutrophil elastase-mediated disruption of intercellular E-cadherin junctions has been shown to facilitate neutrophil transmigration across epithelial barriers (Ginzberg et al., 2001). Similarly, interactions between cytoskeletal elements of fibroblasts and

the external matrix may be susceptible to proteolytic modification by this proteinase. Furthermore, the requirement for neutrophil elastase-mediated cleavage of endothelial CD11b/18 to allow neutrophils to infiltrate lung matrix is consistent with the role of this proteinase in degrading adhesion molecules that immobilise leukocytes during inflammatory cell trafficking (Cai and Wright, 1996).

More direct collaborative interactions between neutrophil elastase and MMPs have been shown to influence extracellular matrix function and remodelling *in vitro*. For example, exogenously added neutrophil elastase can augment fibroblast-mediated contraction of three-dimensional collagen gels (Skold et al., 1999). The mechanism for this appears to involve neutrophil elastase-mediated activation of latent MMPs (Zhu et al., 2001). In this model, collagen gel contraction was also accompanied by the degradation of extracellular matrices secreted by fibroblasts following prolonged co-culture with monocytes. Thus, apart from causing matrix protein loss, neutrophil elastase also appears to influence the rearrangement of extracellular matrix that might ultimately be relevant to disease pathogenesis.

Unlike MMP-mediated inactivation of IL-1β, neutrophil elastase appears to be involved in processing this cytokine to its active form (Black et al., 1991). In a similar manner, it can convert IL-8 to more potent, truncated variants. Neutrophil elastase also degrades and inactivates TNF-α (Scuderi et al., 1991). Because TNF-α has been shown to bind ECM constituents, it is possible that this action may alter the activity of matrix-bound TNF-α. Neutrophil elastase degrades the pleiotropic cytokine IL-2, generating small peptides that regulate T-cell adherence to the ECM and other functions related to T-cell activation (Ariel et al., 1998). The same proteinase produces biologically active fragments of collagen and elastin that stimulate collagen synthesis in cultured fibroblasts (Gardi et al., 1999) and can induce pulmonary fibrosis (Gardi et al., 1990).

1.2.ix The role of neutrophil elastase in diseases of the lung

The notion of neutrophil elastase as a principal mediator of lung inflammation and destruction was reinforced from observations that unopposed elastase activity characterised premature lung destruction in individuals with hereditary α_1-AT deficiency (Laurell and Eriksson, 1963). Since that time, its matrix-degrading capacity has been implicated in the clinical

exacerbation of other lung diseases such as cigarette smoke-induced emphysema, chronic bronchitis, cystic fibrosis, bronchiectasis and bronchiolitis obliterans. Many of these diseases have in common neutrophil-dominated airway inflammation. In almost all of these diseases, neutrophil elastase has emerged as an important modulator of alveolar inflammation, epithelial injury and interstitial matrix damage.

The promiscuous nature of neutrophil elastase and its broad substrate repertoire have led to the hypothesis that any imbalance in the equilibrium between elastase and its natural inhibitors may result in, or at least intensify, these pathological states. Thus, although connective tissue digestion is its best-known tissue manifestation, neutrophil elastase activity can also intervene to amplify pathogenic pathways such as mucus hypersecretion, impairment of ciliary function, cytokine and growth factor activation, augmentation of inflammation and degradation of cell receptors and other molecules (reviewed in Bernstein et al., 1994).

The ability of neutrophil elastase to sequester and kill bacteria underlines its role as a key effector of the innate immune system. Intracellular elastase kills gram negative bacteria by cleaving surface antigens that regulate microbial plasma membrane integrity. Neutrophil elastase-mediated killing of *Klebsiella pneumoniae* occurs by the non-oxidative cleavage of a specific bacterial target, the OmpA protein (Belaaouaj et al., 2000). In a similar manner, the degradation of other, as yet unspecified, virulence factors appears to explain the ability of neutrophil elastase to counter infections by spirochaetes (Garcia et al., 1998), fungi (Tkalcevic et al, 2000) and schistosomal parasites (Freudenstein-Dan et al., 2003).

The observation that emphysematous and fibrotic lung changes often co-exist have given rise to the theory that these two structural anomalies may represent the polar ends of the spectrum of lung extracellular matrix remodelling. Evidence that neutrophil elastase activity may be involved in the development of both airspace enlargement and interstitial matrix accumulation has come from descriptive reports and experimental studies. Raised levels of neutrophil elastase-α1-PI complex, measured to reflect elastase burden, have been reported in the lungs of patients with established IPF (Obayashi et al., 1997; Yamanouchi et al., 1998). Moreover, extracellular neutrophil elastase has been found in areas of interstitial and honeycomb fibrosis (Hojo et al., 1997; Obayashi et al, 1997). Although these studies strengthen the view that uncontrolled neutrophil elastase activity is not purely destructive in chronic lung disease, its role in promoting fibroproliferative changes remains ill defined.

1.2.x Neutrophil elastase-deficient mice as experimental models of human disease

The expression and function of the neutrophil elastase gene (*NE*) in humans and mice share important similarities. In both, it spans five exons of similar sizes containing conserved intron/exon junctions, including the codons of the primary His-Asp-Ser catalytic triad (Belaaouaj et al., 1997). The genomic sequence of *NE* in each species also predicts the expression of a precursor pro-elastase, which in mice, consists of 265 amino acids, two less than the human homolog. These two gene products share sequence homology of approximately 83% (NCBI BLAST® Conserved Sequence website). The synthesis of neutrophil elastase is also restricted to the early stages of myelocytic development in both cases. Furthermore, human neutrophil elastase is inhibited by protein products of two of the five murine α_1-PI genes (Paterson and Moore, 1996). Such overlapping characteristics between the two species lend themselves to the use of genetically modified mice with neutrophil elastase abnormalities to model major human diseases. Although exhaustive comparisons between the enzymatic activities of human and murine neutrophil elastase have not been completely characterised, both enzymes are known to cleave major substrates such as elastin and synthetic compounds that contain substituted nitroanilide groups (Bernstein et al., 1994).

Two strains of neutrophil elastase-deficient ($NE^{-/-}$) mice have been generated by targeted mutagenesis and used for examining the role of this proteinase in host immunity and connective tissue injury (Belaaouaj et al., 1998; Tkalcevic et al., 2000). Whilst the progeny of $NE^{-/-}$ mice develop normally in the absence of infective stimuli, with preserved neutrophil migration, phagocytosis, oxidative burst and degranulation, they have increased vulnerability to sepsis and death when challenged systemically with gram negative bacteria (*Klebsiella pneumoniae* and *Escherichia coli*) (Belaaouaj et al., 1998). Likewise, their survival is severely compromised following exposure to pathogenic *Aspergillus fumigatus* (Tkalcevic et al., 2000). Outside the realm of infections, neutrophil elastase activity has also been implicated in cigarette smoke-induced emphysema Whilst neutrophil elastase deficiency may confer partial resistance to cigarette smoke-induced emphysema (Shapiro, 2002), its role in modulating fibrotic lung repair has not been previously evaluated.

1.3 Pulmonary fibrosis

Pulmonary fibrosis is the cardinal pathologic feature uniting a large group of disorders collectively known as the diffuse parenchymal lung diseases (DPLD). Over 200 clinical entities come under this heading, including those arising from known causes such as exposure to inorganic particulates, infective agents, irradiation and autoimmune reactions, but also those of uncertain aetiology (reviewed in Demedts et al., 2001). Numerically, the largest group of fibrotic lung diseases comprises those associated with connective tissue (collagen vascular) disorders. While many DPLDs may arise from chronic exposure to environmental agents (such as dust) or infection (including mycobacteria), a large number may also develop following acute exposure to certain drugs. Bleomycin is an anti-neoplastic agent whose clinical use is associated with the development of pulmonary fibrosis in up to 3 – 5% of patients (Cooper, 2000). Pulmonary fibrosis may manifest as part of a systemic disorder, or present purely as a lung-limited disease.

The nomenclature for pulmonary fibrotic disorders has evolved considerably since the first description of Liebow and Carrington over 30 years ago (Liebow and Carrington, 1969). Scadding introduced the term 'diffuse fibrosing alveolitis', and divided pulmonary fibrotic disease into two groups that were either aetiologically identifiable or obscure (Scadding, 1974). The second group was defined with the aid of histopathological information. Since that time, classification systems have depended more and more on composite information gleaned from pulmonary imaging, cytopathology and histopathology. Over the past decade, the spectrum of idiopathic interstitial pneumonias has become better defined; as a result, the different disease manifestations are now distinguished as discrete pathological entities, at least in histologic terms (Muller and Colby, 1997; Katzenstein and Myers, 1998). The latest international classification uses an integrated clinical, radiologic and pathologic approach to segregate the many different forms of DPLDs into broad aetiological subgroups (Figure 1.2, ATS/ERS International Multidisciplinary Consensus Classification, 2002). One of its key objectives was to emphasise greater attention on the IIP subgroup, now recognised as a large and important collection of clinically important diseases. Efforts were made to narrow and standardise the pathologic identification of the individual disease variants within this subgroup.

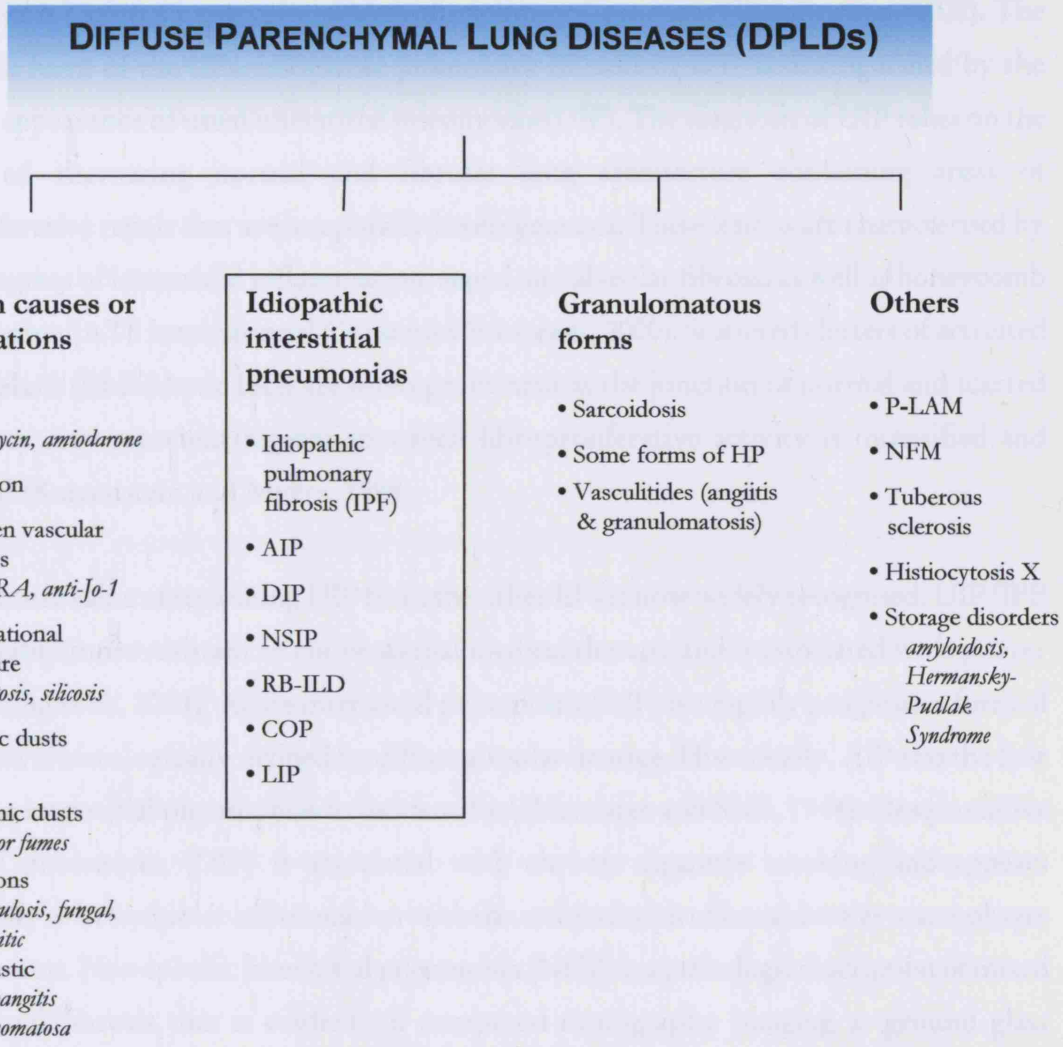

Figure 1.2 Revised classification of the diffuse parenchymal lung diseases (DPLDs)

AIP: acute interstitial pneumonia; anti-Jo-1: polymyositis/pulmonary fibrosis syndrome; COP, cryptogenic organising pneumonia; DIP, desquamative interstitial pneumonia; HP: hypersensitivity pneumonitis; LIP: lymphocytic interstitial pneumonia; NSIP: non-specific interstitial pneumonia; P-LAM: pulmonary leiomyomatosis; NFM: neurofibromatosis with lung disease; RA: rheumatoid arthritis; RB-ILD: respiratory bronchiolitis interstitial lung disease; SSc: systemic sclerosis; UIP: usual interstitial pneumonia.

(adapted from ATS / ERS International Multidisciplinary Consensus Classification, 2002)

1.3.i The idiopathic interstitial pneumonias

The idiopathic interstitial pneumonias consist of acute and chronic disorders of unknown aetiology but sufficient difference to warrant separate clinico-pathological descriptions

(reviewed in ATS/ERS International Multidisciplinary Consensus Classification, 2002). The commonest form of the IIPs, idiopathic pulmonary fibrosis or IPF, is distinguished by the histologic appearance of usual interstitial pneumonia (UIP). The diagnosis of UIP relies on the presence of alternating normal and fibrotic lung architecture containing areas of fibroproliferative repair that are temporally heterogeneous. These lesions are characterised by variable degrees of interstitial inflammation, septal and alveolar fibrosis as well as honeycomb transformation (ATS International Consensus Statement, 2000). Scattered clusters of activated myofibroblasts (fibroblastic foci) are often prominent at the junction of normal and scarred areas. These may represent regions in which fibroproliferative activity is intensified and propagated (Katzenstein and Myers, 1998).

The prognostic value of separating UIP from the other IIPs is now widely recognised. UIP/IPF is considerably more resistant to conventional medical therapy and is associated with poorer survival (King et al., 2001). Acute interstitial pneumonia (AIP) is a rapidly progressive form of the IIPs that is histologically defined by diffuse alveolar damage. Historically, AIP was the first form of the interstitial pneumonias to be identified (Hamman and Rich, 1944). Desquamative interstitial pneumonia (DIP) is associated with chronic cigarette smoking and appears histologically as bronchiolar inflammation with the accumulation of intra-alveolar macrophages laden with iron. Non-specific interstitial pneumonia (NSIP) is a pathologic description of mixed alveolitis and fibrosis that is evident on computed tomography imaging as ground glass opacification. NSIP comprises the widest clinical spectrum of the IIPs. Respiratory bronchiolitis-associated interstitial lung disease (RBILD) and cryptogenic organising pneumonia (COP) are manifestations that include elements of bronchiolo-alveolar inflammation and granulation tissue organisation. Lymphoid interstitial pneumonia (LIP) is associated mainly with immunologic disorders including human immunodeficiency virus disease and has characteristic widespread lymphocytic infiltration in the alveoli and interstitium.

Idiopathic pulmonary fibrosis

IPF is the commonest and most widely studied form of IIP. It is a chronic fibrosing pneumonia with a gender predilection for middle-aged males, and a progressive natural history punctuated by episodes of acute disease exacerbation (Gross and Hunninghake, 2001). Approximately two-thirds of patients with IPF are over the age of 60 at the first presentation, with a mean age of 66

at diagnosis (ATS International Consensus Statement, 2000). One widely quoted study from Bernalilo County, New Mexico, has estimated the incidence of IPF at between 7.4 to 10/100, 000 population/year (Coultas et al., 1994). These figures increase with age, and are thought to exceed 100/100, 000 population/year in men over the age of 75. In the same study, an overall prevalence of 20.2/100, 000 in men and 13.2/100, 000 in women, was also estimated, for a mean prevalence of 16.7/100, 000. The latter is consistent with a recent study from Finland that reported a nationwide prevalence of 16 - 18/100, 000 population in that particular country (Hodgson et al., 2002). In contrast, the average prevalence of IPF in the United Kingdom has been estimated at 6.0 / 100, 000 population (Scott et al., 1990).

In established IPF, extensive parenchymal fibrosis results in severe and progressive ventilatory failure. Loss of lung compliance from excessive matrix deposition increases the work of breathing and accelerates an irrevocable decline in lung function. Patients with IPF have a five-year survival rate of 40 - 60% (Hubbard et al., 1996). This prognosis is substantially poorer than fibrosing alveolitis associated with either systemic sclerosis or rheumatoid arthritis (Wells et al., 1998). The overall median IPF survival rate is around 2.8 years (Bjoraker et al., 1998). Epidemiological studies over the past decade have identified a rising trend in the global mortality rates of IPF (Johnston et al., 1990; Mannino et al., 1996). In the United States, the five-year mortality rate of IPF has surpassed those of breast cancer, prostate cancer and hospital-treated acute myocardial infarction (Table 1.2).

TABLE 1.2 COMPARATIVE MORTALITY OF IPF AND OTHER DISEASES

DISEASE	MORTALITY
Lung cancer	85% at 5 years
Idiopathic pulmonary fibrosis	**50% at 5 years**
Acute myocardial infarction (seen and treated in hospital)	25% at 5 years
Breast cancer	20% at 5 years
Prostate cancer	15% at 5 years
Decompensated liver cirrhosis (with variceal bleeding)	50% at 4 years
Coronary artery bypass surgery (three vessel)	30% at 4 years
COPD on long-term oxygen therapy	50% at 3 years

(adapted from Mason et al., 1999)

In a seven-country study, the authors found a large variation in mortality data of IPF. Mortality rates varied from 0.03 – 1.3 per 100, 000 to 0.6 – 1.7 per 100, 000 in post-inflammatory fibrosis, a term that remains diagnostically obscure (Hubbard et al., 1996). Whilst emphasising the difficulties associated with the epidemiological analysis of IPF, this study nonetheless confirmed earlier estimates of the mortality rate of IPF in England and Wales (Johnston et al., 1990).

1.3.ii Epidemiology and disease burden of pulmonary fibrosis

Epidemiological data for most fibrotic lung diseases is limited by their uncommon occurrence, the lack of large population-based studies, and inherent diagnostic ambiguity. In a population-based study in New Mexico, the prevalence of DPLDs was estimated to be 20% higher among men (80.9 per 100, 000 population) than among women (67.2 per 100, 000 population) (Coultas et al., 1984). In the same study, the incidence of DPLDs among men (31.5 per 100, 000 population) was comparable to that among women (26.1 per 100, 000 population). When compared with the frequency data from other registries, prevalences of sarcoidosis and hypersensitivity pneumonitis are lower than in Europe (reviewed by Demedts et al., 2001). However, pulmonary fibrosis secondary to pneumoconioses and connective tissue diseases were relatively more common. Regardless of geographic differences, it is now widely accepted that both the prevalence and incidence of pulmonary fibrotic disorders are approximately five to ten times higher than suggested by a number of earlier studies (Schwartz, 2000).

The incidence of pulmonary fibrosis in connective tissue disorders such as rheumatoid arthritis and systemic sclerosis is also unclear. Pulmonary abnormalities have been found in up to 60% of patients with rheumatoid arthritis on lung biopsy (Cervantes-Perez et al., 1980) and up to 50% when screened by high-resolution computed tomography (Remy-Jardin et al., 1994). However, interstitial changes are routinely found in only about 5% of affected patients when assessed by plain X-rays, due to the relative insensitivity of this modality as a screening tool (reviewed in Wells, 2000). Conversely, radiological involvement is present up to 65% of patients with systemic sclerosis. In addition, post-mortem evidence of pulmonary fibrosis has been reported in up to 75% of deaths from this condition, the highest prevalence amongst connective tissue disorders (Minai et al., 1998). The prevalence of sarcoidosis also varies widely. Rates of incidence have been estimated at 3/100, 000 in Caucasians, 47/100, 000 in African Americans (Freitas and Costa, 1988), and 64/100, 000 in Scandinavians (reviewed by Eklund and Grunewald, 2000).

Pulmonary involvement occurs at some stage in up to 90% of those affected. Epidemiological data for other connective tissue disorders is inadequate. More recently, a global effort has been made to establish patient registries to allow geographic differences in DPLD to be identified and analysed (Thomeer et al., 2001).

1.3.iii Criteria for diagnosing pulmonary fibrosis

In the majority of cases, a confident diagnosis of pulmonary fibrosis is limited by the sensitivities of clinical and radiological considerations, with or without a histopathological contribution. In the case of IPF, a clinical history of insidious breathlessness, digital clubbing, dry cough and the presence of 'fibrotic' auscultatory crackles in an older patient, in the absence of obvious trigger factors, increase the diagnostic specificity (Bourke and Clague, 2000). Laboratory investigations are not useful for diagnosing IPF but may help eliminate hereditary, hypersensitivity or connective tissue disorders. The presence of UIP in lung biopsy material usually confirms the diagnosis of IPF in the correct clinico-radiological setting. In the absence of biopsy information, the certainty of a clinical diagnosis is improved by considering a list of differentiating criteria (Table 1.3).

TABLE 1.3 SIMPLIFIED ATS / ERS CRITERIA FOR THE CLASSIFICATION OF IPF IN THE ABSENCE OF SURGICAL LUNG BIOPSY

Major Criteria

Exclusion of other known causes of DPLD

Abnormal pulmonary function (restrictive ventilatory defect or impaired gas exchange)

Reticular abnormalities on high-resolution CT scanning (with minimal ground-glass opacities)

No biopsy or bronchoalveolar lavage evidence to support an alternative diagnosis

Minor Criteria

Age > 50 years

Insidious onset of unexplained dyspnoea (shortness of breath)

Duration of illness > 3 months

Bibasilar inspiratory crackles

(adapted from ATS/ERS International Multidisciplinary Consensus Classification statement, 2002)

The presence of certain radiological features on high-resolution computed tomography (HRCT) may suggest an 'IPF pattern'. These include subpleurally distributed, linear (reticular) opacities consistent with interlobular septal thickening in the basal lobes, the presence of parenchymal honeycombing with cystic change and traction bronchiectasis. Patchy ground glass opacification (GGO) may also be present, although this is not the most prominent radiologic sign in IPF. Indeed, extensive GGO may suggest an alternative diagnosis such as non-specific interstitial pneumonia (NSIP).

1.3.iv Functional and clinical consequences of pulmonary fibrosis

The characteristic physiological abnormality in pulmonary fibrosis is a restrictive ventilatory defect with relative sparing of airway limitation. Decreased lung volumes (both vital and total lung capacity) and increased 'stiffening' of lung units ultimately contribute to the gradual reduction in pulmonary compliance. Progressive worsening of gas exchange is evident by a steady decline in the diffusive efficiency of lung carbon monoxide transfer ($_{DL}CO$). In some cases, the reduction in $_{DL}CO$ may precede any appreciable contraction in lung volume. Over time, the combination of heterogeneous ventilation-perfusion mismatches as well as increased blood shunting due to alveolar-capillary barrier thickening result in a steady reduction in the arterial partial pressure of oxygen (P_aO_2).

Depending on the stage of clinical disease, patients may frequently experience breathlessness at rest and almost always during physical exertion. With time, as work of breathing progressively increases, the degree of respiratory disability becomes steadily augmented. One adverse effect of worsening interstitial fibrosis on the pulmonary circulation is the development of secondary pulmonary hypertension as a result of chronically elevated pulmonary vascular resistance. This complication leads inexorably to right ventricular overload and right-sided cardiac failure (ATS/ERS Joint Statement, 2000). This combination of abnormal haemodynamics, structural abnormalities and the deleterious effects of chronic hypoxia ultimately contribute to the premature fatality of individuals affected by pulmonary fibrosis. Thus far, no treatment modality with the possible exception of heart and lung transplantation has been shown to restore either the chronic respiratory or pulmonary circulatory dysfunction encountered in established pulmonary fibrosis.

1.3.v Pathologic ECM changes in the fibrotic lung

The normal alveolar interstitium is thin and contains an optimal composition of ECM elements distributed primarily in peribronchial and perivascular locations. The pulmonary matrix, once simply regarded as ground substance, is a complex and biologically active structure. It can bind, sequester and present growth mediators to a variety of cells involved in lung homeostasis. In addition, intact matrix proteins as well as proteolytic matrix fragments can initiate signal transduction pathways involved in normal and pathological lung repair. During fibrogenesis, the heightened synthesis and over-accumulation of ECM proteins, primarily fibrillar collagens, lead to characteristic anatomical changes. As most of this abnormal matrix becomes deposited in interstitial and paraseptal areas, expansion of the alveolar wall that results is often apparent even macroscopically. In many cases, intra-alveolar accumulation of collagen fibres also occurs (Kuhn III et al., 1989). Deposition of fibrotic matrix in this location arises because granulation tissue forms within damaged alveoli and expands to obliterate the airspaces it occupies. As a direct result, the denuded alveolar walls appose against each other to produce histological changes described as 'alveolar collapse-induration' (Burkhardt, 1989).

On the other hand, the accumulation and metabolism of non-fibrillar collagens in pulmonary fibrosis are less well characterised. In fibrotic lung disorders, distinctive changes in the alveolar basement membrane have been described, including fragmentation, abnormal folding and aggregation of amorphous matrix material in areas of damaged basal laminae (Raghu et al., 1985). Increased immunostaining of types IV and V collagen has been reported in areas of airspace fibrosis, an observation that suggests loss of basal lamina integrity to be an important element in pulmonary fibrogenesis (Madri and Furthmayr, 1980). Pathological studies have long indicated that a major pathway of interstitial fibrosis is organisation of a provisional matrix that appears in the alveolus as a consequence of alveolar wall injury. Formation of the provisional matrix may occur early. The appearance of intra-alveolar proteinaceous exudates in diffuse alveolar damage that accompanies the acute respiratory distress syndrome (ARDS), acute interstitial pneumonia (AIP) and some forms of severe infective pneumonia provides substrate for thrombin activation and fibrin formation that precede hyaline membrane deposition. The eventual transformation of this neo-matrix into a fibrotic scar is the result of re-epithelialisation, mesenchymal cell proliferation and incorporation into more permanent collagenised matrix.

Where fibrosis supervenes, the most discernible biochemical abnormality is an absolute increase in lung collagen content. Pulmonary collagen accumulation is the direct result of both enhanced protein synthesis and decreased degradation (Laurent and McAnulty, 1983; Selman et al., 1986). Changes in the relative abundance of many different collagen subtypes are recognised in lung fibrosi; a three to four-fold increase in the ratio of type I to III collagen has been widely quoted (Kirk et al., 1984). Of note, the ratio of type I to III collagen empirically correlates with different stages of fibrotic lung disease although the significance of this observation is not known (Kuhn III et al., 1989). It has also been suggested that increased type III collagen may precede elevations in type I collagen (Bateman et al., 1983). Indeed, in one early study of IPF, increased type I collagen was linked to the presence of late or established lung fibrosis while changes in type III collagen were noted earlier on in the disease (Seyer et al., 1976). In bleomycin-induced pulmonary fibrosis in rodents, increased expression of collagen type VI has also been shown to precede collagen type I (Specks et al., 1995).

In contrast to collagen, elastin turnover in pulmonary fibrosis has not been as widely studied. Despite its durability and limited turnover in the healthy adult lung, increased numbers of elastic fibres have been described in fibrotic lesions in resected specimens of lung affected by IPF (Basset et al., 1986). In addition, increased tropoelastin expression and elastic fibre number have been reported in lungs with silica-induced lung fibrosis although it is likely that these abnormal-appearing fibres are non-functional (Pierce et al., 1995). Similarly, although alterations in different proteoglycans have been described in pulmonary fibrosis, a detailed understanding of their turnover in fibrotic lung disease is far from established (Venkatesan et al., 2000). Regardless of the specific nature of the fibrotic process, wide-ranging changes in fibrotic ECM remodelling inevitably contribute to the increased stiffness and decreased compliance of the chronically scarred lung.

1.3.vi Therapeutic approaches to pulmonary fibrosis

Pulmonary fibrosis is incurable and available therapies offer limited symptomatic efficacy (Mason et al., 1999). In specific cases of secondary pulmonary fibrosis, treatment of the underlying disorder (e.g. rhematologic disease) or removal of the inciting agent (e.g. organic allergens or drugs) may be beneficial. For the most severe forms of the idiopathic interstitial pneumonias, including IPF and fibrotic variants of NSIP, available treatment options consist

entirely of immunosuppressive agents. In such patients, the institution of immune-modulating therapies, including steroids and cytotoxic agents, does not alter the course or prognosis of the disease (ATS/ERS Joint Statement, 2000). Over the years, a paucity of well-conducted placebo-controlled clinical trials has complicated attempts to optimise drug treatment strategies.

Although corticosteroids remain first line treatment agents for many newly diagnosed patients with IPF, an initial therapeutic response has been reported in only 10 - 30% of patients (ATS/ERS Joint Consensus Statement, 2000). However, many early reports came from uncontrolled studies and failed to account for the biologic variability of a disease in which there can be prolonged survival (up to 10 years) in 10% of patients. The adverse effects of prolonged high-dose steroid treatment commonly offset potential benefits associated with its use. In many cases, concomitant use of either azathioprine or cyclophosphamide is employed with limited success as a steroid-sparing strategy. Even so, current 'best' practice for newly diagnosed IPF consists of tapering dose corticosteroids in combination with azathioprine (ATS/ERS Joint Consensus Statement, 2000). Relapsed or accelerated disease is treated with either 'rescue' methyprednisolone and/or cyclophosphamide, although such strategy is often futile.

Up until now, anti-fibrotic strategies using newer anti-mitotic agents, proline analogues and immune-based therapies have also proved disappointing. However, preliminary analyses of several phase II / III trials have highlighted limited benefits in terms of lung function and increased exacerbation-free intervals. These agents include pirfenidone (Azuma et al., 2005), N-acetylcysteine or NAC (IFIGENIA: Idiopathic Pulmonary Fibrosis International Group Exploring NAC I Annual study; www.zambongroup.com) and bosentan, an endothelin-1 receptor antagonist (BUILD-1: Bosentan Use in Interstitial Lung Disease study; www.actelion.com). In addition, a multi-centre, prospective, double-blinded, placebo-controlled phase II trial of etanercept, a soluble TNF-α receptor-Fc fusion protein, in patients with IPF has been completed and await release.

In 1999, considerable interest was generated by the publication of a preliminary trial showing that IFN-γ had a potential therapeutic role in the treatment of steroid-resistant IPF (Ziesche et al., 1999). More specifically, the combination of IFN-γ and corticosteroids was associated with significantly improved lung function and oxygenation indices compared to steroid therapy alone. IFN-γ has previously been shown to suppress both fibroblast proliferation and production of matrix proteins *in vitro* (Narayanan et al., 1992; Gurujeyalakhsmi and Giri, 1995). A much larger

randomised, double-blinded, placebo-controlled trial subsequently failed to confirm the positive effects of IFN-γ reported in the preliminary study (Raghu et al., 2004). In fact, treatment with IFN-γ in steroid-resistant patients with IPF did not affect disease progression, lung function or the quality of life following diagnosis. Worryingly, several accounts of worsening respiratory failure have recently been reported in patients with severe IPF treated with this cytokine (Carvalho et al., 2004). Evaluation of another interferon, IFN-β has also failed to demonstrate therapeutic benefit in this devastating condition (Raghu et al., 2002).

1.3.vii Current concepts of the pathogenesis of pulmonary fibrosis

A central paradigm in the pathogenesis of chronic pulmonary fibrosis proposes that low level, albeit persistent, lung injury produces cycles of alveolar inflammation that prompt infiltrating as well as stimulated resident cells to release a range of soluble mediators. In turn, these factors individually or co-ordinately promote fibroblast activation, proliferation and extracellular matrix production. These processes in turn interact with other phenomena of tissue repair that contribute to the loss of homeostatic matrix regulation (figure 1.3). As a result, disproportionate accumulation of pulmonary connective tissue occurs, with its attendant effects on lung physiology (Chambers and Laurent, 1997).

Early hypotheses on the pathogenesis of pulmonary fibrosis focused on the role of unresolved inflammation as a stimulus for lung injury and subsequent fibrosis. This concept was supported by the observation of abundant inflammatory cells within damaged alveoli and pulmonary interstitium, as well as the increased expression of pro-inflammatory mediators such as interleukin-1β, tumour necrosis factor-α and transforming growth factor-β (Keane and Strieter, 2002). In addition, an imbalance in the expression of T-helper type 1 and type 2 cytokines has also been implicated in the development of pulmonary fibrosis.

However, it has recently been acknowledged that early and repeated epithelial cell stimulation and damage, as well as abnormal interactions with inflammatory and mesenchymal cells, may represent focal points in pulmonary fibrogenesis (Selman, 2000; Gauldie, 2002). This latest theory has emerged because fibrotic lung remodelling persists in many clinical and experimental situations despite the apparent resolution or paucity of pulmonary inflammation. Even so, while aberrant re-epithelialisation may be pivotal to pulmonary fibrosis, the cardinal event remains an

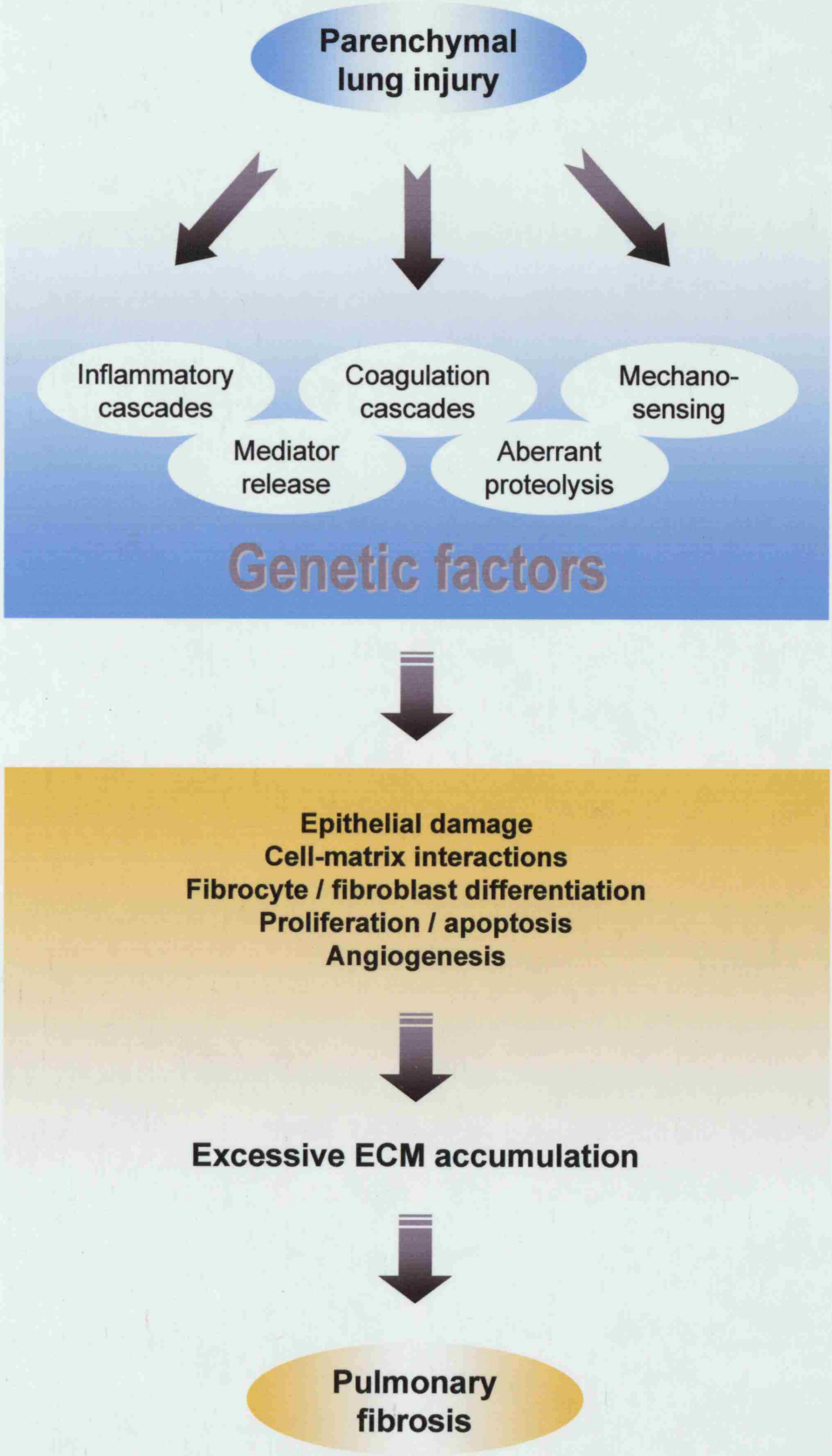

Figure 1.3. Changes in multiple pathways link the progression of lung injury to the excessive accumulation of extracellular matrix that characterises pulmonary fibrosis.

abnormal tissue response to wound healing. Understandably, the hypothesis that disturbed epithelial cell behaviour can drive regenerating lung tissue to resolve as thickened scars amid an exuberant fibrotic reaction has become the subject of intense investigation (Chapman, 2004).

Crucial to the development and maturation of the pulmonary fibrotic response is the secretion of mediators that promote haemostasis, angiogenesis, matrix synthesis and function. Although certain features of tissue repair during lung fibrosis appear at first glance to recapitulate some aspects of lung development, the fibrotic response differs from lung morphogenesis in important respects. In pulmonary fibrosis, the controls that normally govern connective tissue production, assembly and organisation are lost. In addition, although candidate mediators may be identifiable, the triggers responsible for their secretion are not often readily apparent.

1.3.viii Fibrogenic factors implicated in lung remodelling

The number of profibrotic mediators implicated in the pathogenesis of pulmonary fibrosis is large. Among the best-known examples are tumour necrosis factor-alpha (TNF-α), isoforms of platelet-derived growth factor (PDGF), interleukins-1 (IL-1), -4 (IL-4) and -13 (IL-13) and transforming growth factor-beta (TGF-β). TNF-α and PDGF are potent inducers of fibroblast proliferation *in vitro* whose fibrogenic activity appears to be mediated by TGF-β-dependent pathways (Zhang and Phan, 1996). When monitored prospectively over months, mice that overexpress pulmonary TNF-α consistently develop age-related lung fibrosis (Sime et al., 1998). In contrast, TNF-α-deficient or double TNF-α-receptor knockout mice are protected from bleomycin-induced pulmonary fibrosis (Ortiz et al., 1999). Both adenoviral-mediated expression of PDGF-B and exogenously administered recombinant PDGF-BB have been shown to induce pulmonary fibrosis (Yoshida et al., 1995). The expression of PDGF and its receptor (PDGF-R) is also upregulated in the lungs of patients with established IPF (Homma et al., 1995). However, the ability of either TNF-α or PDGF to directly promote collagen production is still not well characterised.

Transient overexpression of IL-1β produces marked lung inflammation and tissue damage that leads to chronic fibrotic lesions (Kolb et al., 2001a). In addition, pulmonary overexpression of GM-CSF (granulocyte-monocyte colony stimulating factor) also produces moderate lung

inflammation and fibrosis in a mechanism that involves increased TGF-β protein expression (Xing et al., 1997). IL-4 and IL-13 are pleiotropic Th-2-derived cytokines that exert profibrotic effects on a number of tissues. Lungs from IPF patients have sustained IL-4 production (Wallace et al., 1995) and very recently, IL-4-deficient mice have been reported to resist bleomycin-induced pulmonary fibrosis (Huaux et al., 2003). Likewise, IL-13-overexpressing mice have been shown to develop spontaneous pulmonary fibrosis (Lee et al., 2001). The finding that alveolar epithelial cells are a source of many of these cytokines is consistent with the hypothesis that these mediators play key roles in modulating aberrant epithelial-mesenchymal interactions within the repairing lung.

However, the best evidence of fibrogenic potential in terms of individual mediators is that for TGF-β. Data from a wide range of experimental models, including the commonly used bleomycin model, have implied a link between increased levels of TGF-β and an enhanced susceptibility to pulmonary fibrosis (reviewed in Thrall and Scalise, 1995; Johnston et al., 1995). Several important lines of evidence support a causal role for active TGF-β as a profibrotic mediator. First, the *in vivo* events that underlie excessive matrix accumulation such as increased fibroblast proliferation, differentiation and ECM synthesis have been reproduced by incubating pulmonary fibroblasts with TGF-β (Raghu et al., 1989; Torry et al., 1994). Second, neutralisation of TGF-β activity or blockade of its signaling, either at the receptor level or intracellularly, inhibits or at least attenuates the development of pulmonary fibrosis in susceptible animals (Giri et al., 1993; Wang et al., 1999; Nakao et al., 1999; Kolb et al., 2001b). Third, *in vivo* transfection of a constitutively active form of the TGF-β gene into the lungs of rodents is sufficient to induce severe and prolonged pulmonary fibrosis (Sime et al., 1997), even in TNF-α receptor knockout mice (Liu et al., 2001).

In humans, immunohistochemical studies have shown that TGF-β expression is increased in a number of cell types, including alveolar macrophages in early fibrotic lesions, and type II alveolar epithelial as well as mesenchymal cells in advanced honeycombed lungs in IPF (Khalil et al., 1991; Khalil et al., 1996b). However, such descriptive studies have failed to directly link the increased presence of TGF-β to either the extent of pulmonary fibrosis or clinical outcome. A number of studies have focused on the functional consequences of certain TGF-β gene polymorphisms in fibrotic lung disease. El-Gamel and colleagues reported two polymorphisms (leucine → proline at codon 10, and arginine → proline at codon 25) in the TGF-β1 leader sequence in a cohort of patients with mixed fibrotic lung pathology undergoing transplantation

(El-Gamel et al., 1999). Of the two polymorphisms, homogygosity for arginine at codon 25 was commoner amongst patients with pre-existing lung fibrosis (either IPF, cystic fibrosis or bronchiectasis), and correlated with an increased risk for post-transplant allograft fibrosis. Of note, the codon 25 arginine allele has previously been linked to increased TGF-β1 production by cells *in vitro* (Awad et al., 1998).

More recently, Xaubet and colleagues reported an association between the codon 10 proline allele and accelerated physiological deterioration in more than a hundred patients with IPF (Xaubet et al., 2003). However, a link between this polymorphism and increased disease susceptibility was not established. Based on protein structure, it had previously been predicted that the leucine to proline substitution at codon 10 might alter TGF-β secretion (Awad et al., 1998). The same polymorphism has also been associated with chronic hepatitis C-induced liver fibrosis (Gewaltig et al., 2002). Interestingly, in an earlier study of osteoporosis in Japanese women, higher levels of serum TGF-β1 had been quantified in subjects carrying the same homozygous codon 10 proline/proline genotype (Yamada et al., 1998). In the Xaubet study, however, blood TGF-β protein levels were not assessed so its functional relevance in IPF remains uncertain.

Insights from the bleomycin model have confirmed that blocking the generation of active TGF-β *in vivo* confers protection against pulmonary fibrosis. Experiments in rats have shown that plasmin can enhance the activation of macrophage-secreted TGF-β in the presence of thrombospondin-1 (TSP-1) and its cell surface receptor, CD36 (Khalil et al, 1996). Disruption of this reaction using a synthetic CD36 blocking peptide inhibited TGF-β activation and abrogated the development of pulmonary fibrosis (Yehualaeshet et al., 1999). In addition, mice lacking αvβ6, an epithelial-restricted integrin, develop intense bleomycin-induced lung inflammation but are protected from bleomycin-induced pulmonary fibrosis (Munger et al., 1999). αvβ6 has been shown to act as a ligand for LAP, an interaction that induces conformational changes in the latent TGF-β complex, allowing active TGF-β to bind to its receptors. These observations provide compelling evidence that TGF-β activation is critical to the development of fibrosis.

1.3.ix Animal models of pulmonary fibrosis

A number of methods have been used to induce experimental pulmonary fibrosis. However, no single approach has managed to comprehensively mimic the human disease in all its complexity. In rats, the inhalation of inorganic asbestos fibres produces granulomatous reactions composed predominantly of macrophages and histiocytes that mature into more uniform fibrotic lesions (reviewed in Lemaire, 1995). Both rodents and larger animals have been used to reproduce the fibrotic lesions induced by silica (Reiser et al., 1983). In all species, the magnitude of pulmonary asbestosis and silicosis appear to depend on the amount and method of fibre inoculation. While the use of such crystalline particles may produce specific forms of pulmonary fibrosis (e.g. silica-induced silicosis), some characteristics of the fibrotic response may be dissimilar to that induced by other more 'acute' agents. Additionally, in studies of rodents exposed to these particles, the degree of fibrotic response may be variable, just as it is in populations of occupationally exposed individuals.

In other studies, thoracic irradiation has also been employed to recapitulate certain aspects of human pulmonary fibrosis (reviewed in Pickrell and Abdel-Mageed, 1995). Ionising radiation generates free radicals which can irreversibly damage DNA leading to subsequent pulmonary inflammation and interstitial fibrosis. Other less commonly used techniques include the instillation of paraquat (Schoenberger et al., 1984), fluorescein isothiocyanate (Christensen et al., 1999) and vanadium pentoxide, an inorganic metal dust (Bonner et al., 1998). Lastly, ozone (O_3) and nitrogen dioxide (NO_2) are environmental pollutants that have been used experimental to induce pulmonary fibrosis in rodents after prolonged direct exposure (Last et al., 1993).

Parenteral administration of bleomycin, a chemotherapeutic agent derived from the *Streptomyces verticillus* mould, consistently produces pulmonary alveolitis that leads to fibrosis in a number of animal species (reviewed in Thrall and Scalise, 1995). Bleomycin is cytotoxic; when administered intratracheally, its actions primarily affect bronchial epithelial cells and alveolar pneumocytes (Hay et al., 1991). The nature and extent of bleomycin-induced lung fibrosis is determined by the route of administration and the dose of drug delivered. Intratracheal administration of bleomycin typically induces fibrosis in peribronchial and focal parenchymal locations, in contrast to subpleural disease following systemic (intravenous or intraperitoneal) routes. While fibrotic lesions resulting from a single dose of bleomycin may be patchily distributed, continuous

administration of the same drug can produce progressive changes involving larger areas of lung (Harrison and Lazo, 1987).

Regardless of administration route, bleomycin-induced lung injury typically begins as an acute neutrophil-rich alveolitis with accompanying alveolar oedema. Both parameters tend to intensify over the first few days following treatment. As the inflammatory response gradually subsides over the ensuing weeks, signs of provisional tissue repair such as epithelial cell hyperplasia and fibrin organisation, become more prominent (Laurent et al., 1981). By the third week of bleomycin exposure, increased collagen synthesis and deposition are usually evident. Over time, even as the initial signals for matrix production recede, the damaged lung may remain irreversibly scarred. In some cases, however, unaffected airspaces may coalesce to produce a mixed histological appearance of interstitial fibrosis and alveolar airspace enlargement (Borzone, 2001).

More recent models of pulmonary fibrosis have included the intra-pulmonary delivery of mediator genes that encode cytokines such as TGF-β, IL-1, GM-CSF and TNF-α in rodents (Gauldie et al., 2002). The use of viral and non-viral delivery vectors to efficiently transduce the expression of peptide growth factors allows in-depth analyses of specific molecular pathways to be undertaken. However, in some circles, the generation of supraphysiologic levels of these mediators has raised concerns that more subtle changes in the tissue response may be masked as a result. One common finding in these models is the dependence of the eventual lung repair process on TGF-β-mediated fibroproliferation (Table 1.4).

TABLE 1.4 EFFECT OF ADENOVIRAL TRANSFER OF PROFIBROTIC MEDIATORS TO RODENT LUNG

Delivered mediator	Myofibroblast number	Extent of fibrosis	TGF-β dependence
TGF-β	++++	++++	Yes
IL-1β	+++	++++	Yes
TNF-α	++	+	Yes
GM-CSF	++	++	Yes

(adapted from Gauldie et al., 2001)

1.4 Transforming growth factor-beta (TGF-β)

1.4.i Structure and assembly of the TGF-β complex

TGF-β is a multifunctional protein originally defined by its ability to induce anchorage-independent growth of kidney fibroblasts in soft agar (Roberts et al., 1981; Moses et al., 1981). It belongs to the wider TGF-β superfamily of growth and differentiation factors that also includes Mullerian inhibitory substance, decapentaplegic proteins, activins, inhibins and bone morphogenetic proteins (BMPs) (Massague, 1990). TGF-β is a key regulator of cell growth, differentiation and function, three fundamental processes that mediate its wider influence on haematopoiesis, morphogenesis, immunity, wound repair and tumorigenesis (Massague 1990). Its importance to normal embryonic, foetal and adult organ development is well described. In particular, its role in balancing the production, organisation and degradation of connective tissue in organ homeostasis is widely appreciated (Lyons and Moses, 1990; Blobe et al., 2000).

TGF-β exists in at least five different isoforms. Three of these isoforms (TGF-β1, -β2 and -β3) have been identified in mammals (Massague, 1998). Mammalian TGF-β isoforms are structurally related and share some 80 to 90% sequence homology (Grande, 1997). Of these, TGF-β1 is the most abundant and best characterised. From gene knockout studies, it has been shown that all three TGF-β isoforms are essential for survival. Disruption of the corresponding genes results in either embryonic or perinatal lethality (Mummery, 2001).

Precursor TGF-β molecules are formed as large peptides containing between 390 – 412 amino acids. Early on in the synthesis process, the precursor TGF-β gene product is proteolytically cleaved by a furin-type endopeptidase at an RRK[KA][RKL] sequence located between amino acids 278 and 279 while still contained within the trans-Golgi apparatus (Dubois et al., 1995). This reaction yields two components, a 25 kDa homodimeric peptide ('mature' TGF-β) from the C-terminus and a 65 – 75 kDa propeptide known as the latency-associated peptide (LAP) belonging to the original N-terminus. The TGF-β monomers dimerise by a single disulphide bridge while two disulphide bridges are formed between the larger LAP monomers (Gentry et

al., 1988). The presence of the LAP moiety facilitates the secretion of the entire heterodimer from the cell and confers latency to it.

The three-dimensional structures of TGF-β1, -β2 and -β3 have been determined. TGF-βs are composed mainly of β-strands although an α-helix and a β-sheet interact between the monomers to form a hydrophobic core. All TGF-β isoforms contain four internal disulphide bridges as well as a disulphide link between the monomers (Archer et al., 1993; Mittl et al., 1996). In addition, the final TGF-β monodimer is stabilised by a number of hydrogen bonds.The LAP portion of the TGF-β molecule is predicted to be rich in β-strands (McMahon et al., 1996).

Most cultured cells secrete latent TGF-β as a large latent complex comprised of the LAP-TGF-β dimer and an additional 120-240 kDa glycoprotein called latent TGF-β binding protein (LTBP). Four LTBPs (LTBP-1, LTBP-2, LTBP-3 and LTBP-4) have been described. All belong to the LTBP/fibrillin superfamily. Members of this family are distinguished by the presence of tandemly repeating epidermal growth factor-like domains in the center of the molecule and a variable number of unique 8-cysteine motifs (Kanzaki et al., 1990). In LTBPs, the third of four 8-cysteine motifs residing in the carboxy terminus interacts directly with LAP through disulphide covalent linking to form the large latent complex (Saharinen and Keski-Oja, 2000). During the production of TGF-β, LTBP is required to direct the processing and secretion of TGF-β from cells (Miyazono et al., 1991). Abnormalities in LTBP at this stage results in the improper folding of the small latent complex and its retention within the *cis*-aspect of the Golgi apparatus (Miyazono et al., 1991). In some cases, the expression of LTBP-1 has been found to be co-regulated with that of TGF-β1 (Taipale et al., 1994). Once extruded from the cell, the role of LTBP is critical for targeting the latent TGF-β complex to the extracellular matrix (Taipale et al., 1994; Koli et al., 2001). Indeed, the amino terminal of LTBP is covalently cross-linked to components of the ECM by a tissue transglutaminase (Nunes et al., 1997). Thus far, only LTBP-1, -3 and -4 have been shown to form covalent bonds with TGF-β (Saharinen and Keski-Oja, 2000).

1.4.ii Cellular sources of TGF-β

The majority of cultured cells studied to date produce TGF-β in a latent form that requires post-translational modification to acquire biological activity (Lyons et al., 1990). These include chinese hamster ovary (CHO) cells, chicken embryonic fibroblasts (Lawrence et al., 1984) and bovine aortic endothelial cells (Schultz-Cherry et al., 1995). In addition, solubilised latent TGF-β complexes have been detected in the culture media of many other cell types, including murine calvarial bone osteoblasts (Bonewald et al., 1991), BSC-40 monkey kidney cells (Lioubin et al., 1991), human erythroleukaemic (HEL) cells (Miyazono et al., 1991) and bovine endothelial cells in monoculture (Flaumenhaft et al., 1992). Rat osteoblast cell lines have been shown to secrete small latent TGF-β complexes that lack the LTBP moiety and are thus unable to target TGF-β to the extracellular matrix in repairing bone (Dallas et al., 1994). Only a few primary cells and established cell lines have been known to secrete active TGF-β. These include cultured BSC-1 African green monkey kidney cells (Tucker et al., 1984), Kato III cells (Horimoto et al., 1994) and certain human glioblastoma cell lines (Olofsson et al., 1992).

Platelets have long been known to be an important and probably the major source of TGF-β in serum (Assoian et al., 1983). TGF-β released from α-granules during platelet degranulation has been purified and shown to be similar to TGF-β released by cultured cells (Wakefield et al., 1988). In the lung, cellular souces of TGF-β include inflammatory cells such as macrophages (Khalil et al., 1996a) and neutrophils (Grotendorst et al., 1989), type II alveolar epithelial cells (Xu et al., 2003) and mesenchymal cells including fibroblasts (Kelley et al., 1991).

1.4.iii Biological functions of TGF-β in the lung

TGF-β demonstrates regulatory effects on a wide range of cell types. It can function either as an agonist or antagonist of inflammatory cell regulation and growth. TGF-β is a potent chemoattractant and mitogen for mesenchymal cells involved in the fibroproliferative response (Blobe et al., 2000). In the pulmonary interstitium, these cells are predominantly fibroblasts and myofibroblasts. TGF-β can also elicit a number of negative growth responses in epithelial and endothelial cells. As a result, numerous studies have focused on the important autocrine tumour-

suppressing properties of this cytokine. The anti-proliferative effect of TGF-β on cultured mink lung epithelial cells occurs via the induction of G1 cell cycle arrest via the prevention of active cyclin E-cdk2 complex formation (Koff et al., 1993). TGF-β is also a potent inducer of apoptosis of epithelia and blood cells (Perlman et al., 2001). Its expression is frequently elevated when tissue growth is perturbed which makes it one of the most important molecular regulators of tissue homeostasis (Cui et al., 1995).

TGF-β is a critical mediator of fibrogenesis. It exerts direct and indirect effects on extracellular matrix production, fibroblast chemoattraction, proliferation and transformation into myofibroblasts. Numerous studies in both animals and humans support a key role for TGF-β in pulmonary fibroproliferation *in vivo*. Its effects on matrix accumulation not only affect interstitial fibroblasts but also airway mesenchymal cells, alveolar epithelial cells and infiltrating leukocytes such as macrophages (Bienkowski and Gotkin, 1995; Coker et al., 1997; Eickelberg et al., 1999).

TGF-β is a uniquely strong promoter of ECM synthesis, particularly of collagen production and accumulation (Ignotz and Massague, 1986; Pentinnen et al., 1988). Its effects on collagen synthesis result from a combination of increased collagen gene transcription, enhanced mRNA stability and decreased degradation of procollagen molecules (reviewed in Cutroneo, 2003). TGF-β-mediated transcription of type I procollagen genes, proα1(I) and proα2(I) involves two different but interacting signaling pathways (reviewed in Cutroneo, 2003). Proα1(I) expression is controlled by the TGF-β activator protein signaling pathway while Proα2(I) expression comes under the domain of the Smad signaling pathway. The outcome of this relationship is the strict synthesis of the two collagen pro-polypeptides (proα1 and proα2) in a 2 : 1 ratio. Along with collagen production, TGF-β also increases fibroblast levels of heat shock protein-47, a procollagen-specific molecular chaperon (Sasaki et al., 2002). This action increases the efficiency of procollagen processing and enhances deposition of stable procollagen molecules into the extracellular milieu.

TGF-β also can enhance the expression of elastin and various early matrix proteins, including tenascin, fibronectin, vitronectin and a number of different proteoglycans (Saharinen et al., 1999). The half-life of the tropoelastin molecule is increased by TGF-β (McGowan et al., 1997). Gene expression of fibronectin and both subunits of the fibronectin receptor in human lung

fibroblasts (Roberts et al., 1988) as well as chondroitin / dermatan sulfate proteoglycans (Bassols and Massague, 1988) are stimulated by the action of TGF-β.

In addition to its direct synthetic effects on the ECM, TGF-β also decreases the proteolytic activity of cells by suppressing the expression and secretion of a number of proteinases including interstitial collagenase and plasmin (Kerr et al., 1990; Laiho and Keski-Oja, 1992). It upregulates the production of tissue inhibitors of metalloproteinases (TIMPs) and plasminogen activator inhibitor-1 (PAI-1), thus tipping the overall balance in matrix turnover towards net accumulation (Wright et al., 1991). Its ability to regulate the expression of matrix receptors including integrins may reveal novel aspects of extracellular matrix remodelling.

1.4.iv The TGF-β signal transduction pathway

'Outside-in' TGF-β signal transmission occurs via serine/threonine kinase receptors consisting of two closely interacting proteins known as type I and type II TGF-β receptors (TβRI and TβRII) (reviewed in Shi and Massague, 2003). TGF-β ligand binding induces the association of these receptors leading to a unidirectional event in which TβRII phosphorylates TβRI to activate it. In turn, the latter signals to the Smad family of intracellular mediators, specifically the receptor-regulated, or R-Smads. Smad-2 is the prototypic member of this group (Smad-3 being the other) and provides a critical link with more downstream signaling events. During the signal transduction process, R-Smads are directly phosphorylated by TβRI on two conserved serine residues. Phosphorylated R-Smads then form heterodimers with the next component of the signaling cascade, Smad-4.

Following association with Smad-4, the Smad complex translocates to the cell nucleus and is then able to bind to one of many DNA-binding partners (including transcriptional co-activators and co-repressors) to either positively or negatively regulate gene expression. An additional group of Smads, the inhibitory Smads (Smad-6 and -7) counteracts the affects of the R-Smads to block Smad-mediated TGF-β signaling (reviewed in Attisano and Wrana, 2002). Termination of Smad signaling is less well understood. It might be achieved by dephosphorylation via as yet unidentified phosphatases or by ubiquitination and proteasome-mediated degradation of activated R-Smads (Randall et al., 2002).

The delivery of active TGF-β to its receptor is enhanced by the action of various proteoglycans that do not actually participate in the signal transduction process. The best characterised of these are glypicans, small glycoproteins containing heparan sulfate glycosaminoglycan (GAG) sidechains linked to the extracellular membrane by a glycosylphosphatidyl inositol anchor (Cheifetz et al., 1988). Acting as chaperone proteins, glypicans reversibly bind TGF-β and deliver it to the TβRII/TβRI complex where it can interact with the receptor complex to initiate intracellular signaling (De Crescenzo et al., 2001). Similarly, the recognition of R-Smads by the TGF-β receptor complex is both facilitated and enhanced by a number of auxiliary proteins. For example, Smad-2 and Smad-3 are recruited to the cell membrane surface and immobilised there by the SARA (Smad anchor for receptor activation) molecule (Tsukazaki et al., 1998).

However, Smad-independent pathways of TGF-β signaling also exist. Acting via TAK1 (transforming growth factor β-activated kinase 1), TGF-β can activate MAPK (mitogen activated protein kinase)-associated signaling pathways which include the signaling molecules ERK (extracellular signal-regulated kinase), p38 and JNK (Jun N-terminal kinase) (Chen et al., 1993). These pathways mediate the effects of TGF-β on the expression of several 'early gene' products such as c-Jun, Jun B and c-Fos. Moreover, TGF-β exerts variable effects on c-Myc expression via Smad-dependent interactions with its p15 promoter. Myc can bind to a Myc-interating zinc-finger transcription factor, Miz-1, to block the expression of a cell cycle inhibitory protein, p15(INK4b) (Seoane et al., 2001). However, TGF-β is able to prevent recruitment of Myc to the p15(INK4b) transcriptional initiator by Miz-1, with the net effect of relieving gene repression, thereby unblocking Myc-dependent arrest of cell cycle events. This is one example of molecular manipulation by TGF-β to modulate cellular responses to changes in the external cellular environment (Orian and Eisenmann, 2001). In fibroblasts, factor(s) that bind at the TGF-β1 control element within the c-Myc promoter increases the expression of this gene (Kim et al., 1993). Furthermore, TGF-β is able to rapidly activate Rho family guanosine triphosphatases (GTPases) and protein kinase B (PKB, synonymous with Akt) (reviewed in Attisano and Wrana, 2002).

The apparent simplicity of the TGF-β signaling pathway sharply contrasts with the diversity of cell-specific gene responses that it triggers. Even within the relatively small area of matrix remodelling following lung injury, this cascade exerts a very broad influence on fundamental

processes that regulate ECM turnover and organ function. However, in order to have any bearing at all on tissue remodelling, TGF-β must first be available in its active conformation for any of its ligand binding actions to be biologically relevant.

1.4.v Mechanisms of TGF-β activation

TGF-β is secreted almost exclusively as a latent molecule. Biological activity is only gained when the mature TGF-β homodimer is separated from the LAP dimer so that it can interact with its high affinity surface receptor (Gleizes et al., 1997; Ribeiro et al., 1999). The presence of TGF-β receptors on most cell types (Tucker et al., 1984) and the ubiquitous nature of the TGF-β molecule itself suggest that the activation of latent TGF-β must form an integral part in any biological processes regulated by this growth factor.

Cultured cells do not normally secrete active TGF-β or activate significant amounts of latent TGF-β. Only a few primary or established cell lines have been found to secrete active TGF-β in their conditioned media (Koli et al., 2001). However, a variety of physicochemical conditions have been shown to promote TGF-β activation *in vitro* including heat, detergents, extremes of pH, urea and enzymatic processing (Brown et al., 1990) (Table 1.5). Of these, proteolysis has been the most extensively studied. Plasmin is the archetypal proteinase that is able to proteolytically separate the LAP component from the mature TGF-β molecule in order to effect activation (Lyons et al., 1990; Sato et al., 1990). In some studies, the TGF-β activating potential of plasmin has been demonstrated in the presence of urokinase-type and tissue-type plasminogen activators (Nunes et al., 1995).

Plasmin-mediated TGF-β activation has been documented in cell-free conditions (Lyons et al., 1988; Lyons et al., 1990), in monocultures of endothelial cells (Flaumenhaft et al., 1992) and in co-culture systems comprising bovine endothelial cells and smooth muscle pericytes (Antonelli-Orlidge et al., 1989; Sato et al., 1990). In the last, endogenous activation of TGF-β is dependent upon the binding of mannose-6-phosphate (M6P) residues on LAP with insulin growth factor-like-II receptors (M6P/IGF-IIR) expressed on the surface of pericytes (Dennis and Rifkin, 1991). Using the same co-culture system, LTBP-1 has also been shown to participate in the activation process since the presence of anti-LTBP-1 antibodies prevents the detection of active

TGF-β (Nunes et al., 1997). It is now known that the interaction between LTBP with the extracellular matrix requires cross-linking enzymatic activity of a tissue transglutaminase (tTg). This observation provides proof that mechanisms exist to concentrate latent TGF-β complexes in the extracellular matrix.

TABLE 1.5 **CONDITIONS / MECHANISMS OF TGF-β ACTIVATION**

	In vitro	*Cell culture*	*In vivo*
Non-proteolytic	heat	EC / pericyte co-culture	radiation
	pH extremes	TSP-1	TSP-1
	detergents		IL-13 / MMP-9
	chaotropes		αvβ6
	radiation		
	TSP-1		
	deglycosylation		
	sialic acid / MP6		
Proteolytic	plasmin / uPA	plasmin / uPA	plasmin
	cathepsin B	MMP-2 / MMP-9	
	cathepsin D	calpain	
		MT1-MMP-αvβ8	

EC endothelial cell; TSP-1, thrombospondin-1; M6P, mannose-6-phosphate

Plasmin has also been shown to liberate and activate latent TGF-β complexes from extracellular matrices assembled by cultured fibroblasts and epithelial cells (Taipale et al., 1992; Taipale et al., 1995). Other examples implicating the plasminogen/plasmin system in TGF-β activation include an *in vivo* role for surface-bound uPA on peritoneal macrophages (Nunes et al., 1995) and the prominence of the CD36/plasmin system localised on the surface of activated rat alveolar macrophages isolated from bleomycin-treated rats (Yehualaeshet et al., 1999).

Other proteinases have been implicated in TGF-β activation. The gastric cancer Kato III cell line has been reported to activate secreted latent TGF-β1 in conditioned media by utilising a serine proteinase other than plasmin (Horimoto et al., 1995). Abe and co-workers have reported that calpain is capable of activating latent TGF-β (Abe et al., 1998) while subtilisin-like endoproteinases (Chu and Kawinski, 1998), thrombin (Benezra et al., 1993), cathepsins (Lyons et al., 1988) as well as matrix metalloproteinases MMP-2 and MMP-9 have also been shown to possess similar capabilities (Yu and Stamenkovic, 2000).

In contrast, the physiologic regulation of TGF-β activation is less well understood. Inevitably, *in vitro* findings have been extrapolated to suggest that plasmin, increased acidity and even reactive oxygen species may participate in TGF-β activation *in vivo* (Grainger et al., 1994; Barcellos-Hoff and Dix, 1996). However, these mechanisms are only thought to function in very restricted situations such as within lysosomal granules or peri-osteoclastic environments (Lawrence, 1996). Although the greatest potential relevance of proteolytic regulation of TGF-β activation has been assigned to plasmin-mediated mechanisms, their perceived importance *in vivo* is not supported by findings from murine genetic studies. The observation that mice lacking plasminogen or its endogenous activators, urokinase plasminogen activator (uPA) or tissue plasminogen activator (tPA), do not succumb to the adverse autoimmunity or premature death that affect TGF-β-null animals suggests that there must be other mechanisms that can activate TGF-β in the absence of plasmin. In addition, data from *in vitro* studies have shown that even high concentrations of plasmin may be insufficient to release active TGF-β from all the latent complexes (Lyons et al., 1988; Taipale et al., 1995). The high concentration of plasmin inhibitors in plasma also would restrict its functionality as the sole TGF-β activator (Flaumenhaft et al., 1992).

Increased local expression of thrombospondin-1 (TSP-1) due to platelet degranulation has been shown to play a role in wound healing processes (Reed et al., 1995). TSP-1 is a large, trimeric protein produced by many cell types. TSP-1 null mice have widespread visceral abnormalities and delayed dermal repair, the latter associated with a concomitant decrease in wound-associated TGF-β activity (Murphy-Ullrich and Poczatek, 2000). However, administration of the KRFK synthetic peptide to mimic the TGF-β binding site on TSP-1 stimulates TGF-β activation and restores the wild type wound phenotype. The same reaction, inhibition of TGF-β activation, can be prevented by anti-LAP antibodies (Schultz-Cherry et al., 1994). TSP-1 appears to play an important role in several cell-associated mechanisms of TGF-β activation, namely the

CD36/TSP-1 system on stimulated macrophages (Khalil et al, 1996), TSP-1-LAP interactions in a variety of organs (Crawford et al., 1998) and a metalloproteinase-dependent TSP-1 mediated mechanism on erythrocytes infected with *plasmodium falciparum* parasites (Omer et al., 2003). One hypothetical scenario might involve the initial removal of latent TGF-β complexes from the matrix by proteolysis and the delivery of such complexes to cell surfaces for activation by TSP-1. Interestingly, TSP-1-deficient mice display many phenotypic similarities to those present in TGF-β-deficient pups (Crawford et al., 1998).

The role of integrin-mediated TGF-β activation is gaining increasing appreciation. The LAP portions of TGF-β1 and β3 contain RGD motifs that are recognised by a number of integrins including αvβ6. In humans, increased αvβ6 expression has been detected in the airways of smokers and individuals with fibrosing alveolitis (Weinacker et al., 1995). *In vitro* studies have shown that the binding of αvβ6 to LAP in injured epithelial cells leads to the activation of latent TGF-β. This mechanism has been proposed to account for the protection of β6 integrin deficient mice against bleomycin-induced pulmonary fibrosis (Munger et al., 1999). In addition to resistance against fibrosis, these animals also have increased pulmonary inflammation, another process that comes under the regulation of TGF-β. Under normal conditions, the expression of αvβ6 is prominent in terminally differentiated epithelial cells in the lung, skin and kidneys during organogenesis in mice. However, this expression is turned off in normal adult cells, only to re-emerge following wounding of adult dermal and lung epithelia. Beyond αvβ6, other integrins such as αvβ1, αvβ5 and αvβ8 have also been shown to bind to LAP (Ludbrook et al., 2003). The αvβ8 interaction with LAP-β1 results in membrane type 1 (MT1)-MMP-dependent activation of TGF-β at the cell surface, a process that precedes cell growth and extracellular matrix production (Mu et al., 2002). LAP-β3 also possesses similar RGD sequences, and perhaps not surprisingly, αvβ6 has been shown to activate latent TGF-β3 *in vitro* (Annes et al., 2002). However, the ability of other integrins to LAP-TGF-β processing has yet to be elucidated.

Like the integrin-mediated syatems, the interaction of MMP-9 with its docking receptor, CD44, on transformed keratinocytes also provides an example of cell-based TGF-β activation (Yu and Stamenkovic, 2000). Together, these reports argue for the importance of multiple and co-existing pathways of TGF-β activation, and particularly, the relevance of tissue-specific and cell-specific proteolytic mechanism.

1.4.vi Post-translational regulation of TGF-β activity

In addition to the association of active TGF-β with LAP, several arrangements exist to ensure that TGF-β activation is controlled homeostatically to prevent adverse effects. Circulating (free) TGF-β in its active conformation is rapidly bound by α2-macroglobulin and cleared by an efficient scavenging system centred in the liver (O'Connor-McCourt and Wakefield, 1987). A potential negative feedback loop to keep levels of active TGF-β in check has been inferred from studies showing that TGF-β itself can stimulate the expression of α2-macroglobulin in adrenocortical cells (Shi et al., 1990).

Endogenous proteoglycans antagonists also exist to limit TGF-β activity in the extracellular matrix. Decorin is a ubiquitous leucine-rich proteoglycans that has two binding sites which recognise active TGF-β (Yamaguchi et al., 1990). It binds and sequesters biologically active TGF-β in both inter- and extracellular matrices, thus preventing TGF-β from stimulating cell surface TGF-βRII and I receptors. Transgene expression of decorin in the mouse lung has been shown to reduce the extent of pulmonary fibrosis following bleomycin administration (Kolb et al., 2001b). Biglycan and fibromodulin are similar proteoglycans that can interfere with TGF-β activity *in vitro* but have not been shown to exhibit similar properties *in vivo* (Hildebrand et al., 1994; Kolb et al., 2001c).

1.4.vii Identification of TGF-β in human forms of pulmonary fibrosis

Over the years, considerable evidence has been amassed to implicate TGF-β in the pathogenesis of human pulmonary fibrosis (Crouch, 1990; Bienkowski and Gotkin, 1995). Increased TGF-β expression has been reported in the lungs of patients with diverse forms of pulmonary fibrosis including IPF, pulmonary fibrosis associated with connective tissue disorders, occupational hazards and thoracic irradiation and sarcoidosis (Broekelmann et al., 1991; Corrin et al., 1994; Salez et al., 1998). In the fibrotic lung, the distribution of TGF-β may be altered in two main ways; its abundance in locations where it is normally found may increase, and its presence may be detected in unusual sites. For example, TGF-β overexpression has been localised to areas of mature fibrosis as well as peri-lesional parenchyma in the lungs of patients

with established IPF (Broekelmann et al., 1991; Border and Noble, 1994). Interstitial cells and areas of honeycombing in fibrotic lungs have been shown to contain altered expression of TGF-β receptors and increased LTBP-1 (Khalil et al., 2001). Furthermore, increased TGF-β levels have been identified within a variety of inflammatory and resident lung cells (Khalil et al., 1989; Khalil et al., 1996). Lung and dermal fibroblasts from patients with scleroderma complicated by pulmonary fibrosis differ functionally from normal fibroblasts. For instance, fibroblasts derived from scleroderma-affected skin overexpress TGF-β receptors and produce greater quantities of collagen and other ECM macromolecules than normal fibroblasts (Yamane et al., 2002).

BAL fluid from individuals with IPF contains significantly greater amounts of biologically active TGF-β compared to samples from unaffected individuals (Khalil et al., 2001) or from patients with hypersensitivity pneumonitis (Hagimoto et al., 2002). Increased quantities of bioactive TGF-β also correlate with enhanced epithelial cell pro-apoptotic potential (Hagimoto et al., 2002). Increased plasma levels of TGF-β may be due to either increased production by cells or increased mobilisation from tissue stores, or a combination of both. In patients undergoing bone marrow transplantation, higher plasma TGF-β concentrations appear to predict the development of radiation-induced pulmonary fibrosis, although this link has yet to be confirmed in an appropriately powered study (Anscher, 1993).

The genetic importance of TGF-β in pulmonary fibrosis has become an increasingly important area of research. Seven polymorphisms in the human gene encoding TGF-β on chromosome 10q13 have been reported (Cambien et al., 1996). Three of these reside in the coding region of the TGF-β1 gene, including two in exon 1 (codons 10 and 25) and one in exon 5 (codon 263). Grainger and colleagues showed that the differential production of TGF-β between individuals was partly dictated by polymorphisms in codons 10 and 25, both encoding parts of the leader sequence of TGF-β1 (Grainger et al., 1999). In each case, single base substitutions were responsible for the change in amino acids encoded: thymine to cytosine (leucine to proline) at codon 10 and guanine to cytosine (arginine to proline) at codon 25. However, data on the functional effect of codon 10 Pro are conflicting. Confusingly, both higher (Perrey et al., 1998) and lower (Yamada et al., 2000) levels of serum TGF-β have been reported with this particular polymorphism. More recently, the codon 10 Pro allele has been associated with a predisposition to hepatitis C-induced liver fibrosis (Gewaltig et al., 2002). On the other hand, the codon 25 Arg

allele has been associated with greater production of TGF-β by stimulated lymphocytes isolated from Arg/Arg homozygous patients undergoing lung transplantation (El-Gamel et al., 1999). In the same cohort of patients, homozygosity was also associated with a significantly higher incidence of pre-transplant fibrotic lung changes as well as the development of post-transplantation lung allograft fibrosis.

However, in a controlled study, neither the codon 10 Pro nor codon 25 Pro allele was associated with an increased susceptibility to IPF (Xaubet et al., 2003). This conclusion is not surprising, given the heterogeneity of growth factors implicated in this disorder and the broader complexity of its pathogenesis and disease progression. However, subgroup analysis revealed that in the majority of patients with IPF, the codon 10 Pro allele was correlated with more rapid deterioration in lung function and worsening in gas exchange. Interpreted another way, patients with this allele may be at greater risk of accelerated progression to terminal respiratory failure due to their disease. However, only a prospective study would be able to address this hypothesis in any detail.

1.4.viii Generation of active TGF-β in the fibrosing lung

A mandatory requirement for the control of TGF-β action in pulmonary fibrosis is the extracellular processing of latent TGF-β to produce the biologically active cytokine. This is crucial because only the mature TGF-β molecule can bind to its cell surface receptor to elicit the desired biological response. Although both latent and active forms of TGF-β are increased in lungs with pulmonary fibrosis, mechanisms of TGF-β activation are poorly understood. Consequently, TGF-β activation has been the subject of intense research for a number of years.

Experiments in bleomycin-injured rats have shown that plasmin can proteolytically regulate the activation of macrophage-secreted TGF-β in the presence of a cell surface receptor, CD36 and its ligand TSP-1 (Khalil et al, 1996a). The mechanism involves the RFK sequence on TSP-1 interacting directly with the LAP molecule to induce a conformational change that unmasks the TGF-β receptor binding site on active TGF-β. Unlike other mechanisms, the LAP moiety remains associated with the 'active' TGF-β component after interacting with TSP-1. The *in vivo* specificity of this hybrid plasmin/TSP-1-dependent mechanism was determined using a

competitive CD36 synthetic peptide that abrogated both bleomycin-induced TGF-β activation and pulmonary fibrosis (Yehualaeshet et al., 1999).

As previously alluded to, mice lacking the epithelial-restricted αvβ6 integrin develop intense bleomycin-induced lung inflammation but are protected from bleomycin-induced pulmonary fibrosis (Munger et al., 1999). αvβ6 has previously been shown to act as an integrin receptor for the matrix proteins fibronectin (Busk et al., 1992), tenascin (Prieto et al., 1993) and vitronectin (Huang et al., 1998). In more recent years, αvβ6 has also been shown to bind LAP (Munger et al., 1998). This particular interaction induces conformational changes in the latent TGF-β complex that allows the mature TGF-β to bind to its cellular receptors and thus initiate TGF-β signaling in epithelial cells (Munger et al., 1999). Hence, there is no release of active TGF-β into the pericellular / peri-matrix environment.

More recently, transgenic mice that overexpress interleukin-13 (IL-13) have been shown to develop spontaneous fibrosis in the airways and lung parenchyma (Lee et al., 2001). The fibrogenic effects of IL-13 were found to be dependent on the generation of active TGF-β. TGF-β activation in IL-13 overexpressing mice was dependent on the activity of a serine proteinase (possibly uPA) and MMP-9 but was independent of CD44. Little is known about how these different factors interact although CD44, which acts as a 'docking receptor' for MMP-9, has previously been shown to be vital for MMP-9-mediated activation of surface-localised latent TGF-β in transformed keratinocytes *in vitro* (Yu and Stamenkovic, 2000).

1.5 Summary, hypothesis and objectives of this thesis

Pulmonary fibrosis is characterised by the excessive accumulation and abnormal arrangement of lung extracellular matrix following diverse forms of lung injury. The progressive nature of parenchymal lung scarring is frequently associated with relentless respiratory morbidity and premature fatality in affected individuals. Extensive experimental and clinical evidence have implicated TGF-β as the key fibrogenic mediator in the pathogenesis of this disorder. An increasing number of studies also indicate neutrophil elastase may play roles in lung disease

beyond that of matrix destruction. Previous studies have shown that neutrophil elastase inhibitors abrogate the pulmonary fibrotic process in the bleomycin model. Until now, genetically modified mice have not been used to elucidate the role of neutrophil elastase in regulating aberrant lung extracellular matrix accumulation. Hence, the mechanism by which neutrophil elastase can stimulate the fibroproliferative process remains unknown. In particular, the potential ways by which neutrophil elastase influences the generation of active TGF-β, either directly or indirectly, in the repairing lung parenchyma remain speculative.

The primary objective of this thesis is to examine the hypothesis that **neutrophil elastase deficiency is associated with resistance to fibrotic lung development.** A secondary aim of assessing the relevance of TGF-β to fibrotic resistance associated with neutrophil elastase deficiency will also be pursued. In essence, the experimental work will seek to:

1. Characterise and compare the pulmonary fibrotic response of wild type (WT) and $NE^{-/-}$ mice to intratracheal instillation of the pro-fibrotic drug bleomycin,
2. Evaluate the extent of bleomycin-induced pulmonary inflammation and lung injury in both genotypes of mice and relate their contribution to the eventual development of pulmonary fibrosis, and
3. Examine the production, localisation and activation of TGF-β in the lungs of bleomycin-injured WT and $NE^{-/-}$ mice.

CHAPTER TWO

MATERIALS AND METHODS

2.1 Generation of gene-targeted mice

2.1.i Neutrophil elastase-deficient ($NE^{-/-}$) mice

$NE^{-/-}$ mice were generated and maintained by Dr. Jürgen Roes at University College London (Tkalcevic et al., 2000). Briefly, the NE gene (Figure 2.1 A) was initially isolated from a P1 mouse embryonic stem cell library to construct a replacement vector (strain 129/Sv; Genome Systems, USA). This targeting vector (Figure 2.1 B) contained the *Cre* recombinase gene, the neomycin resistance gene flanked by loxP sites, mutations at restriction enzyme sites in exons 1

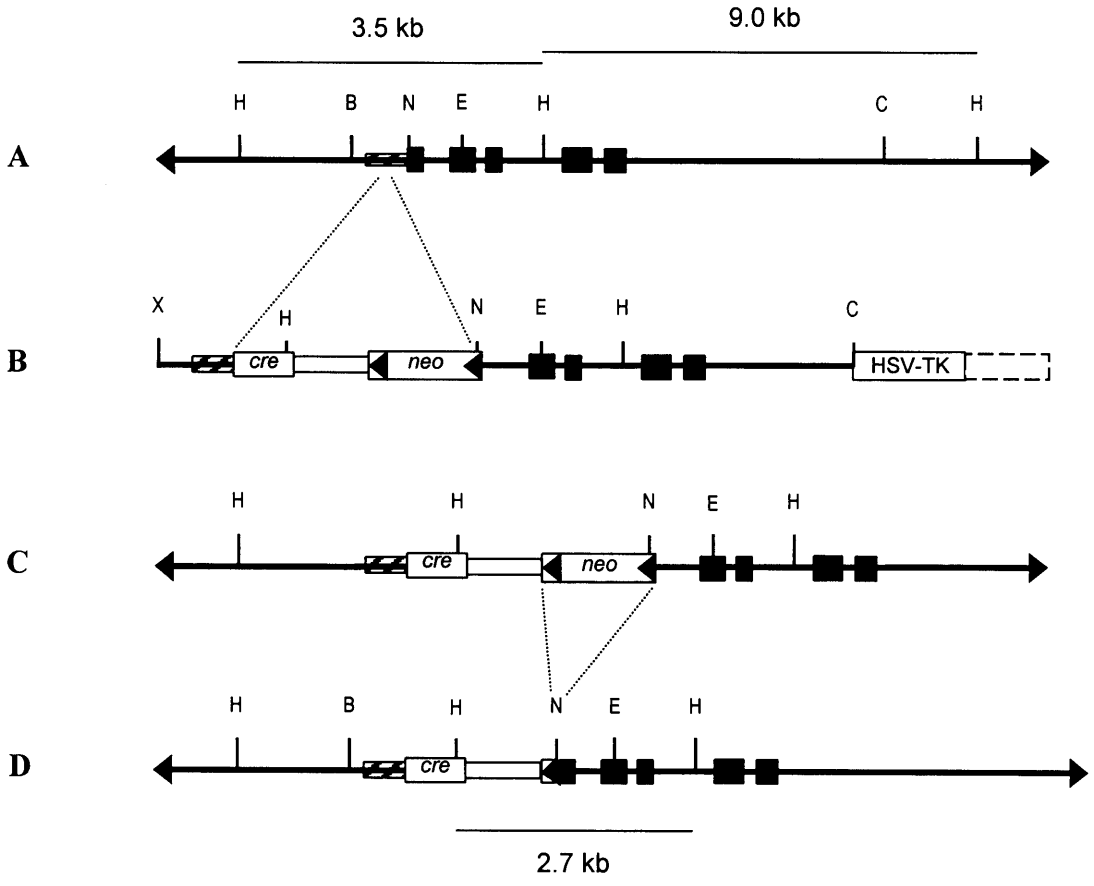

Figure 2.1 Schematic of the neutrophil elastase genomic loci (A), the targeting vector (B), the targeted loci (C) and the targeted loci following the deletion of *neo* by *Cre*-mediated recombination (D). Solid boxes represent exons, the closed empty box represents an intron with polyadenylation site and the closed hashed box represents the neutrophil elastase promoter. Key: *H*, HindIII; *B*, BamHI; *N*, NcoI; *E*, EagI; *C*, ClaI; *neo*, neomycin gene; *Cre*, Cre recombinase.

and 2, and a HSV-TK cassette. The targeting vector was transfected into embryonic stem cell loci and incorporated by homologous recombination (Figure 2.1 C). The *cre* and *neo* (neomycin resistance) genes were incorporated between the NE gene coding region and promoter and enhancer elements. Transient expression of *cre* removed *neo* (Figure 2.1 D). Stably transfected clones were analysed by PCR, DNA sequencing and Southern Blotting. In correctly targeted ES clones, the NE gene was inactivated by a deleted ATG translation site (exon 1) and a 4-bp frameshift mutation in exon 2. These clones were microinjected into blastocysts and chimeric offspring were mated to obtain founders with germline transmission of the inactivated NE gene.

In vivo and *in vitro* analyses have shown that these NE-deficient mice are phenotypically normal in the absence of an immune challenge. Spontaneous infections or signs of inflammatory disease have not been routinely observed either macroscopically or histopathologically (Roes, personal communication). Flowcytometric analysis of bone marrow leukocytes has revealed normal numbers of myeloid precursors and mature granulocytes (Tkalcevic et al., 2000). Unstimulated neutrophils from these animals have normal granularity and demonstrate normal degranulation, and phagocytic activity, as well as respiratory burst when stimulated with phorbol esters or opsonised *candida albicans*. Furthermore, their migration into inflamed serosal cavities in response to thioglycollate injection is equivalent to that of wild type mice (Tkalcevic et al., 2000).

2.2 Animal procedures

Animals used for experiments ranged from 12 to 16 weeks of age and weighed between 20 - 30 g each. To prevent opportunistic infections within the colony, 2.5% enrofloxacin (Baytril®, Bayer AG, Leverkusen Germany) was administered prophylactically to the drinking water given to all animals commencing a week prior to each study. Mice of both genders were distributed equally across experiments, and all procedures were performed in strict accordance with the Home Office Animals (Scientific Procedures) Act 1986.

2.2.i Bleomycin instillation

Bleomycin sulphate (Bleo-Kyowa®, Kyowa Hakko UK Ltd., Slough, UK) was freshly prepared on the day of use. Each vial containing 15 units of lyophilized bleomycin sulphate (1 unit = 1 mg = 1000 I.U.) was dissolved in 1 ml sterile 0.9% saline. The drug was confirmed to be endotoxin-free (personal communication, Kyowa Hakko UK Ltd., Japan). Animals were anaesthesized with 4% halothane (Merial®, Dublin, Eire) administered by constant flow oxygen (5 litres/minute). An area of skin over the ventral neck surface was sterilised with chlorhexidine, and a 1 cm transverse incision was made at the base of the neck. The underlying trachea was then exposed, and a 1 ml syringe used to inject 50 μl of either 0.05 units bleomycin or saline directly into the airway. Following injection, the skin wound was closed with absorbable silk sutures, and the animal was allowed to recover. Changes in gross body weight were recorded daily for the first week after injection of bleomycin or saline and on alternate days thereafter. At sacrifice, euthanasia was obtained with 0.2 ml of a fentanyl citrate : fluanisone mixture (Hypnorm®, Janssen, Belgium) injected intraperitoneally.

2.2.ii Bronchoalveolar lavage

Bronchoalveolar lavage (BAL) fluid was collected at specific time points following bleomycin or saline instillation. Lavage was performed using a 1 ml syringe attached to a 20-gauge cannula which was secured intratracheally. Six sequential aliquots of approximately 400 μl ice-cold sterile 0.9% saline were instilled into the lungs, left for 5 seconds and recovered under gentle pressure. Air (200 μl) was injected after each aliquot to prevent trapping of the lavaging fluid within the tracheal deadspace. Retrieved BAL fluid was placed in sterile 15 ml polypropylene tubes kept on ice. On average, 2 ml of BAL fluid was collected from each animal. For protein analyses, cell separation was achieved by centrifugation at 1000 *g* for five minutes.

2.2.iii Collection of lung tissue

For protein and RNA analyses, unperfused lungs were dissected free from the airways and heart, blotted dry, wrapped in foil and snap-frozen in liquid nitrogen. Lungs were stored at

-80°C until used. Frozen lungs were thawed, and their lung weights recorded prior to use. For histological analysis, the pulmonary vasculature was first cleared using 10 - 15 ml isotonic saline introduced via a 25-gauge butterfly cannula placed in the right atrium. The trachea was then cannulated using a 21-gauge needle, and 10% formalin was carefully instilled into the lungs at a constant pressure of 25 cm H_2O with care to avoid overinflation. Fixed lungs were dissected en bloc from the thorax, placed in fresh formalin and stored at 4°C until processed.

2.3 Analysis of lung collagen content and distribution

2.3.i Measurement of tissue hydroxyproline content by high performance liquid chromatography

Lung collagen content was quantified by measuring hydroxyproline in acid-hydrolysed lung samples. This involved a single-step reverse-phase high performance liquid chromatography (HPLC) method (Campa et al., 1990). Hydroxyproline is a secondary imino acid that constitutes approximately 12.2% of the dry weight of collagen (Laurent et al., 1981). It is present in much smaller amounts in several other proteins. HPLC has been shown to be a convenient, reproducible and sensitive method for measuring hydroxyproline content in lung tissue (Campa et al., 1990). Previous methods for measuring hydroxyproline content included radioactive assay (Rojkind and Gonzalez, 1974) and colorimetric reactions (Edwards and O'Brien, 1980).

2.3.i.a Sample preparation

Snap-frozen lungs were placed in a ceramic pestle containing liquid nitrogen and crushed to a fine powder using a mortar. Twenty mg of each powdered sample were added to 2 ml of 6 M HCl and hydrolysed at 110°C for 16 hours. Activated charcoal (20 - 30 mg) was then added to each hydrolysate to decolourise it prior to filtration through a 0.65 μm DA membrane filter (Millipore, Watford, UK). Filtrates were diluted 1:100 with purified water to a total volume of 1

ml, transferred to a microcentrifuge tube and dried down under vacuum and heat using a Speed-Vac sample concentrator (Savant, UK).

2.3.i.b Pre-column sample derivatisation

All HPLC solvents were purchased from BDH-Merck Ltd. (Leicester, UK) unless otherwise specified. Purified water was deionised by reverse osmosis using a Millipore Water Purification System (RO10 and Milli-Q Plua, Watford, UK). Each dried filtrate was dissolved in 100 µl purified water, buffered with 100 µl 0.4 M potassium tetraborate (pH 9.5) and reacted with 100 µl 36 mM 7-chloro-4-nitrobenzo-2-oxa-1,2-diazole (NBD-Cl; Sigma Chemical Co., Poole, UK) dissolved in methanol. At least three trans-4-hydroxy-L-proline standards (Sigma-Aldrich Co. Ltd., Poole, UK) were derivatized in parallel. NBD-Cl reacts with primary and secondary amino acids to produce light-absorbing chromophores. As reaction products with the latter preferentially absorb light within the 450 - 550 nm range, the absorbance of hydroxyproline at 495 nm therefore exceeds that of primary amino acids in the same sample (Campa et al., 1990). Measurement of the hydroxyproline-NBD-Cl reaction product allows the amount of derivatised amino acid to be quantified and related to hydroxyproline standards within each experiment. Reducing the derivatisation time to 25 minutes further minimises interference from primary amino acids.

Derivatisation reactions were terminated with 50 µl 1.5 M HCl to lower the sample pH. To ensure that all samples were compatible with the HPLC running buffer, 150 µl of concentrated buffer A (167 mM sodium acetate in 26% acetonitrile v/v, pH 6.4) were added to each sample and filtered through a 0.2 µm pore filter. An aliquot (100 µl) of this mixture was then injected onto the HPLC column which was maintained continuously at 40°C in a heated column oven.

2.3.i.c Chromatographic conditions

Freshly prepared running buffers A (50 mM sodium acetate in 8% v/v acetonitrile, pH 6.4) and B (75% v/v acetonitrile) were filtered through a 0.22 µm pore size GV filter prior to each experiment. The HPLC system was purged of air bubbles prior to each use, and the column was equilibrated in buffer A for 40 minutes. Three NBD-Cl derivatised standards, each containing 50

pmol hydroxyproline, were then injected on to the column to initiate a 'run'. Samples were separated on LiChroCART cartridge columns (LiChroCART LiChrospher, 250 mm length x 4 mm diameter, 5 μm particle size, 100 RP-18; BDH-Merck Ltd., Leicester, UK), protected by a directly-coupled precolumn (LiChrosorb, 4 x 4 mm, 5 μm particle size, 100 RP-18) (table 2.1).

Derivatised samples were eluted through the column by gradually altering the relative proportions of the running buffers over time (figure 2.2). Post-column detection was performed by measuring the colourimetric absorbance of eluted products at 495 nm using a flow-through variable wavelength monitor. The signal was computerised (System Gold Integrator, Beckman-Coulter Ltd., High Wycombe, UK) for quantitative analysis. In this way, the biochemical constituents of each sample were separated and visualised on a real-time graph on an LCD monitor. Hydroxyproline elutes from the column between 5 and 7 minutes after injection, between glutamine (3.5 minutes) and serine (7 - 9 minutes), preceding the shift of the gradient to predominantly organic buffer B. The total running and column regeneration time was approximately 25 minutes per sample.

Column characteristics	LiChrospher 100 RP-18 (250 x 4 mm, 5μm particle size)		
Buffers (mobile phase)	*Buffer A*	8% aqueous acetonitrile (v/v)	
		50 mM sodium acetate, pH 6.4	
	Buffer B	75% aqueous acetonitrile (v/v)	
		25% water	
Column flow rate	1.00 ml/min		
Column temperature	40°C		
Detection wavelength	495 nm		
Elution gradient	Time (min)	*% buffer A*	*% buffer B*
	0	100	0
	5	95	5
	6	20	80
	12	20	80
	12.5	100	0
	25	100	0
Collection time	15 seconds between 3.5 and 7 minutes		

Table 2.1 Chromatographic conditions for the separation of hydroxyproline by reverse-phase HPLC.

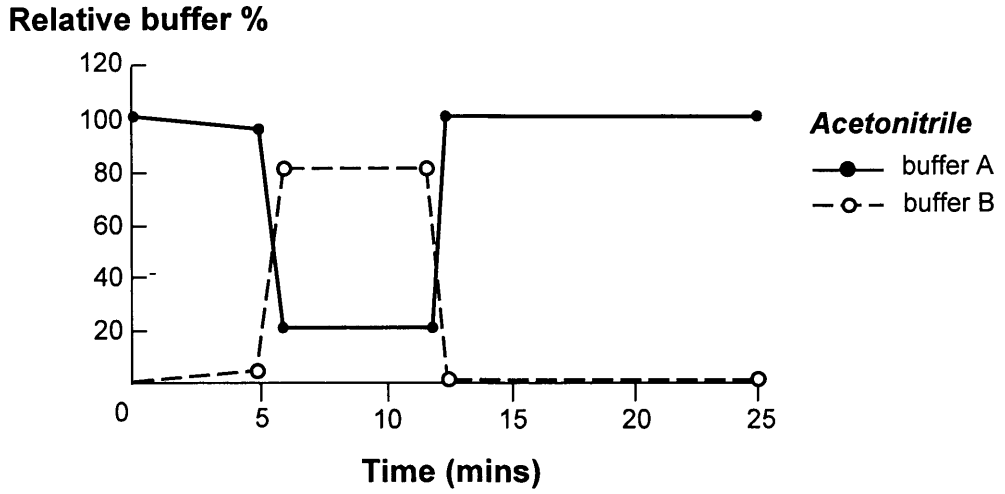

Figure 2.2 Changes in the acetonitrile gradient during the elution of hydroxyproline by reverse-phase HPLC.

The hydroxyproline content in each sample was determined by comparing the area under the hydroxyproline chromatographic peak in each sample ('HPLC number') to the average of three standards isolated under identical conditions. To determine total lung collagen, this value and other key variables were considered thus:

Total lung collagen (mg) = (HPLC number) (A x B x C x D) (lung weight/aliquot weight) $(1/10^9)$ (100/12.2)

where ***A***, hydrolysate dilution factor; ***B***, derivatisation volume/injection volume ratio; ***C***, concentration factor; ***D***, molecular weight of hydroxyproline (MW = 131); 10^9, conversion from pg to mg, and ***12.2***, percentage of collagen weight as hydroxyproline.

2.3.ii Histological analysis

2.3.ii.a Tissue processing and preparation

Lungs for paraffin wax processing (section 2.2.iii) were fixed overnight in 10% formalin at 4°C. Fixed tissues were serially dehydrated in 15% sucrose, 50% ethanol and 70% ethanol for 24 hours each at 4°C before being embedded parasagittally in molten wax using a Leica TP 1050 Vacuum Tissue Processor (Leicester, UK).

2.3.ii.b Routine histochemistry

Tissue processing was performed by Mr. Steve Bottoms, UCL. For routine histology, 4-μm thick paraffin sections were cut using a Shandon AS325 microtome (Cheshire, UK) and adhered onto SuperFrost® slides (BDH-Merck Ltd., Leicester, UK). Tissue sections were dewaxed in xylene and rehydrated in decreasing concentrations of ethanol using an automated stainer (Sakura DRS601 Diversified Stainer, Bayer, UK). Sections were stained with haematoxylin and eosin (Shandon, Pittsburgh, USA) or Masson's trichrome (Sigma-Aldrich Co. Ltd., Poole, UK). Sections were then rehydrated through increasing concentrations of ethanol and mounted in xylene (Sakura Coveraid, Bayer, UK). Photomicrographs were captured using an Olympus BX40 microscope with KS300 Imaging Software (Zeiss GmbH, Germany).

2.4 Assessment of lung injury and inflammation

2.4.i Indices of lung injury

2.4.i.a Alkaline COMET assay

Bleomycin-induced cytotoxicity is dependent on the ability of bleomycin to cleave deoxyribonucleic acid (DNA) in the presence of molecular oxygen and a metal ion (reviewed in Hay et al., 1991). DNA damage in lung cells was assessed as an early marker of bleomycin-induced injury using the alkaline COMET assay in conjunction with Dr. Peter Clingen at the Ludwig Cancer Institute, UCL (Spanswick et al., 1999). This assay detects single-stranded DNA scission in electrophoresced individual cells labeled with a fluorescence nuclear stain.

The pulmonary vasculature of untreated, saline- or bleomycin-treated WT and $NE^{-/-}$ mice was cleared with ice-cold 0.9% saline, as previously described, and lungs were instilled with 2 ml dispase (Calbiochem, Nottingham, UK). The proximal trachea was ligated, and the lungs were removed intact from the thoracic cavity. Dispase-filled lungs were placed in a 15-ml polypropylene tube containing 3 ml fresh dispase and incubated for an hour at room temperature. Each pair of lungs was then transferred to a petri dish containing 5% FCS-supplemented DMEM and minced using scissors and forceps. The resulting crude cell preparations were carefully sieved through a 100-μm cell strainer and resuspended at 5 x 10^4 cells/ml in DMEM containing 10% DMSO.

The COMET assay was carried out on ice and in subdued lighting. Briefly, a single-cell suspension of each sample was embedded in 1% low melting point agarose on a frosted microscope slide and incubated for 1 hour in lysis buffer (100 mM disodium EDTA, 2.5 M NaCl, 10 mM Tris-HCl, pH 10.5) containing 1% Triton X-100 to unwind supercoiled DNA. Slides were then incubated in alkali buffer (50 mM NaOH, 1 mM disodium EDTA, pH 12.5) for 45 minutes, followed by electrophoresis in the same buffer for 25 minutes at 18 V (0.6 V/cm), 25 mA. During electrophoresis, intact DNA remains within the nucleus while damaged (uncoiled) DNA migrates towards the anode, forming a smeared 'tail' effect that fluoresces red when stained with propidium iodide (2.5 μg/ml for 30 minutes). Images were visualized with a Nikon inverted microscope mounted with a high pressure mercury light source, 510 to 560 nm excitation filter and 590 nm barrier filter (Nikon UK Ltd., Kingston-Upon-Thames, UK). In these studies, the

COMET assay was used qualitatively to compare the extent of DNA breakage in lung cells between bleomycin-treated WT and $NE^{-/-}$ mice. The sensitivity of the assay is less than one strand break per 10^7 base pairs (Clingen et al., 2001).

2.4.i.b Measurement of BAL fluid lactate dehydrogenase levels

Lactate dehydrogenase (LDH) is an abundant cytoplasmic enzyme that catalyses the interconversion of lactate and pyruvate. Its extracellular release following cellular plasma membrane disintegration is widely quantified as an index of cytotoxicity. In the current studies, aliquots (50 µl) of cell-free BAL fluid were placed in a microwell plate and an equal volume of a tetrazolium-based assay substrate was added and allowed to react for 30 minutes at room temperature (Promega CytoTox 96® non-radioactive cytotoxicity assay, Southampton, UK). Free LDH in BAL fluid was allowed to catalyse the conversion of yellow tetrazolium salt into a red formazan product. Reactions were terminated by lowering the pH using an acetic acid-based stopping mixture, and the stable product was detected at 490 nm using a microtitre spectrophotometer. Relative amounts of LDH were expressed as the ratio of absorbance in bleomycin-treated samples to that of saline-treated controls.

2.4.ii Cellular indices of pulmonary inflammation

2.4.ii.a Fluorescence activated cell sorting

Initial BAL fluid leukocyte composition was determined 24 hours following saline or bleomycin instillation using a triple-staining fluorescence-activated cell sorting (FACS) protocol from Dr. Jurgen Roes, UCL (Roes and Rajewsky, 1993). Approximately 1 x 10^6 cells were incubated with fluorochrome-conjugated antibodies to Gr-1 (Ly-6G), a granulocyte marker, CD11b/18 and F4/80, a macrophage marker (all from BD PharMingen, Cowley, UK). Erythrocytes were lysed with BD Pharm Lyse™ lysis buffer. Stained cell populations were analysed with a FACSCalibur flow cytometer using CellQuest software (Becton Dickinson, USA). Differentially-stained leukocytes were discriminated according to gating conditions based on their specific light-scatter profiles.

2.4.ii.b Total and differential BAL fluid leukocyte counts

To assess inflammatory cell counts in BAL fluid, samples were centrifuged at 2000 rpm for 10 minutes at 4°C, and the cell pellets were resuspended in 200 µl of red cell lysis buffer (Sigma-Aldrich Co. Ltd., UK). Total leukocyte counts in each cell suspension were determined using a haemocytometer chamber. Aliquots of each suspension containing approximately 1 x 10^5 cells were then loaded into cytospin chambers and centrifuged at low speed (1000 rpm, 3 minutes) onto coated glass slides (Shandon Cytospin 3 System, Pittsburgh, USA). Slides were allowed to air dry prior to staining with Wright-Giemsa (Diff-Quik®, BDH-Merck, UK). Differential leukocyte profiles were determined by enumerating at least 500 cells on each stained slide, distinguished on the basis of morphological differences (figure 2.3).

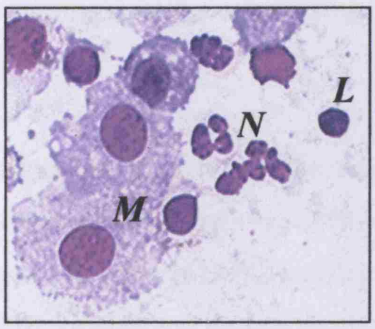

Figure 2.3 Differential leukocyte morphology

***M**, macrophages*
***N**, neutrophils*
***L**, lymphocytes*

2.4.ii.c Lung tissue neutrophil burden

Myeloperoxidase (MPO) is an antimicrobial enzyme found mainly in neutrophils and at much lower concentrations in monocytes and macrophages. MPO accounts for approximately 5% of the total dry weight of the neutrophil (Klebanoff, 1968). It catalyzes the oxidation of halides and other electron donors in the presence of hydrogen peroxide to produce reactive oxygen species. MPO activity has been correlated to neutrophil numbers in inflamed pulmonary tissues (Venge, 1994; Schneider and Issekutz, 1996), and its assessment therefore provides a quantitative indicator of tissue neutrophil burden.

The spectrophotometric method for measuring MPO activity was based on a protocol used in Professor A. W. Segal's laboratory (Winterbourn et al., 1988) and modified for use with homogenised lung tissue. Calcium/magnesium-free phosphate buffered saline (PBS) was freshly

prepared from tablets (Oxoid Ltd., Basingstoke, UK), and all other reagents were obtained from Sigma-Aldrich Co. Ltd. (Poole, UK). Aliquots of lung powder (50 mg) were placed in 2 ml RIPA buffer (PBS containing 1% Nonidet P-40, 0.5% sodium deoxycholate and 0.1% sodium dodecyl sulfate). Each tissue solution was homogenised using a rotor-blade tissue tearor (Kinematica GmBH, Swizerland). Homogenates were kept on ice for one hour after which they were ultracentrifuged at 25,000 x g for 15 minutes to release intra-granular MPO into the supernatant. A substrate reaction mixture was freshly prepared for each experiment, comprising citrate buffer (0.1 M, pH 5.5), O-Dianisidine (DMB, 0.32 mM) dissolved in ethanol and 30% hydrogen peroxide. Five hundred µl of this mixture was place in labeled bijous and allowed to warm to 37°C. Fifty µl of each homogenate supernatant was added to the substrate mixture and reacted for 5 minutes at 37°C (reaction time). The mixture was then removed from the water bath and kept at room temperature (incubation time) before each reaction was terminated by the addition of a stopping mixture comprising 35% perchloric acid (v/v) and 20% DMSO (v/v) in deionised water.

Absorbance of samples and horseradish peroxidase (HPO) standards (0.00131 units/ng protein) at 560 nm were determined. MPO and HPO activities are linear at concentrations of 0.1 – 10.0 ng. *In vitro*, 1 unit of MPO activity is defined as the amount of activity that oxidises 1 micromole of DMB, an electron donor, per minute at 25°C. MPO activity in lung samples were expressed relative to that of HPO standards as units/mg protein. The peroxidase – substrate reaction is both time and temperature sensitive; peroxidase activity deteriorates with increasing periods of incubation under standard laboratory conditions. Consequently, preliminary experiments were performed to establish the optimal incubation time at room temperature prior to termination.

2.4.iii Measurement of neutrophil elastase activity in BAL fluid

Neutrophil elastase activity in samples of BAL fluid was measured photometrically using the chromogenic substrate methoxy-succinyl-L-alanyl-L-alanyl-L-prolyl-L-valinyl-*p*-nitroanilide (MeOSAAPVNA). Hydrolysis of this compound has been shown to be the most efficient means to determine neutrophil elastase activity *in vitro* (Nakajima and Powers, 1979). Incorporation of a MeO-Suc group significantly increases the solubility of the substrate, enhancing the elastase enzymatic reactivity towards the terminal anilide portion. As a result, much less neutrophil elastase is required to hydrolyse this compound than other commonly used substrates including SAAPNA

(Bieth, 1998). Moreover, MeOSAAPVNA recognises enzymatic specificity for neutrophil elastase as it is not cleaved by either neutrophil-derived cathepsin G or proteinase 3 (Nakajima and Powers, 1979).

2.4.iii.a Sample preparation and analysis

Lyophilised MeOSAAPVNA (Elastase Colorimetric Substrate I, Calbiochem, Nottingham, UK) was dissolved in 1 mM 1-methyl-2-pyrrol-idinone (Sigma-Aldrich Co. Ltd., Poole, UK) to form 1 M stock solutions that were stored at -40°C until used. Purified human neutrophil elastase (product 324681, Calbiochem, Nottingham, UK) was diluted sequentially to establish a standard reference range. BAL fluid was collected from WT and $NE^{-/-}$ mice seven days after either saline or 0.05U bleomycin instillation. Samples were first concentrated ten-fold using Centricon® Centrifugal Filter Units (Millipore, Watford, UK) with the appropriate cut-off pore size prior to analysis. To assess free elastase activity, cell-free BAL fluid and neutrophil elastase standards were diluted in a buffer containing 0.1 M Tris, 0.5M NaCl and 0.01% NaN_3 (pH 7.5) and equilibrated at 37°C for two minutes prior to the addition of 5 mM MeOSAAPVNA. The total reaction volume was 120 µl. A reaction temperature of 37°C was chosen for its physiological relevance. At the end of each incubation period, the rates of hydrolysis of the MeOSAAPVNA substrate (i.e. changes in optical density / absorbance) were measured at 410 nm using a 96-well microplate spectrophotometer (Multiskan MCC 340 plate reader, Titertek®, AL, USA). Appropriate controls using assays that lacked either enzyme or substrate were incorporated into every experiment. By convention, one neutrophil elastase enzyme unit is defined as that which releases 1 mmol of *p*-nitroanilide from the substrate per minute at 25°C. For comparative reasons, the unit of elastolytic activity in the BAL fluid samples was defined as a change in optical density at 410 nm per minute per 0.06 ml (volume of sample analysed).

2.4.iii.b Comparison of different preparations of purified neutrophil elastase

Additional experiments were performed to assess the ability of human neutrophil elastase obtained from a commercial source (Calbiochem, Nottingham, UK) and Dr. Caroline Owen (Harvard Medical School, Boston, USA) to hydrolyse MeOSAAPVNA. For these assays, increasing concentrations of neutrophil elastase were incubated with 1 mM of the substrate in a

reaction mixture containing 0.1 M Hepes, 0.5 M NaCl, 0.1% Brij buffer (pH 7.5) for 10 minutes at 25°C. Changes in absorbance were measured in units of optical density using the same microtitre spectrophotometer.

2.4.iv Evans blue dye assay for assessing alveolar-capillary permeability

Evans blue dye (EBD) is a stable and non-toxic azo dye with unique properties for the assessment of vascular permeability in acute lung injury (Evans et al., 1988; Standiford et al., 1995). It binds avidly and stably to circulating albumin (Patterson et al., 1992) and achieves a volume of distribution very close to that of native albumin and ^{125}I-albumin with negligible competition from other substances (Sear et al., 1953). The translocation of albumin-bound EBD out of the vasculature therefore provides a reliable method for quantifying extravascular protein accumulation. In pulmonary tissues, EBD accrual follows a rapid and linear pattern whilst its egress out of the same compartment is much slower, occurring over many hours (Green et al., 1988; Dallal and Chang, 1994). Although the pharmacokinetics of EBD and ^{125}I-albumin are comparable in many aspects (Sear et al., 1953; Huggins et al., 1963), the former has been shown to accumulate in pulmonary tissue faster than the radiolabelled protein in perfused rodent lungs (Dallal and Chang, 1994).

2.4.iv.a Dye administration

Evans blue dye (Sigma-Aldrich Co. Ltd., Poole, UK) was prepared at a stock concentration of 10 mg/ml, filtered through a 0.45 μm filter and kept at room temperature. EBD was administered at a dose of 20 mg/kg intravenously via the tail vein of anaesthesised mice using a 29-gauge insulin needle. Vasodilatation of the vein was increased by placing the mice in a warming box kept at 35°C for 20 minutes prior to injection. Digital pressure applied at the base of the tail further increased venous stasis and facilitated injection of the dye. The injected dye was allowed to circulate intravascularly for one hour before the mice were sacrificed. In preliminary studies, it was found that the one-hour circulation time was sufficient for the dye to be distributed systemically and accumulate in viscera.

2.4.iv.b Quantifying EBD accumulation in BAL fluid, lungs and plasma

Blood was collected via cardiac puncture using a 21G needle and placed into heparinised microcentrifuge tubes kept on ice. Bronchoalveolar lavage was then performed (section 2.1.ii), and the pulmonary vasculature was cleared with ice-cold 0.9% saline. BAL samples were centrifuged at 1000 *g* for five minutes to remove cells prior to analysis. Finally, the lungs were dissected free and snap-frozen in liquid nitrogen. Evans blue dye exhibits light absorbance between 580 - 650 nm. In these studies, EBD absorbance in plasma, BAL fluid and lung homogenates was measured at 620 nm using a microwell plate method modified from published protocols (Standiford et al., 1995; Kaner et al., 2000).

Heparinised blood samples were centrifuged at 1500 rpm for 15 minutes to sediment the erythrocyte pellet. An aliquot (200 µl) of the separated plasma was then diluted 1 : 30 with normal saline prior to measurement. Samples of cell-free BAL fluid were analysed undiluted in triplicates of 100 µl volume. To quantify the extent of tissue-trapped EBD, snap-frozen lungs were weighed and powdered using a pestle and mortar. Approximately 200 mg of lung powder were then homogenised in 2 ml calcium / magnesium-free PBS. Four ml of formamide were added to each homogenate, and the samples were incubated for 16 hours at 37°C. The mixture was then centrifuged at 4000 rpm for 15 minutes, and the supernatant was removed for spectrophotometric analysis. Data were expressed as the ratio of EBD absorbance in samples (BAL fluid or homogenised lung tissue) to plasma EBD absorbance.

2.4.v Measurement of BAL fluid total protein

Total protein was assayed in cell-free BAL fluid and lung tissue homogenates using the Pierce BCA Protein Assay method (Perbio Science Ltd., Cheshire, UK). This assay combines the Biuret reaction (reduction of Cu^{++} to Cu^{+} by alkalinised protein) with a sensitive colourimetric detection of the cuprous cation (Cu^{+}) using a bicinchoninic acid (BCA)-based reagent. The purple coloured reaction product of this assay, formed by the chelation of two molecules of BCA with one cuprous ion, exhibits a strong absorbance between 540 nm to 590 nm that is linear with increasing protein concentrations over a broad working range of 20 µg/ml to 2000 µg/ml. Briefly, 200 µl of the working reagent (BCA + 4% cupric sulfate) and 25 µl of either a protein standard or BAL fluid/lung homogenate sample were pipetted into a 96-well plate. The diluent

used in bronchoalveolar lavage or lung homogenisation was used as a blank (negative) control. The plate was gently rocked and incubated at 37° for 30 minutes after which the reaction was terminated by cooling on ice. The corrected absorbance of each well was then measured at 540 nm using a microtitre plate spectrophotometer.

To eliminate the possibility that other substances might interfere with the measurement of protein in cell-free BAL fluid, protein precipitation with trichloroacetic acid (TCA) was also performed in some samples prior to analysis. Briefly, approximately 30 mg of lung tissue was dissolved in 800 µl serum-free DMEM and 20% (w/v) TCA made up in purified deionised water. The mixture was incubated overnight at 4°C. The following day, each sample was ultracentrifuged at 14,000 rpm for 15 minutes at 4°C and the supernatant discarded. The pellet was washed twice in 200 µl ice cold acetone, resuspended in 200 µl 0.1M NaOH and incubated for 1 hour at 4°C. 50 µl of this was removed and reacted with 100 µl 0.1M NaOH. From this, 25 µl was used for protein measurement using the Pierce BCA Protein Assay. Protein standards were made up in 0.1 M NaOH and assayed in parallel with BAL fluid samples.

2.4.vi Polyacrylamide gel electrophoresis

Proteins in cell-free BAL fluid specimens were also separated by one-dimensional polyacrylamide gel electrophoresis (PAGE) to assess their relative abundance. All reagents used were obtained from Sigma-Aldrich Co. Ltd. (Poole, UK). Samples (20 µl) were diluted 1:4 in 0.5M Tris-HCl (pH 6.8) sample buffer (7 µl) containing 10% sodium dodecyl sulfate (SDS), 2 β-mercaptoethanol, glycerol and 0.05% bromophenol blue and heated at 95°C for 5 minutes. Approximately 10 µg of protein per sample were loaded. A 4% acrylamide stacking gel (pH 6.8) composed of 0.5% Tris-HCl, 10% SDS, 30% acrylamide/bis, 10% ammonium persulphate and TEMED was poured on top of a 12% separating gel containing 1.5M Tris-HCl (pH 8.8) and the prerequisite buffers and catalyst. Molecular weight standards were incorporated into the outermost lanes of each gel (MultiMark Multi-coloured Protein Standards, NOVEX, Oxford, UK). The gel electrode assembly was placed in a Mini PROTEAN II electrophoresis chanber (BIO-RAD, Richmond, CA). Running buffer was added to the upper and lower chambers, and the proteins electrophoresed at 90 – 100 V for 1.5 hours. The gels were then fixed and stained for 2 hours in 0.1% Coomassie blue (R-250, Invitrogen Ltd., Renfrewshire, UK).

2.5 Assessment of TGF-β production, activation and localisation

2.5.i Ribonuclease Protection Assay (RPA) of TGF-β mRNA expression

The detection and quantification of TGF-β mRNA in WT and $NE^{-/-}$ lung tissue was performed using a RiboQuant Multi-Probe RNase Protection Assay (PharMingen, Cowley, UK) in conjunction with Dr. Sarah E. Dunsmore, UCL. Total RNA was isolated using a trizol-based protocol from the lungs of mice injected seven days previously with either saline or bleomycin. A template set containing, amongst others, murine TGF-β_1, TGF-β_2 and TGF-β_3 cDNA, and GAPDH, a housekeeping gene, was used for bacteriophage T7 polymerase-directed synthesis of [^{32}P]-labelled probes. The probe set was hybridised in excess to the target RNA in solution, after which free probe was digested with RNases. The remaining RNase-protected probes were purified, resolved on a denaturing polyacrylamide gel and quantified by phosphorimaging. The relative density of each TGF-β band was converted to pixels and graphed as a ratio to GAPDH density.

2.5.ii The mink lung epithelial cell-based PAI-1/luciferase assay

The mink lung epithelial cell (MLEC)-based bioassay measures TGF-β activity by utilising its ability to upregulate plasminogen activator inhibitor-1 (PAI-1) in an appropriate reporter gene system (Abe et a., 1994). This method has been shown to be more specific than ELISA-based systems to quantify TGF-β activity (Abdelouahed et al., 2000). MLECs permanently transfected with the expression construct p800neoLUC containing a truncated PAI-1 promoter fused to the firefly luciferase reporter gene (figure 2.4) were obtained from Dr. Daniel B. Rifkin (New York University School of Medicine, NY, USA). This promoter fragment contains two regions that are necessary for maximal induction of PAI-1 gene expression by TGF-β (Keeton et al., 1991). The addition of 0.2 to > 30 pM active recombinant TGF-β has been shown to induce a dose-dependent increase in luciferase activity, including a linear response between 1 to 10 pM (Abe et al., 1994).

Specificity of the assay for TGF-β was confirmed using neutralising antibodies to all three mammalian isoforms, TGF-β1, -β2, and β3, with negligible interference by other known inducers of PAI-1, including basic fibroblast growth factor, platelet-derived growth factor, recombinant interleukin-1α and epidermal growth factor (Abe et al., 1994).

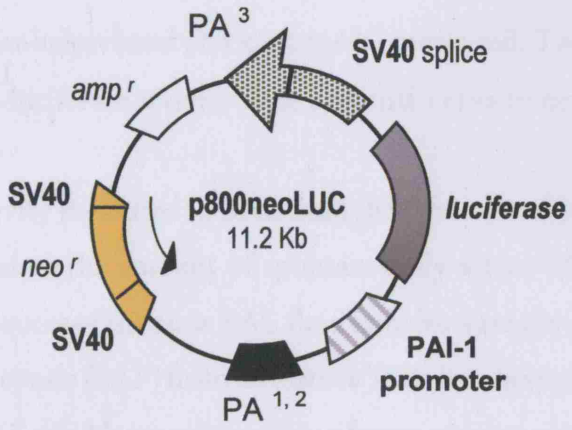

Figure 2.4 The p800*neo*LUC expression construct containing a truncated TGF-β-inducible PAI-1 promoter linked to a firefly luciferase reporter gene.

PA, plasminogen activator; *amp*^{r}, ampicillin resistance cassette; *neo*^{r}, neomycin resistance cassette; *SV40*, Simian virus 40.

Confluent MLECs (passages 22 to 32) were cultured in supplemented Dulbecco's modified Eagle's media (DMEM, Gibco-BRL, Paisley, UK) containing penicillin (200 units/ml), streptomycin (200 units/ml), L-glutamine (4 mM), FCS (10% v/v) and gentamicin (250 μg/ml Geneticin G418, Sigma-Aldrich Co. Ltd., UK). Cells were incubated at 37°C in a humified chamber of air containing 10% CO_2, examined daily using an inverted phase-contrast microscope and subcultured upon reaching 80 - 90% confluence. When passaged at a ratio of 1 : 30 ratio, near-confluence was reached on average within 4 - 5 days.

2.5.iii Measurement of active and total TGF-β levels in BAL fluid

For each experiment, MLECs were plated at a density of 1.6 x 10^4 cells/100 µl/well in a 96-well plate (TPP, Zurich, Swizerland) and allowed to attach for 4 hours at 37°C. The medium was then removed and cells were washed with sterile PBS. Each well was refilled with either 100 µl control (serum-free) medium, control medium containing a range of acid-activated TGF-β1 (0.1 to 1.2 ng/ml, R & D Ltd., Abingdon, UK) or cell-free BAL fluid. TGF-β standards were prepared at least an hour beforehand and kept at 4°C until used. Their incorporation into the assay allowed a TGF-β-luciferase activity dose response curve to be constructed.

Luciferase activity measured in BAL fluid that was not subjected to additional *in vitro* treatment corresponded to the amount of spontaneously active TGF-β in those samples. In certain experiments, aliquots of the same BAL fluid samples were also heated *in vitro* to dissociate the latency-associated peptide (LAP) from its mature TGF-β moiety prior to addition to MLECs (protocol outlined in 2.5.vi). Measurement of luciferase activity of such samples indicated the amount of total (spontaneously active plus heat-activated) TGF-β. Thus, the proportion of latent TGF-β could be determined by direct subtraction of the two values. All measurements were made in triplicate.

Following a second incubation at 37°C in 10% CO_2 for 16 - 20 hours, the plated MLECs were visually inspected for gross changes in viability and morphology. The overlying medium was then aspirated and the cells washed with PBS before being lysed in 100 µl of Reporter Lysis Buffer (Roche Molecular Biochemicals, UK). After gentle agitation at room temperature for 20 minutes, 30 µl of cell lysate from each well were transferred to a 96-well Optiplate (Packard Bioscience, Berkshire, UK). Luciferase substrate (150 µl) was injected automatically into each well using a Tropix TR717 Microplate Luminometer (Applied Biosystems, CA, USA) and the resultant luciferase activity was measured at a wavelength of 620 nm.

2.5.iv Quantification of activatable TGF-β in homogenised lung tissue

Lung tissue (50 mg) was homogenised in serum-free DMEM containing 0.5 mM phenylmethylslufonyl fluoride (PMSF; Sigma Chemical Co., Poole, UK) and 5 μM Ilomastat. (GM6001; Chemicon, Harrow, UK). The resultant homogenates were heated at 80° for 5 minutes and centrifuged at 1800 rpm for 15 minutes. Supernatants were removed and assayed for active TGF-β using the PAI-1/luciferase assay. The residual tissue was washed in serum-free DMEM, re-homogenised, heated under the same conditions and centrifuged. Supernatants were removed and assayed for active TGF-β. This extended extraction procedure was repeated for a total of five times on the same aliquot of lung tissue. The amount of active TGF-β remaining in the final residual pellet was less than 5% of the total measured.

2.5.v Activation of latent TGF-β by neutrophil elastase or plasmin

Neutrophil elastase and plasmin were also reacted with latent TGF-β, both in purified form and in BAL fluid, to assess whether they could activate TGF-β. In experiments where purified TGF-β was used, the substrate (40 nM recombinant human LAP-TGF-β, R & D Systems Ltd., Abingdon, UK) was diluted in DMEM containing 0.1% BSA (pH 7.5). Reactions were performed by placing the reaction microtitre tray on an agitator maintained at 37°C. In experiments where BAL fluid was used, specimens were collected from WT and $NE^{-/-}$ mice seven days following the IT instillation of 0.05 U bleomycin. In preliminary experiments, 0.1 M Hepes and 0.1% Brij were evaluated as potential buffers but DMEM containing 0.1& BSA was found to give the most consistent results. 0.1% Brij also interfered with the MLEC / PAI-1 assay rendering measurement of TGF-β activity inaccurate.

2.5.vi Analysis of proteinase-mediated release of TGF-β from intact lung tissue

For the analysis of proteinase-mediated TGF-β elution from lung tissue, lungs were removed *en bloc* from the thoracic cavity of WT and $NE^{-/-}$ mice seven days following the

instillation of 0.05 U bleomycin as previously described. Following dissection, each pair of lungs was carefully instilled with approximately 100 – 150 µl of Optimal Cutting Temperature compound (OCT; Sakura Finetek, Torrance, CA) diluted 1 : 1 (v/v) in normal saline to inflate the alveoli. Care was taken to avoid over-distension and leakage of the OCT out of alveoli. The distal trachea was then tied off and the lungs fast frozen in a mould containing neat OCT surrounded by liquid nitrogen. Tissues were stored at -80°C until used.

To prepare lung slices for elution, each OCT-embedded block of lung tissue was mounted on a pre-chilled chuck in a cryostat maintained at -22°C. Contiguous lobar sections of 10-µm thickness were cut and approximately 200 lung slices were placed in each well of a 12-well microtitre plate kept at the same temperature. Lung slices were then immersed in 1.5 ml of elution buffer containing DMEM, 0.25% BSA and 30 nM neutrophil elastase (Calbiochem, Nottingham, UK) or plasmin (Sigma Chemical Co., Poole, UK) for two hours at 37°C. Enzymatic reactions were stopped by adding 0.5 mM PMSF and 5 µM ilomastat. Eluates were removed by centrifugation and concentrated down to 800 µl by centrifugal filtration (Centricon® Filter Units, Millipore, Watford, UK). The volume of each concentrated eluate was then halved, with one part kept for measuring spontaneously active TGF-β and the remainder for heat activation of latent TGF-β (to assess the total TGF-β pool). Latent TGF-β activation was achieved by heat treatment at 80°C for 10 minutes in the presence of proteinase inhibitors (0.5 mM PMSF and 5 µM ilomastat). Active TGF-β was then measured using the MLEC/PAI-1 luciferase assay.

Steps were also taken to estimate the total area of lung sections used for the elution experiment. During the microtoming process, every 10th slice of sectioned lung was adhered on to a poly-L-lysine-coated slide for haematoxylin staining. This enabled the lung area used for eluting TGF-β in each mouse to be estimated using computerised image analysis. In essence, the sum of area of lung measured per slide and the number of slides approximated to the total area of lung from which TGF-β was eluted. As each lung lobe assumes a three-dimensional shape and the transected area varies as the lobe is sequentially cut, this approach maximised the accuracy in estimating the parenchymal elution area.

2.5.vii Optimisation experiments

In some experiments, samples of BAL fluid and homogenised lung tissue were pretreated *in vitro* to activate latent TGF-β prior to the MLEC PAI-1/luciferase assay. This involved heating aliquots of the appropriate samples at 80°C to liberate mature TGF-β from its latency associated peptide. Preliminary time course experiments were performed to determine the optimal duration for recovering maximal amounts of active TGF-β. In order to minimise the loss of TGF-β activity due to proteolytic degradation during the optimisation process, a number of non-selective and selective protease inhibitors were also incorporated into the experiments. These included a Protease Inhibitor Cocktail (Roche Molecular Biochemicals, UK), PMSF to inhibit serine proteinases and Ilomastat, a matrix metalloproteinase inhibitor. Experiments were also performed to assess whether these compounds interfered with either mink lung epithelial cell viability or luciferase activity. All measurements were made in triplicate.

2.5.viii TGF-β immunohistochemistry

TGF-β immunolabeling in paraffin-embedded lung sections was performed using two different antibodies, one directed against latent TGF-β1 (LAP-TGF-β1) and the other against active TGF-β1. Serial paraffin-embedded lung sections were cut, adhered to poly-L-lysine-coated slides and heated in 1% citrate buffer (pH 6.0) for 10 minutes to uncover antigenic sites. Antigen unmasking was not performed prior to staining for latent TGF-β to avoid activating latent cytokine. Specimens were then incubated in 3% hydrogen peroxide to quench endogenous peroxidase activity and pre-blocked using normal serum derived from the host of the secondary antibody.

Primary antibody labeling was performed overnight at 4°C using either a goat polyclonal anti-human LAP-TGF-β1 antibody (R&D Systems, Abingdon, UK), a rabbit monoclonal antibody raised against the amino-terminal 30 amino acids of mature (active) TGF-β (LC1-30, gift from Dr. Kathleen Flanders, National Cancer Institute, Bethesda, MD) or isotype-specific control antibodies (Dako Limited, Cambridgeshire, UK). The optimal working dilution of each primary antibody was determined by preliminary dose response staining procedures. The appropriate peroxidase-conjugated biotinylated second layer antibodies were then added, and the chromogenic

product obtained following hydrolysis of 3,3'-diaminobenzidine (DAB). Haematoxylin counterstaining was performed to distinguish cells from extracellular material. The results were examined using a Zeiss K300 Image Analysis system (Zeiss, Gottingen, Germany).

2.6 Statistical analysis

All data are expressed as mean ± standard error of the mean (SEM), unless otherwise indicated. For lung collagen measurements, each treatment group contained at least eight animals. Differences between treatment groups were analysed using one-way analysis of variance by ranks (ANOVA) (Prism®, GraphPad Software Inc., San Diego, CA). Post-test analysis of mean values between groups was performed using Dunn's Multiple Comparison Test. Comparisons of non-parametric indices in which there were fewer variables in each group (e.g. lung permeability assays) were performed using unpaired student's t-test. In each case, probability (P) values of < 0.05 were considered statistically significant.

CHAPTER THREE

BLEOMYCIN INSTILLATION INDUCES A PULMONARY FIBROTIC RESPONSE IN 129S6/SvEv MICE

3.1 Background

3.1.i Bleomycin

The bleomycin family of compounds was first purified by Umezawa and colleagues from a culture broth of *Streptomyces verticillus* moulds as copper chelates (Umezawa et al., 1966). Although all bleomycin glycopeptides share the same molecular backbone, substitution of the terminal amine moiety produces a class of related but different compounds (Figure 3.1). All bleomycins contain a bithiazole component that binds DNA, a metal binding domain that contains pyrimidine and imidazole components, and a carbohydrate moiety. Bleomycin exists in several different isoforms. Commercial preparations of bleomycin consist predominantly of bleomycin A_2 (55 - 70%) and B_2 (25 - 32%) (Hay et al., 1990).

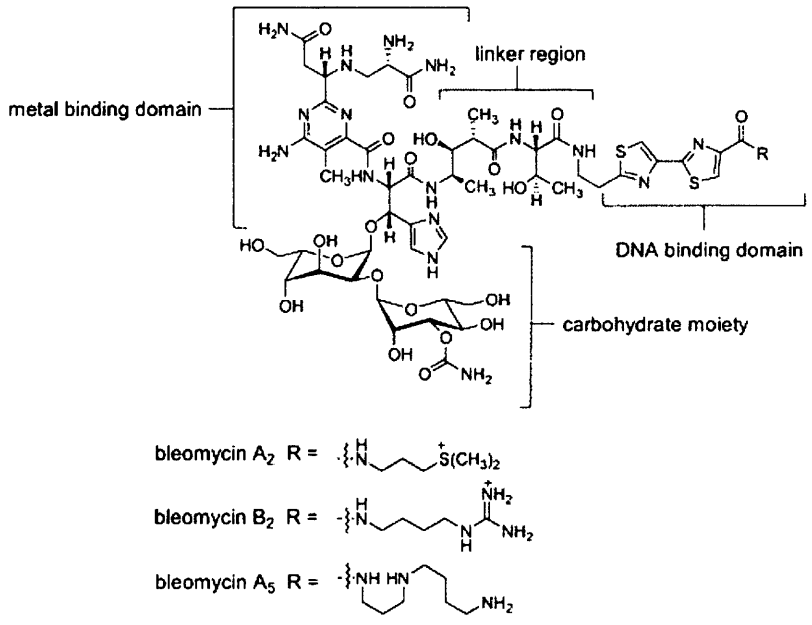

Figure 3.1

Bleomycin was originally purified to be used as an anti-tumour drug. Over the years, it has been incorporated into treatment regimens for germ-cell tumours, non-Hodgkin's lymphoma, Kaposi's sarcoma and various squamous cell carcinomas affecting the oesophagus, external genitalia as well as the head and neck (Thrall and Scalise, 1995). The pharmacologic preference for bleomycin has been primarily attributed to its lack of immunosuppressive effects on the bone marrow and

peripheral blood cells. However, bleomycin administration has been associated with the development of lung toxicity, and in particular, an increased predisposition to pulmonary fibrosis. This adverse potential has been exploited for inducing experimental lung fibrosis in a variety of animal species.

Bleomycin exerts its anti-tumour properties by inducing cytotoxicity resulting from sequence-selective oxidative damage of DNA and RNA (Hecht, 1986). It concomitantly binds a metal ion (most commonly bivalent iron, Fe^{++}) and DNA in the presence of oxygen. In the case of iron, rapid oxidation of Fe^{++} to Fe^{+++} results in the reduction of oxygen and the generation of free hydroxyl radicals. 'Activated' bleomycin consisting of a drug-iron-oxygen hybrid then removes the 4'-hydrogen atom from the C4' of the deoxyribose moiety of a pyrimidine 3' to a guanine, initiating a pathway that ends with the formation of a pyrimidine propenal and subsequent DNA strand scission (Giloni et al., 1981). Bleomycin can also produce lipid peroxidation which may be an additional means for inducing pulmonary toxicity independent of and additional to DNA scission (Hay et al., 1990).

3.1.ii The bleomycin model of pulmonary fibrosis

Bleomycin was first reported to induce pneumonitis in dogs in 1971 (Fleischmann et al., 1971). Since then, a large body of information has been collected on bleomycin-induced pulmonary fibrosis in various animal species. Early experiments employed parenteral (intravenous and intramuscular) routes of bleomycin delivery. In addition to mice and rats, dogs, hamsters, rabbits, pheasants and non-human primates have also been used (reviewed in Thrall and Scalise, 1995). Snider and colleagues were the first to utilise the single-dose intratracheal technique of bleomycin instillation (Snider et al., 1978), an approach that has gained popularity ever since.

Although single-dose intratracheal instillation of bleomycin is convenient, the lung fibrosis that results may be short lasting or limited in extent, particularly when low dose bleomycin is used. To circumvent this, bleomycin has also been administered either as a continuous infusion or as repeated boluses over time. Indeed, mice receiving bleomycin from a subcutaneous osmotic pump over a one-week period appear to have increased lung collagen and more evenly distributed fibrotic lesions compared to animals receiving daily bleomycin injections of an equal cumulative dose (Harrison and Lazo, 1987). The number of repeat injections of bleomycin also influences the

development of fibrosis. Hamsters given three weekly intratracheal instillations of the drug develop more extensive and progressive fibrotic changes compared to control animals that receive only a single dose (Zia et al., 1992).

Increased rates of collagen synthesis are detectable as early as three to four days following the intratracheal instillation of bleomycin (Thrall and Scalise, 1995; Van Hoozen et al., 2000). Rates of collagen synthesis may remain elevated for up to 14 days as described in studies using mice (Sikic et al., 1978), rats (Phan et al., 1980) and rabbits (Laurent and McAnulty, 1983). In most studies, maximal collagen accumulation is usually quantified in the subacute stage of lung repair, typically between 21 to 28 days following bleomycin administration. In the majority of cases, total lung collagen levels will have reached a plateau by 30 days, by which time collagen synthesis rates would also have normalised. Data from several bleomycin time course studies in mice have shown that maximal lung collagen content, as quantified by hydroxyproline concentration, may persist for up to 60 days following instillation of the drug (Shahzeidi et al., 1993; Munger et al., 1999; Zuo et al., 2002). Similar trends have been reported in studies using rats. In these rodents, increases in lung collagen content may remain elevated for at least 60 days and occasionally up to 120 days after the administration of bleomycin (Thrall et al., 1979; Hesterberg et al., 1981 and Borzone et al., 2001). In some, chronic fibrosis may be accompanied by focal loss of interstitial connective tissue, a process similar to the remodelling of alveoli in emphysema (Borzone et al., 2001). In other words, histologic differences may exist between mice and rats treated with bleomycin, but these characteristics remain incompletely characterised.

In the main, histopathological features of pulmonary fibrosis induced by bleomycin include alveolar epithelial damage, type II pneumocyte hyperplasia, fibroblast activation and proliferation, as well as expansion of the pulmonary interstitium due to increased extracellular matrix deposition (Grande et al., 1998). Localised increases in fibroblast numbers are often evident in peribronchiolar locations and in areas adjacent to alveolar buds (Adler et al., 1986). Many of these features are also present in pulmonary fibrosis induced by other agents. In bleomycin-induced lung damage, extracellular matrix remodelling often coincides with active alveolar repair and may also occur before cellular inflammation has completely subsided.

3.2 Results

3.2.i Biochemical (collagen) response to IT bleomycin instillation

Lungs from untreated adult wild type (WT) mice contained 1.64 ± 0.06 mg total collagen. Intratracheal instillation of single doses of 0.025U, 0.05U and 0.10U bleomycin increased this amount in a dose-dependent manner when measured at 30 days following instillation (**figure 1a**). Total lung collagen increased by 1.5-fold (2.39 ± 0.19 mg vs. 1.64 ± 0.06 mg, $P < 0.05$), 1.8-fold (2.95 ± 0.25 mg vs. 1.64 ± 0.06 mg, $P < 0.001$) and 2.0-fold (3.24 ± 0.23 mg vs. 1.64 ± 0.06 mg, $P < 0.001$) at the 0.025U, 0.05U and 0.10U doses of bleomycin respectively.

When assessed over a more detailed time course, increases in lung collagen content were appreciable as early as 15 days following the instillation of bleomycin (**figure 1b**). At this time point, the mean value of total lung collagen was higher than that in untreated controls (2.29 ± 0.11 mg vs. 1.64 ± 0.06 mg, $P < 0.01$) but lower than the amount of total lung collagen measured at 30 days (2.29 ± 0.11mg vs. 2.95 ± 0.25 mg, $P < 0.01$). Maximal collagen accumulation was evident by 30 days following bleomycin instillation, as no further increases in collagen content were detected beyond this point (studies were performed up to 60 days).

3.2.ii Morphologic changes in the lung following bleomycin instillation

Low power microscopic examination of WT lungs obtained 30 days following bleomycin instillation showed characteristic architectural abnormalities of damaged and fibrotic areas interspersed with relatively normal lung parenchyma (**figure 2a**). The degree of alveolar distortion within such fibrotic lesions was better appreciated at higher magnification (**figure 2c**). Expansion of the interstitial space by dense collagen-rich matrix contributed to the loss of alveolar airspaces. In areas of established fibrosis, some of these collagenous fibrils penetrated into the distorted alveoli and obliterated their lumen. In other places, the fibrillar bundles within the alveolar walls appeared looser, suggesting more recent matrix deposition. The abundance, distribution and size of blood vessels were not assessed in this study. In general, however, fewer capillaries were seen

1 (a)

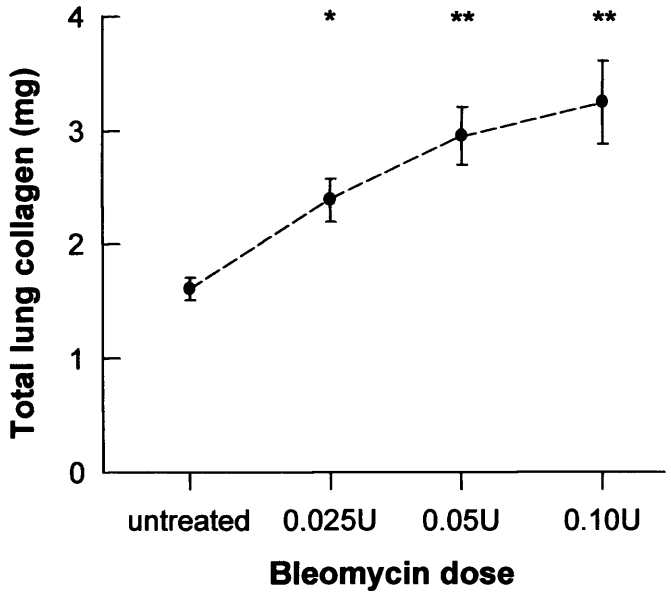

1 (b)

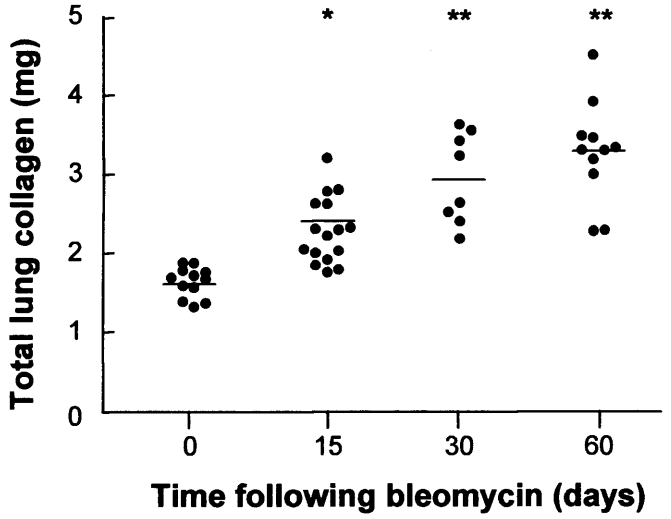

Figure 1. **Characterisation of bleomycin-induced collagen response in adult wild type 129S6/SvEv mice.**

1 (a). **Collagen dose response.** Total lung collagen was measured in adult 129/SvEv mice 30 days following intratracheal instillation of 0.025 unit, 0.05 unit or 0.10 unit bleomycin. Values are expressed as mean ± SEM. * *P < 0.01 (vs. untreated),* ** *P < 0.001 (vs. untreated)*

1 (b). **Collagen time course.** Total lung collagen was analysed at baseline (day 0, untreated group) and 15, 30 and 60 days following instillation of the 0.05 unit bleomycin dose. Values are expressed as mean ± SEM. * *P < 0.01 (vs. untreated),* ** *P < 0.001 (vs. untreated)*

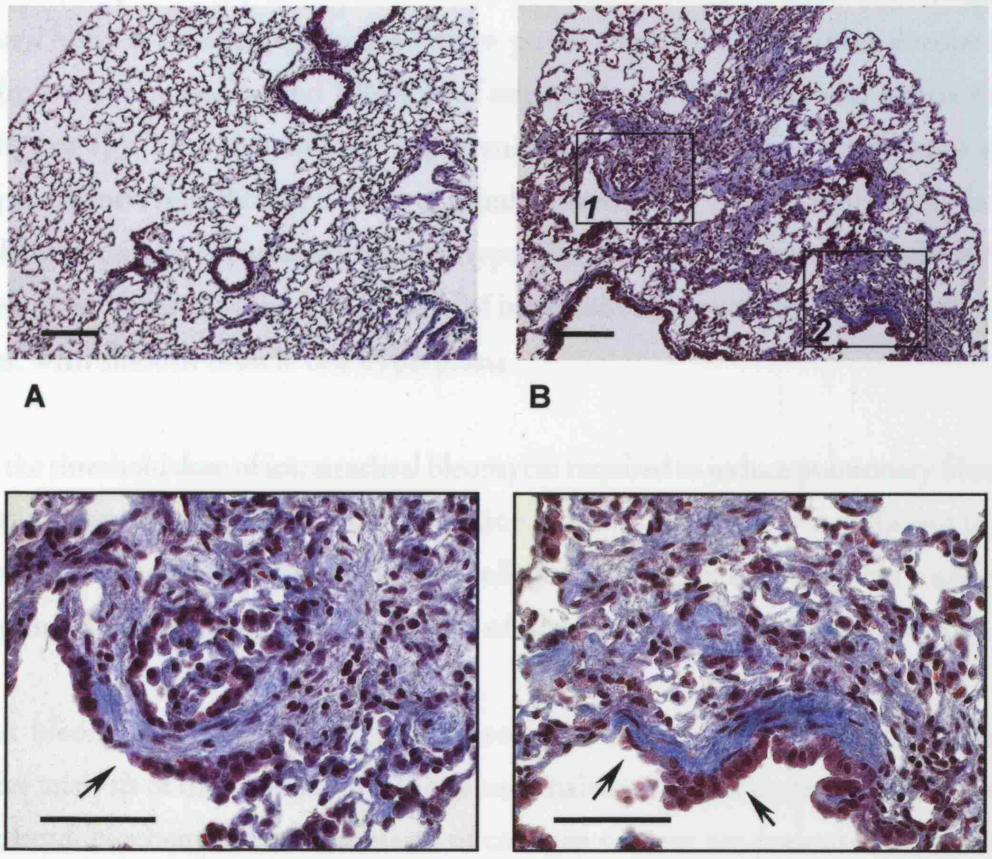

***Figure 2.* Histological changes in lungs of wild type 129S6/SvEv mice 30 days following the instillation of either saline or 0.05 U bleomycin.**

2 (a). Saline instillation, low power (*bar*, 250 μm).

2 (b). 0.05 U bleomycin instillation, low power (*bar*, 250 μm).

2 (c). Enlarged inset from panel B (box 1) showing reactive epithelium (arrow) with underlying collagenous matrix (*bar*, 100 μm).

2 (d). Enlarged bottom inset from panel B (box 2) showing mesenchymal cells and increased matrix underneath a damaged and hyperplastic epithelial lining (arrows) (*bar*, 100 μm).

Masson's trichrome stain

within areas of fibrotic change compared to areas of normal lung. Lungs from saline-treated controls appeared strikingly different (**figure 2b**). Focal areas of fibrotic change were absent in these specimens. When viewed at higher magnification, these alveoli appeared open with relatively normal interstitial thickness between adjacent airspaces (**figure 2d**).

Specific features of pulmonary fibrosis were identified in the bleomycin-treated WT lungs. Areas of subpleural fibrosis were best appreciated at low power (**figure 3a**) while intra-alveolar fibrosis resulting from the compression and 'filling in' of normal alveoli by extracellular matrix were also evident (**figure 3b**). This morphologic appearance has previously been described as alveolar 'collapse-induration'. In addition, clusters of spindle-shaped cells, most likely fibroblasts and/or myofibroblasts were also apparent adjacent to hyperplastic epithelia (**figures 3c and 3d**). Groups of these cells were closely associated with areas of increased collagenous matrix deposition and in some cases, with smooth muscle cell hyperplasia.

Although the threshold dose of intratracheal bleomycin required to induce pulmonary fibrosis was not formally assessed, intratracheal administration of the 0.025U dose was sufficient to elicit a fibrotic response. In addition to increased lung collagen content, WT mice treated with this dose of bleomycin displayed morphologic evidence of fibrotic lung remodelling (**figure 4**).

Given that bleomycin-induced pulmonary fibrosis has a heterogenous distribution, a semi-quantitative analysis of the architectural lung abnormalities was not undertaken in the current studies. Instead, biochemical measurements of collagen content are presented in this thesis as quantitative data. Morphologic observations are offered as a qualitative assessment of changes characteristic of pulmonary fibrosis.

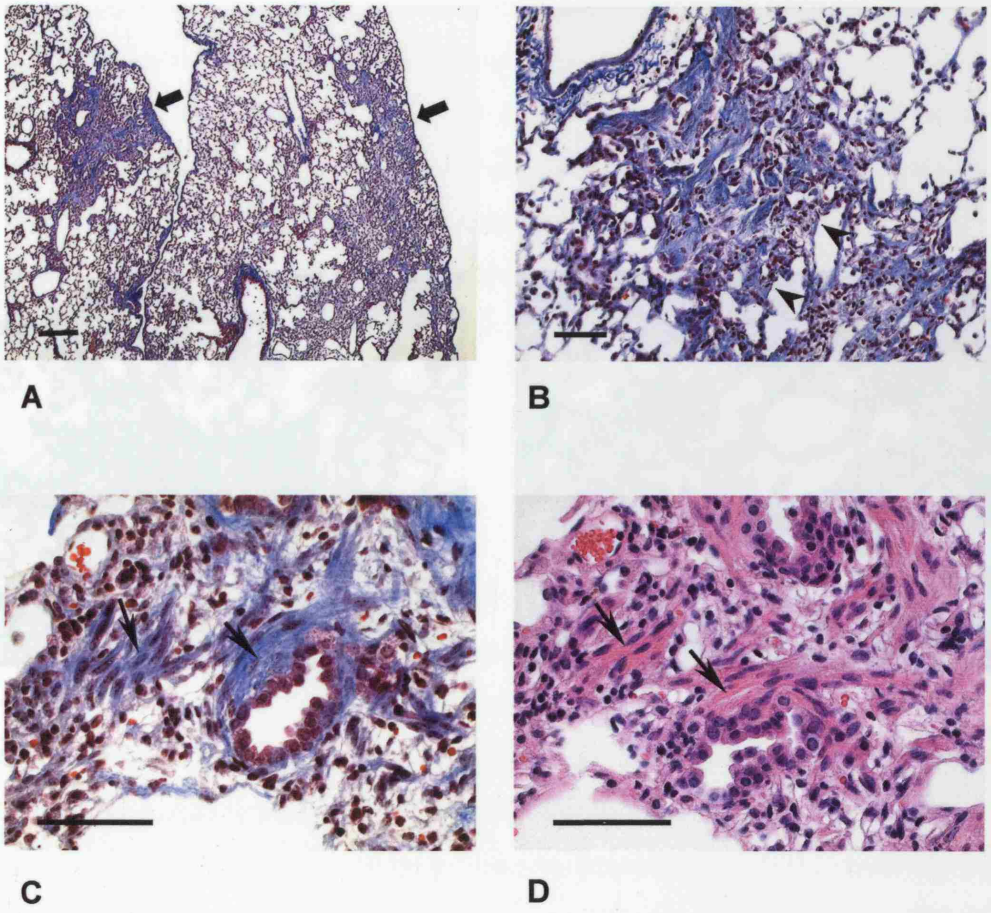

Figure 3. **Specific histolopathologic features in WT lungs 30 days following instillation of 0.05U bleomycin.**

3 (a). Subpleural fibrosis. Larger areas of fibrosis typically extend to the limits of the visceral lung pleura (arrows). *Masson's trichrome stain* (*bar*, 200 μm).

3 (b). An area of intra-alveolar fibrosis demarcated by denuded alveolar basement membrane (arrowheads). *Masson's trichrome stain* (*bar*, 100 μm).

3 (c) and (d). Sequential sections stained with Masson's trichrome (c) and haematoxylin and eosin (d) highlighting two fibroblast-rich lesions (arrows) associated with increased extracellular matrix deposition (*bar*, 100 μm).

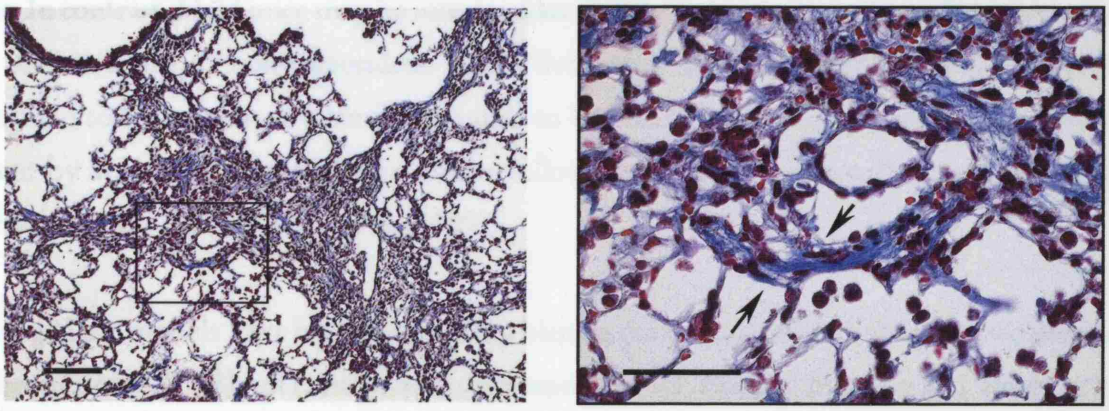

***Figure 4.* 0.025 U bleomycin is sufficient to induce fibrotic scar formation in the lungs of WT mice.**

30 days following the instillation of 0.025 U bleomycin, lungs of wild type 129S6/SvEv mice develop areas of pulmonary fibrosis. Interstitial thickening and airspace obliteration can be appreciated at low power (left panel). Collagen-rich bands are evident at higher magnification (right panel, between arrows).

Masson's trichrome stain

Left panel: *bar*, 250 μm; right panel: *bar*, 100 μm.

3.3 Discussion

3.3.i Bleomycin induces pulmonary fibrosis in 129S6/SvEv mice

Susceptibility to bleomycin-induced pulmonary toxicity in mice is subject to genetic influence. Differential susceptibility is manifested as a phenotypic variability in the degree of pulmonary fibrosis among different strains of mice. However, the biological basis for this susceptibility is incompletely understood. As a rule, most mice bearing the H-2b haplotype such as the C57BL/6 strain tend to be bleomycin-sensitive and are therefore described as fibrosis-prone. In contrast, H-2d mice may be intermediate (DBA/2) or non-responders (BALB/c). H-2k mice (C3Hf/Kam) are non-responders. 129S6/SvEv mice are H-2b and thus would be predicted to respond to bleomycin in a similar manner to C57BL/6 mice which increase lung collagen content by approximately 40% two weeks following intratracheal instillation of bleomycin (Shahzeidi et al., 1993; Madtes et al., 1999).

Mouse genetic models have been used to map bleomycin susceptibility linkage to two loci: one on chromosome 17, Blmpf1, and one on chromosome 11, Blmpf2 (Haston and Travis, 1997; Haston et al., 2002). A putative interaction between these two loci is believed to determine the abundance of lung tissue bleomycin hydrolase, an endogenous thiol-dependent aminopeptidase that metabolises bleomycin to its inactive by-products (Haston et al., 2002). The same enzyme has been implicated as an MHC class I epitope-processing proteinase with the ability to modulate bleomycin-induced inflammatory injury within the lung. Of note, fibrosis-prone C57BL/6N mice have decreased levels of bleomycin hydrolase compared to fibrosis-resistant BALB/c animals (Filderman and Lazo, 1991). Other fibrosis susceptibility genes have been localised to the TNF-α cluster on chromosome 6 and the FGF-10 cluster on chromosome 13, but their functional significance is not known (Barth et al., 2002). Moreover, the physiologic basis upon which these factors may influence the sensitivity of 129S6/SvEv mice to the fibrotic effects of bleomycin remains unclear. Specifically, the ability of neutrophil elastase in cleaving bleomycin hydrolase is not known.

In general, mice with a 129/Sv background develop pulmonary fibrosis in response to bleomycin administration (Munger et al., 1999; Zuo et al., 2002) or asbestos fibre inhalation (Warshamana et al., 2002). They have also been shown to develop fibroproliferative lung injury following ozone

inhalation (Savov et al., 2004). However, the degree of susceptibility to fibrosis may vary within the generic 129/Sv group. At least seven different parental 129 substrains exist. Although all strains are haplotypically H-2b and are predicted to be fibrosis-prone, the rate and/or persistence of fibrogenesis may vary when compared to other H-2b strains. For example, lesions of asbestos-related fibrosis form earlier in C57BL/6 compared to 129/Sv mice (Warshamana et al., 2002), but histological changes of bleomycin-induced pulmonary fibrosis tend to persist longer in 129/Sv mice than in age-matched C57BL/6 mice (Morris et al., 2002).

The current studies demonstrate the susceptibility of 129S6/SvEv mice to bleomycin-induced pulmonary fibrosis. These animals consistently developed a two-fold increase in lung collagen content as well as characteristic histological changes of pulmonary fibrosis. The use of hydroxyproline as a marker of collagen accumulation is reliable and widely adopted (reviewed in McAnulty and Laurent, 1995). Following bleomycin instillation, a time-dependent increase in lung hydroxyproline content in 129S6/SvEv mice was observed. This increase reached a maximal level 30 days following bleomycin administration. At this time point, the morphologic changes of pulmonary fibrosis were extensive and reproducible, and at a dose of 0.05U, the mortality rate remained relatively low.

Previous studies using mice belonging to various 129 substrains have shown that bleomycin-induced increases in lung collagen may vary between 50% to 100% above baseline values over a 30-day experimental period (Munger et al., 1999; Betsuyaku et al., 2000; Zuo et al., 2002). This variability may be due to a number of factors such as substrain differences, the dose of bleomycin employed or the age of mice subjected to treatment. Munger and colleagues used the Sv/129ter ('susceptible to teratomas') substrain, whereas Zuo and co-workers used the SvJ (Jackson Laboratories), and not SvEv, mice. The dose of bleomycin used in the current studies was 0.05U which equates to 3 mg/kg of body weight for a typical 30 g mouse. Others have previously used an equivalent dose in the same strain of mice (Munger et al., 1999; Betsuyaku et al., 2000). Some of the animals used in the current study were older than three months of age. The possibility that older mice may have a greater predilection for accumulating more collagen following bleomycin-induced lung injury, while appreciated, was not directly tested.

The minimal dose of bleomycin required to induce pulmonary fibrosis in mice is not known. In the present study, a dose of 0.025U bleomycin was sufficient to induce parenchymal lung fibrosis albeit to a lesser degree than that produced by the standard 0.05U dose. A smaller number of

fibrotic lesions developed in response to 0.025 U bleomycin, and these lesions tended to be smaller in size. True threshold studies to determine the lowest dose of intratracheal bleomycin needed for inducing lung fibrosis in the 129S6/SvEv mice were beyond the scope of this thesis.

The maximal collagen response following bleomycin instillation was established in the present study. Total lung collagen measured two weeks after bleomycin instillation was 50% greater than saline values and comparable to the 45% increase described by Munger and colleagues in a previous study (Munger et al., 1999). By 30 days following instillation, the bleomycin-induced mean increase in lung collagen was approximately 80% greater than saline controls. This value was higher than that reported in the Munger study.

At the 60-day time point, however, comparable increases in bleomycin-induced lung collagen were observed between this and the previous study. Detailed studies aimed at comparing the kinetics of collagen deposition in 129/Sv and other mouse strains are limited (Morris et al., 2002).

3.3.ii The bleomycin model replicates key pathological features of pulmonary fibrosis in humans

Bleomycin administration is the most widely used animal model of experimental pulmonary fibrosis (Thrall and Scalise, 1995). The histological characteristics it produces in murine lungs are particularly well described (Grande et al., 1998). Changes in pulmonary extracellular matrix turnover resulting from bleomycin treatment are quantitative and reproducible. The natural history of bleomycin-induced lung damage combines an antecedent lung injury that culminates in fibroproliferative lung repair via a series of overlapping pathological stages. The bleomycin model has been used extensively to elucidate *in vivo* mechanisms of the pathogenesis of pulmonary fibrosis, including fibrogenic growth factor activation (Munger et al., 1999), molecular control of critical signaling pathways (Zhao et al., 2002) and the potential for using gene transfer approaches to modulate the fibrotic response (Kolb et al., 2001b). More recently, the bleomycin model has been used to demonstrate that bone marrow-derived progenitor cells can traffic to the lung to participate in tissue repair (Hashimoto et al., 2003; Phillips et al., 2004). Bleomycin was chosen over other experimental models of pulmonary fibrosis (such as fluorescein isothiocyanate or FITC, cadmium chloride and particulate silica) because of its consistency in inducing widespread and progressive fibrosis that morphologically mimics lung

fibrosis in the human lung. The development of durable non-granulomatous fibroblast-rich lesions places bleomycin at an advantage over FITC and silica. The propensity of cadmium for inducing a mixed fibrotic and emphysematous reaction in animals (Snider et al., 1988) made it unsuitable as a model for the current studies.

In the present studies, the initial changes of lung damage following bleomycin injection were localised predominantly to peribronchial sites. As time passed, the intensity of fibroproliferative changes increased, and in particular, the extent of interstitial and intra-alveolar collagen deposition increased. Several of the morphological changes in bleomycin-treated wild type 129S6/SvEv mice merit further discussion. Firstly, although areas of pulmonary fibrosis were scattered throughout the lung parenchyma, a marked subpleural distribution was evident in most of the animals examined. A similar pattern of lung fibrosis has been described in other strains of mice exposed to bleomycin, in particular C57BL/6 mice. These changes may reflect underlying mechanisms that concentrate the activation of fibrogenic mediators at focal sites thus localising the fibroproliferative response. One other possibility is that blood-derived leukocytes may be preferentially retained in certain regions due to the production and release of proteinases that aid in their transmigration. Enzymes such as matrilysin (Li et al., 2002) or neutrophil elastase (McGarry Houghton et al., 2002), may act by targeting specific substrates in the alveolar-capillary barrier that have a bearing on neutrophil accumulation. Interestingly, a subpleural predilection of pulmonary fibrosis also features in certain forms of human interstitial lung disease such as idiopathic pulmonary fibrosis. However, the pathological reasons for this are unclear.

Secondly, the increased deposition of interstitial collagen, together with the proliferation of mesenchymal cells in the same compartment, resulted in the 'filling in' of airspaces by connective tissue. In many areas of distorted alveolar architecture, intra-alveolar buds became more prominent. This particular feature has also been described in a number of clinically important fibrotic lung disorders (Usuki and Fukuda, 1995). In such disorders, intra-alveolar buds may be found in association with fibroblast-rich cell clusters that are termed fibroblastic foci in lungs affected by IPF (Karzenstein and Myers, 1998). In the current studies, groups of spindle-shaped mesenchymal cells resembling fibroblasts/myofibroblasts that were closely associated with increased collagen-rich matrix were identified. These cells may form the murine equivalent of fibroblastic foci. Fibroblastic-dominant scars have previously been described in the bleomycin model of pulmonary fibrosis in mice (Zhang et al., 1994) and in rodents that develop lung fibrosis as a result of overexpressing transforming growth factor-beta (TGF-β) (Sime et al., 1997). In the

bleomycin model, most cells expressing procollagen mRNA also express α-smooth muscle actin, a myofibroblast marker.

However, caution has been raised in recent years regarding the validity of bleomycin-induced pulmonary fibrosis as a model of IPF (Borzone et al., 2001). The contentions are that the accelerated development of fibrosis following bleomycin exposure does not mimic the tempo of the disease in humans and that bleomycin-induced fibrosis is not pathologically compatible to IPF due to the lack of fibroblastic foci. Furthermore, there is a suspicion that the fibrotic changes induced by bleomycin may co-exist with focal matrix loss and alveolar enlargement mimicking localised emphysema when lung damage progresses beyond a certain point in time (Borzone et al., 2001). However, such changes have not been reported in other studies. They may simply represent an anomaly of parenchymal lung repair, a process in which focal loss of matrix components is not entirely unexpected. Fibroblast-rich lesions were certainly evident in the lungs of bleomycin-treated WT mice in the current studies. Alveolar tissue breakdown was not an appreciable histological feature even at 60 days.

In truth, bleomycin-induced pulmonary fibrosis in mice may be regarded as long lasting in relation to the lifespan of these animals. In many cases, collagen-rich fibrous scarring can persist up to 120 days following administration of the drug in rats (Borzone et al., 2001) and up to at least 90 days in hamsters (Zia et al., 1992). In the current studies, pulmonary fibrosis was present in the lungs of wild type mice 60 days after a single instillation of 0.05U bleomycin. The induction of fibroblasts and myofibroblasts, together with upregulation of collagen deposition and interstitial tissue scarring, provide evidence of the progressive nature of bleomycin-induced pulmonary fibrosis. This is crucial because the majority of clinically important fibrosing lung diseases are also characterised by a progressive tendency. While 'fibroblastic foci' may be sparser in bleomycin-treated mice compared to humans with established IPF, the current experiments show that fibroblast-rich lesions in the lung parenchyma can certainly be produced by bleomycin administration. Overall, the fibrotic response to bleomycin instillation is highly consistent within a large batch of mice. Only a small degree of inter-group variability in terms of collagen quantification was observed. While bleomycin instillation does not provide an experimental equivalent of IPF, the strengths of this particular model lie in its robust reproducibility and versatility. IPF is only one example of human pulmonary fibrosis, itself a collection of myriad disorders unified pathologically by common morphologic and biochemical changes.

CHAPTER FOUR

NEUTROPHIL ELASTASE PLAYS A CRUCIAL ROLE IN THE DEVELOPMENT OF BLEOMYCIN-INDUCED PULMONARY FIBROSIS

4.1 Background

4.1.i Neutrophils as effector cells in fibrotic lung disease

Loss of homeostatic control of neutrophil proteinases and oxidative radicals has been linked to the development of chronic lung disorders such as chronic obstructive pulmonary disease and cystic fibrosis. Neutrophil-derived proteinases can target a wide range of alveolar, vascular and extracellular matrix substrates. While the majority of these reactions destroy lung tissue, neutrophilic inflammation has also been implicated in the parenchymal damage that accompanies fibroproliferative lung remodelling. Inappropriate recruitment and retention of neutrophils in the distal lung are recognised phenomena in fibrotic lung disorders. However, a mechanistic explanation for their pathogenicity in pulmonary fibrosis remains elusive.

Increased numbers of pulmonary neutrophils are present in idiopathic pulmonary fibrosis (Borok et al., 1990), hypersensitivity pneumonitis (Pardo et al., 2000), pulmonary asbestosis and silicosis as well as lung fibrosis associated with rheumatoid arthritis (Crystal et al., 1981). Lung neutrophilia and increased expression of neutrophil chemoattractants have also been observed in the inherited (familial) form of IPF (Bitterman et al., 1986). Up to two-thirds of patients with IPF may have increased numbers of alveolar neutrophils, as assessed by bronchoalveolar lavage (BAL Cooperative Group Steering Committee, 1990). Declining numbers of pulmonary neutrophils have previously been associated with an improved response to corticosteroid therapy in the same condition (Rudd et al., 1981). Evidence that a positive correlation may exist between BAL fluid neutrophilia and the clinical severity, as well as the radiologic extent, of IPF has also been reported (Wells et al., 1998). Pathologically, the importance of episodic neutrophil-mediated alveolitis to progressive or uncontrolled fibroproliferation in the pathogenesis of IPF has been postulated (Gross and Hunninghake, 2001).

One reason for the chronic accumulation of neutrophils in IPF may be alveolar mucus retention, also known as mucostasis. This phenomenon is thought to account for the increased sequestration of neutrophils within cysts of honeycombed lungs in IPF (Schwarz and Brown, 2002) and could explain why such lungs might be more prone to neutrophil-mediated injury. Architectural changes in chronic IPF are characteristically described as being temporally

heterogeneous. The co-existence of established fibrosis and more recently deposited ECM raises the possibility that recurrent bouts of localised parenchymal injury might be pathogenically important to the development of pulmonary fibrosis (Gross and Hunninghake, 2001). Low-level sequential lung injury mediated by neutrophils could produce precisely such abnormalities in the lung architecture. Accumulation of neutrophils within the lung would help perpetuate alveolar injury and promote matrix repair in discrete areas of lung parenchyma. On this basis, neutrophil trapping may be a crucial pathogenetic event in fibrotic interstitial ECM remodelling.

In the bleomycin model, the accumulation of neutrophils at various stages of lung injury and fibrosis is well recognised (Haslett et al., 1989; Serrano-Mollar et al., 2002). The development of bleomycin-induced pulmonary fibrosis has specifically been correlated to the duration of neutrophil activation as assessed metabolically by (^{18}F)-2-fluoro-2-deoxy-D-glucose uptake in lung parenchyma (Jones et al., 1998). Moreover, increased levels of macrophage inflammatory protein (MIP)-2, a murine functional homologue of IL-8, have been observed in mice developing bleomycin-induced pneumopathy (Keane et al., 1999). Neutralisation of MIP-2 in the lung leads to decreased neutrophil infiltration and attenuation of the subsequent pulmonary fibrotic response. Furthermore, the administration of pentoxifylline, N-acetylcysteine and pirfenidone has been shown to limit the extent of bleomycin-induced fibrosis, in part by decreasing neutrophil inflammation (Entzian et al., 1998; Hagiwara et al., 2000; Iyer et al., 2000). More recently, confinement of neutrophils to perivascular areas due to a failure of alveolar infiltration has been proposed as a mechanism contributing to the resistance of matrilysin-deficient mice to bleomycin-induced pulmonary fibrosis (Li et al., 2002). However, the precise role of neutrophils in either initiating or propagating pulmonary fibrotic response is far from resolved.

4.1.ii Neutrophil elastase : potential pathogenic roles in pulmonary fibrosis

The uncontrolled proteolytic capacity of neutrophil elastase has long been associated with the development and exacerbation of pulmonary emphysema (Senior et al., 1977; Snider 1991). As a result, the vast majority of studies concerning this proteinase in lung disease have focused on its role in destructive lung disorders of one form or another. Over the past fifteen years, a pathologic function for neutrophil elastase in the development of pulmonary fibrosis has been reported in clinical and experimental studies. Early reports of elevated antiproteinases in BAL fluid and serum from patients with interstitial lung disease indirectly suggested that an

increased neutrophil elastase burden might be prevalent in such conditions (Sibille, 1988; Mordelet-Dambrine et al., 1988). More specifically, increased neutrophil elastase activity has been correlated to diminished lung function and increased disease severity of IPF (Borzi et al., 1993). To some extent, these observations have been corroborated by more recent studies. For example, Cailes and colleagues showed that BAL fluid from patients with IPF contained greater quantities of immunoreactive neutrophil elastase (Cailes et al., 1996). In addition, neutrophil elastase : alpha-1 proteinase inhibitor complex levels were higher in the lungs of these patients than in healthy controls. In a separate study of patients with IPF, Yamanouchi and co-workers correlated increased levels of neutrophil elastase : alpha-1 proteinase inhibitor complex with increased amounts of lactate dehydrogenase (LDH) in BAL fluid and lowered arterial oxygen tension (PaO_2) (Yamanouchi et al., 1998).

Levels of α1-PI : neutrophil elastase complexes in alveolar fluid provide an estimate of neutrophil elastase burden within the lung. In individuals with IPF, levels of these complexes range between 600 and 1000 ng/ml in BAL fluid (Obayashi et al., 1997; Yamanouchi et al., 1998). These quantities represent a six-to-seven fold increase over levels of α1-PI : neutrophil elastase complexes typically found in healthy non-smoking individuals. Perhaps more importantly, immunoreactive neutrophil elastase has been identified in areas of established interstitial and honeycomb fibrosis in the lungs of individuals with IPF (Hojo et al., 1997; Obayashi et al, 1997). This observation indicates that neutrophil elastase is present in measurable quantities at sites of fibrotic lung matrix remodelling. Despite these findings, a correlation between raised levels of neutrophil elastase in either the BAL or tissue compartment and the pathological development of fibrosis in the lung has not been established.

Animal studies have provided additional insights into the role of neutrophil elastase in pulmonary fibrosis. The increased predisposition of beige mice, a strain genetically defective in neutrophil degranulation, to bleomycin-induced pulmonary fibrosis was initially interpreted as proof that elastase-mediated ECM degradation was critical for preventing fibrogenesis (Phan et al., 1983). However, it is now clear that neutrophils derived from these animals possess and release a pro-elastase compound from which the biologically active enzyme can readily form. This finding has called into question previous assumptions that neutrophil elastase plays a solely degradative role in chronic lung diseases characterised by aberrant ECM turnover (Cavarra et al., 1997). Since then, a number of controlled *in vivo* studies have demonstrated the ability of physiological (SLPI and α1-PI) and synthetic (ONO-5046) inhibitors of neutrophil elastase to abrogate the fibrotic response

following bleomycin exposure (Nagai et al., 1992; Mitsuhashi et al., 1996; Taooka et al., 1997; Maeda et al., 1999). Nonetheless, these data derive from approaches that inhibit the activity of released neutrophil elastase in the extracellular milieu. Crucially, mechanistic explanations of how neutrophil elastase may promote the pulmonary fibrotic process remain unknown. Similarly, the potential benefits of these compounds in human pulmonary fibrosis have not been tested.

In this chapter, the importance of neutrophil elastase in the development of bleomycin-induced pulmonary fibrosis will be addressed. The approach taken will compare *in vivo* changes in lung histopathology and collagen accumulation in gene-targeted mice that are deficient in neutrophil elastase and wild type mice with normal levels of the enzyme.

4.2 Results

4.2.i Development of neutrophil elastase-deficient ($NE^{-/-}$) mice

Initial studies were aimed at characterising the general features of untreated WT and $NE^{-/-}$ mice housed under conventional conditions and provided access to food and water *ad libitum*. Like their WT counterparts, $NE^{-/-}$ mice mated and reproduced normally. $NE^{-/-}$ progeny did not exhibit obvious developmental abnormalities and had normal feeding habits. Representative animals from each colony were screened for infections according to the University College London Biological Services policies. Overt signs of opportunistic infection were not apparent in any of the animals studied. When matched for age and gender, WT and $NE^{-/-}$ mice had similar growth rates (**figure 5a**), with comparable fractional weight gain between monthly intervals. Full growth, in terms of final body weight and size, was attained in both genotypes between four to six months of age. Overall, untreated male animals (both WT and $NE^{-/-}$) tended to be heavier than female mice at three, four-and-a-half and six months of age. Unexplained mortality in untreated mice was not noticeable in either group of animals.

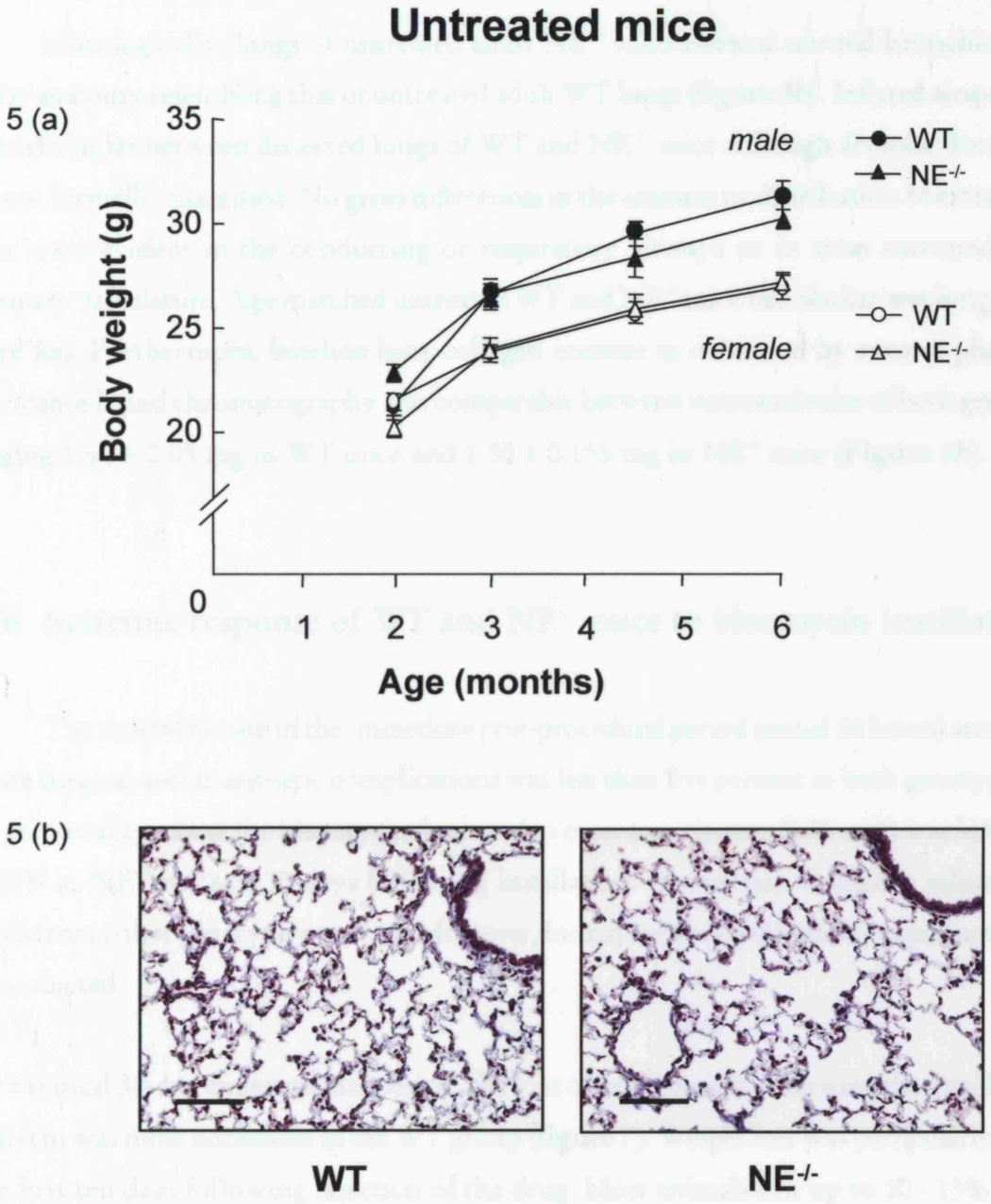

***Figure 5.* Untreated WT and NE$^{-/-}$ mice share similar baseline characteristics.**

5 (a). WT and NE$^{-/-}$ mice provided with access to food and water *ad libitum* and housed under standard conditions were weighed at two, three, four-and-a half and six months of age (n = 10 in each group).

5 (b). Representative light photomicrographs showing the alveolar architecture in untreated 12-week old WT and NE$^{-/-}$ mice. Masson's trichrome staining. *Bar*, 100 μm.

4.2.ii Pulmonary characteristics of healthy adult $NE^{-/-}$ mice

Histologically, lungs of untreated adult $NE^{-/-}$ mice showed normal bronchiolar and alveolar anatomy resembling that of untreated adult WT lungs (**figure 5b**). Inflated airspace sizes appeared similar between dissected lungs of WT and $NE^{-/-}$ mice although alveolar dimensions were not formally quantified. No gross differences in the amount or distribution of extracellular matrix were evident in the conducting or respiratory airways or in areas surrounding the pulmonary vasculature. Age-matched untreated WT and $NE^{-/-}$ mice had similar wet lung weights (**figure 6a**). Furthermore, baseline lung collagen content as measured by reverse phase high performance liquid chromatography was comparable between untreated mice of both genotypes, averaging 1.64 ± 0.05 mg in WT mice and 1.50 ± 0.155 mg in $NE^{-/-}$ mice (**Figure 6b**).

4.2.iii Systemic response of WT and $NE^{-/-}$ mice to bleomycin instillation

The mortality rate in the immediate post-procedural period (initial 24 hours) attributable to acute surgical and anaesthetic complications was less than five percent in both genotypes. The average mortality rate at the bleomycin dose used in most experiments (0.05 unit) was 36% in WT and 23% in $NE^{-/-}$ mice at 30 days following instillation. In contrast, deaths in saline-treated animals from either genotype were rare. However, formal survival and lethality experiments were not conducted.

Over a typical 30-day experimental period, the loss of body weight following the instillation of bleomycin was most noticeable in the WT group (**figure 7**). Weight loss was particularly marked in the first ten days following injection of the drug. Most animals lost up to 10 - 15% of their initial body weight. Mice gained weight from 14 days onward so that by the end of the experimental period, bleomycin-treated WT mice were at their initial body weights. In comparison, mean weight loss in bleomycin-treated $NE^{-/-}$ mice remained consistently under five percent of the starting value for the first ten days following injection of the drug. The plateau effect – apparent lack of normal growth – in bleomycin-treated $NE^{-/-}$ mice between days 14 and 30 may be explained by averaging. When analysed separately, some individual animals did gain weight at normal rates. When considered as a group, weight was regained from 7 days onward so that by the end of the experimental period, bleomycin-treated $NE^{-/-}$ mice were also at their initial body weights. The average body weights of surviving bleomycin-treated WT and $NE^{-/-}$ mice were

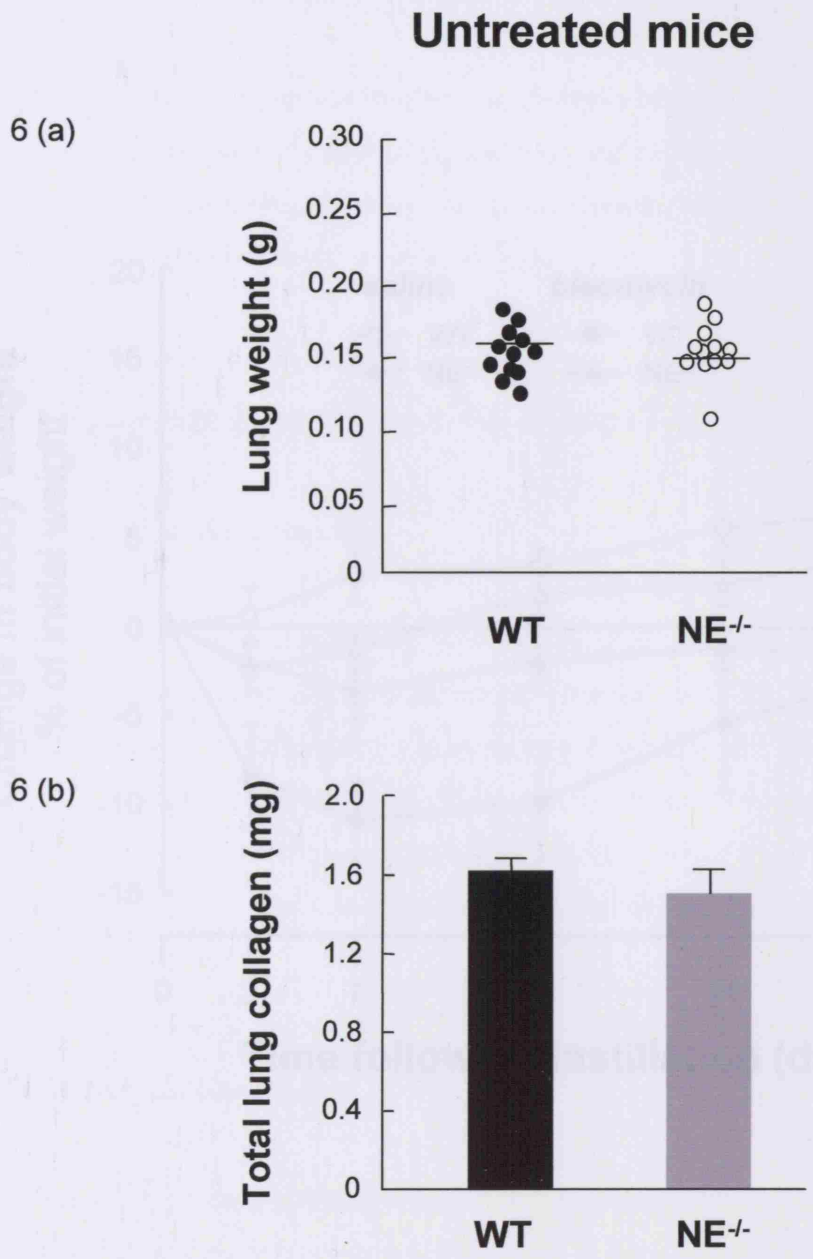

Figure 6. **Average lung weight and collagen content are not different in untreated WT and NE$^{-/-}$ mice.**

6 (a). Wet weights of unperfused and unlavaged lungs from untreated WT and NE$^{-/-}$ mice were compared following removal from the thoracic cavity. Bar denotes the group (n = 12) mean.

6 (b). Total lung collagen in an aliquot of the lung samples weighed in Panel A was determined by measuring hydroxyproline content using reverse-phase HPLC. Values are expressed as mean total lung collagen ± SEM (n = 12 in each group).

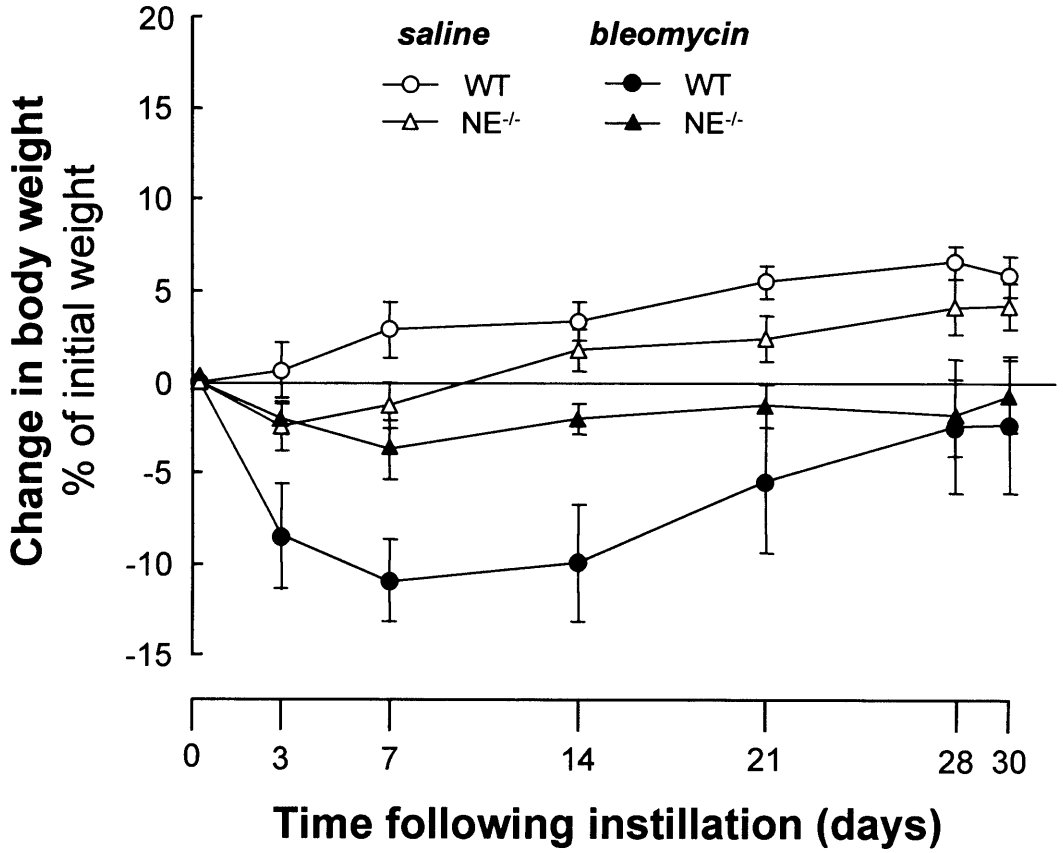

Figure 7. **Bleomycin response: changes in body weight.**

Bleomycin (0.05 unit / animal) or saline was instilled intratracheally into adult WT or $NE^{-/-}$ mice. Body weights were measured prior to treatment and at regular intervals until sacrifice 30 days later. Results are expressed as percentage change in weight compared to baseline body weight (day 0). Each point represents the mean ± SEM (n = 8 in each group).

comparable at the time of sacrifice. In saline-treated animals, average body weight increased by approximately five percent in both WT and $NE^{-/-}$ genotypes over the 30 day experimental period.

Throughout the study, moderate to severe decreases in body mass were associated with signs of increased morbidity such as ruffled fur, anorexia and reduced response to tactile stimuli. In adherence with guidelines stipulated in the animal procedures project license, mice that lost more than 20% of initial body weight were sacrificed.

4.2.iv Changes in lung collagen following IT bleomycin instillation

4.2.iv.i Bleomycin dose response

Lung collagen accumulation was evaluated in WT and $NE^{-/-}$ mice following the intratracheal instillation of two different doses of bleomycin (0.05 U and 0.10 U). Both doses of the drug induced a two-fold increase in lung collagen content in WT mice 30 days after instillation (**Figure 8**). In contrast, neither dose of bleomycin induced any significant increase in lung collagen in $NE^{-/-}$ mice over the same period of time. However, a trend suggesting that the higher dose of bleomycin (0.01 U) was associated with a slight increase in measured collagen content was observed.

4.2.iv.ii Bleomycin time course

Total lung collagen in untreated WT and $NE^{-/-}$ mice averaged 1.6 ± 0.12 mg per animal. Over a period of 60 days following the instillation of 0.05U bleomycin, lung collagen in saline-treated WT and $NE^{-/-}$ mice did not differ from untreated values at any point and averaged between 1.5 and 1.8 mg per animal (**figure 9**). Instillation of 0.05U bleomycin into WT mice induced an increase in total lung collagen over saline-treated values by 1.5-fold (2.29 ± 0.11 mg vs. 1.54 ± 0.07 mg, $P < 0.0001$), 1.8-fold (2.95 ± 0.25 mg vs. 1.61 ± 0.12 mg, $P < 0.001$) and 1.8-fold (3.274 ± 0.23 mg vs. 1.83 ± 0.07 mg, $P < 0.01$) at 15, 30 and 60 days respectively. In contrast, total lung collagen in bleomycin-treated $NE^{-/-}$ mice was not significantly altered from saline-treated values at any time point.

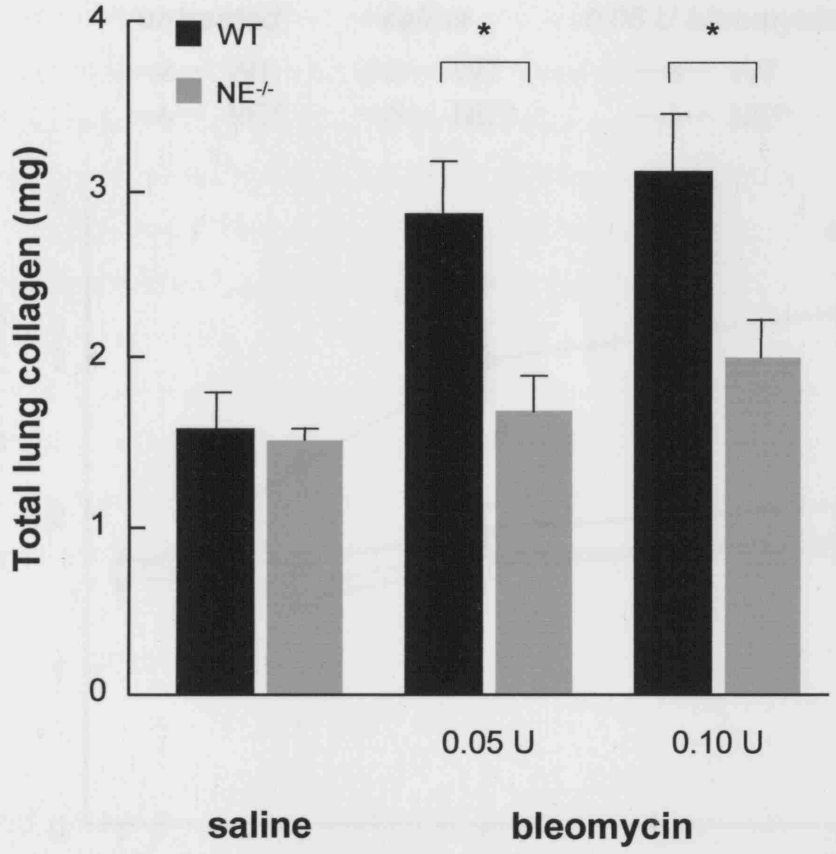

Figure 8. **Bleomycin response: changes in lung collagen content.**

Total lung collagen was determined by the measurement of hydroxyproline content 30 days following the instillation of either saline, 0.05 unit or 0.10 unit bleomycin. Values are expressed as mean total lung collagen ± SEM (n = 7 in each treatment group). * *P < 0.001*

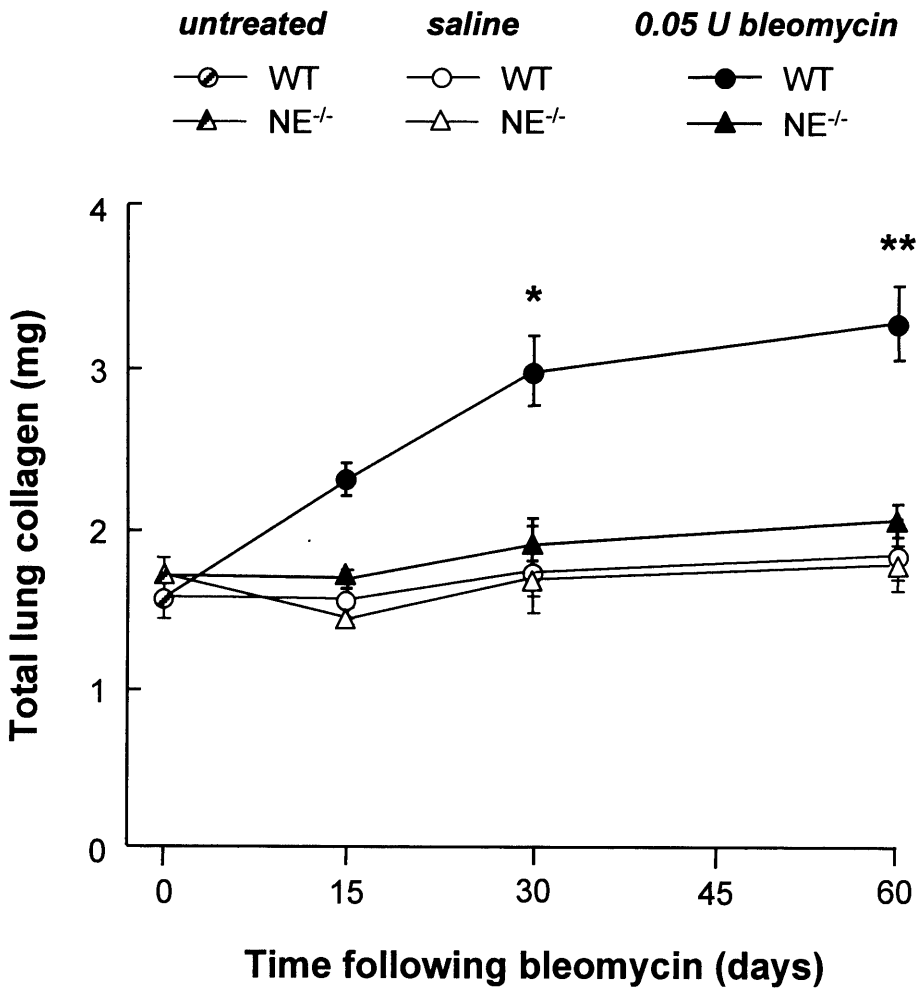

Figure 9. **Lung collagen remains unchanged in bleomycin-treated $NE^{-/-}$ animals.**

Total lung collagen was analysed in WT and $NE^{-/-}$ lung homogenates at baseline (0), 15, 30 and 60 days following instillation of either saline (open symbols) or 0.05 unit bleomycin (closed symbols). Values are expressed as mean total lung collagen ± SEM (minimum of eight animals per treatment group). * *P < 0.0001 (bleomycin-treated WT vs. bleomycin-treated $NE^{-/-}$ animals),* ** *P < 0.005 (bleomycin-treated WT vs. bleomycin-treated $NE^{-/-}$ animals).*

4.2.v Morphologic differences in ECM accumulation following bleomycin instillation

As described in the previous chapter, histological examination of lungs from WT mice showed large areas of interstitial fibrosis 30 days following the instillation of 0.05 U bleomycin. At low power, these fibrotic lesions were seen to intersperse with smaller areas of unaffected lung. The obliteration of alveoli within such fibrotic areas resulted from a combination of interstitial thickening from collagen accumulation (blue thread-like staining, *left* middle panel, **figure 10**), increased presence of mesenchymal cells and the development of intra-alveolar fibrosis (best appreciated at high power, *left* bottom panel, **figure 10**). Increased numbers of inflammatory cells were also prominent within damaged alveoli and at the periphery of fibrotic scars. Occasionally, clusters of spindle-shaped cells resembling fibroblasts / myofibroblasts in areas of dense matrix deposition were apparent at higher magnification (*left* bottom panel). By comparison, fibrotic lesions were scarce in the lungs of bleomycin-treated $NE^{-/-}$ mice. In these specimens, the most characteristic morphologic features were increased numbers of inflammatory cells and areas of apposed alveolar walls due to collapsed alveoli, mimicking foci of alveolar induration (*right* middle and lower panels). True interstitial thickening due to fibrotic collagen accumulation was not apparent. Normal lung architecture was present in all saline-treated WT and $NE^{-/-}$ lungs examined (top panels).

Lung histology was also examined 15 days following the instillation of 0.05 U bleomycin. At this time point, lungs of WT mice contained characteristic, albeit smaller, areas of increased extracellular matrix than lungs that were collected at 30 days (**figure 11**). These changes were predominantly peribronchiolar and pericapillary in location. In contrast, corresponding sections from bleomycin-treated $NE^{-/-}$ lungs had minimal changes of ECM deposition. When followed up to 60 days, large areas of bleomycin-treated WT lungs had areas of increased matrix accumulation, and inflammatory hypercellularity (left panels, **figure 12**). These changes were easily appreciated at low power. The presence of collagen-rich ECM arranged in a ribbon-like pattern was particularly prominent around the terminal airways and blood vessels. By comparison, lungs from $NE^{-/-}$ mice had more focal deposition of matrix (right panels, **figure 12**) as well as areas where groups of alveoli had collapsed. Loss of alveolar walls leading to airspace coalescence was also evident in bleomycin-treated $NE^{-/-}$ mice.

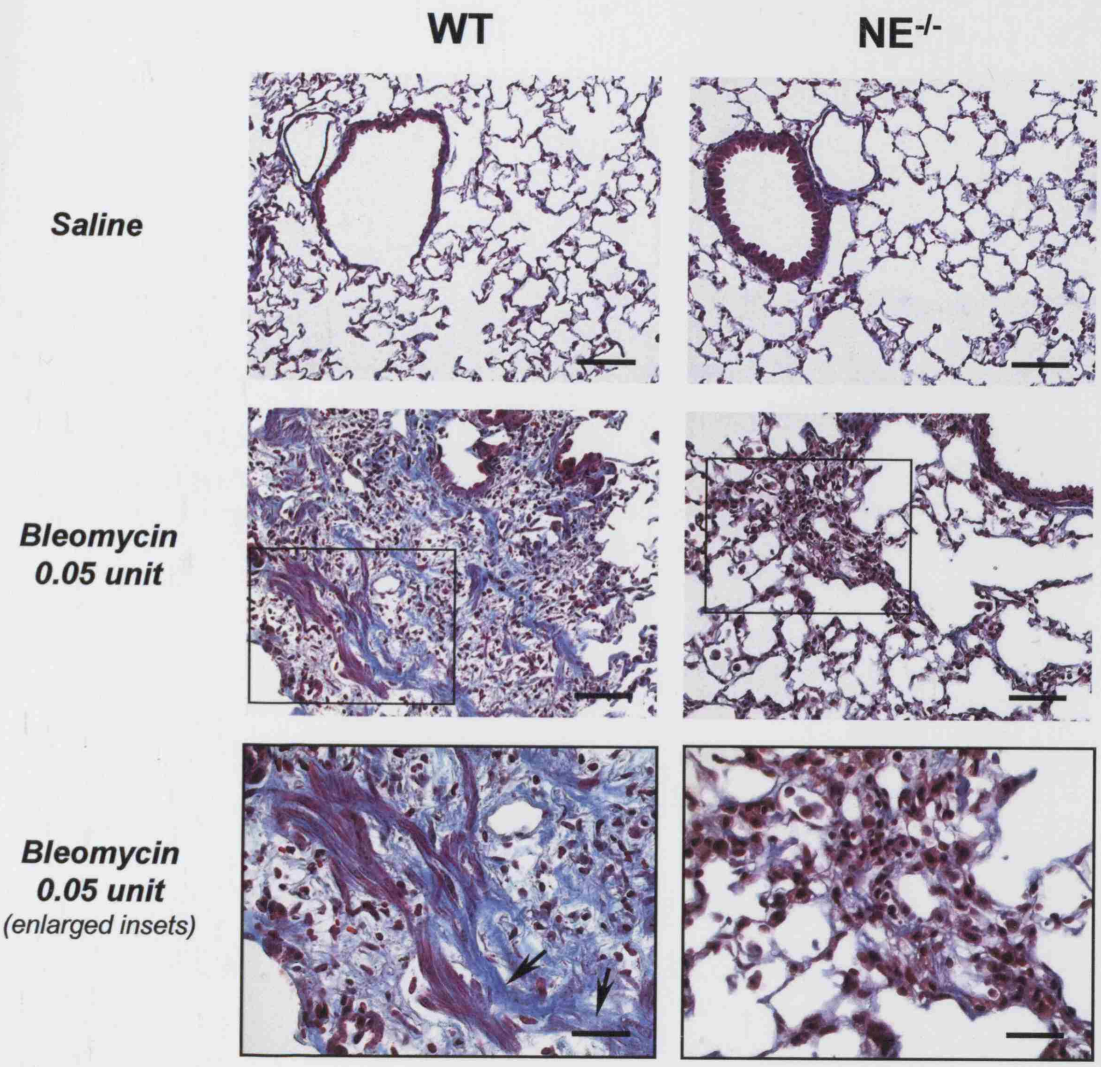

Figure 10. **Lung histology 30 days following IT saline or bleomycin.**

Top panels, Representative photomicrographs of lung sections from WT and $NE^{-/-}$ mice 30 days following saline instillation. *Bar*, 100 μm.

Middle panels, Low power photomicrographs of WT and $NE^{-/-}$ lungs 30 days following 0.05 U bleomycin instillation. *Bar*, 100 μm.

Bottom panels, Detail of insets from middle panels showing magnified areas of bleomycin injury in WT (left) and $NE^{-/-}$ (right) lung. Arrows indicate blue-staining collagen-rich extracellular matrix. *Bar*, 50 μm.

Masson's trichrome stain

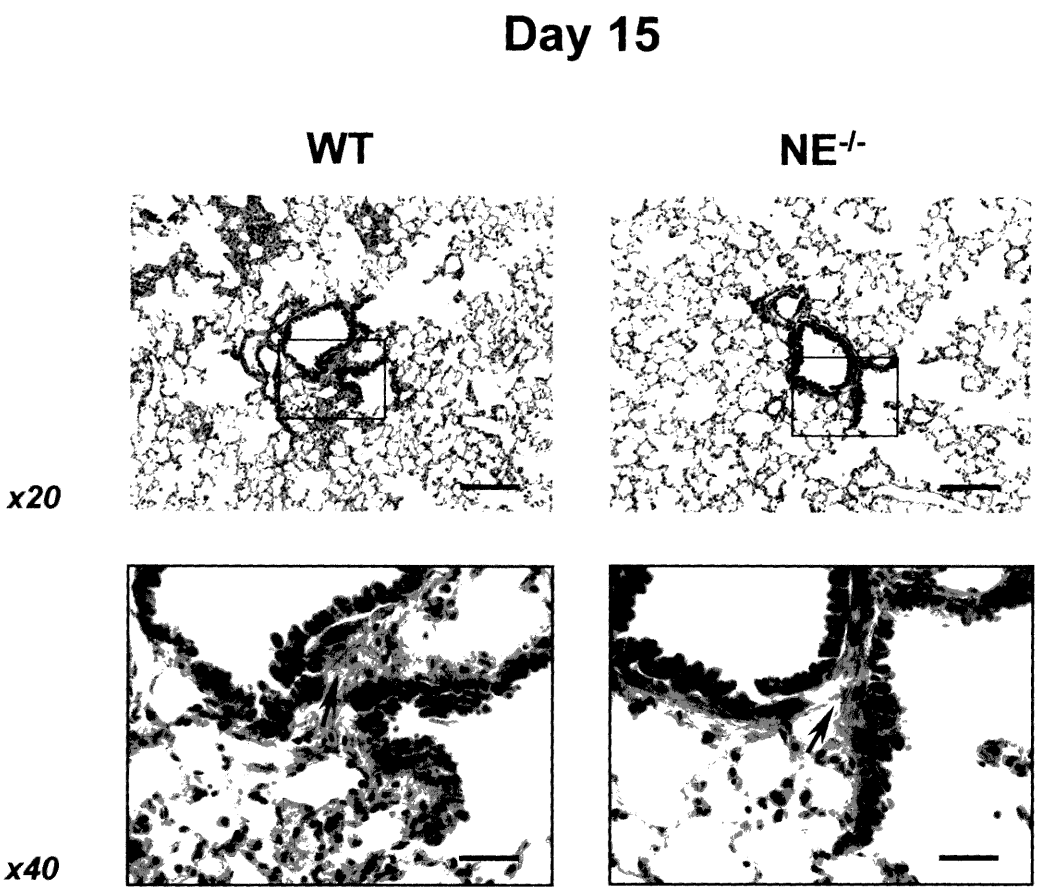

Figure 11. **Lung histology 15 days following IT bleomycin.**

Top panels, Low-power photomicrographs showing lung parenchymal architecture from WT and $NE^{-/-}$ mice 15 days following 0.05U bleomycin instillation. *Bar*, 100 μm.

Lower panels, Magnified areas with arrows indicating increased peribronchiolar matrix deposition in WT (left panel) and $NE^{-/-}$ (right panel) lungs. *Bar*, 100 μm.

Masson's trichrome stain

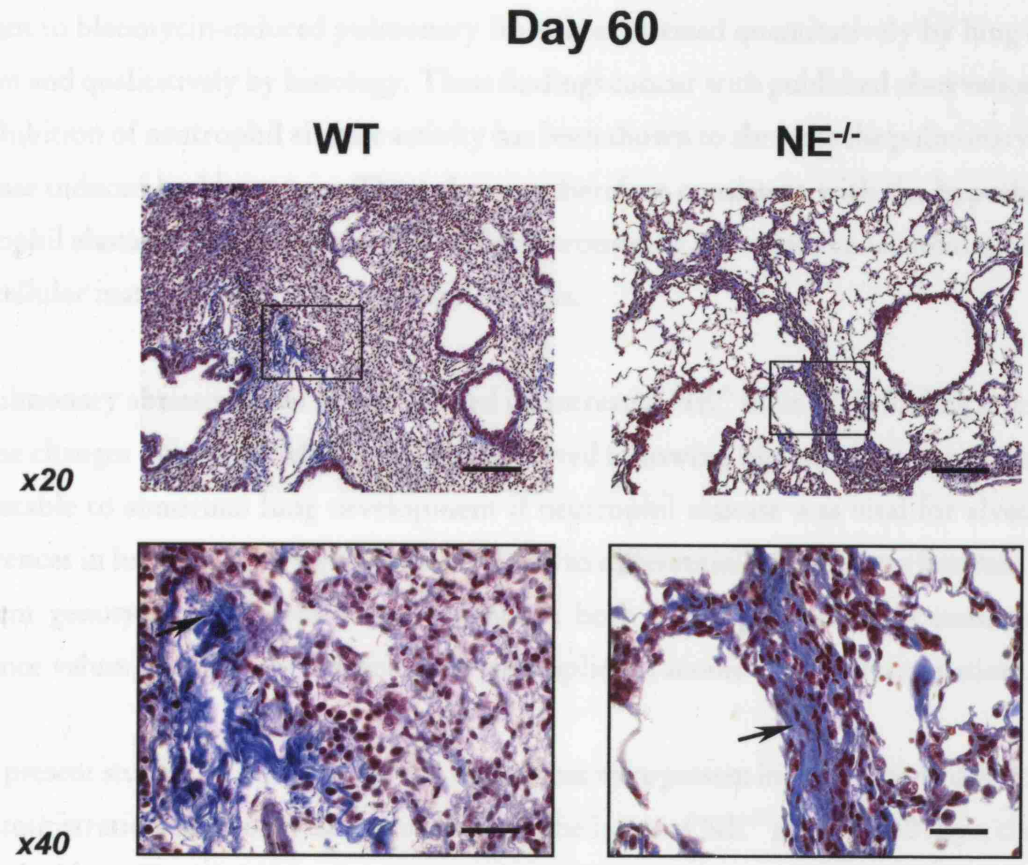

Figure 12. **Lung histology 60 days following IT bleomycin.**

Top panels, Low-power photomicrographs of WT and $NE^{-/-}$ lungs taken 60 days following instillation of 0.05U bleomycin. *Bar*, 100 μm.

Lower panels, Detail of insets from top panels showing areas of increased collagen-rich matrix deposition (arrows). *Bar*, 100 μm.

Masson's trichrome stain

4.3 Discussion

The current studies demonstrate that $NE^{-/-}$ mice bred on a 129S6/SvEv background are resistant to bleomycin-induced pulmonary fibrosis as assessed quantitatively by lung collagen content and qualitatively by histology. These findings concur with published observations where the inhibition of neutrophil elastase activity has been shown to abrogate the pulmonary fibrotic response induced by bleomycin. These data are therefore consistent with the hypothesis that neutrophil elastase can play a pathogenic role in promoting the excessive accumulation of lung extracellular matrix typical of pulmonary fibrosis.

No pulmonary abnormalities were observed in untreated $NE^{-/-}$ mice. This finding is important because changes in lung ECM remodelling observed following bleomycin treatment might be attributable to abnormal lung development if neutrophil elastase was vital for alveogenesis. Differences in lung collagen were also not related to differential growth rates between the two different genotypes. Moreover, lung weights in both genotypes were also consistent with reference values provided by the commercial supplier (Taconic website information).

In the present studies, pulmonary fibrotic lesions that were present in WT lungs 15 days following the administration of bleomycin were absent in the lungs of $NE^{-/-}$ mice. By 30 days, the lack of established lung fibrosis in bleomycin-treated $NE^{-/-}$ mice was obvious. Unlike older studies that relied on exogenously administered compounds to temporarily neutralise neutrophil elastase activity, the use of $NE^{-/-}$ mice provides the opportunity to assess the role of neutrophil elastase in bleomycin-induced pulmonary fibrosis in a state of true deficiency. Administration of neutrophil elastase inhibitors (α1-PI, SLPI and ONO-5046) has been associated with reductions in BAL fluid neutrophil numbers, the extent of lung tissue neutrophil inflammation and the degree of pulmonary fibrosis in bleomycin-treated animals (Nagai et al., 1992; Mitsuhashi et al., 1996; Taooka et al., 1997). However, such studies have important limitations. For example, exogenously administered inhibitors have a very short half-life *in vivo*. In one study, blood α1-PI levels did not remain elevated for any substantial time following the administration of purified anti-proteinase but declined over the course of bleomycin-induced lung injury (Nagai et al., 1992). More specifically, exogenous α1-PI failed to suppress elastolytic activity attributable to neutrophil elastase. On the other hand, ONO-5046 succeeded in attenuating lung collagen accumulation when given in the first 14 days following bleomycin administration but not when administered

beyond this period (Taooka et al., 1997). In all these studies, the interpretation of findings was limited by the individual pharmacokinetic considerations of each inhibitor which were not extensively studied in any of the reports. Doubts about the extent of neutrophil elastase inhibition in these earlier studies are not pertinent to the current experiments because the use of genetically engineered $NE^{-/-}$ mice means that this serine proteinase is completely absent from birth.

Two previous studies, one in rats (Thrall et al., 1981) and the other in hamsters (Clark and Kuhn III, 1982) have studied bleomycin-induced pulmonary fibrosis following peripheral blood neutrophil depletion using anti-serum. In each, depletion of the pulmonary neutrophil pool was incomplete and neutrophils were observed in the lungs of 'depleted' animals soon after the instillation of bleomycin. By a week following bleomycin administration, circulating neutrophils were back to their pre-treatment numbers. Not surprisingly, the development of pulmonary fibrosis failed to be retarded using such an approach. This strategy is clearly unsuited for delineating the role of the neutrophil in a complex disorder such as pulmonary fibrosis or any model that requires neutrophil elastase inhibition for days or weeks rather than hours.

The resistance of $NE^{-/-}$ mice to bleomycin-induced pulmonary fibrosis in the current was not the result of a delayed fibrotic response. Lung collagen content in these animals consistently failed to increase even when analysis was carried out 60 days after the drug was instilled. Despite lacking a collagen response, the lungs of $NE^{-/-}$ mice treated with bleomycin were not histologically normal. In addition to isolated areas of thickened interstitial septae, there was evidence of alveolar collapse where the walls of adjacent alveoli had become apposed. At low power, these areas produced an image of linear scars through the parenchymal field. However, areas of true fibrotic scarring or fibroblast-associated matrix accumulation were scarce. The presence of prominent inflammation in $NE^{-/-}$ lungs 60 days following bleomycin instillation was a consistent observation. Although the true reason for this is not known, it is possible that prolonged neutrophil infiltration may be one consequence of enhanced IL-8-mediated neutrophil chemotaxis arising from a lack neutrophil elastase proteolytic activity (Leavell et al., 1996). Moreover, degradation of native (and hence, unused) α1-AT in the lungs of $NE^{-/-}$ mice by matrix metalloproteinases such as MMP-12 may generate fragments that are chemotactic for neutrophils (Banda et al., 1988).

Some sections of bleomycin-treated $NE^{-/-}$ lungs showed evidence of epithelial denudation, apposition of alveolar walls and increased intra-alveolar cellularity. This combination of pathological findings has previously been described by Burkhardt as alveolar 'collapse-induration'

(Burkhardt, 1989), although Kaufmann first coined the term in the early part of the last century (Kaufmann, 1922). The supposition that it might represent a pre-fibrotic phenomenon remains unresolved. In a study of histologic patterns of pulmonary fibrosis, Basset and colleagues distinguished different types of architectural changes, including one that they called 'obliterative changes' (Basset et al., 1986). They noted that this particular process was frequently associated with alveolar atelectasis and collapsed mural components. Fukuda and colleagues also described the importance of fused and coalesced alveolar walls during the progression of lung damage as a precursor of fibrotic lung remodelling (Fukuda et al., 1987). If such changes are indeed pre-fibrotic in nature, their presence in bleomycin-treated $NE^{-/-}$ lungs that do not succumb to eventual fibrosis suggests that the fibroproliferative process is inefficient and somehow terminates prematurely in animals that lack neutrophil elastase. Precisely how this is achieved or regulated is yet unknown.

It is possible that pulmonary fibrosis develops very early in bleomycin-treated $NE^{-/-}$ mice and resolves just as rapidly. The notion that pulmonary fibrosis might be a reversible process is not without clinical basis. In patients with post-transplant organising pneumonia associated with bronchiolitis obliterans, intra-alveolar fibrosis can resolve with prolonged corticosteroid therapy (Katzenstein et al., 1986). Likewise, pulmonary fibrosis that complicates the acute respiratory distress syndrome is thought to be reversible in some survivors of this devastating condition, as lung function parameters can improve over time (McHugh et al., 1994). Thus, lung repair may only confer lasting structural effects in the setting of extensive injury in which the fibrotic tissue that forms prevents alveolar re-expansion. Although there was evidence of alveolar injury in bleomycin-treated $NE^{-/-}$ mice, this damage appeared to be insufficient to generate the collagenised scars that lead to permanent pulmonary fibrosis.

The phenotype of $NE^{-/-}$ mice in the bleomycin model as characterised in this thesis indicates that compensatory mechanisms to replace the absence of neutrophil elastase activity cannot induce fibrosis within 60 days of lung injury. It also suggests that neutrophil elastase activity may play a dual role in initiating and propagating bleomycin-induced pulmonary fibrosis. There are several possible mechanisms by which this enzyme may act to promote fibroproliferative repair in the lung. Neutrophil elastase has the potential to regulate leukocyte migration, augment lung injury and proteolyse molecules that regulate extracellular matrix turnover. Previous studies have shown that neutrophil elastase-mediated digestion of collagen and elastin can generate peptide fragments that are fibrogenic when instilled into rabbit lungs (Gardi et al., 1990). These degradation products

stimulate collagen synthesis, increase lung fibroblast numbers and enhance the deposition of new matrix within interstitial lung tissue. However, the level of elastolysis following bleomycin instillation is estimated at less than 0.1% of total lung elastin (Starcher and Petersen, 1999), mitigating against fibrogenic elastin fragments as being a prime endogenous mechanism *in vivo*. In the current study, the nature and products of elastin and collagen degradation were not specifically assessed. The similarities in alveolar leak between WT and $NE^{-/-}$ lungs at three and seven days following bleomycin treatment suggest that matrix breakdown may be comparable. It is acknowledged that the solubilisation of other matrix molecules that may not necessarily comprise structural lung elements might also be important to pulmonary fibrosis. This will be discussed in greater detail in a later chapter.

CHAPTER FIVE

BLEOMYCIN-INDUCED INJURY AND INFLAMMATION IN WT AND $NE^{-/-}$ MICE

5.1 Background

5.1.i Lung injury precedes fibrotic lung repair

Conditions present during the early inflammatory stages of lung injury can influence successful resolution or progression to chronic fibrotic remodelling. The acute respiratory distress syndrome (ARDS) is a clinical example of this theory. In ARDS, the more severe the initial lung injury, the greater the likelihood that alveolar damage will lead to fibroproliferative consequences (Griffiths and Evans, 1995).

Lung injury may be assessed by many indices such as inflammatory cell burden, cellular DNA damage or the degree of alveolar-capillary barrier dysfunction. Changes in cellular inflammation may be distinguished between lung tissue and BAL fluid. Inflammatory cells may be further characterised by their lineage, activation state, temporal persistence in tissue or mediator secretion. As leukocyte numbers may fluctuate substantially over the course of an inflammatory response, such changes may provide limited information on the damage sustained by resident cells. Moreover, leukocyte numbers do not necessarily reflect the severity of lung injury. For example, leukocyte numbers are increased in bacterial pneumonia, yet there is little lasting injury to the lung parenchyma. One reason for this may be that leukocyte clearance mechanisms are preserved. The analysis of cellular DNA damage provides an additional indicator of cytotoxicity. However, under certain circumstances such as cellular apoptosis, DNA damage may form part of normal tissue repair and not a product of cytotoxicity. Alveolar leak causing the flooding of protein-rich exudate into alveolar airspaces is a hallmark of non-repairable damage to endothelial and epithelial cells. The formation of pulmonary oedema disrupts alveolar function and prolongs the course of lung damage. In chronic lung injury, oedema fluid must be removed to ensure successful alveolar repair and to prevent the development of further complications such as pulmonary fibrosis.

The regulatory mechanisms governing the progression of lung injury to pulmonary fibrosis have not been completely uncovered. Pulmonary fibrosis may manifest in patients with no previous history of obvious lung injury. Thus, the same signals that are elaborated to downregulate or turn off inflammation may actually perpetuate fibrosis. In this context, cellular products such as cytokines or proteinases appear to provide some of the fibrogenic signals that drive fibroproliferative lung repair.

5.1.ii Proteolytic substrates of neutrophil elastase that promote lung injury

Studies in animals have shown that inhibiting neutrophil elastase catalytic activity confers beneficial effects against both the induction and intensification of lung injury. These studies have utilised various stimuli to elicit lung injury, including bacterial endotoxin, TNF-α, oleic acid, thrombin, phorbol esters and bleomycin (reviewed by Lee and Downey, 2001). Collectively, they support a prime effector role for neutrophil elastase in the development of lung injury. Different neutrophil elastase inhibitors have proven to be effective in abrogating the intensity of lung injury *in vivo*, including SLPI (Mulligan et al., 1993), ONO-5046 (Sakamaki et al., 1996) and related compounds, as well as erythromycin (Azuma et al., 1998).

Apart from components of the extracellular matrix (elastin, collagen, fibronectin, proteoglycans), neutrophil elastase can cleave biologically important soluble proteins including complement factors, coagulation cascade factors and cytokines as well as cell surface adhesion molecules. Unwanted neutrophil elastase activity not only destroys structural lung components but can also influence the inflammatory response by modulating leukocyte chemotaxis, cytokine activation and microvascular injury (reviewed in Lee and Downey, 2001). However, the relative importance of each elastase-mediated response may only dominate temporarily during the course of lung injury.

The ability of neutrophils to reach sites of lung damage is critical for perpetuating lung injury. Lung neutrophil influx has been shown to result from neutrophil elastase-induced secretion of IL-6, IL-8 and GM-CSF by injured airway epithelial cells (Bedard et al., 1993). Neutrophil elastase can also stimulate mononuclear cells to release leukotriene B4, a neutrophil chemoattractant derived from arachidonic acid metabolism (Owen and Campbell, 1999) and to directly increase the expression of IL-8, a key neutrophil chemoattractant and stimulant (Chen et al., 2004). Furthermore, neutrophil elastase-mediated degradation of fibronectin and complement factor C5 generates biologically active products that can establish chemotactic gradients to direct neutrophil infiltration into injured tissue (Banda et al., 1988). Similar properties have also been ascribed to collagen degradation peptides generated *in vitro* by the digestion of intact collagen following exposure to purified neutrophil elastase (Gardi et al., 1994). Although neutrophil elastase can cleave CXCL12 (stromal cell-derived factor-1) and its receptor CXCR4 (Levesque et al., 2003), molecules thought to be involved in haematopoietic progenitor cell (HPC) release from the bone marrow, neutrophil elastase activity is not required in the actual mobilisation of HPC induced by granulocyte colony stimulating factor in studies using neutrophil mice deficient in both elastase

and cathepsin G (Levesque et al., 2004). Hence, the accumulated evidence suggests that lung injury itself induces neutrophil chemoattractants other than neutrophil elastase and the latter plays a role in enhancing but not initiating tissue neutrophil influx.

A heightened pro-coagulant milieu is also an important feature of alveolar inflammation. Neutrophil elastase activity promotes coagulation in several ways. The catalytic activity of cell surface-bound neutrophil elastase, and to some extent that of cathepsin G, can enhance the activation of cofactor Va and promote the formation of prothrombinase complexes (Allen and Tracy, 1995). Thrombin generation is critical for stabilising the terminal fibrin plug at sites of micro-haemostasis during alveolar injury. Neutrophil elastase can also cleave and inactivate anti-coagulant molecules such as antithrombin III, α1-antiplasmin and protein C that act to inhibit fibrin crosslinking and retard fibrinolysis (Sie et al., 1987; Eckle et al., 1991).

A final way in which neutrophil elastase can exacerbate lung injury is by causing microvascular damage that leads to alveolar-capillary hyperpermeability. Neutrophil elastase activity can directly injure epithelial and endothelial cells as well as the basement membrane that supports them. It can efficiently detach epithelial (Amitani et al., 1991) and endothelial cells (Yang et al., 1996) from their substratum and induce apoptosis and cytolysis. Neutrophil elastase-mediated proteolysis of endothelial cadherins has been shown to induce pulmonary microvascular injury (Carden et al., 1998). Finally, this serine proteinase cleaves collagen type IV, fibronectin and laminin deposited in alveolar basement membranes, an action that compromises the integrity of this important tissue (Heck et al., 1990).

5.1.iii Markers of bleomycin-induced lung injury

The manifestations of bleomycin-induced DNA damage include the straightforward scission of single or double-stranded DNA, modification of deoxyribose sugar moieties and the release of unaltered free nucleic acid bases (Suzuki et al., 1969). The products of DNA scission are the easiest to analyse and quantify *in vitro*. In order to be DNA-toxic, bleomycin must first enter cells, penetrate the nuclear membrane and become activated in very close proximity to DNA. *In vitro* studies using ^{3}H labelled bleomycin have shown that the initial accrual of bleomycin within cells occurs rapidly in a dose-dependent manner with a slower secondary accumulation pattern after the first few minutes (Lyman et al., 1986). Cellular necrosis, as evidenced by elevated lactate

dehydrogenase levels, may result from excessive non-repairable DNA damage. Bleomycin may also have cytotoxic effects via DNA degradation-independent processes such as lipid peroxidation.

Pulmonary administration of bleomycin induces a 'classic' neutrophil-rich inflammatory infiltrate that gives way to a more sustained influx of mononuclear cells comprising macrophages and lymphocytes (Janick-Buckner et al., 1989). Eosinophils may also appear transiently at around seven to ten days post-injection. In one study using hamsters, up to eight times the normal number of leukocytes were quantified in alveoli four days following a single 1U intratracheal dose of bleomycin (Chandler et al., 1983). Recruitment of inflammatory cells into the alveolar and interstitial structures is usually accompanied by capillary congestion and the formation of perivascular oedema (reviewed in Thrall and Scalise, 1995). The resultant detachment and death of epithelial cells may produce areas of denuded basement membrane, evident at light microscopy level but best appreciated at electron microscopy (Burkhardt, 1989). Severe endothelial cell damage may be evident histologically as patchy intra-alveolar haemorrhage. The analysis of soluble epithelial and endothelial biomarkers such as surfactant proteins and endothelium-expressed adhesion molecules provides an additional (albeit indirect) means for assessing injury to these cells (Azuma et al., 2000; Pan et al., 2002).

During both the acute and subacute phases of bleomycin-induced lung injury, the development of alveolar hyper-permeability due to the loss of alveolar-capillary barrier integrity is pathophysiologically important. The formation of pulmonary oedema, particularly changes in the transepithelial movement of macromolecules, has been the subject of intense investigation over many years (Yi et al., 1998; Balharry et al., 2005). The extent of oedema fluid accumulation has itself been correlated to the severity of ensuing bleomycin-induced pulmonary fibrosis (Yasui et al., 2001). Physiological parameters are more variable. For example, decreased lung compliance occurs early in bleomycin-induced lung injury as a result of interstitial oedema and alveolar injury, or may only become evident later when lung collagen content increases (Hesterberg et al., 1981). Lung compliance may also be preserved until quite late, being apparently normal even when lung tissue collagen content has increased. This disparity has still not been adequately explained.

The following sections will present results relating to the characterisation of bleomycin-induced lung injury and inflammation in WT and $NE^{-/-}$ mice.

5.2 Results

5.2.i Bleomycin-induced pulmonary inflammation

5.2.i.i Elastolytic activity

Continuous (kinetic) and discontinuous (fixed-time) assays were performed to determine the optimal conditions for measuring neutrophil elastase activity. The initial hydrolysis rate of MEOSAAPVNA, a specific neutrophil elastase substrate, was determined using a range of enzyme concentrations (**figure 13**). Enzymatic consumption of the substrate was constant ten minutes following initiation of the hydrolytic reaction. Subsequently, fixed-time (10-minute) reactions were performed to delineate the linear concentration range of neutrophil elastase required to fully hydrolyse the same amount of MEOSAAPVNA substrate (**figure 14**). Using these conditions, mean BAL fluid neutrophil elastolytic activity in bleomycin-treated $NE^{-/-}$ mice was almost undetectable (0.032 ± 0.009 OD) and was not different from values in saline-treated animals. In fact, mean neutrophil elastase activity in BAL samples collected from saline-treated WT mice and bleomycin-treated $NE^{-/-}$ samples fell below the linear range of detection (**figure 15**).

5.2.i.ii Leukocyte recruitment and extravasation

Cytocentrifuged BAL fluid from WT and $NE^{-/-}$ lungs contained increased numbers of polymorphonuclear neutrophils and alveolar macrophages as early as four hours after bleomycin instillation (**figure 16**). Granulocyte precursor cells were also present at this early stage, distinguished by their larger horseshoe or band-shaped nuclei and lack of nuclear segmentation. In contrast, BAL fluid from saline-treated animals of either genotype contained mostly unstimulated resident macrophages with few neutrophils or granulocyte precursors. Quantitative analysis by fluorescence-activated cell sorting on the basis of Gr-1 (Ly-6G) antigen expression showed that comparable numbers of neutrophils were present in the BAL fluid of both WT and $NE^{-/-}$ mice 24 hours following saline or bleomycin administration (top graph, **figure 17**).

Histologic examination of haematoxylin and eosin-stained lung sections of bleomycin-treated WT and $NE^{-/-}$ mice also showed marked tissue neutrophilia at 24 hours (bottom panels, **figure 17**).

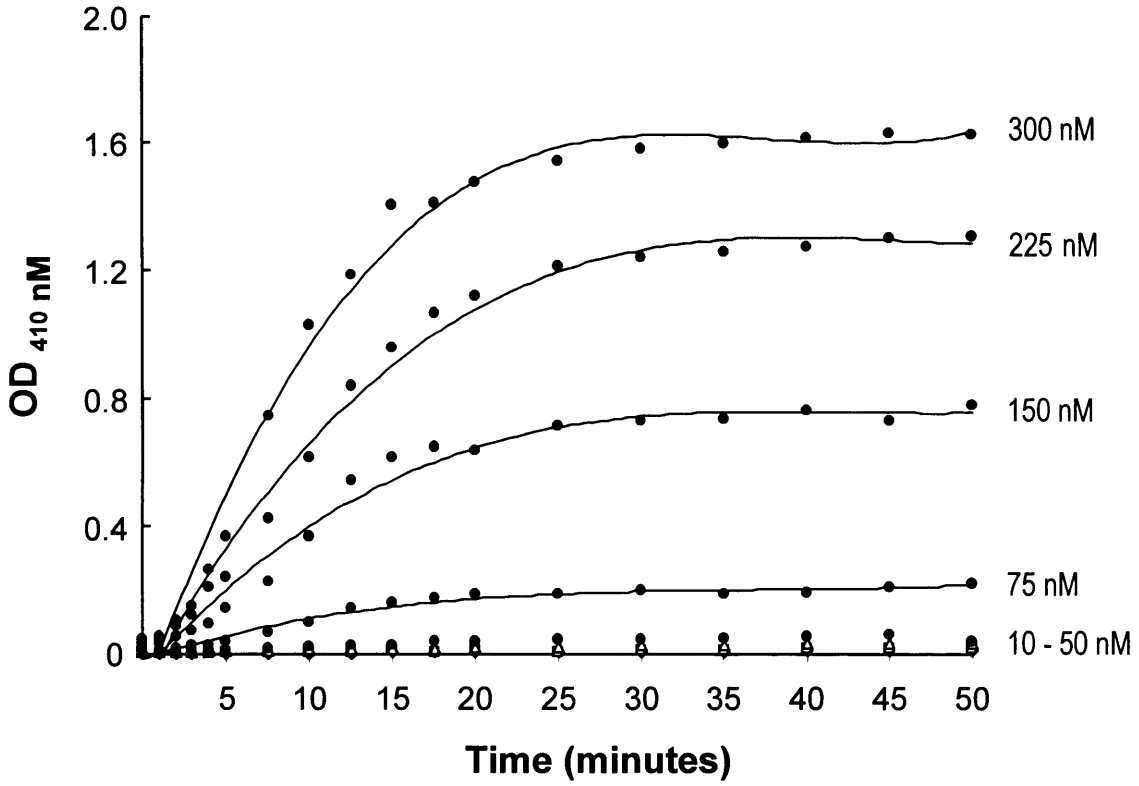

Figure 13. **Initial rates of MEOSAAPVNA hydrolysis.**

MEOSAAPVNA (5 mM), a highly specific neutrophil elastase substrate, was reacted with increasing concentrations of the proteinase (10 - 300 nM) at 25°C. Time-dependent variation in the concentration of the reaction product (measured in units of optical density at 410 nm) was assessed to optimise catalytic conditions. Each point represents the mean ± SEM of a triplicate.

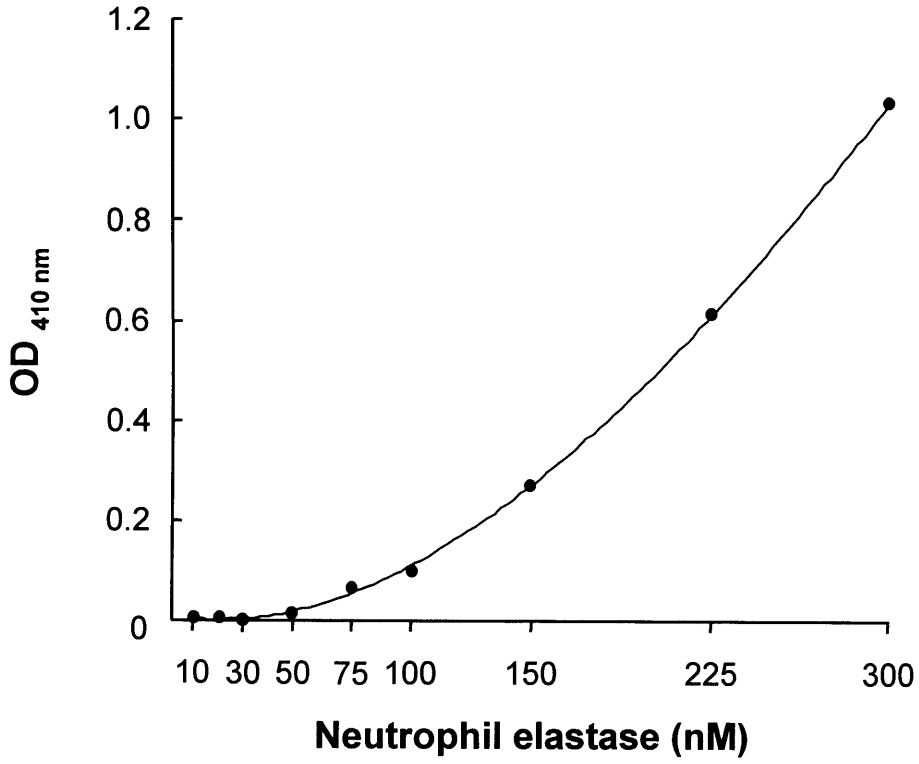

Figure 14. **Linear range of neutrophil elastase concentration required to hydrolyse MEOSAAPVNA.**

Purified neutrophil elastase (10 - 300 nM) was allowed to proteolytically react with 5 mM MEOSAAPVNA over 10 minutes at 25°C to produce a fixed-time elastolytic curve. Each point represents the mean ± SEM of a triplicate.

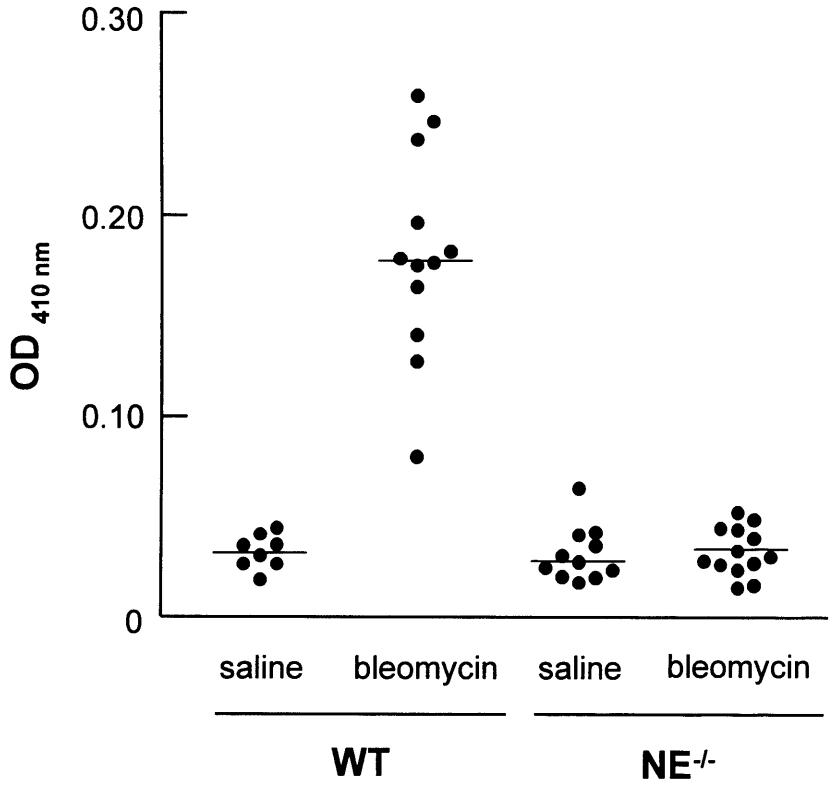

Figure 15. **Neutrophil elastolytic activity in cell-free BAL fluid of bleomycin and saline-treated WT and $NE^{-/-}$ mice.**

Neutrophil elastolytic activity in BAL fluid was compared between saline or bleomycin-treated WT and $NE^{-/-}$ mice following the removal of neutrophils. Aliquots of BAL samples were incubated with 5 mM MEOSAAPVNA at 25°C to produce a fixed-time elastolytic curve. Each point represents the mean ± SEM of a triplicate.

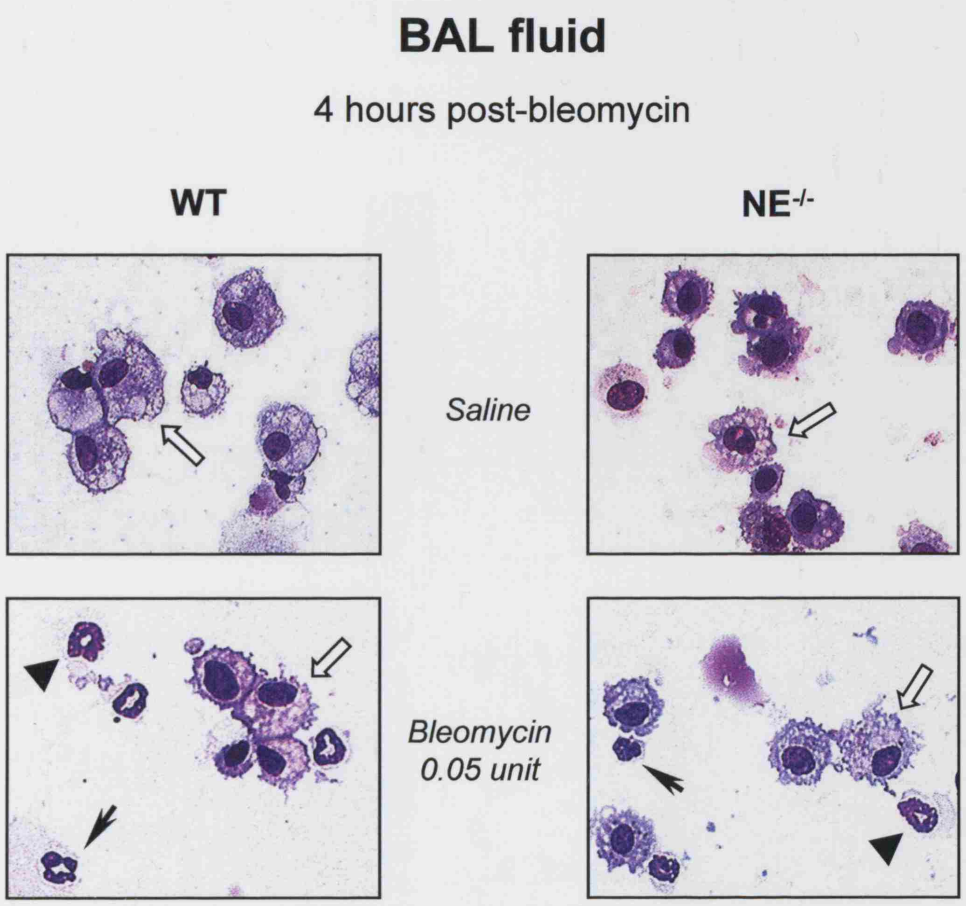

Figure 16. **The absence of neutrophil elastase does not prevent the influx of neutrophils into the lungs of bleomycin-treated $NE^{-/-}$ mice.**

Wright-Giemsa-stained cytospins of bronchoalveolar lavage (BAL) fluid collected from WT and $NE^{-/-}$ mice four hours following the instillation of 0.05 unit bleomycin. Mature neutrophils are denoted by arrows, immature granulocytes by arrowheads and alveolar macrophages by open arrows.

x40 objective

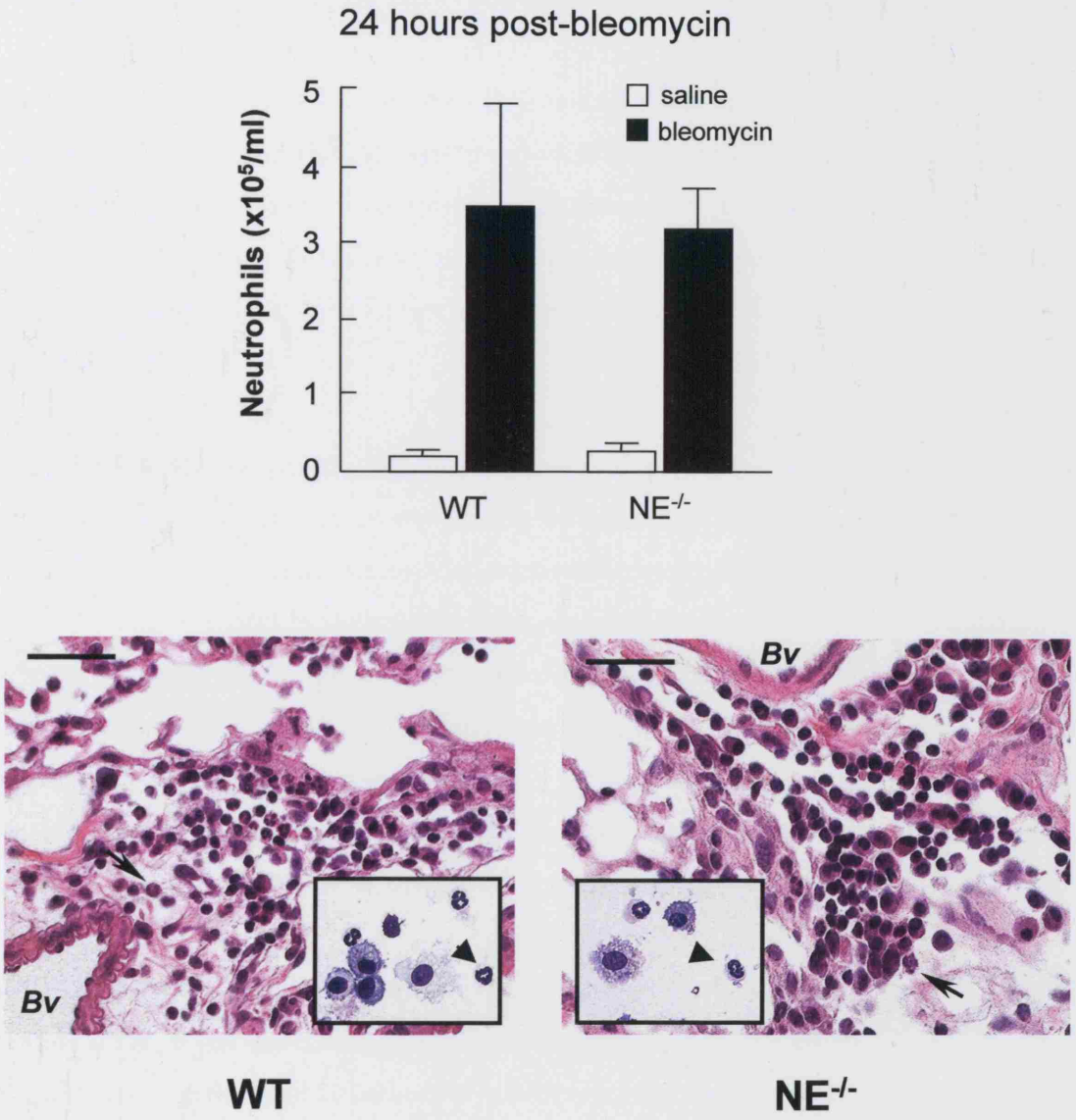

Figure 17. **Characterisation of early neutrophilia in BAL fluid and lung tissue of bleomycin-treated WT and NE$^{-/-}$ mice.**

Top panel, Flow cytometric analysis of leukocyte Gr-1 expression using a fluorochrome-conjugated antibody (BDH-Merck, UK) on uncentrifuged BAL fluid of WT and NE$^{-/-}$ mice 24 hours post-bleomycin instillation (n=6 in each group).

Bottom panels, Neutrophils (arrows) are seen in haematoxylin and eosin-stained WT and NE$^{-/-}$ lungs 24 hours following bleomycin instillation. *Bv* indicates blood vessels. ***Insets,*** Neutrophils are also present in BAL fluid collected at the same time point (arrowheads, *Wright-Giemsa staining*).

x40 objective

Some of these cells were seen to marginate intravascularly, while others had extravasated from blood vessels to collect in perivascular areas. The morphologic features of these neutrophils and those in BAL fluid collected at the same time were very similar.

Examination of lung sections obtained three days following bleomycin treatment showed that the initial extent of tissue neutrophil infiltration was variable between WT and $NE^{-/-}$ mice (**figure 18**). Neutrophils were consistently observed to accumulate for longer within the perivascular perimeter in $NE^{-/-}$ lungs, with a delayed advance into adjacent alveoli. In contrast, neutrophils in the lungs of bleomycin-treated WT mice had dispersed more widely amongst the alveolar spaces by this time.

Representative Wright-Giemsa stained cytospin preparations of BAL cells from bleomycin-treated WT and $NE^{-/-}$ mice from day 7 are shown in **figure 19** (top panels). Neutrophils and macrophages, the most abundant leukocytes, were easily distinguished by their gross morphology. A number of enlarged and hyper-vacuolated macrophages were seen in both groups of mice. Differences in the pattern of tissue leukocyte infiltration between bleomycin-treated WT and $NE^{-/-}$ mice are shown in the bottom panels of **figure 19**. While many leukocytes (including a large number of neutrophils) were widely dispersed in the lung parenchyma of WT mice, there was a greater tendency for leukocytes to remain in the perivascular margin in the lungs of $NE^{-/-}$ animals. Scattered among these cells were a small number of eosinophils and lymphocytes.

Figure 20 summarises the changes in total leukocyte numbers in BAL fluid from WT and $NE^{-/-}$ mice at one, three, seven and ten days following the administration of either saline or bleomycin. At the earliest time point (day 1), leukocyte numbers were not significantly different between any of the treatment groups. Bleomycin instillation of WT mice induced a leukocytosis in BAL fluid that increased quite sharply between days three and seven and decreased between days seven and ten. In WT mice, maximal leukocyte counts, observed at day seven, were 220% higher than those at one day following the instillation of bleomycin ($1.19 \pm 0.13 \times 10^6$/ml vs. $0.36 \pm 0.04 \times 10^6$/ml, $P < 0.0001$). In contrast, increases in leukocyte counts in $NE^{-/-}$ BAL fluid following bleomycin instillation were of a smaller magnitude over the same time period. Peak leukocyte numbers were also observed on day seven but were only 100% higher than at day one ($0.68 \pm 0.05 \times 10^6$/ml vs. $0.34 \pm 0.03 \times 10^6$/ml, $P < 0.01$). As a result, peak leukocytosis in $NE^{-/-}$ BAL fluid was quantitatively smaller than in corresponding WT samples ($P < 0.05$). Saline instillation induced equivalent changes in leukocyte counts in both WT and $NE^{-/-}$ mice.

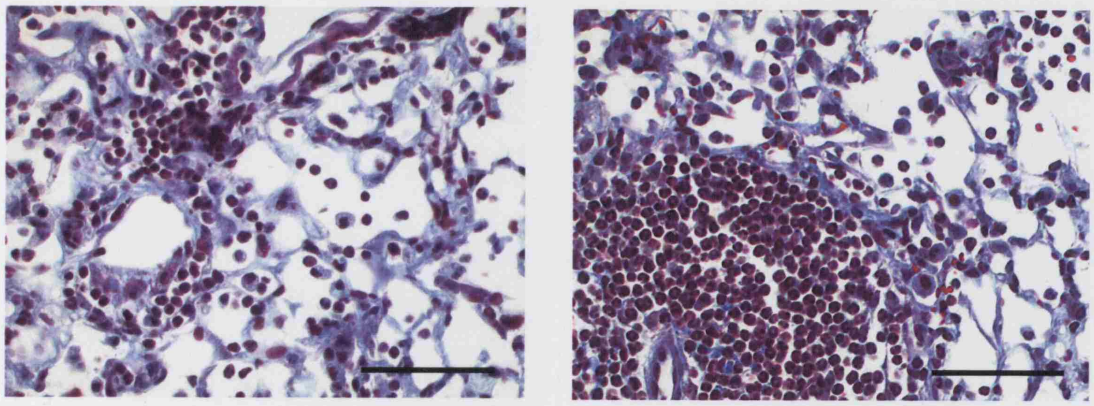

Figure 18. **Lungs of WT and $NE^{-/-}$ mice have intense neutrophil infiltration three days following bleomycin instillation.**

Neutrophils and other inflammatory cells are observed perivascularly and in the deeper lung parenchyma (*bar*, 100 μm).

Masson's trichrome stain

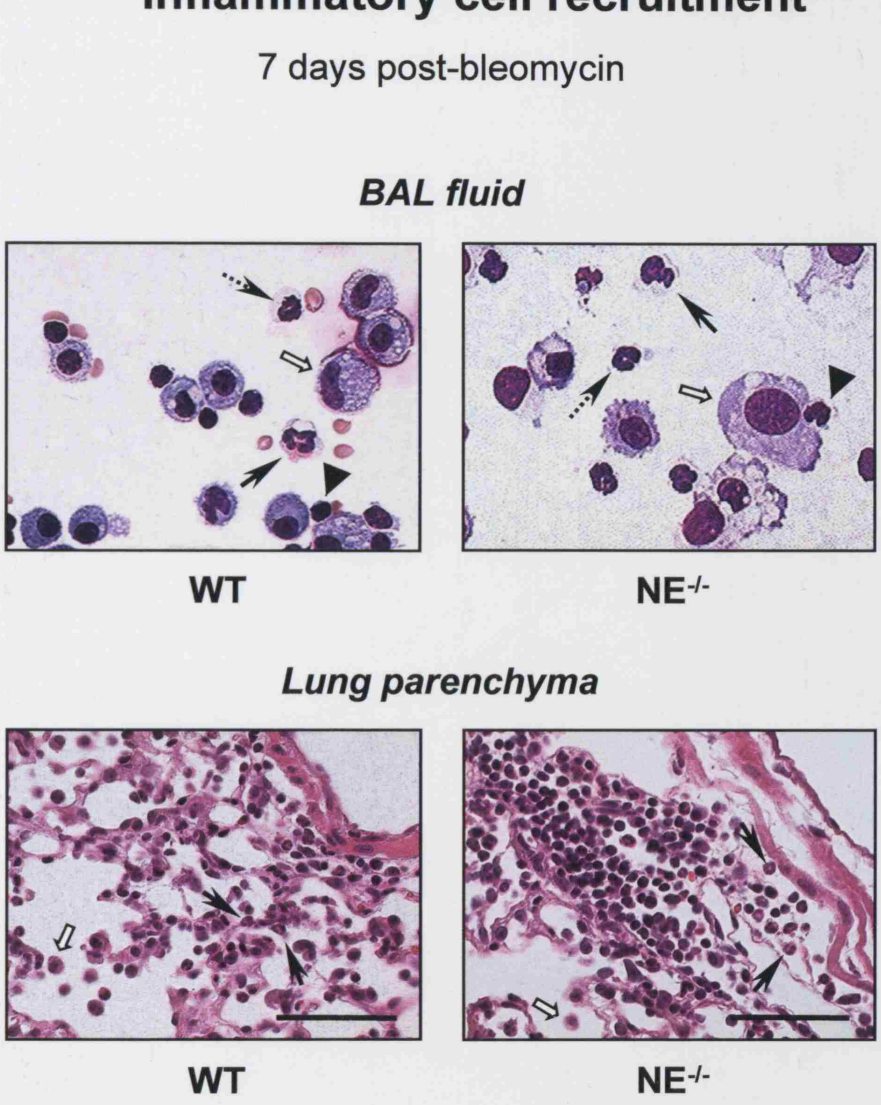

Figure 19. **Bleomycin instillation induces a classical inflammatory response represented by a mixed leukocytosis in both WT and $NE^{-/-}$ mice.**

Top panels, Mature neutrophils with hypersegmented nuclei (closed arrows), immature polymorphs (dashed arrows), macrophages (open arrows) and lymphocytes (arrowheads) are prominent in BAL fluid from bleomycin-treated WT and $NE^{-/-}$ mice. Wright-Giemsa stain. *x40 objective.*

Bottom panels, Haematoxylin & eosin-stained sections show the infiltration of neutrophils (closed arrows) and macrophages (open arrows) into bleomycin-injured WT and $NE^{-/-}$ lung parenchyma. *Bar*, 50 μm.

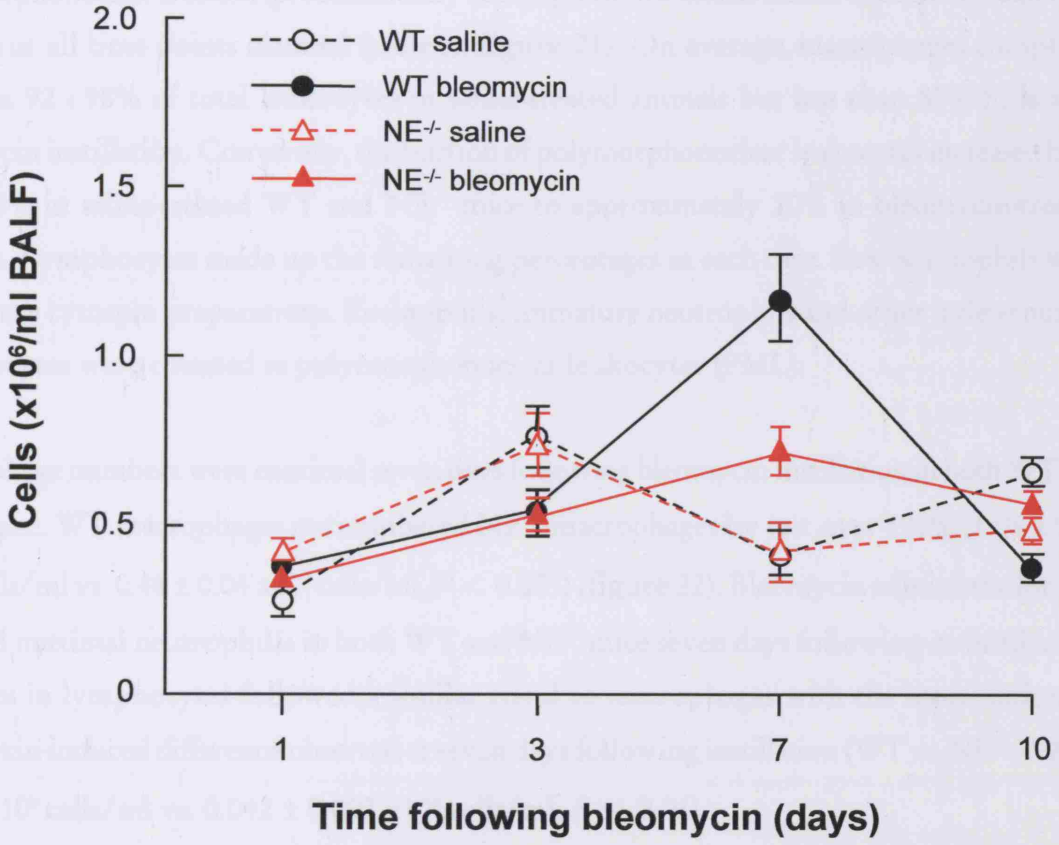

***Figure 20.* WT and NE$^{-/-}$ BAL fluid have maximal leukocytosis seven days following bleomycin instillation.**

Cell pellets in BAL fluid collected from WT and NE$^{-/-}$ mice one, three, seven and ten days following the instillation of either saline or bleomycin were isolated by centrifugation and resuspended in red cell lysis buffer. Leukocytes were enumerated using a haemocytometer chamber and expressed as x10^6 counts per ml BAL fluid. Each point represents the mean ± SEM of 4 - 12 animals.

5.2.i.iii Differential leukocyte profile in BAL fluid

The cellular composition of BAL fluid of bleomycin-treated WT and $NE^{-/-}$ mice was identified by examining cytospins. Saline treatment did not induce significant changes in leukocyte fractions compared to untreated samples. However, bleomycin instillation decreased the percentage of mononuclear cells (comprising macrophages and lymphocytes) whilst increasing the polymorphonuclear fraction (predominantly neutrophils) to a similar extent in both WT and $NE^{-/-}$ animals at all time points assessed (table in **figure 21**). On average, macrophages comprised between 92 - 98% of total leukocytes in saline-treated animals but less than 80% following bleomycin instillation. Conversely, the fraction of polymorphonuclear leukocytes increased from under 5% in saline-treated WT and $NE^{-/-}$ mice to approximately 20% in bleomycin-treated animals. Lymphocytes made up the remaining percentages in each case. Few eosinophils were seen in the cytospin preparations. Eosinophils, immature neutrophils and other indeterminate granulocytes were counted as polymorphonuclear leukocytes (PML).

Macrophage numbers were maximal seven days following bleomycin instillation in both WT and $NE^{-/-}$ mice. WT macrophages outnumbered $NE^{-/-}$ macrophages by just over 100% (1.05 ± 0.14 x10^6 cells/ml vs. 0.48 ± 0.04 x10^6 cells/ml, $P < 0.001$) (**figure 22**). Bleomycin administration also induced maximal neutrophilia in both WT and $NE^{-/-}$ mice seven days following its instillation, Changes in lymphocytes followed a similar trend to macrophages with the most noticeable bleomycin-induced difference observed at seven days following instillation (WT vs. $NE^{-/-}$: 0.093 ± 0.015 x10^6 cells/ml vs. 0.042 ± 0.007 x10^6 cells/ml, $P < 0.01$).

5.2.i.iv Lung tissue neutrophil burden

Total lung neutrophil abundance was assessed by quantifying myeloperoxidase (MPO) activity in homogenised lung tissue. As enzyme - substrate reactions involving MPO are time- and substrate-dependent, preliminary experiments were performed to determine the optimal conditions for peroxidation analysis. A range of standard horseradish peroxidase (1 to 5 ng) was used to construct the standard curve. Incubation of samples for more than 15 minutes led to loss of peroxidase activity (**figure 23**). Consequently, a 15-minute incubation period was chosen for all subsequent experiments.

BAL FLUID INFLAMMATORY CELL COMPOSITION

DIFFERENTIAL LEUKOCYTE FRACTIONS

		WT		$NE^{-/-}$	
		Saline	*Bleomycin*	*Saline*	*Bleomycin*
Day 3	Mac	96.6 (0.9)	74.6 (3.7)	96.5 (1.7)	78.8 (3.2)
	PML	3.1 (0.8)	20.9 (2.4)	3.3 (1.7)	18.6 (2.4)
	Lymp	0.4 (0.2)	4.5 (1.9)	0.2 (0.2)	2.8 (2.8)
Day 7	Mac	93.4 (1.2)	73.9 (1.8)	92.3 (1.3)	71.8 (2.4)
	PML	5.0 (1.2)	18.2 (1.0)	5.3 (0.7)	21.5 (1.9)
	Lymp	1.9 (0.5)	7.9 (1.1)	2.4 (0.7)	6.4 (1.0)
Day 10	Mac	93.7 (0.7)	69.0 (1.1)	98.5 (0.2)	79.0 (2.0)
	PML	3.6 (0.8)	20.2 (1.3)	1.1 (0.1)	12.4 (1.6)
	Lymp	2.7 (0.6)	10.9 (0.6)	0.5 (0.2)	8.6 (0.5)

Mean % (SEM)

***Figure 21.* Changes in BAL fluid leukocyte composition are equivalent between WT and $NE^{-/-}$ mice following saline or bleomycin instillation.**

Differential cell fractions were determined by cell counting of cytocentrifuged BAL fluid from saline and bleomycin-treated WT and $NE^{-/-}$ mice. Approximately 1×10^5 cells were centrifuged onto each slide, stained with Diff-Quick® Wright-Giemsa, and a minimum of 400 cells counted. Cells were differentiated on the basis of morphological features and divided into three main groups (Mac, *macrophages*; PML, *polymorphonuclear leukocytes*; Lymp, *lymphocytes*). Values represent mean percentages with SEM in brackets.

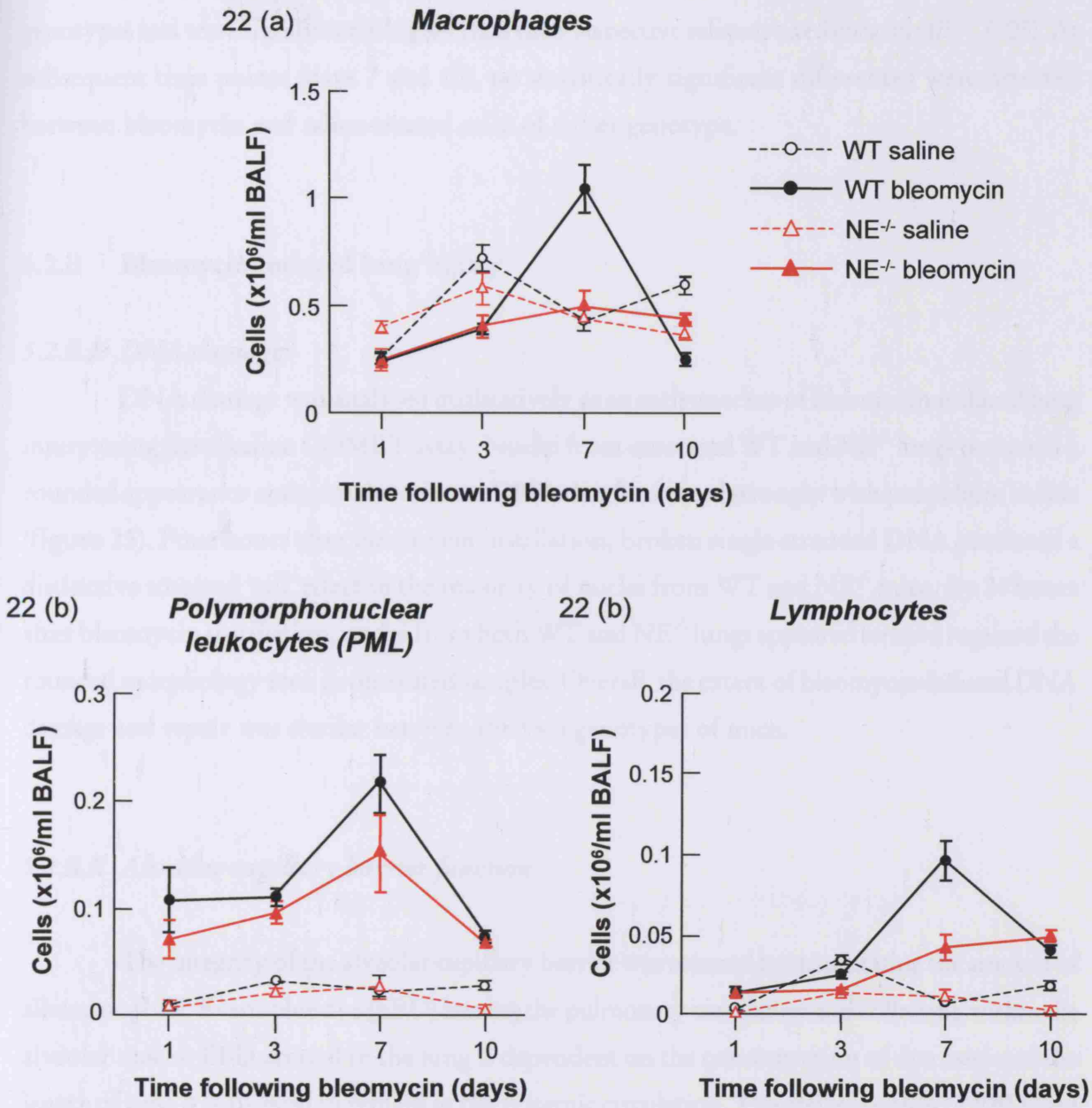

Figure 22. **Changes in differential inflammatory cell indices following bleomycin instillation.**

Time course changes in BAL fluid cellularity were assessed in saline and bleomycin-treated WT and $NE^{-/-}$ mice. Cells were differentiated visually on Wright-Giemsa (Diff-Quick®)-stained cytospins. Cell numbers were calculated using the percentage of each cell type present and the total leukocyte count for each given sample. Values represent the mean ± SEM of 4 - 12 animals per group.

MPO activity in lung homogenates was highest in both WT and $NE^{-/-}$ mice three days following the administration of 0.05U bleomycin (**figure 24**). Values were comparable between the two genotypes and were significantly higher than their respective saline-treated controls ($P < 0.05$). At subsequent time points (days 7 and 10), no statistically significant differences were detected between bleomycin and saline-treated mice of either genotype.

5.2.ii Bleomycin-induced lung injury

5.2.ii.i DNA damage

DNA damage was analysed qualitatively as an early marker of bleomycin-induced lung injury using the alkaline COMET assay. Nuclei from untreated WT and $NE^{-/-}$ lungs possessed a rounded appearance and contained intact DNA that fluoresced strongly with propidium iodide (**figure 25**). Four hours after bleomycin instillation, broken single-stranded DNA produced a distinctive smeared 'tail' effect in the majority of nuclei from WT and $NE^{-/-}$ mice. By 24 hours after bleomycin instillation, nuclei from both WT and $NE^{-/-}$ lungs appeared to have regained the rounded morphology seen in untreated samples. Overall, the extent of bleomycin-induced DNA damage and repair was similar between the two genotypes of mice.

5.2.ii.ii Alveolar-capillary barrier function

The integrity of the alveolar-capillary barrier was assessed by quantitating the amount of albuminophilic Evans blue dye (EBD) leaving the pulmonary circulation and collecting within the alveolar spaces. EBD accrual in the lung is dependent on the concentration of dye used and the length of time it is allowed to remain in the systemic circulation. The concentration of EBD used in these studies was chosen from the literature. **Figure 26** shows that intravascular distribution of the dye for either one or three hours was associated with a similar degree of pulmonary dye retention and recovery in BAL fluid. The one-hour circulating time was thus chosen for subsequent experiments.

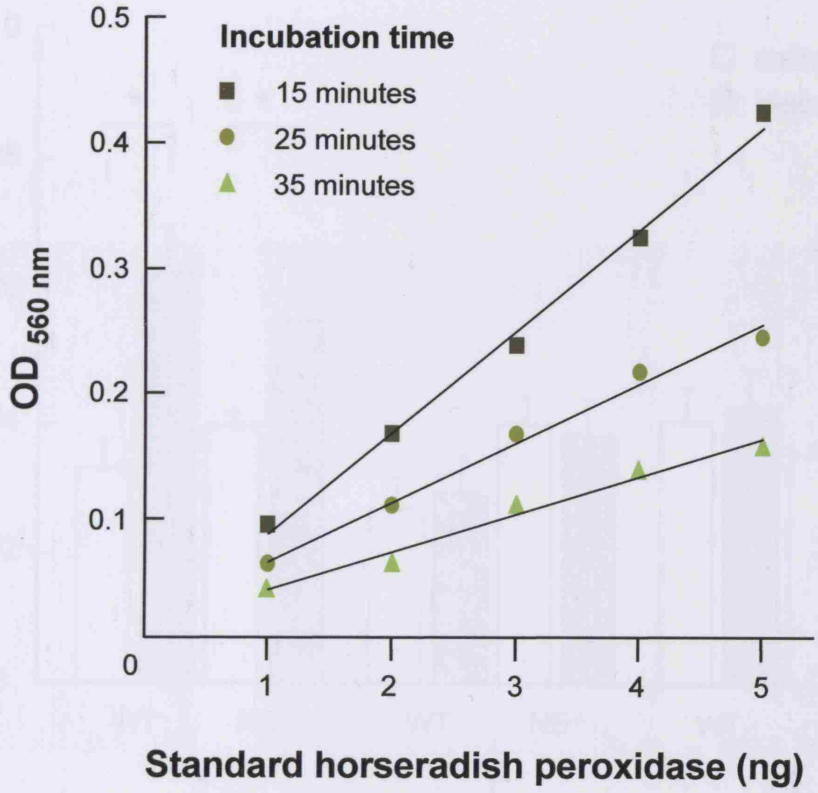

Figure 23. **Determination of optimal incubation time for measuring horseradish peroxidase activity.**

Analysis of the efficiency of standard horseradish peroxidase to hydrolyse ethanol-dissolved O-Dianisidine (DMB, 0.32 mM) by varying the duration of incubation. Reactions were performed at 37°C for 5 minutes followed by incubation at room temperature for 15, 25 or 35 minutes. Values represent absorbances read at 560 nm.

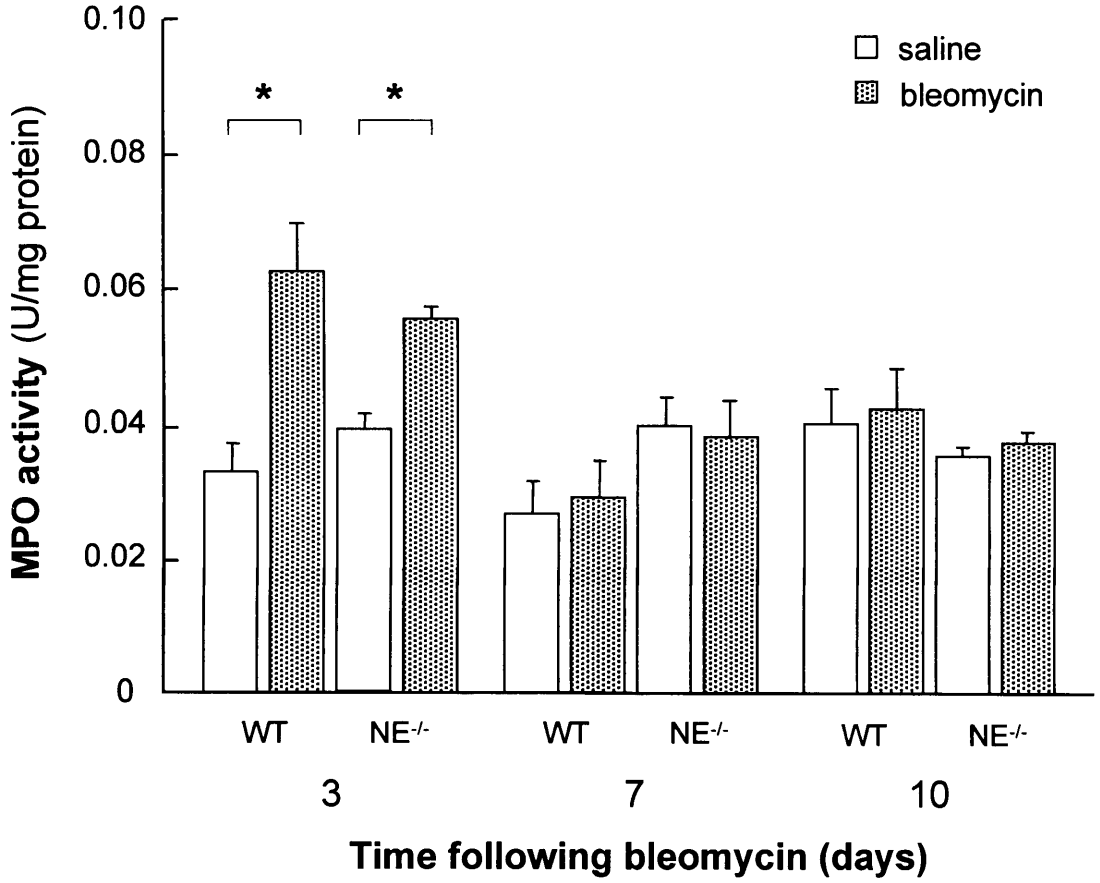

Figure 24. **Lung tissue neutrophil burden is similar in WT and NE$^{-/-}$ mice following bleomycin-induced lung injury.**

Myeloperoxidase (MPO) activity, taken as an index of neutrophil burden, was determined in homogenised lung tissue by measuring the hydrolysis of *O*-dianisidine (DMB). A standard curve for the reaction was generated using known concentrations of horseradish peroxidase (0.1 - 10.0 ng, specific activity 0.00131 units/ng protein). Total protein content in the same samples was quantified with the BCA assay. Values are expressed as mean ± SEM. * $P < 0.05$.

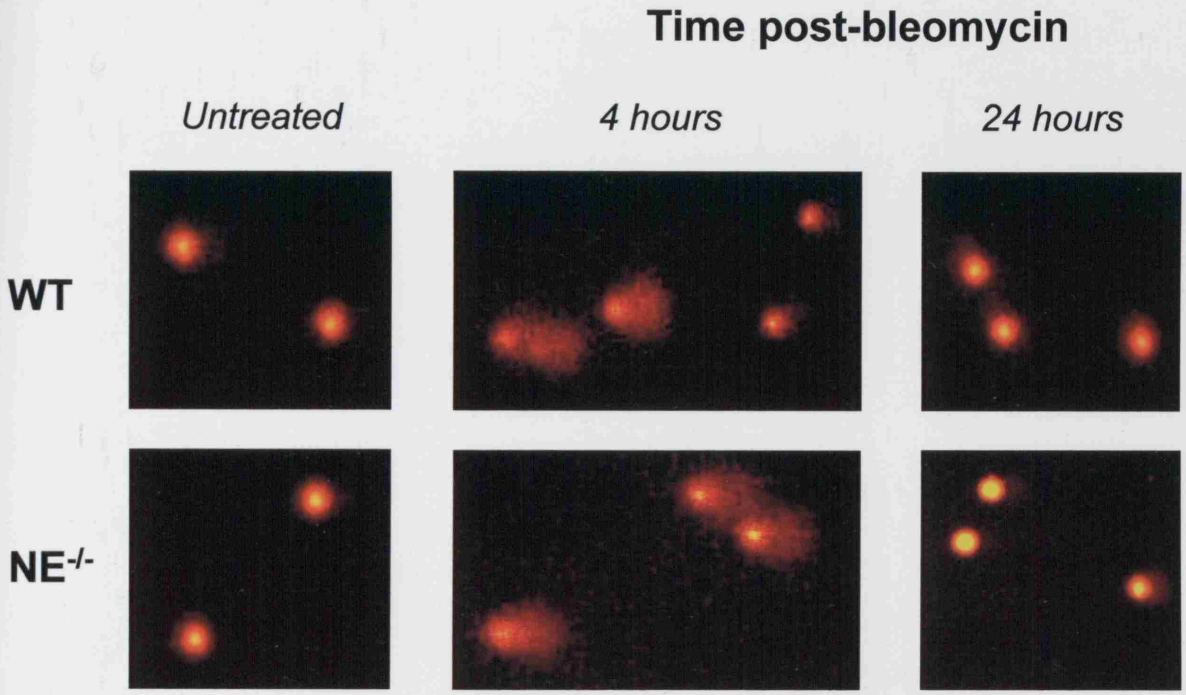

***Figure 25.* Analysis of DNA damage in lung cells by the COMET assay.**

DNA damage and repair was assessed in cells isolated from dispase-digested lungs. Cells were lysed, treated under alkaline conditions to uncoil their DNA and subjected to single-cell gel electrophoresis on agarose-coated microscope slides. Images of intact and damaged nuclear DNA stained with propidium iodide were taken of representative fields from each animal (n = 2 mice in untreated group; n = 3 mice in each bleomycin-treated group).

Cells and images prepared by F Chua, assay performed by PH Clingen

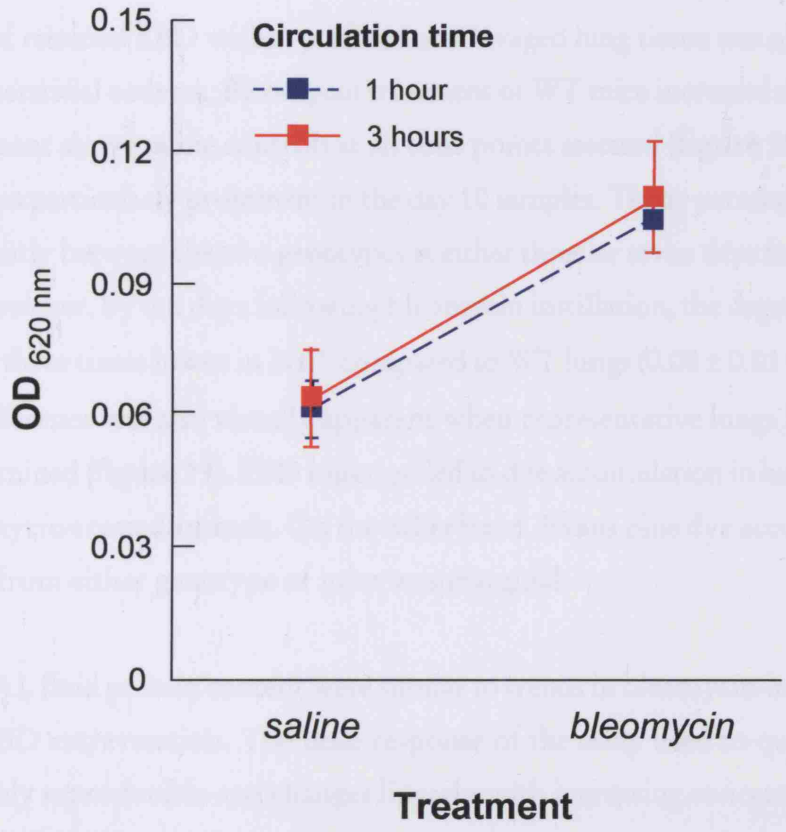

Figure 26. **Recovery of Evans blue dye from murine BAL fluid is similar following either one or three hours of intravascular circulation.**

Evans blue dye (20 mg/kg) was injected intravenously one day following intratracheal bleomycin or saline instillation and allowed to circulate for one or three hours prior to animal sacrifice. Accumulation of dye in the alveolar compartment was assessed by determining dye absorbance at 620 nm in cell-free BAL fluid. Each point represents the mean ± SEM of four animals.

Alveolar leak was evident three days following IT bleomycin instillation into WT mice and reached peak values at seven days following treatment (**figure 27**). At both these time-points, alveolar leak was comparable in bleomycin-treated $NE^{-/-}$ mice. By 10 days following bleomycin instillation, alveolar leak in $NE^{-/-}$ mice was significantly below values measured in WT animals ($NE^{-/-}$ vs. WT permeability index: 0.09 ± 0.01 vs. 0.25 ± 0.05, $P < 0.01$). In contrast, saline treatment exerted a marginal effect on alveolar barrier integrity in both WT and $NE^{-/-}$ lungs.

The amount of retained EBD within perfused and lavaged lung tissue was also quantified as an estimate of interstitial oedema. Bleomycin treatment of WT mice increased dye sequestration in this compartment above saline controls at all time points assessed (**figure 28**). The recovery of trapped dye was particularly prominent in the day 10 samples. Tissue permeability index did not differ significantly between the two genotypes at either three or seven days following bleomycin treatment. However, by ten days following bleomycin instillation, the degree of interstitial dye retention was three times lower in $NE^{-/-}$ compared to WT lungs (0.08 ± 0.01 vs. 0.22 ± 0.05, $P < 0.01$). This difference was also visually apparent when representative lungs from each group of mice were examined (**figure 29**). EBD injection led to dye accumulation in lung tissue and airway walls of bleomycin-treated animals. On the other hand, Evans blue dye accumulation in saline-treated lungs from either genotype of mice was marginal.

Changes in BAL fluid protein content were similar to trends in bleomycin-induced alveolar leak assessed by EBD extravasation. The dose response of the assay used to quantitate BAL fluid protein is highly reproducible and changes linearly with increasing concentrations of albumin (**figure 30**, panel A). Bleomycin instillation induced a progressive and comparable increase in BAL fluid protein in both WT and $NE^{-/-}$ mice that was maximal a week following administration (**figure 31**). By the tenth day, however, average protein levels in $NE^{-/-}$ BAL fluid had decreased to nearly two-thirds that of WT samples ($NE^{-/-}$ vs. WT: 0.86 ± 0.12 vs. 1.38 ± 0.15 mg/ml, $P < 0.05$). Saline treatment did not alter BAL fluid protein levels in either WT or $NE^{-/-}$ mice compared to untreated controls (not shown). Analysis of BAL fluid samples using one-dimensional gel electrophoresis confirmed that the most abundant protein in specimens from bleomycin-treated WT and $NE^{-/-}$ mice migrated between 60 – 70 kDa (**figure 32**). Although monomeric albumin has a molecular weight of 66 kDa, this band could contain a number of admixed proteins, not necessarily just albumin. Although not pursued in the current studies, dilution of samples and repeat analysis using either a sepharose blue gel or non-denaturing PAGE with Western Blotting for albumin would be appropriate in confirming the nature of the most abundant protein.

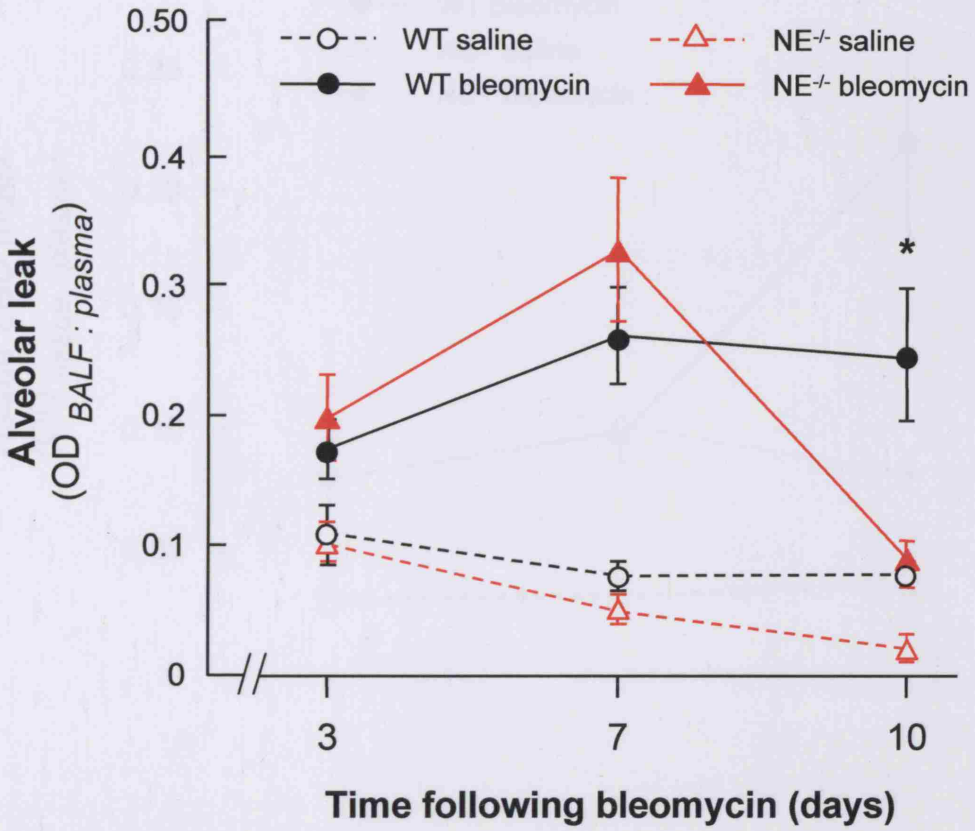

Figure 27. **Bleomycin-induced alveolar hyper-permeability (leak) resolves earlier in NE$^{-/-}$ mice.**

Evans blue dye (EBD, 20 mg/kg) was injected intravenously three, seven or ten days following intratracheal bleomycin or saline instillation. Accumulation of dye in alveoli was assessed by bronchoalveolar lavage. The BAL fluid : plasma ratio of EBD absorbance at 620 nm was used to indicate the extent of alveolar-capillary leak. Each point represents the mean ± SEM of three animals. * *P < 0.01 (bleomycin-treated WT vs. NE$^{-/-}$ mice)*

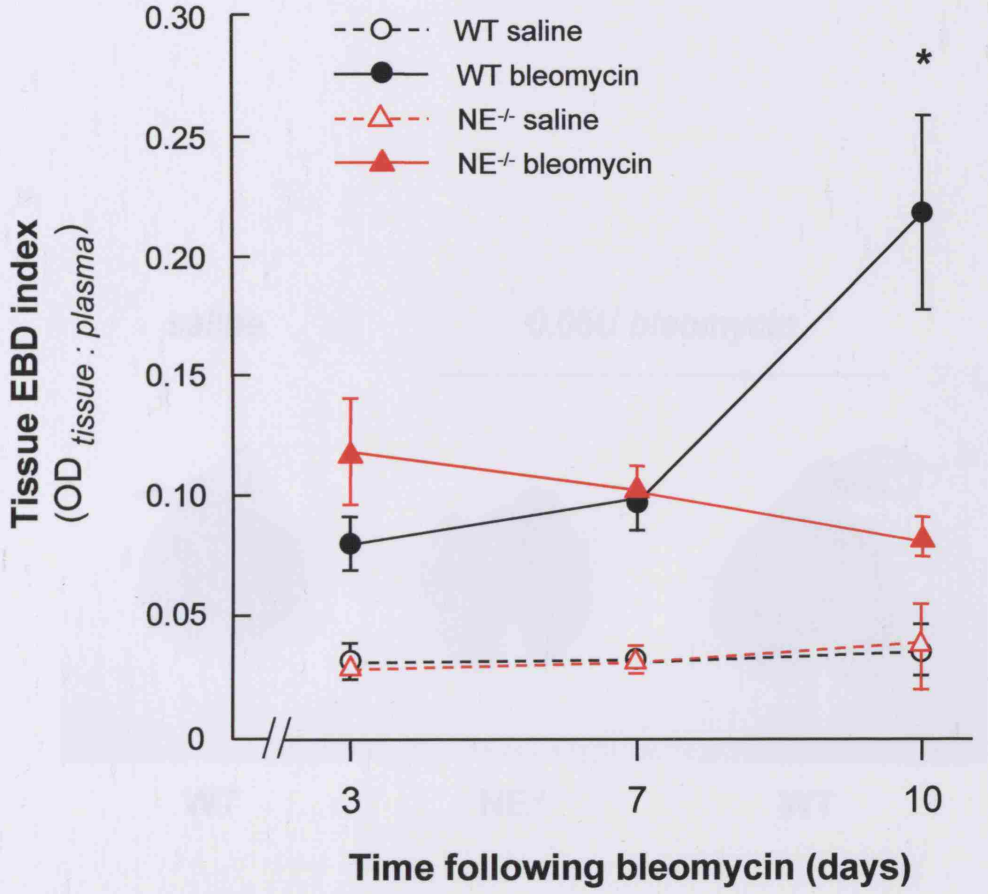

Figure 28. **Bleomycin-induced interstitial oedema in $NE^{-/-}$ mice is significantly less than in WT mice at 10 days following instillation.**

Accumulation of albuminophilic Evan blue dye in the pulmonary interstitium was analysed by homogenising lung tissue to extract trapped dye. The tissue : plasma ratio of EBD absorbance at 620 nm was used to indicate the extent of pulmonary interstitial oedema. Each point represents the mean ± SEM of three animals. * *$P < 0.01$ (bleomycin-treated WT vs. $NE^{-/-}$ mice)*

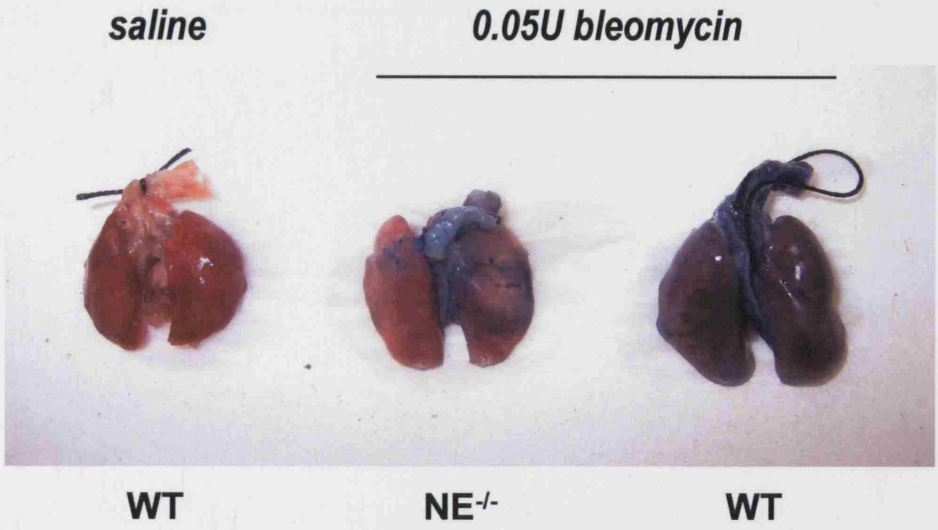

Figure 29. **Macroscopic appearance of lungs following EBD injection.**

Evans blue dye (EBD, 20 mg/kg) was injected via the tail vein ten days following intratracheal bleomycin or saline instillation and allowed to circulate systemically for one hour. Lungs were removed *en bloc* from the thoracic cage without prior saline perfusion.

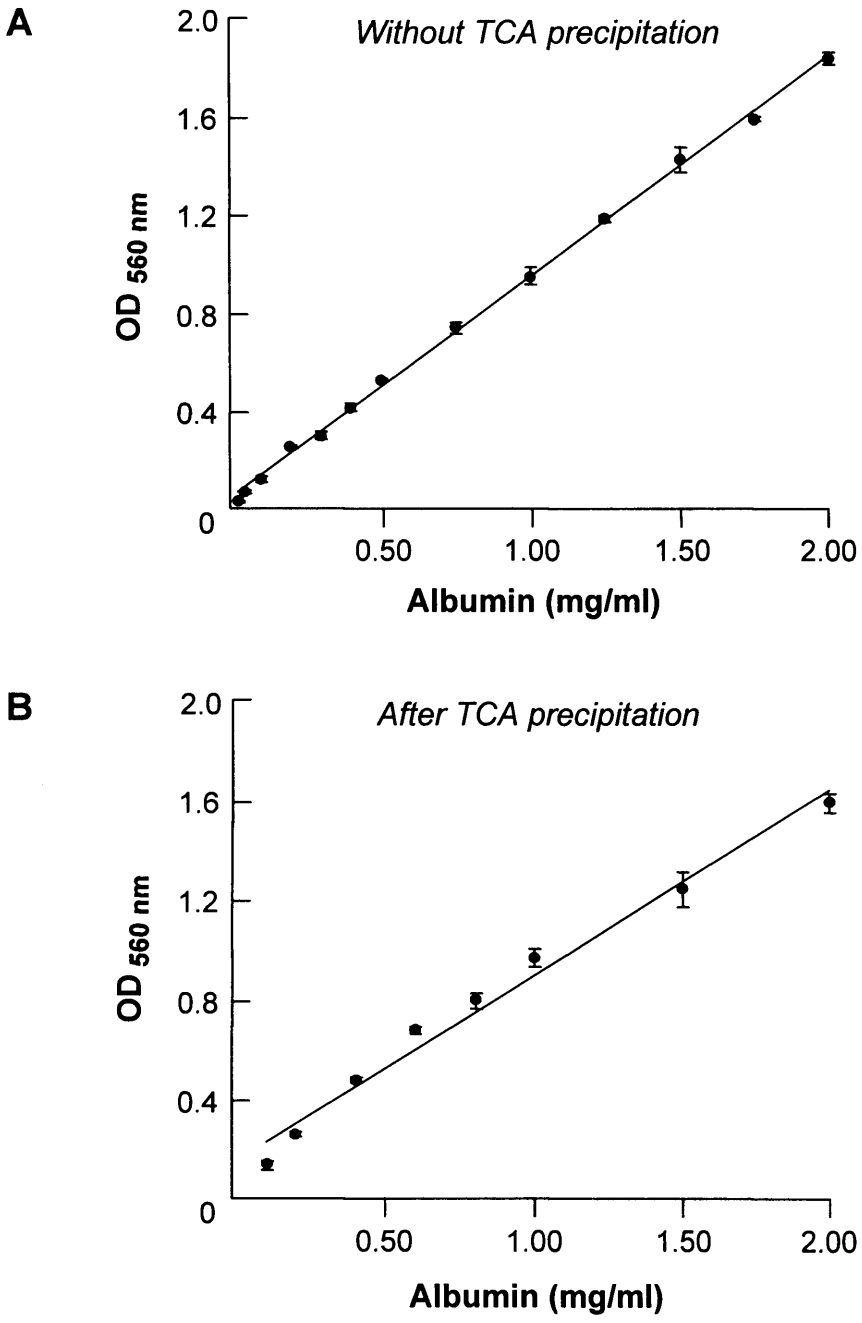

Figure 30. **Standard curve for the BCA protein assay.**

The Pierce bicinchoninic acid (BCA) assay was used to measure the albumin concentration in BAL fluid (panel A) and homogenised lung samples (not shown). Bovine serum albumin standards were supplied by the manufacturer. Some albumin standards were precipitated with trichloroacetic acid prior to use in the assay (Panel B). Each point represents the mean ± SEM of a triplicate.

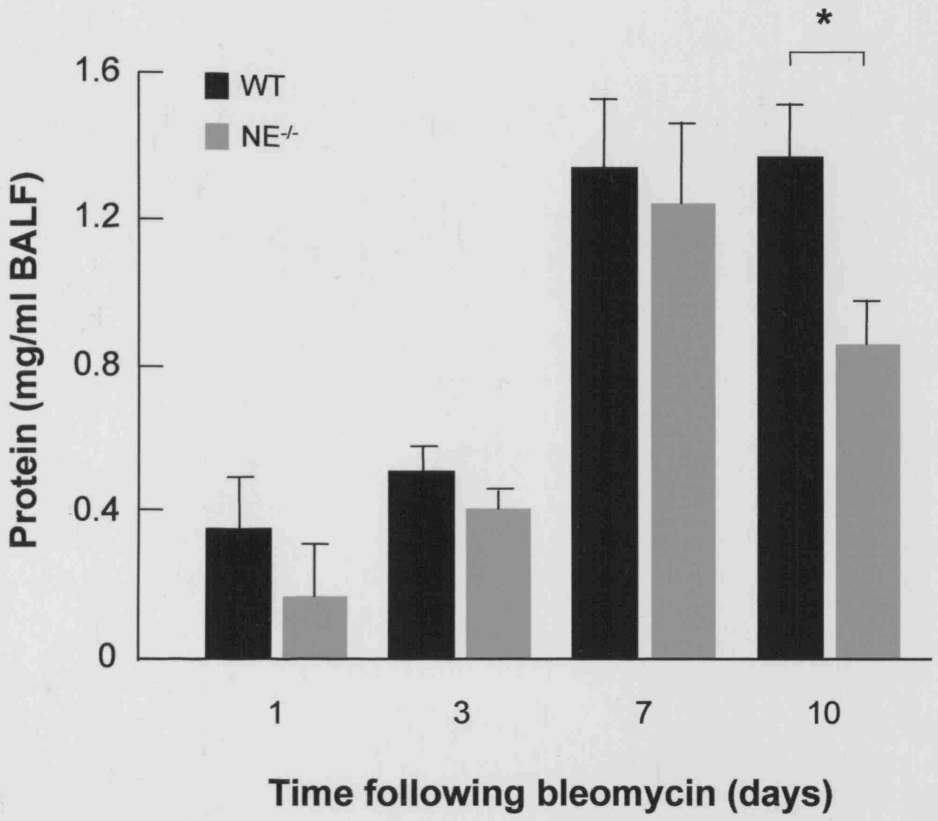

Figure 31. **Bleomycin instillation induces a progressive increase in BAL fluid albumin in WT and NE$^{-/-}$ mice that peaks at seven days.**

Albumin concentration in cell-free BAL fluid was measured spectrophotometrically using the Pierce BCA assay. Each sample was analysed in triplicate by measuring the absorbance of the reduced cuprous (Cu^{+})-containing products at 560 nm. Comparison against a standard albumin curve enabled the protein content in each sample to be determined. Values are expressed as mean ± SEM. Values from untreated and saline-treated animals were significantly less than bleomycin-treated values at all time points (less then 0.2 mg/ml BALF, data not shown). n = 5 in each treatment group. * $P < 0.05$

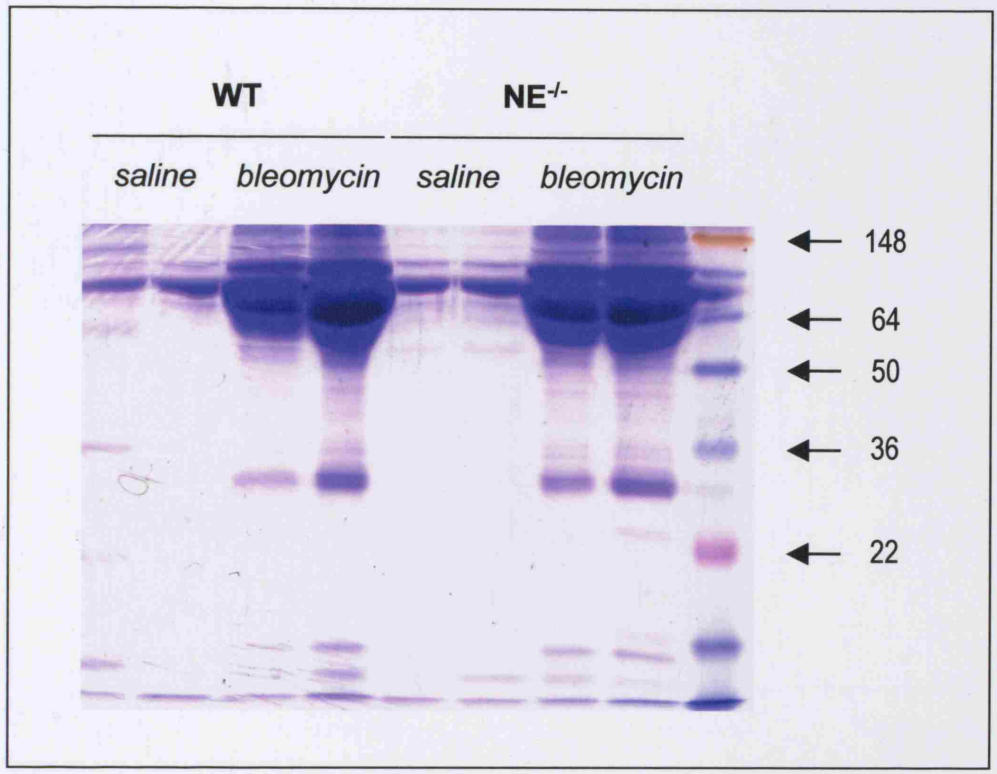

Figure 32. **BAL fluid protein from bleomycin-treated WT and NE$^{-/-}$ mice is primarily composed of albumin.**

Representative sodium dodecyl sulfate-polyacrylamide gel electrophoresis (SDS-PAGE) using BAL fluid from WT and NE$^{-/-}$ mice collected seven days after saline or bleomycin instillation and resolved using a 12% separating gel. Standard molecular weight markers were incorporated to aid identification of different proteins. In this particular gel, each lane indicates BAL fluid from one animal.

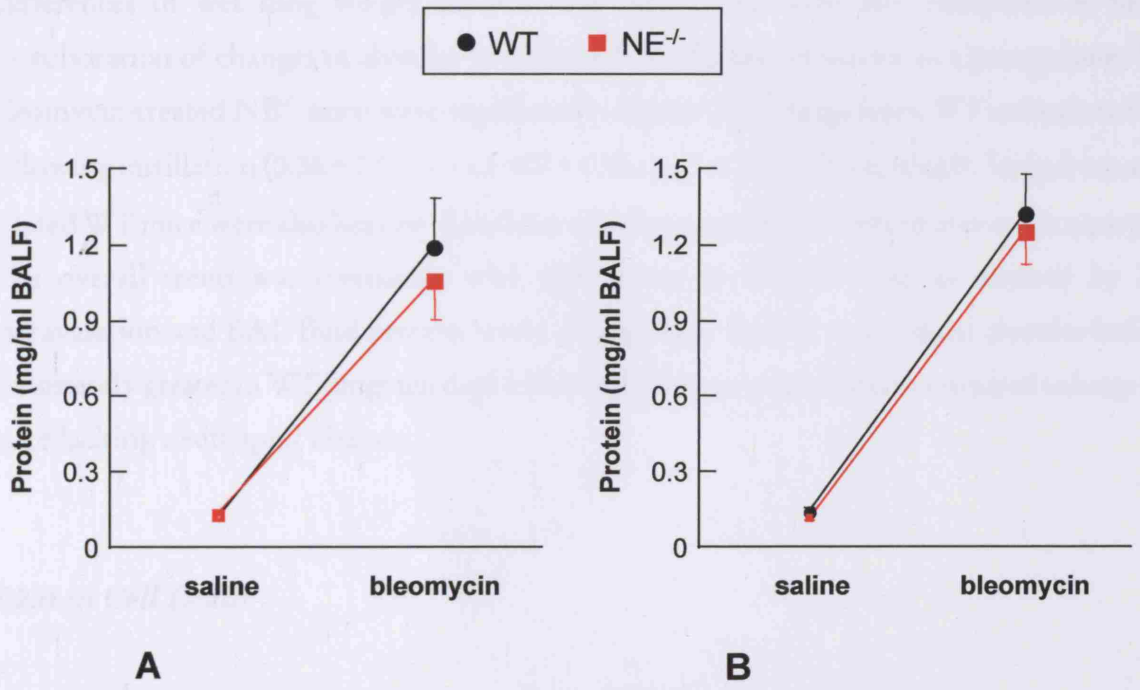

Figure 33. **Measurement of BAL fluid protein is not interfered by other substances.**

The Pierce bicinchoninic acid (BCA) assay was used to measure total protein in cell-free BAL fluid collected from WT and $NE^{-/-}$ mice 10 days following the instillation of either saline or bleomycin. Samples in Panel B were precipitated with trichloroacetic acid prior to analysis. Changes in absorbance were measured at 560 nm. Each point represents the mean ± SEM of a minimum of six different samples.

Moreover, the development of a band around the 30 kDa mark in BAL fluid of both bleomycin-treated WT and $NE^{-/-}$ mice remains unexplained. It is likely that the induction of this protein is related to bleomycin exposure due to its absence following saline treatment but its identity is unclear. Because lipids are known to interfere with the assay used to quantitate BAL fluid protein, standards (**figure 30b**) and samples (**figure 33**) were also precipitated with trichloroacetic acid (TCA) in parallel experiments. The degree of similarity in the amounts of BAL fluid protein measured with and without the TCA precipitation step indicated that the measurement of soluble protein in these samples was not altered by interfering substances.

Differences in wet lung weight in WT and $NE^{-/-}$ mice were also compared as further corroboration of changes in alveolar protein leak. As **figure 34** shows, as a group, lungs from bleomycin-treated $NE^{-/-}$ mice were significantly lighter than lungs from WT animals ten days following instillation (0.36 ± 0.012 g vs.0.407 ± 0.011 g, $P < 0.05$). Interestingly, lungs from saline-treated WT mice were also heavier than those of saline-treated $NE^{-/-}$ littermates at this time point. The overall trend was consistent with differences in alveolar leak as assessed by EBD extravasation and BAL fluid protein levels. Using these various techniques, alveolar leak was consistently greater in WT lungs ten days following bleomycin instillation compared to lungs from mice lacking neutrophil elastase.

5.2.ii.iii Cell Death

The amount of lactate dehydrogenase (LDH) in the extracellular compartment (BAL) was measured as an index of cell death. LDH in BAL fluid from bleomycin-treated WT and $NE^{-/-}$ mice was maximally increased above saline-treated values seven days following bleomycin instillation (**figure 35**). Although levels of LDH did not differ significantly between the two groups of mice at any time point assessed, WT values tended to be slightly higher particularly at the earlier time points. LDH levels in saline-treated BAL fluid from both genotypes were comparable.

5.2.ii.iv Morphologic changes

Bleomycin instillation in WT and $NE^{-/-}$ mice was associated with changes consistent with

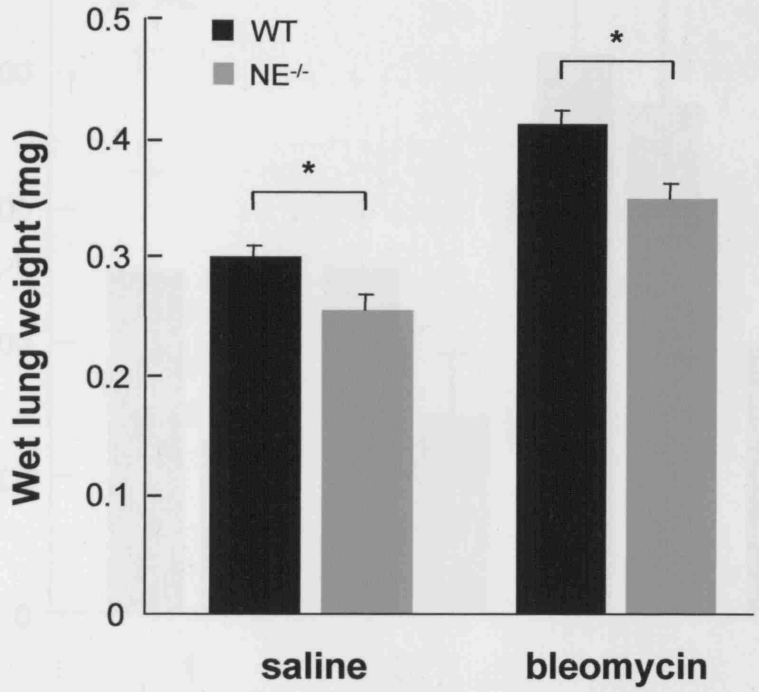

Figure 34. **Changes in wet lung weight ten days following bleomycin instillation.**

Wet lung weight was determined by weighing snap frozen lungs (without airways) harvested from WT and $NE^{-/-}$ mice ten days following 0.05 U bleomycin or saline instillation. Each bar represents the mean of eight to thirteen animals (error bars denote SEM). * $P < 0.05$.

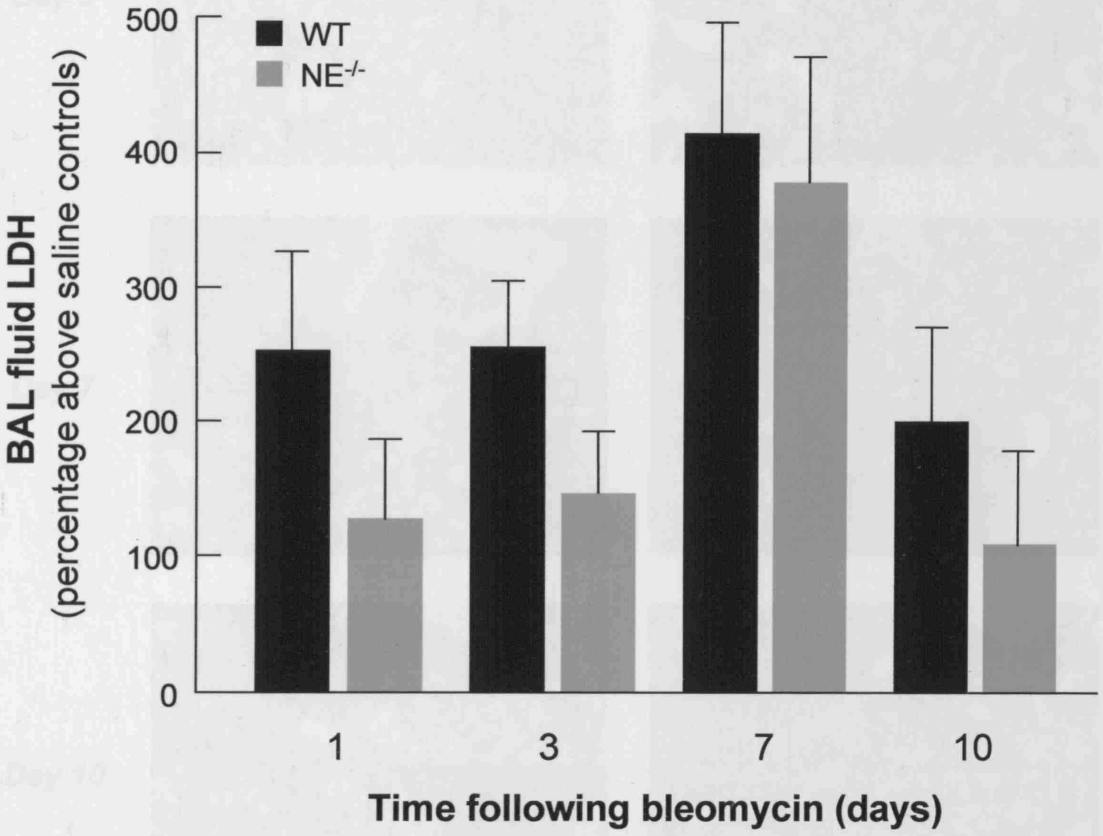

Figure 35. **Quantification of lactate dehydrogenase in BAL fluid.**

Levels of lactate dehydrogenase (LDH) in cell-free BAL fluid were measured using a colourimetric assay based on the enzymatic conversion of a tetrazolium salt into a red formazan product. Absorbances were analysed in triplicate at 490 nm. Values are expressed as percentage mean above saline values ± SEM. Levels of LDH from untreated animals were below saline values (not shown). n = 5 in each treatment group.

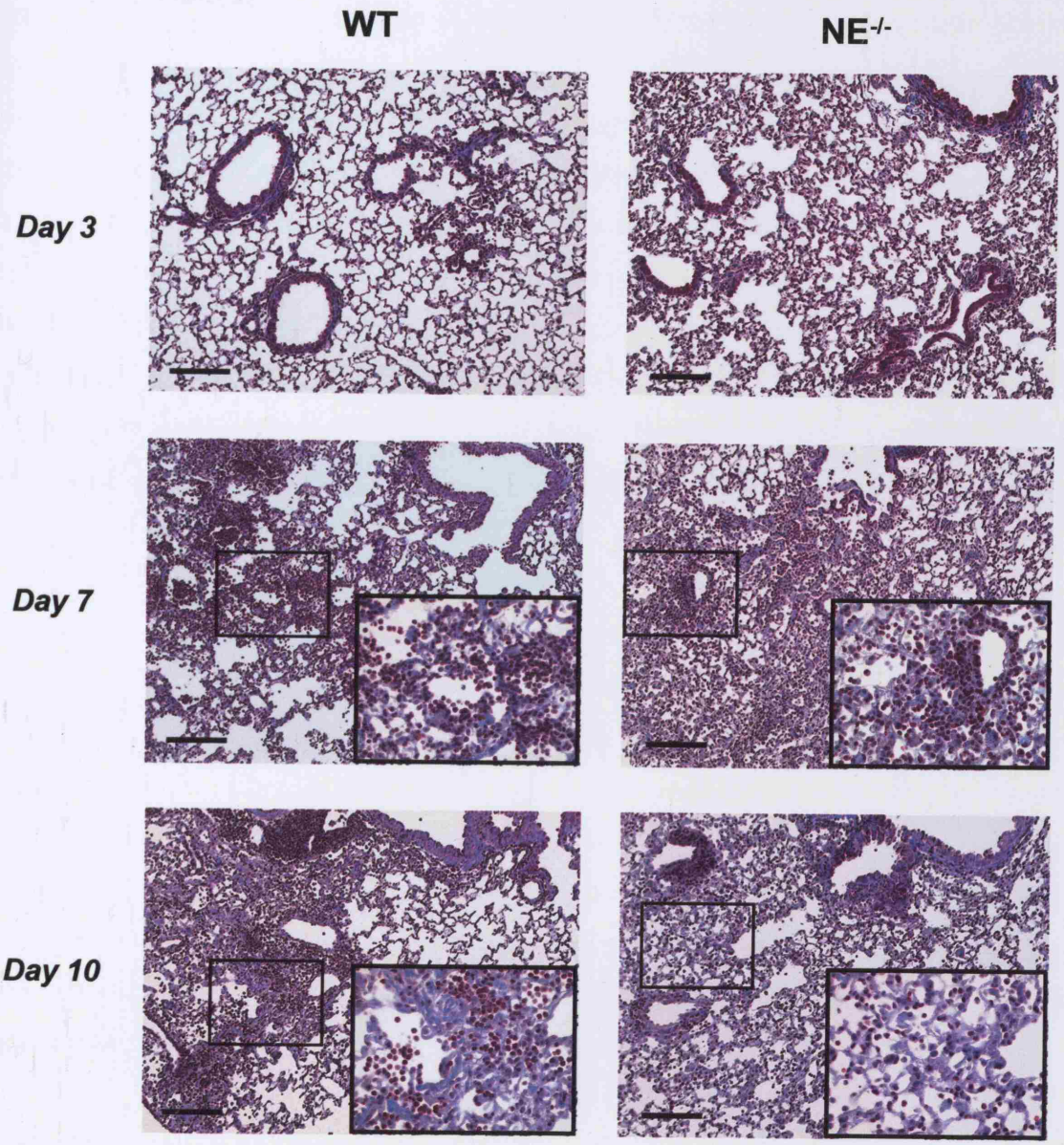

Figure 36. **Bleomycin instillation induces an intense alveolitis and alveolar damage in WT and NE$^{-/-}$ mice.**

Histology of paraffin-embedded lung sections of WT and NE$^{-/-}$ mice collected three, seven and ten days following the instillation of 0.05 U bleomycin showing widespread inflammatory foci in the parenchyma. Changes of lung injury were absent in the lungs of saline-treated control animals (not shown). *Bar*, 100 mm.

Masson's trichrome staining

acute lung injury. Three days following the administration of bleomycin, interstitial oedema and inflammation particularly in perivascular and peribronchiolar locations were the most obvious changes in the lungs of both genotypes of mice (**figure 36**, top panels). It was apparent even at low power that the overall alveolar architecture was disrupted. Injury to the pulmonary microvasculature was evidenced by the presence of erythrocytes in the alveolar airspaces which was best appreciated at high magnification. The intensity of alveolitis became increasingly pronounced and by seven days following bleomycin instillation, multifocal sites of inflammation had appeared throughout the lung parenchyma. The infiltrating leukocytes were a mixture of polymorphonuclear (neutrophils) and mononuclear cells (macrophages and lymphocytes). Marked disruption of the alveolar-capillary barrier in both bleomycin-treated WT and $NE^{-/-}$ mice was indicated by the loss of alveolar compartmentalisation (**figure 36**, middle panels). Overall, the degree of lung damage was comparable between bleomycin-injured WT and $NE^{-/-}$ lungs at the end of the first week.

By the tenth day following bleomycin instillation, numerous alveoli in WT lungs were filled with a combination of inflammatory cells, cellular debris and fibrinous exudates (**figure 36**, left lower panel). In addition, type II epithelial cell hyperplasia was noticeable particularly adjacent to congested alveoli. Bleomycin-treated $NE^{-/-}$ lungs also appeared abnormal although architectural damage seemed attenuated at this time point. In terms of inflammatory changes, many animals from both genotypes displayed features of persistent parenchymal inflammation that lasted into the third or fourth week following bleomycin administration. In comparison, morphologic features of persistent alveolar injury were absent in saline-treated WT and $NE^{-/-}$ mice (not shown). Any noticeable alveolar abnormality resolved within days of saline instillation.

The presence of tissue neutrophils throughout the entire duration of acute lung injury (days 3 – 10) was a pathologic hallmark in both WT and $NE^{-/-}$ lungs. However, neutrophils appeared to be dispersed over a wider area in the lungs of bleomycin-treated WT mice. In these specimens, neutrophils were often present within injured alveoli and scattered throughout the lung parenchyma (**figure 37**). In lungs from bleomycin-treated $NE^{-/-}$ mice, neutrophils aggregated predominantly around the smaller capillaries with less infiltration into the airspaces.

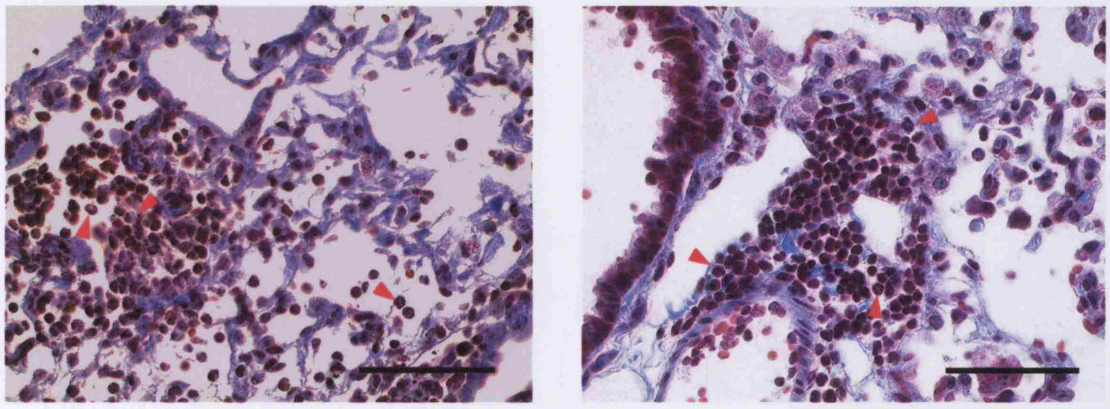

Figure 37. **Neutrophils are prominent in WT and $NE^{-/-}$ lungs seven days after bleomycin instillation.**

In bleomycin-treated WT lungs, neutrophils are dispersed over a large area of damaged lung and appear within injured alveoli. In $NE^{-/-}$ lungs, neutrophils have a greater tendency to remain associated with perivascular areas. *Bar*, 100 μm.

Masson's trichrome staining

5.3 Discussion

The findings presented in this chapter relate to: (1) the role of neutrophil elastase in recruiting neutrophils to sites of damaged lung, (2) the importance of neutrophil elastase in the severity of bleomycin-induced lung injury and inflammation, and (3) the relevance of particular aspects of lung injury to the eventual development of bleomycin-induced pulmonary fibrosis.

5.3.i Neutrophil elastase activity is not required for neutrophil recruitment to bleomycin-injured lungs

Implicit to the hypothesis that neutrophil-mediated matrix damage precedes fibrotic lung remodelling is the requirement that these cells must leave the bloodstream to reach sites of lung injury. The present data show that despite not possessing neutrophil elastase, neutrophils were able to infiltrate the alveoli of bleomycin-treated $NE^{-/-}$ mice. Both mature and immature forms of neutrophils breached the alveolar-capillary barrier to enter the perivascular space within hours of bleomycin instillation. The redundancy of neutrophil elastase in this process suggests that neutrophil transmigration from the vasculature does not solely depend on the proteolysis of an elastase-sensitive substrate. Closer inspection revealed that, compared to WT lungs, neutrophils in bleomycin-treated $NE^{-/-}$ lungs were retained for longer within the perivascular vicinity before they penetrated the surrounding alveoli. This observations suggests that neutrophil elastase might exert a rate-limiting effect on lung tissue neutrophil accumulation.

Proteolytic cleavage of the pulmonary ECM has long been thought to play a key role in regulating neutrophil influx into the lung (Watanabe et al., 1990; Bonnefoy and Legrand, 2000). However, the evidence that neutrophil elastase plays a direct role in mediating neutrophil migration into the lung has been conflicting. Studies in inflamed lungs have shown that neutrophils can migrate unimpeded into the alveoli of $NE^{-/-}$ mice infected by *klebsiella pneumoniae* (Belaaouaj et al., 1998). More recently, these observations have been extended to pulmonary infections caused by other gram-negative bacteria including *pseudomonas aeruginosa* (Hirche et al., 2004). Chronic exposure of $NE^{-/-}$ mice to cigarette smoke also leads to the development of pulmonary emphysema accompanied by alveolar neutrophilia (Shapiro, 2002). Likewise, neutrophil elastase deficiency does not impair neutrophils infiltrating into thioglycollate-inflamed serosal cavities (Tkalcevic et

al., 2000) or traversing through endothelial cell layers *in vitro* (Allport et al., 2002). Furthermore, in experimental bullous pemphigoid induced by the administration of antibodies targeting murine subepidermal BP180 ligand, the absence of neutrophil elastase does not prevent pathologic neutrophil accumulation in the skin of mice lacking this serine proteinase (Liu et al., 2000). In other words, neutrophil elastase does not appear to be necessary for neutrophil tissue penetration.

Emigration of neutrophils from the pulmonary circulation crucially relies on physical adaptation to sequestration (Doerschuk et al., 2000). *In vitro* observations that neutrophil elastase can bind competitively to CD11/18 have led to the suggestion that neutrophil elastase localised to the cell surface might proteolytically elute ligands involved in neutrophil immobilisation and thereby promote neutrophil migration. Functional proof has come from murine studies in which neutrophil elastase-mediated cleavage of CD11b/18 facilitated the migration of activated neutrophils into alveoli previously exposed to bacterial lipopolysaccharide (Cai and Wright, 1996). In contrast, other stimuli such as hyperoxia and activated complement factor 5 (C5a) do not depend on CD18-proteolysis for neutrophil recruitment (Doerschuk et al., 1990). It is possible that bleomycin may exert its pro-inflammatory effects on neutrophil influx in a CD18-independent manner. Even when a particular stimulus elicits neutrophil emigration primarily through CD18-dependent pathways, anti-CD18 antibodies only block such emigration by 60 - 80% which means that about 20 - 40% of neutrophils may be emigrating through CD18-independent pathways (Doerschuk et al., 2000).

Cytokine heterogeneity in terms of neutrophil chemoattraction has been described in the bleomycin model. Neutrophil elastase activity does not appear to be essential for mediating neutrophil migration in response to either IL-1β or TNF-α whereas zymosan-induced neutrophil adhesion and transmigration are significantly decreased following pharmacological inhibition of neutrophil elastase activity (Young et al., 2004). These observations confirm the versatility of neutrophils in utilising different molecular pathways to find their way into injured lung tissue.

A series of studies by Walker and colleagues has shown that neutrophils can seek out and traverse gaps between neighbouring endothelial cells (Burns et al., 2003). Neutrophils have even been observed to adhere to the surface of fibroblasts embedded within an interstitial barrier to aid their own migration across that lining (Behzad et al., 1996). More recent studies have shown that the coordinated release of syndecan-1, a heparan sulfate proteoglycan, and KC, an epithelium-derived CXC chemokine, by matrilysin (MMP-7) promotes transepithelial neutrophil migration in the

setting of bleomycin-induced lung injury (Li et al., 2002). By acting as a 'sheddase' to cleave the ectodomain of epithelial syndecan-1, matrilysin generates a gradient of ectodomain-bound KC that functions to direct and facilitate neutrophil infiltration into alveolar airspaces following the initiation of lung injury. In matrilysin-deficient animals, neutrophils were seen to congregate perivascularly but could not penetrate into alveoli. A similar observation has been made in the present studies, suggesting that a neutrophil elastase-sensitive substrate may enhance alveolar neutrophil infiltration. As yet, it is not known if the delayed tissue influx in $NE^{-/-}$ lungs affects subsequent tissue repair.

The kinetics of inflammatory cell infiltration in the current study are consistent with those in the reported literature. Peak neutrophilia occurring at seven days post-bleomycin instillation has also been described in other murine bleomycin studies (Izbicki et al., 2002; Teder et al., 2002). The histological presence of neutrophils for a number of weeks after bleomycin administration suggests that neutrophil inflammation may be a more sustained phenomenon in 129S6/SvEv mice than in other strains previously studied. The persistent lung tissue neutrophilia, particularly prominent in bleomycin-treated $NE^{-/-}$ mice, implicates a role for these cells in tissue remodelling events and in more chronic sequelae such as pulmonary fibrosis.

5.3.ii The absence of neutrophil elastase does not decrease the severity of bleomycin-induced lung injury or inflammation

The deleterious effects of unopposed neutrophil elastase activity on alveolar structures has been implicated in the development of both clinical and experimental forms of acute lung injury. Local elastase : anti-elastase imbalances resulting from inadequate antiproteinase defenses are believed to underpin many manifestations of acute and chronic lung injury. Pretreatment with neutrophil elastase inhibitors in animal models of acute lung injury consistently attenuates characteristic parameters such as BAL fluid neutrophilia and alveolar-capillary permeability. In guinea pigs treated with *E. coli* endotoxin, inhibition of neutrophil elastase activity by ONO-5046 decreased BAL fluid neutrophilia and alveolar-capillary permeability as assessed by the proportion of radiolabeled albumin in BAL fluid to that in plasma and the wet-to-dry lung weight ratio (Sakamaki et al., 1996). Similarly, in dogs subjected to ischaemic reperfusion lung injury, ONO-5046 minimised lung extravascular water accumulation which led to improved lung compliance and decreased levels of pro-inflammatory IL-6 and IL-8 in the circulation (Yamazaki et al, 1999).

Inhibitors of neutrophil elastase also exert protective effects in thrombin-induced pulmonary oedema (Saldeen et al., 1991), IgG immune complex-induced lung injury (Bless et al., 1997) and organic acid-induced lung and systemic injury (Kaneko et al., 1997). Despite these findings, a unifying mechanism to account for the role of neutrophil elastase in lung injury has not been described.

Because of its short half-life *in vivo* (less than 32 minutes in murine lungs; Lazo and Pham, 1984), maximal DNA damage caused by bleomycin could be expected to occur rapidly and coincide with deleterious effects on the lung epithelium. It follows that an enhanced rate of DNA repair might correlate with increased resistance to bleomycin-induced lung toxicity. In the current study, acute changes in single-stranded DNA damage and repair following bleomycin instillation did not distinguish WT from $NE^{-/-}$ lung cells. The cytotoxic effects of bleomycin at such early time points were likely to obscure any changes in DNA damage attributable to neutrophil elastase. The observed changes in single-stranded DNA breakage correlated with increases in lung poly (ADP-ribose) polymerase (PARP) activity in both bleomycin-treated WT and $NE^{-/-}$ mice during the period of acute lung injury (data not shown due to limited numbers). PARP is an enzyme of lung DNA repair and measurement of its activity has been linked to the sensitivity of murine lungs to bleomycin and its associated effects on cellular integrity (Hoyt and Lazo, 1992).

The administration of exogenous α_1-PI and SLPI when given either prior to or concomitantly with bleomycin has been shown to decrease total BAL fluid leukocytes in the first week following bleomycin instillation (Nagai et al., 1992; Mitsuhashi et al., 1996). Intraperitoneal injection of twice-daily SLPI for 10 days starting from the day of bleomycin administration also decreases lung tissue leukocyte accumulation. Similarly, when ONO-5046, a synthetic neutrophil elastase inhibitor, is administered together with bleomycin instillation over a ten-day period, BAL fluid inflammatory cell numbers are decreased for up to a month afterwards (Taooka et al., 1997). In the latter, suppression of leukocytosis was also associated with early reductions in BAL fluid IL-1β, PDGF-A and IGF-1. Even though the use of these inhibitors appeared to attenuate non-specific indices of inflammation, their effects were temporary.

Precisely why neutrophil elastase deficiency does not protect against bleomycin-induced lung injury is not entirely clear. As previously mentioned, it is possible that the severity of early bleomycin-induced lung damage made it difficult to attribute particular aspects of alveolar injury to neutrophil elastase. Neutrophil depletion has previously been shown to ameliorate the *in vivo*

development of experimental lung injury (Albertine, 1988). However, such studies used granulocyte-neutralising antibodies active in the peripheral circulation but failed to suppress bone marrow production of new granulocytes, resulting in incomplete neutrophil depletion in the bloodstream. The administration of exogenous α1-PI also attenuates bleomycin-induced cellular inflammation although this is not a result of diminished neutrophil elastase activity in the treated animals (Nagai et al., 1992). Other non-proteolytic pathways of lung injury may be involved, including the contribution of hydrogen and oxygen radicals as well as immune-mediated mechanisms of tissue damage. It is possible that such processes may interact with neutrophil elastase-mediated pathways to accentuate lung tissue injury following the instillation of bleomycin.

5.3.iii Neutrophil elastase activity delays alveolar-capillary barrier repair following bleomycin-induced lung injury

Disintegration of the alveolar-capillary barrier causing alveolar flooding in the context of acute lung injury is associated with an increased likelihood of progression to pulmonary fibrosis (Matthay, 2004). In acute lung injury in general and the bleomycin model in particular, fibroproliferative complications may be initiated while the injured alveoli remain hyper-permeable to macromolecules and cells. In the present studies, morphologic signs of gross alveolar cell damage including vacuolisation, cytoplasmic expansion and detachment from the basement membrane were evident within days of bleomycin instillation in both WT and $NE^{-/-}$ mice.

Alveolar barrier damage can occur due to the release of cytotoxic products by transmigrating neutrophils. However, this is usually characterised by a temporary and reversible decrease in the transepithelial resistance (Nusrat et al., 1997). More lasting effects of alveolar barrier injury may develop following other insults. Hence, a morphologic assessment of barrier breakdown without correlation to physiological dysfunction only provides an incomplete analysis of alveolar injury. In the present studies, comparisons of alveolar barrier macromolecular selectivity provided one of the most striking differences of alveolar injury between bleomycin-treated WT and $NE^{-/-}$ animals. In essence, hyper-proteinaemia in BAL fluid induced by bleomycin treatment decreased considerably earlier in $NE^{-/-}$ mice than in WT animals which suggested more prolonged damage of the epithelial barrier in the latter.

The use of Evans Blue dye (EBD) enabled the permeability of both the endothelial and epithelial linings in both groups of mice to be assessed in greater detail. EBD must traverse both these barriers and their respective basement membranes in order to get into BAL fluid. On the other hand, EBD that is extracted from lung tissue is trapped within the pulmonary interstitium and need only have traversed the endothelial barrier to enter this compartment. The observation that bleomycin treatment significantly and comparably increased BAL fluid and lung tissue permeability in both WT and $NE^{-/-}$ lungs up to seven days indicated that the severity of bleomycin-induced tissue damage may have masked specific neutrophil elastase-mediated effects on the alveolar barrier or that neutrophil elastase activity is not required for the initial degradation of this barrier. Evidence for the latter is supported by studies where the removal of neutrophil elastase or cathepsin G activity from the supernatant of activated neutrophils does not affect the microvascular permeability of cultured endothelial cells (Gautam et al., 2001). Put another way, the earlier resolution of alveolar barrier leak in bleomycin-treated $NE^{-/-}$ mice suggests that deleterious neutrophil elastase activity may be more important during the reparative phase of barrier injury.

At least two potential mechanisms can explain the time frame allowing unopposed neutrophil elastase activity to retard alveolar-capillary barrier repair during bleomycin-induced lung injury. As previously mentioned, neutrophil elastase might act early during the acute phase but its effects only become evident when the alveolar damage induced by bleomycin has subsided. Alternatively, it might act on one or more substrates in the barrier approximately a week post-instillation of bleomycin when its impact on barrier repair is likely to be greatest. Neutrophil elastase has been shown to degrade proteins within tight cell junctions involved in maintaining cellular integrity and tissue compartmentalisation. These include VE-cadherins in endothelial cells (Carden et al., 1998) and E-cadherins that separate mature epithelial cells (Ginzberg et al., 2001). However, if cadherin proteolysis was the primary mechanism for elastase-mediated barrier injury, it would not explain why alveolar leak is no different between the two genotypes of mice in the first seven days following bleomycin instillation. Unless of course, cadherin proteolysis itself occurs as a late event, either on its own or in combination with neutrophil elastase-induced detachment of epithelial cells and degradation of type IV collagen. Although possible, evidence to support this premise is not presented in the current studies.

The mechanism most consistent with the present data is one where neutrophil elastase activity modulates the activity of a second molecule which allows it to potentiate and prolong alveolar

barrier dysfunction. One candidate is TGF-β, a molecule that has been shown to disrupt the integrity of cellular components of the alveolar-capillary barrier in a number of ways. TGF-β can increase endothelial permeability by increasing the gaps between adjoining cells (Hurst et al., 1999). This effect results from myosin light chain kinase-dependent signaling leading to endothelial cell contraction, a phenomenon that is itself dependent on the proliferative state of these cells. More recently, TGF-β has been shown to directly increase alveolar cell permeability *in vivo*, in a mechanism involving the depletion of intracellular glutathione and an increase in the concentration of its oxidized form, glutathione disulfide (Pittet et al., 2001). Glutathione is depleted from the epithelial lining fluid in animal models of lung injury (Guidot et al., 2000) and in patients with ARDS (Bunnell and Pacht, 1993). Moreover, TGF-β has also been shown to act as a pro-oxidant by increasing the cellular generation of hydrogen peroxide (Das and Fanburg, 1991).

In addition to these actions, TGF-β may also inhibit surfactant component expression and enhance Fas-mediated apoptosis of epithelial cells (Beers et al., 1998; Hagimoto et al., 2002). Fas ligation itself can augment the release of proinflammatory cytokines to promote epithelial cell injury (Chen et al., 1998). Of note, activation of the Fas-fasL pathway has been previously shown to be an important pathogenetic mechanism in bleomycin-induced pulmonary fibrosis (Kuwano et al., 1999). More recently, neutrophil elastase has been shown to mediate apoptosis of human alveolar epithelial cells *in vitro* through a mechanism implicating proteinase activated receptor-1 (PAR-1) (Suzuki et al., 2005). More specifically, the process involved altered mitochondrial permeability, translocation of cytochrome c to the cytosol and enhanced cleavage of death enzymes, caspase-3 and caspase-9, leading to JNK and Akt inhibition. One other physiological abnormality linked to TGF-β activity in the alveoli is the reduction of epithelial sodium and water clearance due in part to the suppressed expression of apical membrane sodium (alphaENaC) channels (Frank et al., 2003). Taken together, these studies suggest that TGF-β activity is important beyond its classic association with fibrotic tissue remodelling during the late phase of lung injury. Its pathogenic role in earlier phases of lung injury is now emerging, particularly in the context of alveolar hyper-permeability. Hence, its sustained actions throughout the evolution of alveolar injury may provide the crucial links that bridge acute lung injury with eventual pulmonary fibrosis.

5.3.iv How does alveolar barrier leak impact on fibrotic matrix accumulation in the lung?

Although severe and persistent alveolar leak is linked to a greater tendency to form pulmonary fibrosis, it is not known whether leak *per se* exerts a rate-limiting effect on the development of fibrotic lesions. What is not disputed is that alveolar leak allows a significant amount of protein-rich oedema fluid containing inflammatory and fibrogenic cytokines to reach the alveolar spaces. Mediators such as IL-1, IL-6 and TGF-β have been measured in increased amounts in pulmonary oedema fluid (Dhainaut et al., 2003; Olman et al., 2004). In the past, inhibition of alveolar surfactant protein function by plasma-derived proteins has previously been demonstrated *in vitro* (Fuchimukai et al., 1987). More recently, abnormalities in surfactant function have been suggested as an additional pathogenic factor in the development of fibroproliferative lung disorders (Gunther et al., 1999). As one of many examples, the surfactant-inhibitory capacity of fibrinogen is markedly enhanced upon its conversion to fibrin and the acquisition of greater hydrophobicity once it has reached the alveolar space (Seeger et al., 1999).

Ultrastructural studies have shown that the invasion of matrix-synthesising fibroblasts into damaged alveoli also commences during this phase (Kuhn III et al., 1989). Tissue accumulation of these cells is associated with discontinuities in the epithelial basal lamina and contributes to the formation of intra-alveolar fibrosis as well as fibroblastic foci within the parenchymal interstitium. The latter consist of matrix-producing fibroblasts/myofibroblasts organized in clusters that are thought to represent sites of active collagen synthesis (Katzenstein and Myers, 1998). The structure of these foci suggests that they arise in areas of prior exudate deposition that provide a substratum for the invading fibroblasts. Fibroblastic foci often coincide with areas of damaged basal laminae and are typically bounded by damaged or reactive epithelium.

Persistent alveolar leak also impairs oxygenation and is linked to higher oxygen debt (hypoxia) as a direct result of the degree of lung injury. In human fibroblasts, the combination of hypoxia and the presence of other injurious mediators such as TGF-β can reduce cellular MMP-1 expression while at the same time amplify the expression of tissue inhibitors of matrix proteinases (TIMP) and collagen type I (Papakonstantinou et al., 2003). Put simply, lung injury induces pulmonary tissue oxygenation that in turn perpetuates adaptive responses including an altered mediator secretion profile that favours fibroproliferative lung repair.

In the clinical setting, a link between alveolar leak and lung fibrosis has been most widely studied in ARDS. In this catastrophic disorder, alveolar hyper-permeability is a pathologic hallmark with negative prognostic implications (Matthay, 2004). The development of fibrosing alveolitis carries a significant risk of death in these patients and is more likely to result from uncontrolled and severe pulmonary oedema (Clark et al., 1994). In recent years, elevated levels of procollagen III, a biological marker of collagen synthesis, have been identified in ARDS patients with more adverse physiological scores (Clark et al., 1994). Hence, the observation that more efficient repair of the damaged alveolar-capillary membrane may somehow protect against later fibrotic sequelae in bleomycin-treated mice lacking neutrophil elastase may have important implications clinically. Studies have shown that neutrophil elastase activity is elevated and α_1-proteinase inhibitor (α_1-antitrypsin) is reduced in BAL fluid of patients with ARDS (Lee et al., 1981; Gando et al., 1997). Critically ill individuals at-risk of developing ARDS also have increased alveolar and circulating levels of neutrophil elastase compared to those who do not develop the syndrome (Donnelly et al., 1995). Furthermore, BAL fluid levels of both SLPI and elafin are markedly increased in ARDS patients suggesting that vigorous attempts at mounting an anti-elastase response within the lung are initiated during severe lung injury but are ultimately inadequate at controlling alveolar damage (Sallenave et al., 1999).

The suppression of alveolar permeability has also been associated with the attenuation of bleomycin-induced pulmonary fibrosis (Iyer et al., 2000; Yasui et al., 2001). Increased alveolar fluid and solute loss due to leak has been documented using radiolabeled albumin and non-albumin tracers such as 99mTc-DTPA (Jordana et al., 1988). This concept has also been studied indirectly. For example, the intratracheal instillation of carbon particles at a time when the alveolar barrier is already repaired following bleomycin-induced injury does not appear to induce additional fibroblast growth or collagen deposition (Adamson and Prieditis, 1995). Once the alveolar leak is plugged and fibrosis is established, further fresh injury is unlikely to influence the magnitude of the resultant fibrosis. Hence, the current findings are consistent with the hypothesis that repair of the alveolar-capillary barrier is an important step in maintaining alveolar architecture and impeding the development of pulmonary fibrosis.

CHAPTER SIX

BLEOMYCIN-TREATED $NE^{-/-}$ MICE HAVE DIMINISHED PULMONARY LEVELS OF ACTIVE TGF-β

6.1 Background

6.1.i Increased TGF-β activity promotes pulmonary fibrosis in animal models

TGF-β is widely regarded as the most potent mediator of tissue fibrosis. TGF-β gene expression and protein production are increased in animal models of pulmonary fibrosis resulting from the administration of bleomycin, silica or asbestos fibres, or irradiation of the thoracic cage (Phan and Kunkel, 1992; Williams et al., 1993; Rube et al., 2000). In the bleomycin rodent model of pulmonary fibrosis, elevations in TGF-β mRNA and levels of procollagen molecules consistently precede the development of pathologic evidence of fibrotic lung damage (Hoyt and Lazo, 1988). Steady-state expression of TGF-β transcripts significantly increase about one week after intratracheal instillation of bleomycin in mice, hamsters and rats (Hoyt and Lazo, 1988; Raghow et al., 1989; Westergren-Thorsson et al., 1993). More recently, the correlation of decreased TGF-β activation (Munger et al., 1999), production (Huang et al., 2002) or tissue abundance (Azuma et al., 2005) with attenuated bleomycin-induced pulmonary fibrosis has further consolidated the importance of TGF-β as a key fibrogenic mediator.

Approaches using antibodies or soluble receptors to neutralise TGF-β activity have proven to be effective at inhibiting the development of bleomycin-induced pulmonary fibrosis (Giri et al., 1993; Wang et al., 1999). Targeted overexpression of decorin, a naturally occurring proteoglycan inhibitor of TGF-β, in alveolar cells also attenuates the lung fibrotic response resulting from prior administration of bleomycin (Kolb et al., 2001b). Moreover, inhibition of Smad3, a stimulatory protein involved in TGF-β signalling, by overexpression of the inhibitory Smad7 protein inhibits the development of bleomycin-induced pulmonary fibrosis (Nakao et al., 1999). More recently, the same protective phenotype against pulmonary fibrosis has been duplicated in mice with a targeted deletion of Smad3 itself (Zhao et al., 2002). In organs other than the lung, the anti-fibrotic properties of decorin have been successfully employed to abrogate renal and gliotic brain scarring, pathological situations in which the profibrotic potential of TGF-β has been implicated (Isaka et al., 1996; Logan et al., 1999). Smad3-null mice also have drastically decreased fibrotic

responses in radiation-induced cutaneous fibrosis (Flanders et al., 2002) and carbon tetrachloride-induced hepatic fibrosis (Schnabl et al., 2001).

Direct evidence that TGF-β is potently fibrogenic has been shown by directly overexpressing active TGF-β in the lungs of host animals (Sime et al., 1997). In the same study, latent TGF-β was not fibrogenic when overexpressed in the lung. Overexpression of active TGF-β induced severe and lasting pulmonary fibrosis with intense myofibroblast induction. Adenoviral-mediated delivery of GM-CSF, IL-1β and TNF-α genes to the alveoli also induces diffuse pulmonary fibrosis. The regulatory processes that underpin excessive lung matrix deposition following the administration of these growth factors appears to be TGF-β dependent (Xing et al., 1997; Kolb et al., 2001a; Liu et al., 2001). These findings strongly suggest a capacity for TGF-β to act as a 'conductor cytokine' in regulating tissue repair pathways that culminate in lung fibrosis (Gauldie et al., 2001).

6.1.ii Mechanisms of fibrogenic activity of TGF-β

Fibroblasts express TGF-β receptors comprising two serine/threonine kinase subunits, TGF-β type I receptor (TβRI) and TGF-β type II receptor (TβRII) (Massague, 1998). The TβRII kinases are constitutively active; ligand binding to TβRII allows the latter to activate the TβRI kinase through phosphorylation of its juxtamembrane domain, mainly at the glycine-serine-rich or GS domains (Heldin et al., 1997). Signals from TGF-β receptor activation are transduced either by a series of latent cytoplasmic transcription factors called Smad proteins or by the entire complex of mitogen-activated protein kinase (MAPK) pathways (Shi and Massague, 2003). However, various degrees of cross-talk exist between the different transduction pathways, as evidenced by the ability of the ras / MEK / ERK MAP kinase cascade to modify the function of Smad-mediated signalling (Mulder, 2000). In addition, the initial presentation of TGF-β to its receptor may occur in association with accessory proteins, such as betaglycan and endoglin, an interaction that can modify the cellular response (Letamendia et al., 1998; Leask et al., 2002).

When the Smad signalling pathway is engaged, TGF-β binding allows TβRI kinase to directly phosphorylatate the receptor-activated Smads (Smad2 and Smad3) on a C-terminal motif while still in the cytoplasm (Derynck et al., 1998). These phosphorylated R-Smads then hetero-

oligomerise with the common mediator Smad4 and translocate to the cell nucleus where they bind to sequence-specific DNA known as Smad-binding elements (SBE) (Zawel et al., 1998). Smad-dependent transcriptional control is reliant upon Smad proteins interacting with the appropriate transcriptional factor(s), including Sp-1, DP1 and Miz-1, to achieve the desired gene effect (Shi and Massague, 2003).

As TGF-β receptors and transcriptional factors in the main are limited, it is likely that alterations in signalling pathways help differentiate biologic responses to TGF-β. In its capacity as a key downstream mediator of pulmonary fibrogenesis, the stimulatory effects of TGF-β are most prominent at two levels: (1) its ability to promote fibroblast growth and activation, and (2) its effects on ECM production and organisation. Although TGF-β can upregulate the synthesis of collagens, elastin, proteoglycans and glycoproteins, most studies of TGF-β-dependent lung matrix production have concentrated on collagen. Active TGF-β specifically induces lung collagen formation by a combination of upregulating collagen gene expression, increasing collagen mRNA stability and inhibiting post-translational collagen protein breakdown (reviewed in Cutroneo 2003). TGF-β-responsive sequences in the human α1 (I) procollagen gene promoter have been identified using transfection studies in NIH/3T3 cells (Jimenez et al., 1994). These TGF-β binding sites are believed to regulate the basal expression of the mouse and rat α1 (I) procollagen genes *(COL1A1)*.

TGF-β usually induces synthesis of α1 (I) and α2 (I) collagen pro-polypeptides in a strict 2 : 1 proportion (Curoneo, 2003). However, TGF-β-mediated regulation of procollagen gene expression may be cell type- and species-specific. For example, TGF-β-stimulated transcription of the α1 (I) procollagen gene *(COL1A1)* appears to be controlled by nuclear factors interacting at the DNA Sp1-like binding site (Gaidarova and Jimemez, 2002). In contrast, transcription of the human α2 (I) procollagen gene *(COL1A2)* is regulated primarily by the TGF-β-dependent Smad signalling pathway (Cutroneo, 2003). Smad3 and Smad4 are required for TGF-β-induced α2 (I) procollagen expression in cultured human skin fibroblasts and act as transcription factors that interact with DNA-bound Sp1 complexes (Chen et al., 2000; Poncelet and Schnaper, 2001).

TGF-β also potently induces fibroblast growth and activation, processes synonymous with the transformation of quiescent fibroblasts into more contractile and metabolically active cells called

myofibroblasts (Desmouliere et al., 1993). Fibroblast phenotype switching is characterised by increased expression of the transdifferentiation marker α-smooth muscle actin (α-SMA). Combined in-situ hybridisation studies have shown that procollagen type I messenger RNA frequently co-localises with immunostaining for α-SMA, an observation consistent with myofibroblasts as a key source of collagen production in the lung (Zhang et al., 1994). Furthermore, TGF-β protects myofibroblasts against apoptotic signals and prolong their survival (Zhang and Phan, 1999).

Most cells secrete TGF-β as a latent molecule comprising the mature TGF-β moiety non-covalently bound its latency-associated peptide (LAP) (Gentry et al., 1988). An important mechanism for controlling TGF-β activity is the post-translational processing that removes LAP from the mature peptide (Lawrence, 1991). Successful LAP-TGF-β separation appears to be critical for TGF-β activity, since enhanced TGF-β expression does not always equate to increased TGF-β activity (Theodorescu et al., 1991). *In vitro*, a number of methods including thermal, acidification and proteolysis, have been shown to activate latent TGF-β (Gleizes et al., 1996).

6.1.iii Proteolytic control of TGF-β activity in the extracellular environment

TGF-β is subjected to proteolytic regulation at various points of its synthetic and secretory pathway. While still within the Golgi apparatus, the TGF-β gene product is digested by a furin-type endopeptidase at a 'RRXR' sequence to produce two monomers that rapidly dimerise (Dubois et al., 1995). The larger N-terminal fragment forms the LAP while the smaller C-terminal portion becomes the mature TGF-β homodimer. Both molecules remain non-covalently bound in a conformation known as the small latent TGF-β complex. Just prior to secretion, a covalent bond is formed between the cysteine-33 residue of LAP and an 8-cys structural motif located in latent TGF-β binding protein (LTBP) molecules (Saharinen and Keski-Oja, 2000). This process is thought to be necessary for rapid and efficient secretion of the large latent TGF-β complex.

Outside the cell, most large latent TGF-β complexes (LTBP-LAP-TGF-β) are targeted to the ECM by a tissue transglutaminase acting on substrate motifs in the N-terminal portion of the LTBP molecule (Nunes et al., 1997). Generation of active TGF-β in the extracellular

microenvironment also implicates two further roles for proteolysis. Serine proteinases such as plasmin, calpain, some cathepsins, neuraminidase, sialidase and endoglycosidase F can cleave the LAP-TGF-β bond to produce active TGF-β *in vitro* (reviewed in Khalil, 1999). Other proteinases, such as MMP-9 (gelatinase B), have been shown to activate latent TGF-β localised to keratinocyte cell surfaces by degrading the LAP component (Yu and Stamenkovic, 2000). Moreover, urokinase-type plasminogen activator (uPA) can increase TGF-β activity in osteoblast cultures in a process which likely requires plasmin as an intermediate mediator (Yee et al., 1993). Finally, the release of ECM-bound latent TGF-β is also proteolysis-sensitive (Taipale et al., 1995).

The importance of proteolysis to TGF-β-dependent matrix remodelling has been characterised in some detail in experimental models of bone tissue development (Dallas et al., 1994). LTBP-1 bound to bone matrix is susceptible to cleavage by purified plasmin and pancreatic elastase, both of which can release tissue stored TGF-β (Dallas et al., 2002). Subsequent activation generates active TGF-β to stimulate the proliferation and migration of osteoblasts, the cells that ultimately orchestrate increased bone formation. In line with this, Geiser and colleagues have discovered that TGF-β1-null mice have decreased bone mass and elasticity within the first few weeks of life before succumbing to fatal multi-organ inflammation (Geiser et al., 1998).

Different lines of evidence from cell co-culture models have built the case for plasmin as a key activator of latent TGF-β (Antonelli-Orlidge et al., 1989; Sato et al., 1990). Lyons and coworkers showed that plasmin can release mature (active) TGF-β from LAP by proteolytically disrupting the non-covalent interactions between them (Lyons et al., 1990). Plasmin also has been shown to efficiently degrade matrix-associated LTBP molecules to liberate small latent TGF-β complexes from cultured fibroblast and epithelial-derived extracellular matrices (Taipale et al., 1992). Although Grainger and colleagues have demonstrated that TGF-β activation is decreased in transgenic mice expressing Apo(a), a structurally homologous competitor of plasminogen (Grainger et al., 1996), the fact that mice lacking plasminogen are spared the lethal phenotype of TGF-β-deficient animals indicates that the plasmin activation mechanism is not the only TGF-β activation pathway operating *in vivo*. Neutrophil elastase has been shown to cleave proteins involved in TGF-β anchorage to the ECM, such as LTBP (Taipale et al., 1995). The potential implications of this observation to the current thesis will be explored in detail in the chapter discussion.

6.2 Results

6.2.i Reproducibility and specificity of the MLEC PAI-1/luciferase assay

The mink lung epithelial cell (MLEC) PAI-1/luciferase bioassay (Abe et al., 1994) was optimised for measuring amounts of active TGF-β in BAL fluid and in tissue obtained from murine lungs. Preliminary experiments determined that the optimal ratio of MLEC lysate to assay substrate required to generate the greatest increment in luciferase activity per given amount of TGF-β was 1:5 (50 μl lysate to 250 μl substrate). Dose response curves produced by two different lysate:substrate ratios are shown in **figure 38**. Aliquots of acid-activated TGF-β over a range of 0.1 to 1.2 ng/ml consistently produced a sigmoid-shaped dose response curve (**figure 39a**). A reproducible linear portion of the curve was obtained between 0.2 and 1.0 ng/ml of active purified TGF-β (**figure 39b**). Luciferase activity in each biological sample (BAL fluid or lung tissue) was determined after subtracting background luciferase activity. Overall, the inter-well variability of luciferase activity within each triplicate of samples or standards was less than ten percent of the mean value.

The specificity of the assay for active TGF-β was verified using a pan-specific TGF-β neutralising antibody (R & D Systems, UK). One hundred μg/ml of this antibody reduced luciferase activity measured in BAL fluid from WT or $NE^{-/-}$ mice to near background levels (**figure 40**).

6.2.ii Activation of TGF-β in lung samples

Aliquots of 100 μl of BAL fluid and 50 mg of homogenised lung tissue (collected according to the protocol described in sections 2.2.ii and 2.2.iii) produced measurements of luciferase activity within the linear portion of the standard curve. Samples were subjected to *in vitro* heat treatment to activate latent TGF-β. Preliminary experiments showed that heating homogenised lung tissue at 80°C for 5 minutes produced maximal amounts of active TGF-β (**figure 41**). BAL fluid required heating at the same temperature for 10 minutes to generate maximal amounts of the active cytokine.

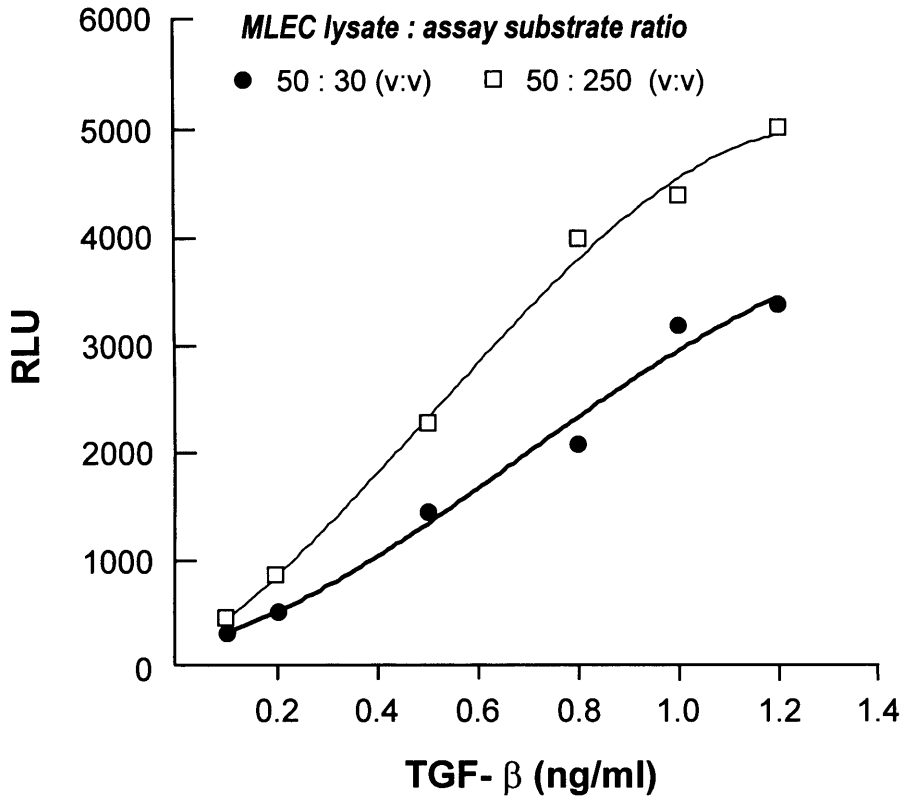

Figure 38. **Determination of optimal cell lysate : luciferase substrate ratio for the MLEC / PAI-1 TGF-β assay.**

PAI-1 transfected mink lung epithelial cells (MLEC) were plated at a density of 1.6×10^4 cells/100 μl/well and incubated with increasing concentrations of TGF-β for 16 hours. The cells were then lysed, and luciferase substrate was added immediately prior to measuring luciferase activity. Amounts of substrate were varied to determine maximum relative light units (RLU). Each point represents the mean of a triplicate measurement.

39 (a)

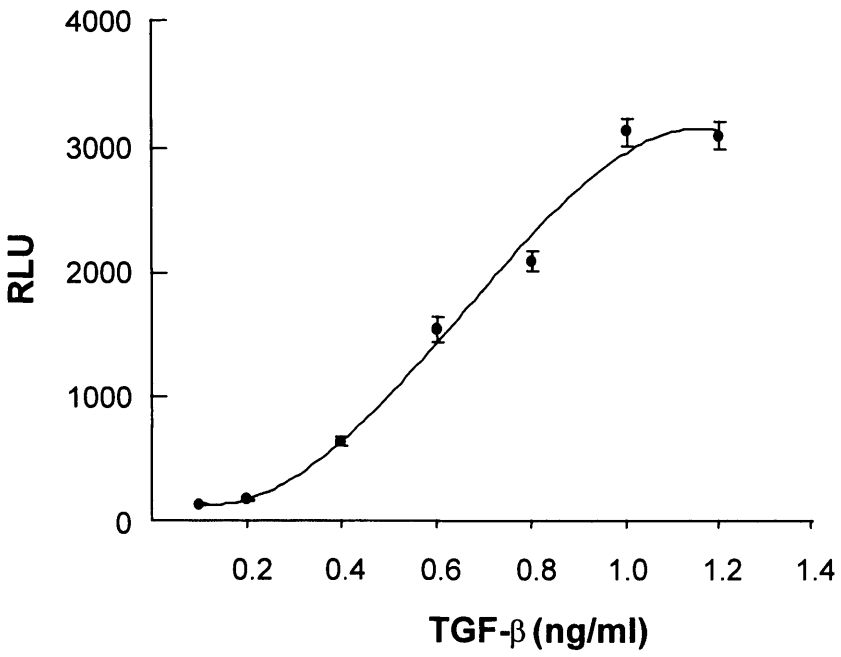

39 (b)

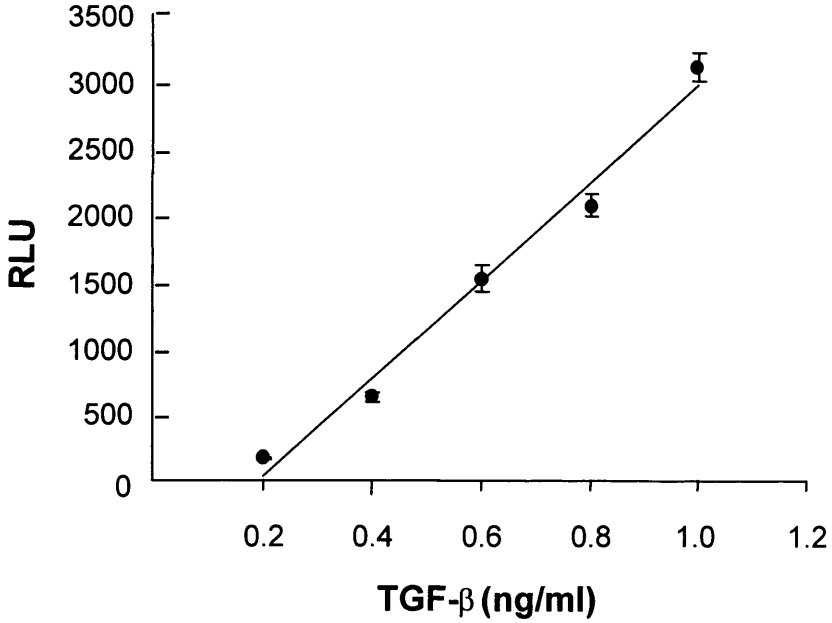

Figure 39. **Representative standard curve of the MLEC / PAI-1 TGF-β assay showing the limits of detection of active TGF-β.**

39 (a). Mink lung epithelial cells (MLEC), stably transfected with a plasminogen activator inhibitor-1 (PAI-1) / luciferase construct, were adhered on a 96-well plate. TGF-β standard curves were constructed using 0.1 - 1.2 ng/ml of acid-activated TGF-β. ***39 (b).*** A linear dose response was consistently obtained between 0.2 - 1.0 ng/ml TGF-β. One hundred μl of cell-free BAL fluid produced readings within this linear range. Each point represents the mean ± SEM of a triplicate. (*RLU*, relative light units)

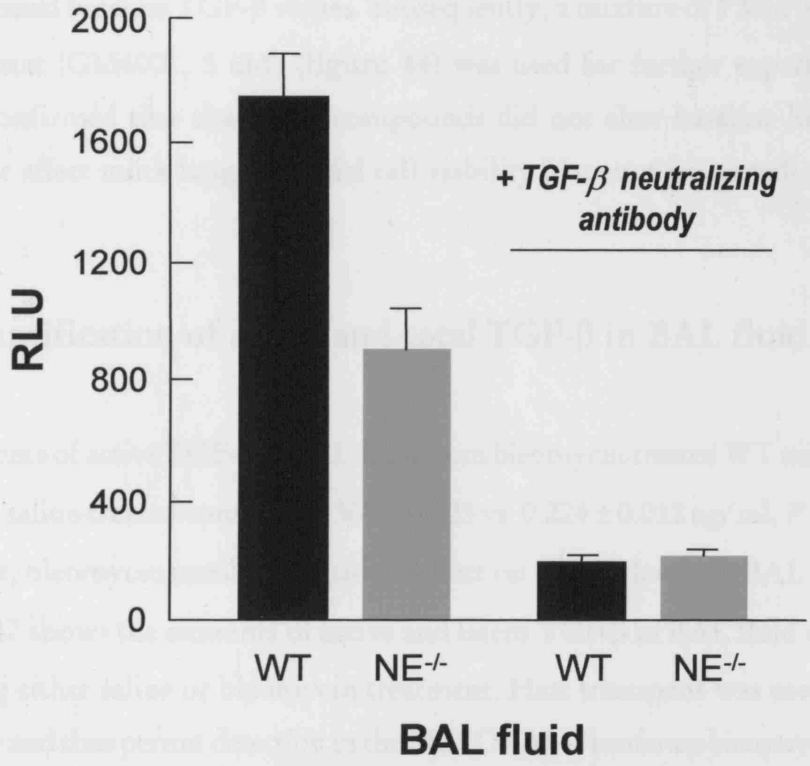

Figure 40. **The MLEC / PAI-1 luciferase assay is specific for active TGF-β in BAL fluid.**

Specificity of the PAI-1/luciferase bioassay for active TGF-β in BAL fluid was confirmed using a pan-specific TGF-β neutralising antibody (R & D, Abingdon, UK) used at a concentration of 100 μg/ml. Background of assay (DMEM control) = 0 ng/ml TGF-β. Values are expressed in relative light units (RLU) as mean ± SEM of a triplicate of pooled BAL fluid.

In some optimisation experiments, diminution of TGF-β activity in heated aliquots of WT but not $NE^{-/-}$ BAL fluid was noted. This result indicated the potential inactivation of TGF-β during the heating process. In addition, loss of exogenously added TGF-β activity was also apparent when assessed under the same conditions (**figure 42**). Following the addition of a mixture of selective proteinase inhibitors prior to heating (Complete® Mini Protease Inhibitor cocktail, Roche Biochemicals, UK), the recovery of both endogenous and exogenous TGF-β activity was significantly increased. However, the addition of this complex antiproteinase preparation to the assay also increased baseline TGF-β values. Subsequently, a mixture of PMSF (0.5 mM) (**figure 43**) and Ilomastat (GM6001, 5 uM) (**figure 44**) was used for further experiments. Control experiments confirmed that these two compounds did not alter baseline luciferase activity (**figures 45**), or affect mink lung epithelial cell viability (data not presented).

6.2.iii Quantification of active and total TGF-β in BAL fluid

Amounts of active TGF-β in BAL fluid from bleomycin-treated WT mice were two-fold greater than in saline-treated controls (0.364 ± 0.023 vs. 0.224 ± 0.012 ng/ml, $P < 0.001$) (**figure 46**). In contrast, bleomycin instillation had no effect on TGF-β levels in BAL fluid from $NE^{-/-}$ mice. **Figure 47** shows the amounts of active and latent TGF-β in BAL fluid of WT and $NE^{-/-}$ mice following either saline or bleomycin treatment. Heat treatment was used to activate the latent cytokine and thus permit detection in the MLEC PAI-1/luciferase bioassay. Approximately 50% of TGF-β in BAL fluid from WT mice (both saline and bleomycin-treated) was present in the latent form. In comparison, $NE^{-/-}$ samples contained a smaller proportion of latent TGF-β that averaged around 30 - 35% of the total pool of cytokine. Following heat activation, bleomycin-treated WT BAL fluid contained the highest amounts of TGF-β with levels that were almost two fold greater than those of saline-treated WT controls (0.747 ± 0.137 vs. 0.434 ± 0.066 ng/ml, $P < 0.05$). In contrast, TGF-β in bleomycin-treated $NE^{-/-}$ BAL fluid did not differ from saline-treated control values following the same heat treatment protocol (0.362 ± 0.042 vs. 0.340 ± 0.013 ng/ml). Thus, the total pool of TGF-β in bleomycin-treated $NE^{-/-}$ BAL fluid was significantly less than that recovered from bleomycin-treated WT animals ($P < 0.02$). Taken together, these results indicate that not only are the levels of soluble active TGF-β significantly decreased in $NE^{-/-}$ mice compared to WT littermates following treatment with an equivalent dose

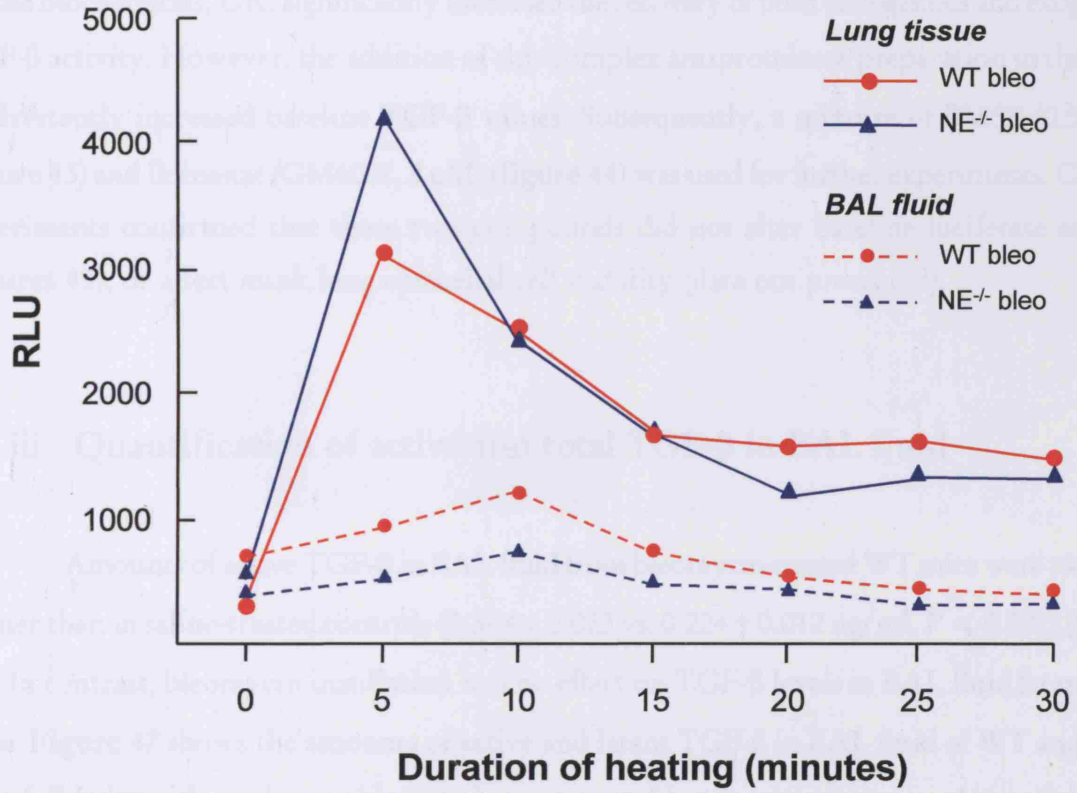

Figure 41. **Time course of heat activation of latent TGF-β in lung tissue and in BAL fluid.**

Pooled BAL fluid from saline and bleomycin-treated WT and $NE^{-/-}$ mice was heated for up to 30 minutes at 80°C to determine the optimum *in vitro* conditions for activating latent TGF-β. Levels of active TGF-β were measured by the PAI-1/luciferase assay. Values are expressed in relative light units (RLU) as the mean ± SEM of a triplicate measurement with each point representing pooled BAL fluid from at least six animals. Error bars do not extend beyond the symbols.

In some optimisation experiments, diminution of TGF-β activity in heated aliquots of BAL fluid from WT but not $NE^{-/-}$ mice was noted. This observation suggested that inactivation of TGF-β might occur during the heating process, possibly as the result of enhanced proteolytic activity. It is possible that neutrophil elastase might contribute to such proteolysis, although its participation is yet unproven. Loss of activity of exogenously added TGF-β was also apparent when the experiment was repeated under the same conditions (**figure 42**). The addition of a mixture of selective proteinase inhibitors prior to heating (Complete® Mini Protease Inhibitor cocktail, Roche Biochemicals, UK) significantly increased the recovery of both endogenous and exogenous TGF-β activity. However, the addition of this complex antiproteinase preparation to the assay inadvertently increased baseline TGF-β values. Subsequently, a mixture of PMSF (0.5 mM) (**figure 43**) and Ilomastat (GM6001, 5 uM) (**figure 44**) was used for further experiments. Control experiments confirmed that these two compounds did not alter baseline luciferase activity (**figures 45**), or affect mink lung epithelial cell viability (data not presented).

6.2.iii Quantification of active and total TGF-β in BAL fluid

Amounts of active TGF-β in BAL fluid from bleomycin-treated WT mice were two-fold greater than in saline-treated controls (0.364 ± 0.023 vs. 0.224 ± 0.012 ng/ml, $P < 0.001$) (**figure 46**). In contrast, bleomycin instillation had no effect on TGF-β levels in BAL fluid from $NE^{-/-}$ mice. **Figure 47** shows the amounts of active and latent TGF-β in BAL fluid of WT and $NE^{-/-}$ mice following either saline or bleomycin treatment. Heat treatment was used to activate the latent cytokine and thus permit detection in the MLEC PAI-1/luciferase bioassay. Approximately 50% of TGF-β in BAL fluid from WT mice (both saline and bleomycin-treated) was present in the latent form. In comparison, $NE^{-/-}$ samples contained a smaller proportion of latent TGF-β that averaged around 30 – 35% of the total pool of cytokine. Following heat activation, bleomycin-treated WT BAL fluid contained the highest amounts of TGF-β with levels that were almost two fold greater than those of saline-treated WT controls (0.747 ± 0.137 vs. 0.434 ± 0.066 ng/ml, $P < 0.05$). In contrast, TGF-β in bleomycin-treated $NE^{-/-}$ BAL fluid did not differ from saline-treated control values when similarly heated (0.362 ± 0.042 vs. 0.340 ± 0.013 ng/ml). Thus, the total pool of TGF-β in bleomycin-treated $NE^{-/-}$ BAL fluid was significantly less than that recovered from bleomycin-treated WT animals ($P < 0.02$). Taken together, these results indicate

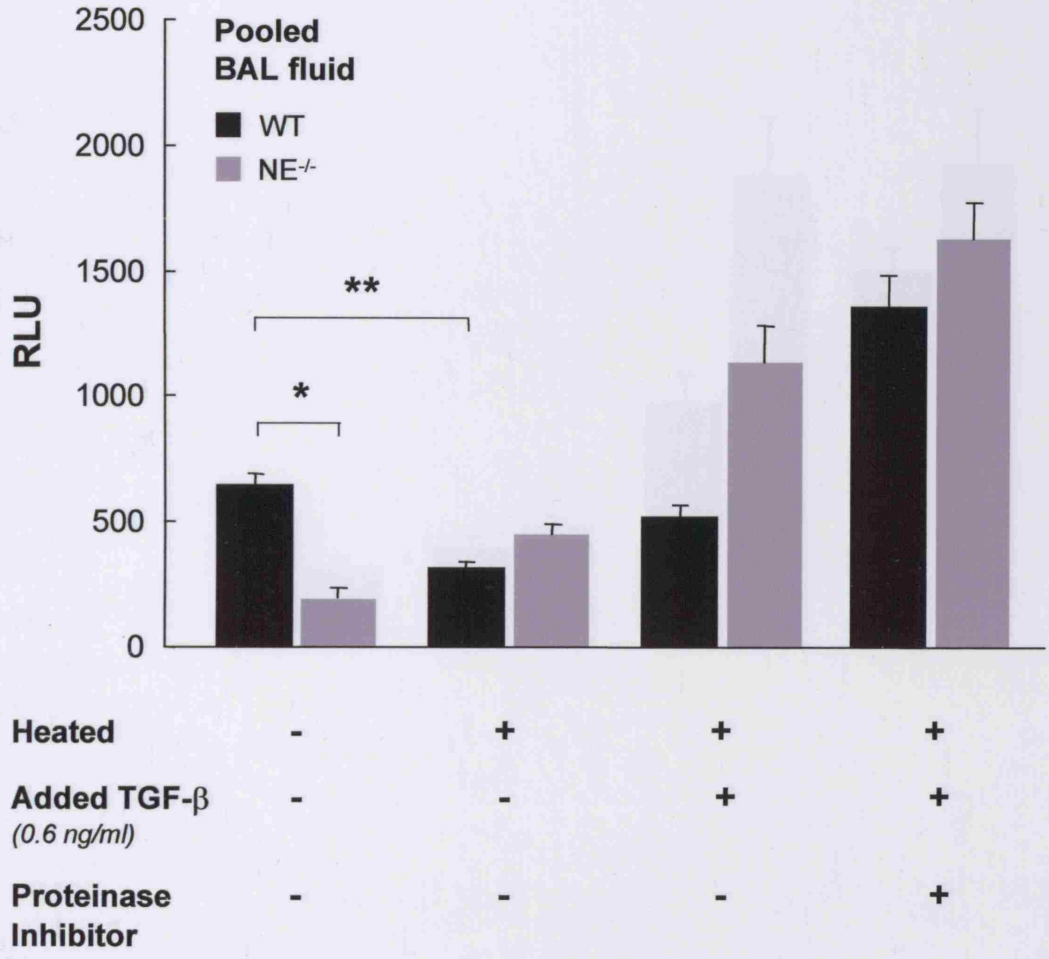

Figure 42. **Proteinase inhibition increases the recovery of heat-activated TGF-β in BAL fluid.**

Levels of active TGF-β were measured in pooled BAL fluid from bleomycin-treated WT and $NE^{-/-}$ mice after heating at 80°C for 10 minutes to activate latent TGF-β. Exogenous acid-activated TGF-β (0.6 ng/ml) was added to selected wells with or without a broad spectrum proteinase inhibitor (Complete® Mini Protease Inhibitor, Roche, UK). Values are expressed in relative light units (RLU) as mean ± SEM with each bar representing pooled BAL fluid from at least six different animals. * $P < 0.01$, ** $P < 0.05$

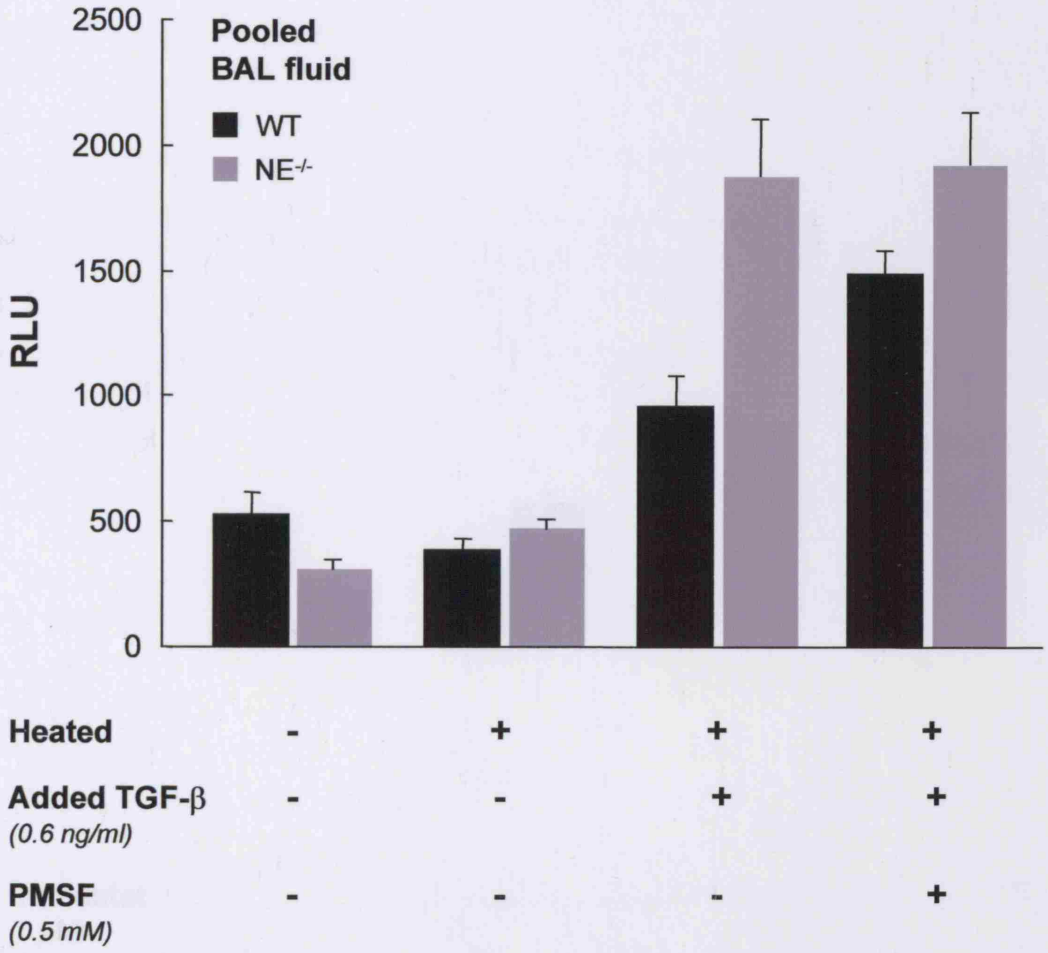

Figure 43. **The addition of PMSF replicates the effects of Complete® Proteinase Inhibitor on the recovery of heat-activated TGF-β.**

Levels of active TGF-β were measured in pooled BAL fluid from bleomycin-treated WT and $NE^{-/-}$ mice after heating at 80°C for 10 minutes to activate latent TGF-β. Exogenous acid-activated TGF-β (0.6 ng/ml) was added to selected wells with or without PMSF, a serine proteinase inhibitor. Values are expressed in relative light units (RLU) as mean ± SEM with each bar representing pooled BAL fluid from at least six different animals. * $P < 0.01$, ** $P < 0.05$

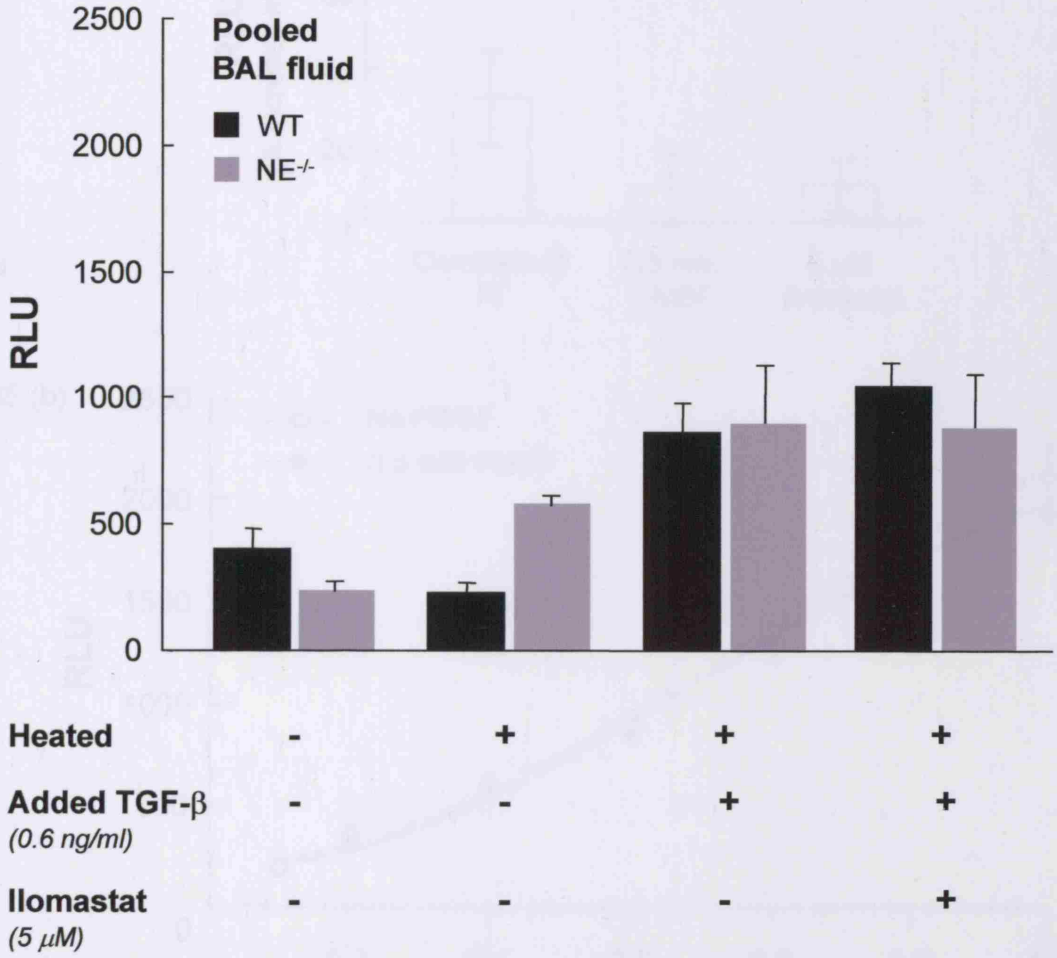

Figure 44. **Metalloproteinase inhibition also reduces loss of TGF-β activity during heat treatment.**

Levels of active TGF-β were measured in pooled BAL fluid from bleomycin-treated WT and $NE^{-/-}$ mice after heating at 80°C for 10 minutes to activate latent TGF-β. Exogenous acid-activated TGF-β (0.6 ng/ml) was added to selected wells with or without Ilomastat (GM6001), a matrix metalloproteinase inhibitor. Values are expressed in relative light units (RLU) as mean ± SEM with each bar representing pooled BAL fluid from at least six different animals. BAL fluid used came from the same batch as in the previous two figures. * $P < 0.01$, ** $P < 0.05$

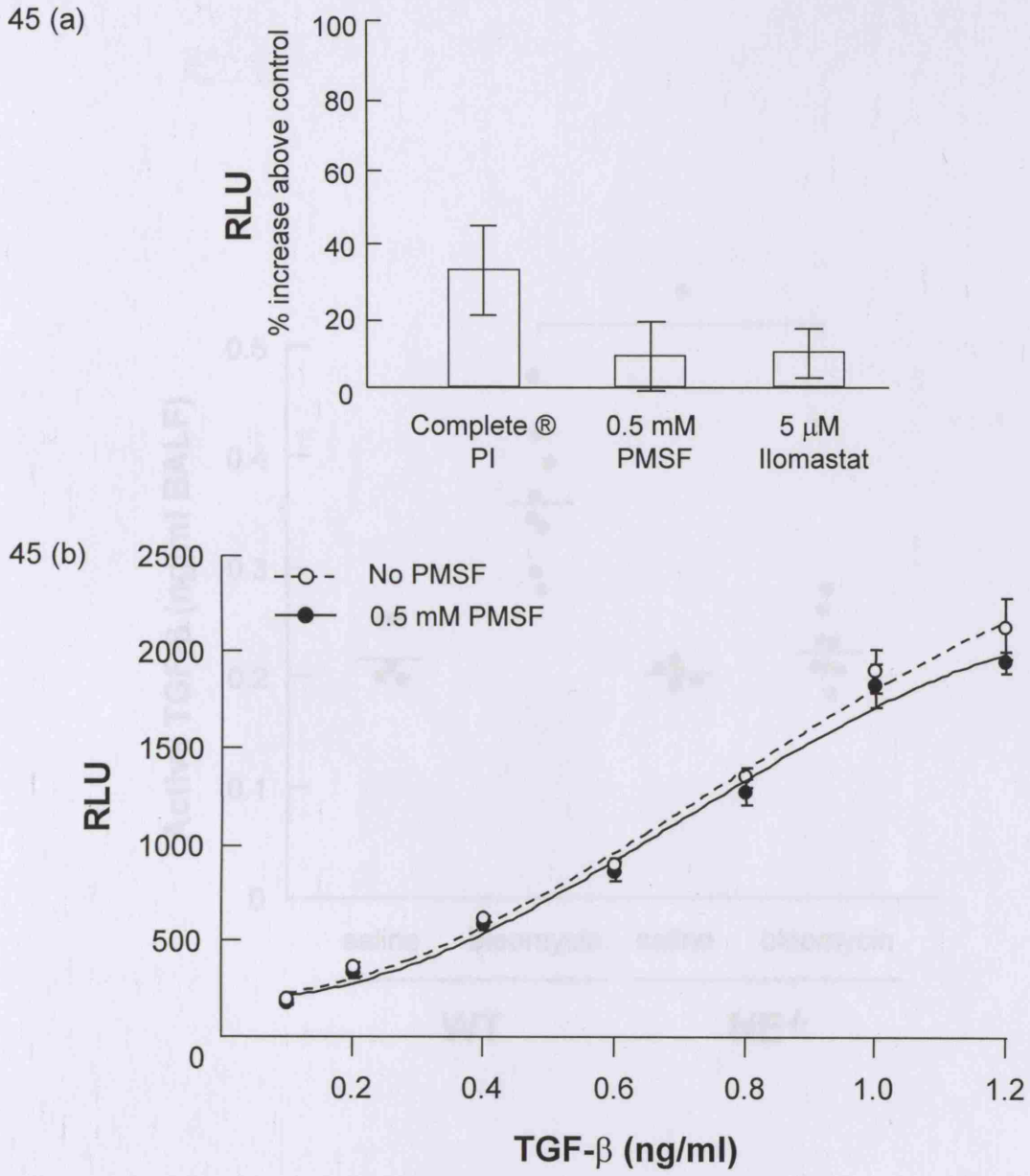

Figure 45. **PMSF and Ilomastat do not interfere with the measurement of active TGF-β in the MLEC / PAI-1 luciferase assay.**

45 (a). 0.5 mM PMSF, 5 μM Ilomastat (GM6001) and Complete® Proteinase Inhibitor were added to mink lung epithelial cells, and luciferase activity was measured after overnight incubation. Data are expressed as percentage increase in relative light units above serum free controls.

45 (b). The effect of 0.5 mM PMSF on the standard curve of the PAI-1 assay was also assessed. Each value represents the mean ± SEM of RLU for each corresponding concentration of TGF-β.

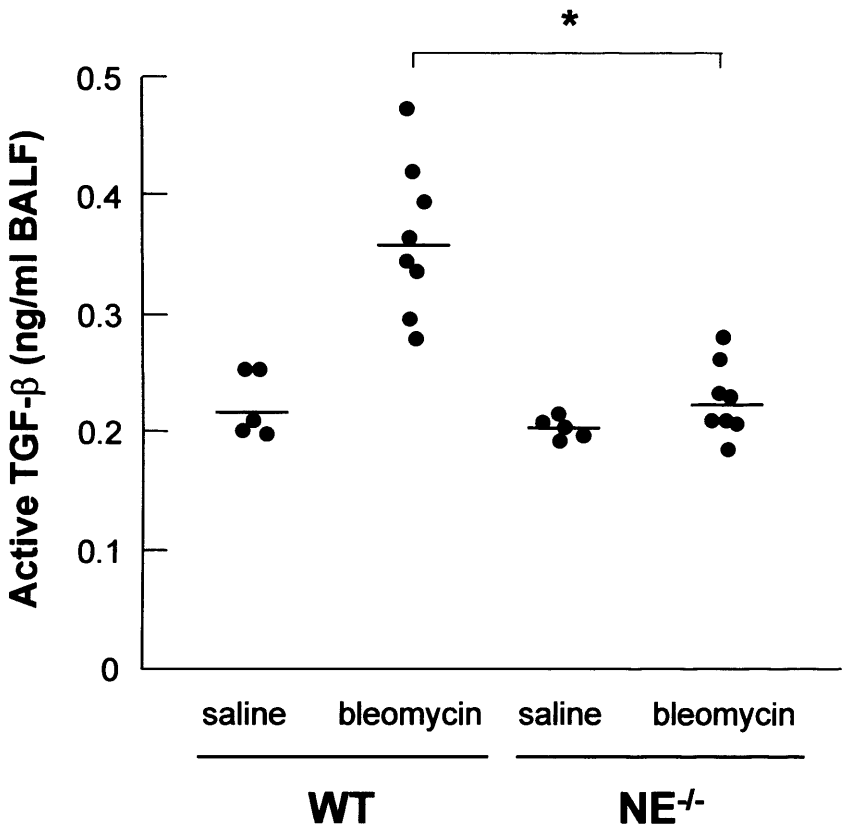

***Figure 46.* BAL fluid from bleomycin-treated NE$^{-/-}$ mice contains decreased amounts of active TGF-β.**

BAL fluid was collected from WT or NE$^{-/-}$ mice seven days following bleomycin or saline instillation and centrifuged to remove cells. Amounts of active TGF-β were measured using the MLEC PAI-1 / luciferase assay. Each point represents the mean of each sample measured in triplicate. * *P < 0.001 (using ANOVA)*

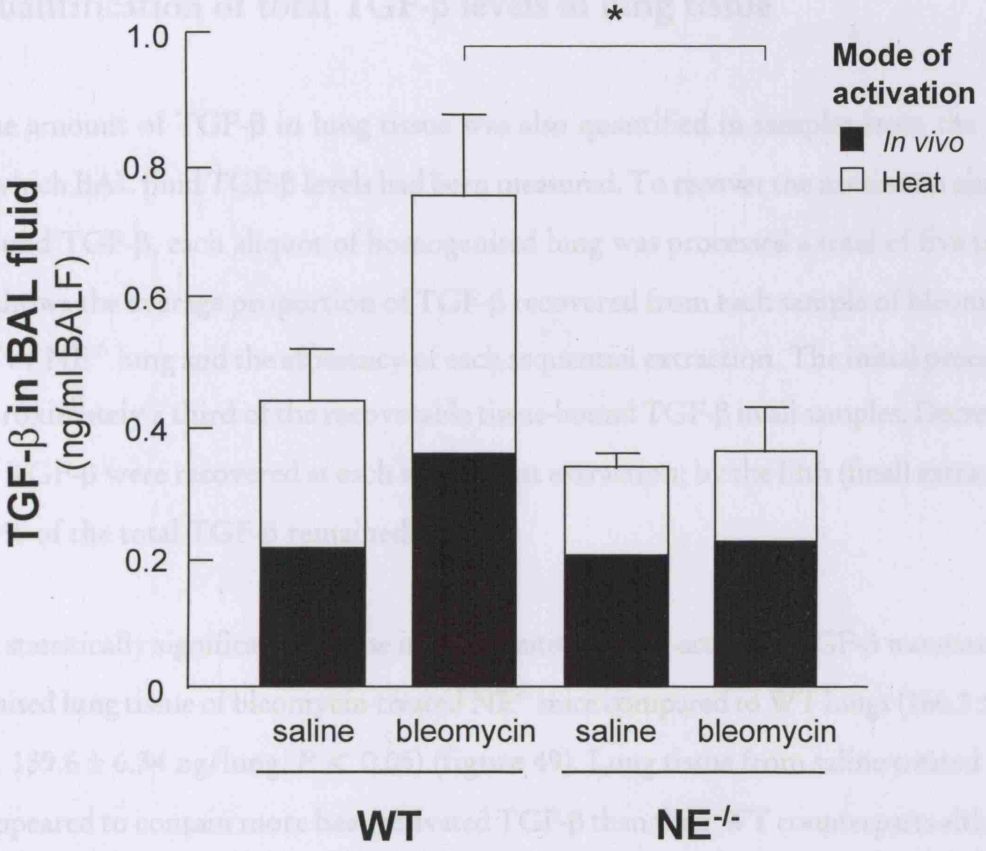

Figure 47. **Latent and total pools of TGF-β are also diminished in BAL fluid from bleomycin-treated NE$^{-/-}$ mice.**

Levels of active TGF-β in cell-free BAL fluid from WT and NE$^{-/-}$ mice were measured using the MLEC PAI-1/luciferase assay. Samples were also heated at 80°C for 10 minutes to activate latent TGF-β. Values are expressed as mean ± SEM of a triplicate. Each bar represents values from five to eight different animals. Solid portions of the bar indicate active TGF-β while open portions of the bar represent latent TGF-β. * $P < 0.02$

that not only are the levels of soluble active TGF-β significantly decreased in $NE^{-/-}$ mice compared to WT littermates following treatment with an equivalent dose of bleomycin, but that the total pool of TGF-β available for activation as represented by cytokine recovered in BAL fluid is also diminished.

6.2.iv Quantification of total TGF-β levels in lung tissue

The amount of TGF-β in lung tissue was also quantified in samples from the same animals in which BAL fluid TGF-β levels had been measured. To recover the maximum amount of tissue-bound TGF-β, each aliquot of homogenised lung was processed a total of five times. **Figure 48** shows the average proportion of TGF-β recovered from each sample of bleomycin-treated WT or $NE^{-/-}$ lung and the efficiency of each sequential extraction. The initial procedure yielded approximately a third of the recoverable tissue-bound TGF-β in all samples. Decreasing amounts of TGF-β were recovered at each subsequent extraction; by the fifth (final) extraction, only 5 – 10% of the total TGF-β remained.

A small but statistically significant increase in the quantity of heat-activated TGF-β was measured in homogenised lung tissue of bleomycin-treated $NE^{-/-}$ mice compared to WT lungs (166.3 ± 9.84 ng/lung vs. 139.6 ± 6.34 ng/lung, $P < 0.05$) (**figure 49**). Lung tissue from saline-treated $NE^{-/-}$ mice also appeared to contain more heat-activated TGF-β than their WT counterparts although this difference did not reach statistical significance.

6.2.v Analysis of pulmonary TGF-β gene expression

Pulmonary TGF-β production was compared between WT and $NE^{-/-}$ mice by measuring mRNA levels with a multi-probe Ribonuclease Protection Assay seven days following bleomycin instillation. **Figure 50** shows the positions of RNAse-protected probes for TGF-β_1, TGF-β_2 and TGF-β_3 as well as that of GAPDH (a housekeeping gene) in these samples. The relative densities of these bands were quantified as a ratio of their pixel intensity to that of GAPDH. TGF-β_1 was the most abundantly expressed isoform in both genotypes of mice following bleomycin-induced

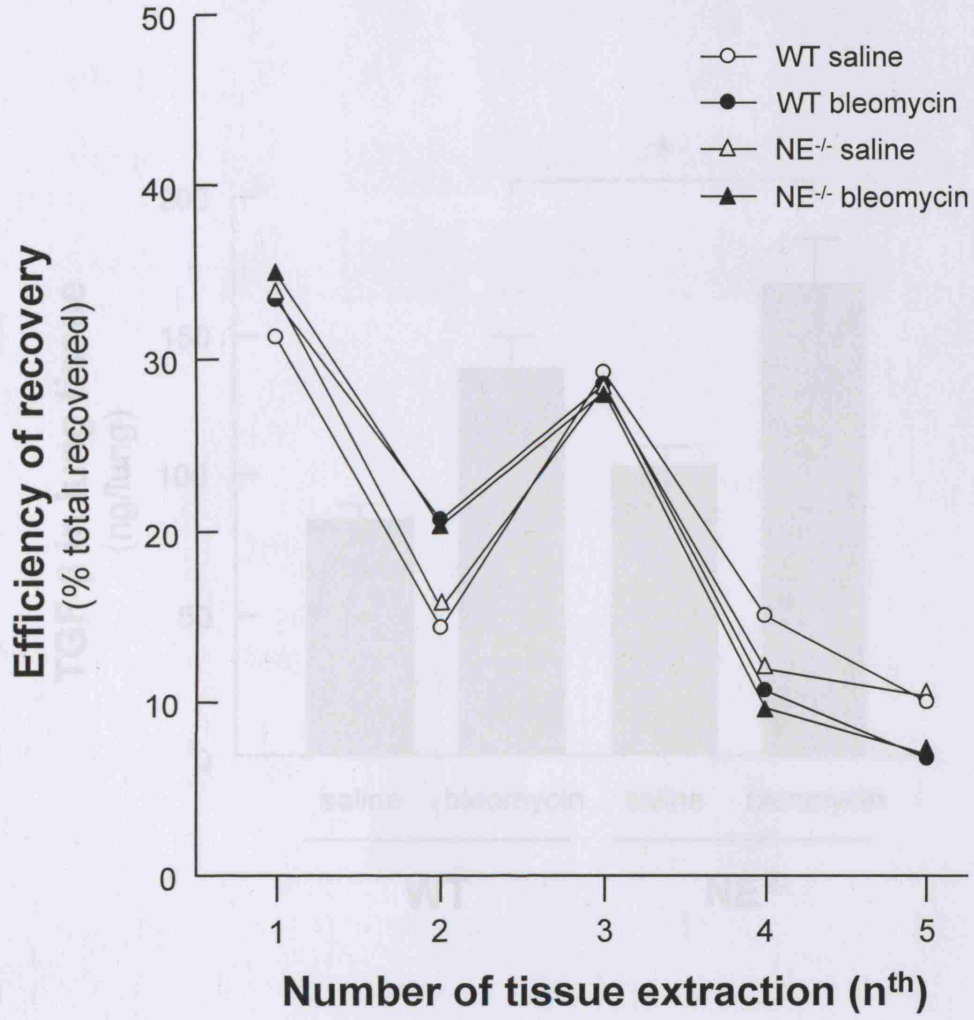

Figure 48. **Recovery of TGF-β from homogenised lung tissue.**

Lung tissue was harvested from WT and NE$^{-/-}$ mice seven days following saline or bleomycin instillation. 50 mg of each sample was homogenised in the presence of proteinase inhibitors (0.5 mM PMSF, 5 μM Ilomastat) and heated at 80°C for 5 minutes to activate latent TGF-β. Each aliquot was processed a total of five times to recover the maximum amount of TGF-β. Residual amounts of TGF-β remaining after the final extraction amounted to < 5% of the total TGF-β in that sample.

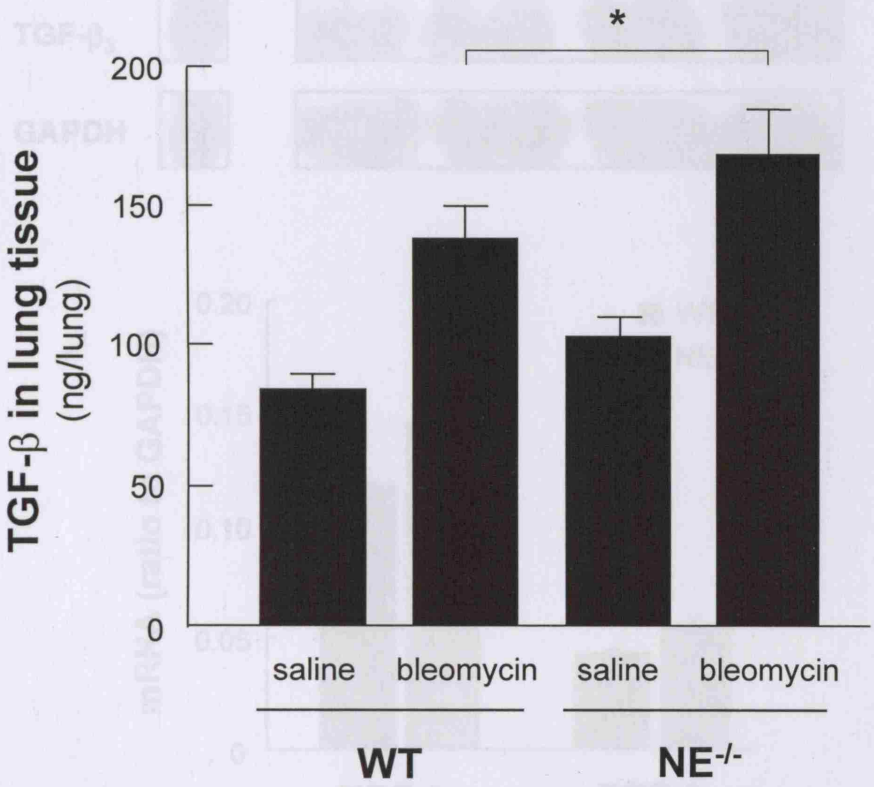

Figure 49. **Greater amounts of heat-activated TGF-β are present in lung tissue of bleomycin-treated NE$^{-/-}$ mice.**

Lung tissue collected seven days following bleomycin instillation was homogenised and heated at 80°C for 5 minutes to activate latent TGF-β. Samples were then added to the MLEC PAI-1/luciferase assay. Values are expressed as mean ± SEM of a triplicate following five extractions from a single lung tissue aliquot to completely recover tissue-bound TGF-β. Each bar represents values from five to eight different animals. * $P < 0.05$

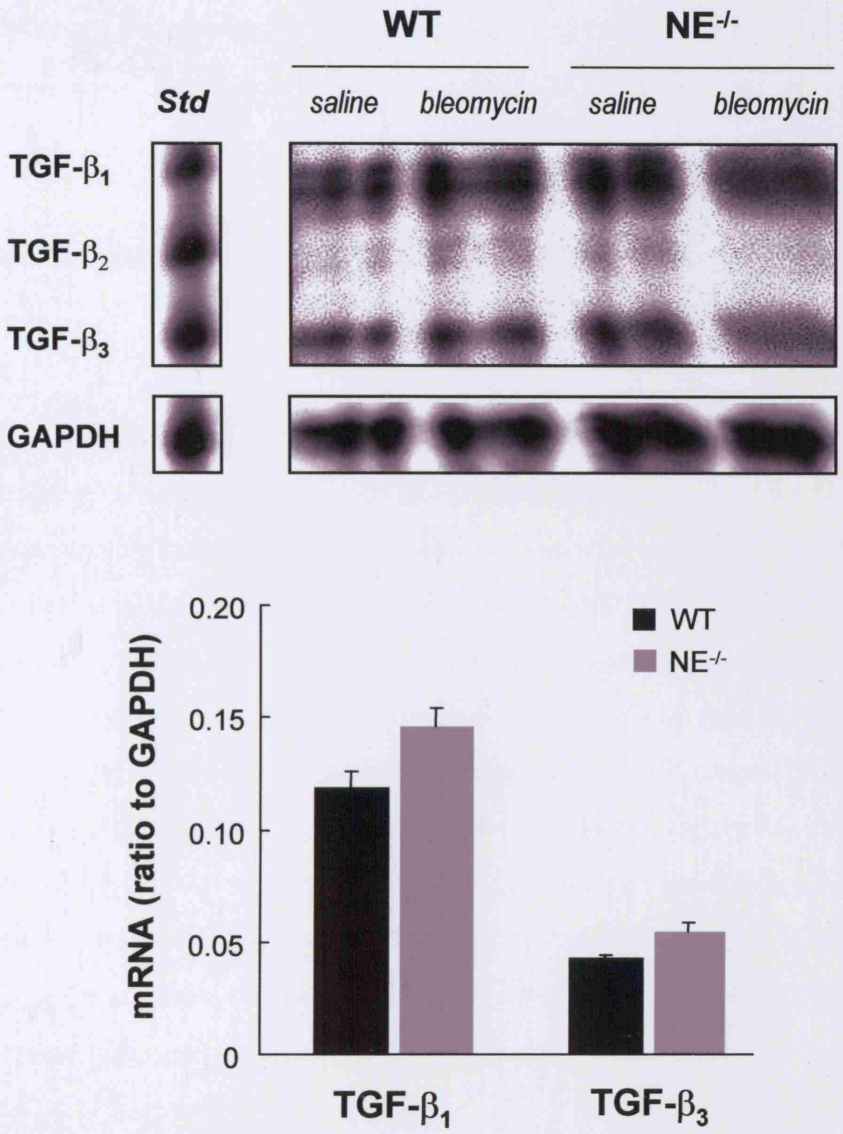

Figure 50. **Lung tissue TGF-β_1 and TGF-β_3 mRNA expression is comparable between WT and NE$^{-/-}$ mice.**

Total RNA was isolated using a Trizol-based protocol from WT and NE$^{-/-}$ lung tissue seven days following saline or bleomycin instillation. Relative TGF-β mRNA levels were determined using a RiboQuant multi-probe RNase protection assay. ***Top panel,*** Relative positions of probes for TGF-β_1, TGF-β_3 and GAPDH (housekeeping gene) are shown. ***Bottom panel,*** The densitometric ratios of protected TGF-β_1 and TGF-β_3 mRNA related to GAPDH are shown as a histogram. Each bar represents the mean value ± SEM (n=8 for bleomycin-treated WT and NE$^{-/-}$ mice). Saline values not shown.

lung injury. In comparison, changes in the expression of TGF-β_3 were smaller and again not significantly different between the two genotypes of mice. At this time point, expression of TGF-β_2 was negligible in both genotypes. No statistically significant differences in the expression of TGF-β isoforms were observed in bleomycin-treated WT and $NE^{-/-}$ mice.

6.2.vi Localisation of active TGF-β in bleomycin-injured WT and $NE^{-/-}$ lungs

Figure 51 shows, at low power (left hand panels), the localisation of immunoreactive TGF-β in WT and $NE^{-/-}$ lungs seven days following the instillation of 0.05 U bleomycin. In lung sections from WT mice, staining for active TGF-β was almost entirely extracellular and was prominent in the interstitium and in locations adjacent to damaged alveoli. Increased staining of active TGF-β was also observed in areas with increased numbers of inflammatory cells (**figure 51**, upper right hand panel). Mature polymorphonuclear neutrophils, discernible by their distinct hypersegmented nuclei, were scattered within many areas of the lungs of bleomycin-treated WT mice where there was increased extracellular staining of active TGF-β (left panel, **figure 52**). In contrast, a much more limited staining pattern was observed in the lungs of bleomycin-treated $NE^{-/-}$ mice although the distribution of active TGF-β was mostly extracellular. In the lungs of saline-treated WT and $NE^{-/-}$ animals, staining of active TGF-β was minor and restricted to the pulmonary endothelial and airway lining (data not shown).

While most of the active TGF-β staining in WT and $NE^{-/-}$ mice appeared to be associated with the extracellular matrix, occasional staining of cells was also evident. However, the cell types involved were not easily identified but were most likely macrophages, fibroblasts and epithelium of bleomycin-treated animals. Staining for latent TGF-β in bleomycin-treated WT and $NE^{-/-}$ lungs also appeared to be more associated with the extracellular matrix than with cells (data not shown).

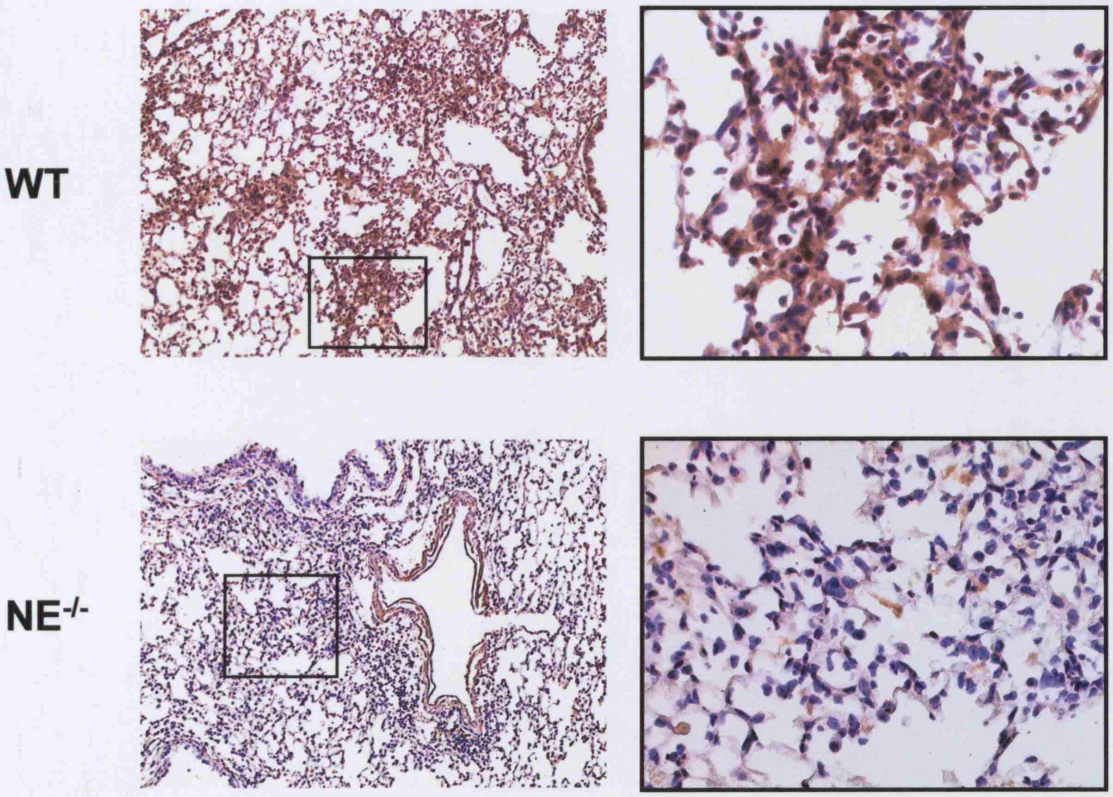

Figure 51. **Staining for active TGF-β is more extensive in bleomycin-treated WT lungs than in bleomycin-treated $NE^{-/-}$ lungs.**

Representative light photomicrographs showing immunolocalisation of active TGF-β in paraffin-embedded WT and $NE^{-/-}$ lungs. Specimens were collected seven days following 0.05 U bleomycin instillation, and active TGF-β (brown) was stained with the LC(1-30) monoclonal antibody. Peroxidase-conjugated biotinylated secondary antibodies were used. The final immunogenic reaction was obtained using 3,3-diaminobenzidine (DAB) as a chromogen.

Low power, *x10 objective*; high power, *x40 objective*

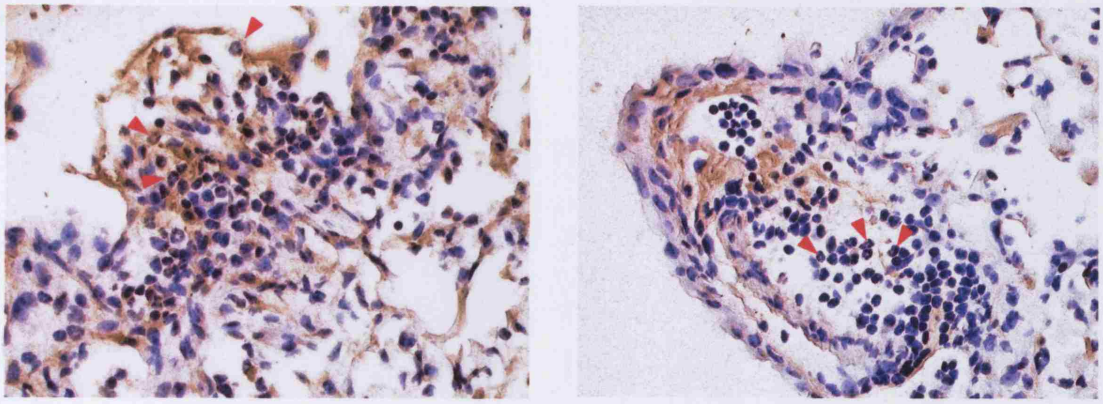

WT NE$^{-/-}$

Figure 52. **Neutrophils are found in areas of TGF-β immunoreactivity in bleomycin-injured WT and NE$^{-/-}$ lungs.**

Haematoxylin counter-stained polymorphonuclear neutrophils (red arrowheads) are present at sites of increased active TGF-β staining (brown staining) in areas of alveolar damage in WT and NE$^{-/-}$ lungs seven days following 0.05 U bleomycin instillation. Active TGF-β was stained with the LC(1-30) monoclonal antibody. Peroxidase-conjugated biotinylated secondary antibodies and 3,3-diaminobenzidine (DAB) were used for the final epitopic identification.

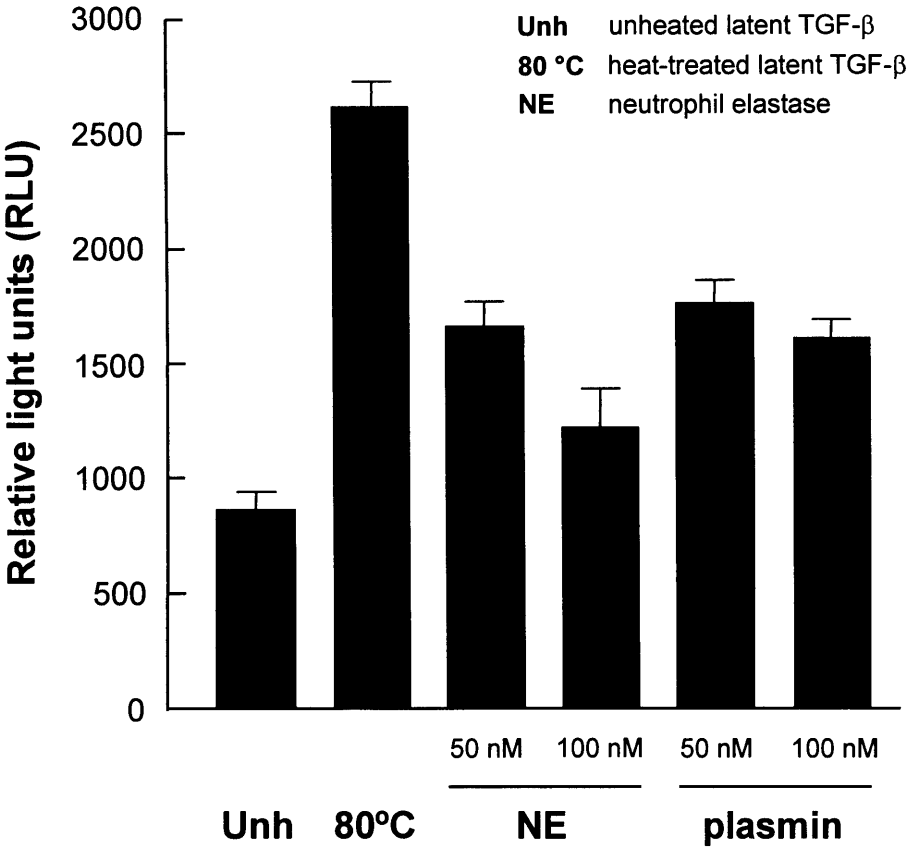

Figure 53. **Purified neutrophil elastase is equipotent to plasmin at activating latent TGF-β *in vitro.***

Purified neutrophil elastase and plasmin were prepared in DMEM containing 0.1% BSA (pH 7.5) and reacted with 40 nM latent TGF-β at 37°C. TGF-β activity was measured by the MLEC PAI-1 / luciferase assay and expressed as RLU (relative light units). Measurements were performed in triplicate. Values represent the mean ± SEM.

6.2.vii Neutrophil elastase is a poor activator of latent TGF-β in BAL fluid

Purified neutrophil elastase at two concentrations, 50 and 100 nM, increased the activity of 40 nM latent TGF-β (LAP-TGF-β1) *in vitro* (**figure 53**). However, the degree of TGF-β activation was only 45% to 64% of that obtained by heat activation. Curiously, decreased TGF-β activation was achieved with the higher (100 nM) concentration of neutrophil elastase. This effect may have been related to proteolytic degradation of TGF-β in the reaction media. In comparison, both 50 and 100 nM plasmin activated latent TGF-β to a similar extent as 50 nM neutrophil elastase. In these experiments, proteinase inhibition with PMSF and Ilomastat was not used during the reaction but were added at the end to terminate proteolysis.

Figure 54 shows that the addition of purified neutrophil elastase (100 nM) to BAL fluid from WT and $NE^{-/-}$ mice collected seven days following 0.05 U bleomycin instillation did not activate latent TGF-β. In contrast, plasmin at a concentration of 1 μM increased TGF-β activity in BAL fluid by ten-fold in bleomycin-treated WT samples and over seven-fold in BAL fluid from bleomycin-treated $NE^{-/-}$ mice. The final amount of active TGF-β following plasmin treatment in the former correlated to > 1.2 ng/ml BAL fluid (from the dose response curve of the MLEC/PAI-1 assay). The amount of plasmin-activated TGF-β in BAL fluid from $NE^{-/-}$ lungs corresponded to 50% of the value in WT samples. Residual neutrophil elastolytic activity following incubation was not measured in these samples but differences in endogenous BAL fluid neutrophil elastolytic activity has been compared between WT and $NE^{-/-}$ mice (**figure 15**).

Plasmin is a serine proteinase whose ability to activate latent TGF-β has often been used as a positive experimental control. One μM plasmin has previously been shown to be more efficient at activating LAP-TGF-β than nanomolar amounts of this proteinase when used *in vitro* (Lyons et al., 1988). While 1 μM plasmin managed to activate latent TGF-β in BAL fluid of $NE^{-/-}$ mice, the degree of activation was significantly less than that in BAL fluid of bleomycin-treated WT mice. This result agrees with the data obtained from heat activation of $NE^{-/-}$ BAL fluid (**figure 47**) and suggests that the amount of latent TGF-β in BAL fluid from bleomycin-treated $NE^{-/-}$ mice is decreased compared to that of bleomycin-treated WT mice.

Experiments comparing the ability of neutrophil elastase and plasmin to release lung tissue-bound TGF-β were performed on three different occasions under the same conditions. **Figure 55** shows

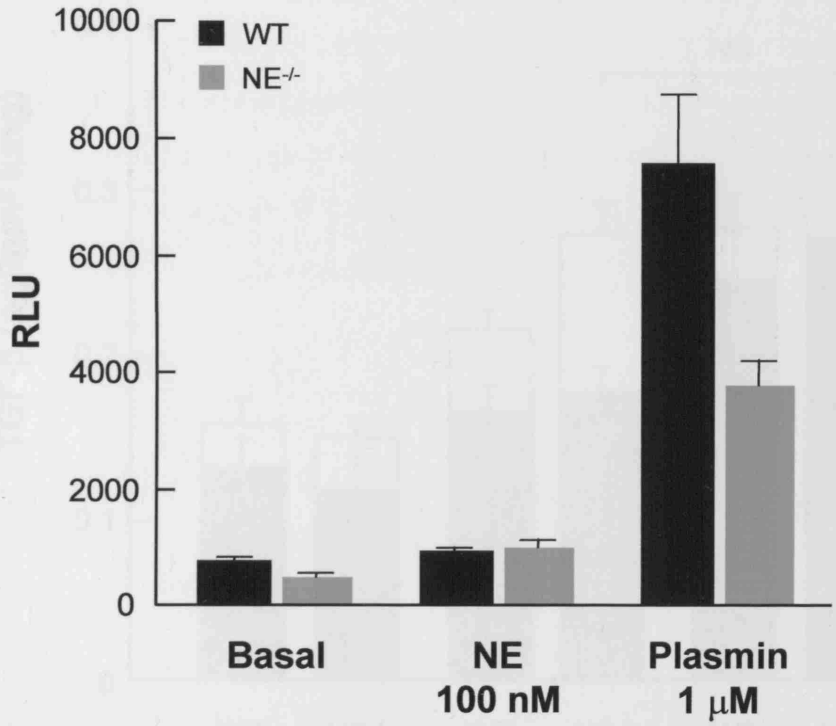

Figure 54. **Neutrophil elastase does not activate latent TGF-β in BAL fluid.**

BAL fluid was collected from WT and $NE^{-/-}$ mice seven days after the intratracheal instillation of 0.05 U bleomycin. Purified neutrophil elastase (NE, 100 nM) and plasmin (1 μM) were added to activate latent TGF-β in these biological samples. Proteolysis was stopped with 0.5 mM PMSF and 5 μM Ilomastat (GM6001). Active TGF-β was measured using the MLEC PAI-1 / luciferase assay. Values represent the mean ± SEM of a triplicate measurement (n = 4 animals in each group).

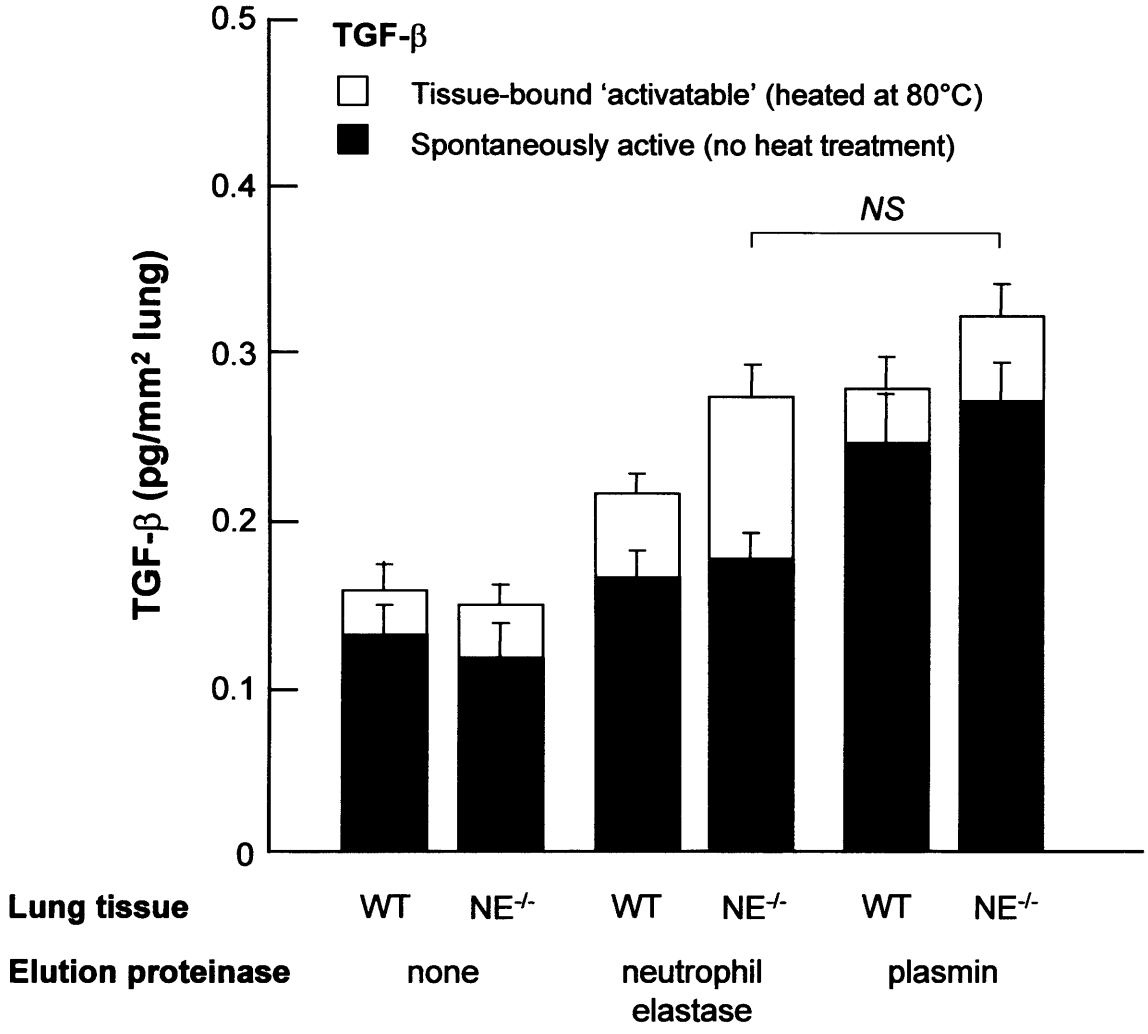

Figure 55. **Neutrophil elastase enhances TGF-β activation by releasing activatable cytokine from lung tissue.**

Fresh-frozen sections of WT and $NE^{-/-}$ lungs collected seven days following instillation of 0.05 U bleomycin were immersed in elution media (proteinase-free DMEM, DMEM containing 30 nM neutrophil elastase or DMEM containing 30 nM plasmin). Enzymatic reactions were stopped with 0.5 mM PMSF and 5 μM Ilomastat (GM6001) at the end of two hours. *In vitro* activation of latent TGF-β in the media was achieved by heating at 80°C for 10 minutes in the presence of the same proteinase inhibitors. Active TGF-β released into the media was measured using the MLEC PAI-1 / luciferase assay.

data from one representative experiment. Baseline amounts of active TGF-β in proteinase-free elution media were not different in lung cryosections of bleomycin-treated WT and $NE^{-/-}$ mice (WT: 0.135 pg/mm^2 lung; $NE^{-/-}$: 0.123 pg/ mm^2 lung). Heat activation of the same samples did not significantly increase the amount of TGF-β recovered. However, incubation of lung tissue with 30 mM neutrophil elastase yielded a small and equivalent increase in the amount of active TGF-β recovered from both WT and $NE^{-/-}$ lung sections. When the same samples were heat-treated, a significant increase in active TGF-β was measured in eluates from bleomycin-treated $NE^{-/-}$ mice ($NE^{-/-}$: 0.28 pg/mm^2 lung; WT: 0.22 pg/ mm^2 lung, $P < 0.05$). The amount of activatable TGF-β susceptible to proteolytic release by neutrophil elastase in the lungs of bleomycin-treated $NE^{-/-}$ mice was approximately 0.10 pg/mm^2 lung, a value which was twice the quantity available in bleomycin-treated WT lungs. Plasmin also released and activated tissue-bound TGF-β in lung sections from WT and $NE^{-/-}$ mice. In plasmin-treated samples, significant amounts of active TGF-β were not generated by heat treatment.

6.3 Discussion

Greater quantities of active TGF-β were present in the lungs of bleomycin-treated WT mice compared to similarly treated $NE^{-/-}$ mice. This result is a previously unpublished finding and may be potentially relevant to the decreased susceptibility of $NE^{-/-}$ mice to bleomycin-induced pulmonary fibrosis. These studies suggest that the increased amounts of active TGF-β in the BAL fluid of fibrosis-susceptible WT mice may be the result of enhanced generation of active TGF-β as compared to fibrosis-resistant $NE^{-/-}$ mice. This particular finding has broader implications for the role of neutrophil elastase in regulating pulmonary TGF-β activation in lung fibrosis. Although previous studies have shown that the fibrotic response in experimental models may be ameliorated by inhibiting neutrophil elastase activity, a pathologic relationship between TGF-β and neutrophil elastase *in vivo* has still not been demonstrated.

6.3.i TGF-β activation is impaired in the lungs of fibrosis-resistant $NE^{-/-}$ mice

Levels of active TGF-β failed to increase in BAL fluid of fibrosis-resistant $NE^{-/-}$ mice despite the development of bleomycin-induced lung injury. Similarly, active TGF-β protein in the lung parenchyma also failed to increase despite comparable levels of TGF-β mRNA in bleomycin-treated WT and $NE^{-/-}$ mice. These findings suggest that TGF-β activation rather than gene expression is impaired in the lungs of bleomycin-treated $NE^{-/-}$ mice. The additional finding that heat-activatable TGF-β was present in greater quantities in the lung tissue of these animals suggested that faulty generation of active TGF-β was likely the result of decreased release of activatable TGF-β from tissue stores. The specific role of neutrophil elastase in regulating pulmonary TGF-β activation has not been previously examined.

Proteolysis of tissue-associated latent TGF-β has been shown to form an important step in the generation of active TGF-β (Taipale et al., 1995; Pedrozo et al., 1999). Difficulties in accurately measuring the *in vivo* activity of TGF-β, particularly at the tissue level, have contributed to the incomplete understanding of TGF-β activation. Additionally, studies of adult fibrosis in a state of TGF-β deficiency are hampered by the lethality of mice deficient in TGF-β and several associated signalling molecules (Mummery, 2001). As a result, animal models in which impairment of the pulmonary fibrotic response resulting from defects in TGF-β activation that do not affect lung development are of great interest (Munger et al., 1999, Yehualaseshet et al., 2000).

Fibrosis-prone bleomycin-treated 129S6/SvEv mice in the current studies have levels of BAL fluid TGF-β that fall within a range similar to that of bleomycin-susceptible C57BL/6 mice (Teder et al., 2002). In their report, Kumar and colleagues showed that approximately 30% of BAL fluid TGF-β collected from bleomycin-injured C57BL/6 mice exists in the active form prior to acidification (Kumar et al., 1996). The proportion of active TGF-β present in bleomycin-treated WT animals in the present studies concurs with this. *In vivo*, less than 500 pg/ml of active TGF-β in BAL fluid can be fibrogenic in mice instilled with adenoviral-mediated TGF-β gene transfer (Kolb et al., 2001; Warshamana et al., 2002). This correlates well with the current findings. Amounts of TGF-β in BAL fluid are not equivalent to TGF-β concentrations present in or associated with cells at the tissue level. It is conceivable, although unproven, that

concentrations of TGF-β would be higher at tissue sites of cytokine activation. Under *in vitro* conditions, concentrations of active TGF-β in the 5-50 pg/ml range have been implicated in fibroblast chemotaxis and extracellular matrix production (Coker et al., 1997). However, in the femtomolar range, the immunoregulatory effects of TGF-β are more likely to predominate over its tissue remodelling properties (Wahl et al., 1989; Coker et al., 1997).

6.3.ii Inhibition of TGF-β activation is associated with lasting protection from bleomycin-induced pulmonary fibrosis in $NE^{-/-}$ mice

In the current studies, the lungs of $NE^{-/-}$ mice were marked by a lack of fibrosis for up to 60 days following the instillation of bleomycin. In contrast, lung collagen content had doubled in bleomycin-treated WT mice by 30 days following instillation and remained elevated for a further 30 days. In fibrosis-resistant $NE^{-/-}$ animals, inhibition of pulmonary TGF-β activation was detectable as early as a week following exposure to bleomycin. Protection against bleomycin-induced fibrosis for an entire two months suggested that compensatory mechanisms of TGF-β activation were either not in evidence or were inadequate to replace the lack of neutrophil elastase.

Although the timing of lung TGF-β expression and activation has been examined in different animal models of pulmonary fibrosis (Khalil et al., 1989; Lee et al., 2001; Warshamana et al., 2002), understanding of the temporal relationship between the upregulation of TGF-β bioactivity and initiation of pulmonary fibrosis is still incomplete. In the present studies, temporal changes in lung TGF-β mRNA expression were not characterised. However, at the time point when it was quantified (day 7 post-bleomycin), pulmonary TGF-β mRNA was significantly increased over saline values in both WT and $NE^{-/-}$ mice, and preceded measurable changes in lung collagen accumulation. This result agrees with the findings of Kaminski and colleagues that upregulation of TGF-β is detectable as early as two days following bleomycin administration, ahead of increased matrix deposition (Kamisnki et al., 2000). In the wider literature, maximal TGF-β mRNA expression following bleomycin instillation has been documented at day 7 (Hoyt and Lazo, 1988; Phan and Kunkel, 1992; Santana et al., 1995), or day 10 (Coker et al., 1997) following instillation of the drug in mice. Coker and colleagues noted a gradual increase in lung collagen following peak

TGF-β gene expression, with the former reaching a maximum value approximately a month after bleomycin injection of fibrosis-susceptible $B_6D_2F_1$ strain mice. In all studies, upregulation of TGF-β mRNA occurred before maximal extracellular matrix accumulation became apparent.

In other models of lung injury, an early rise in TGF-β gene expression preceding slower increases in lung collagen content has also been described. Peak TGF-β transcripts were measured seven days after pulmonary overexpression of granulocyte macrophage colony-stimulating factor using adenoviral-mediated gene delivery (Xing et al., 1997) and fourteen days following the overexpression of TNF-α using a similar vector (Sime et al., 1998). In radiation-induced pulmonary fibrosis, TGF-β gene transcription peaks after a longer delay of between two to three weeks following exposure to radiation, and elevations in total lung collagen similarly take longer to reach a maximum (Yi et al., 1996; Rube et al., 2000).

6.3.iii Neutrophil elastase does not activate latent TGF-β in BAL fluid

In the present *in vivo* experiments, levels of total (latent + active) TGF-β in BAL fluid of bleomycin-treated $NE^{-/-}$ mice amounted to only about half of those in WT samples. This disparity was due to differences in the levels of both latent and active TGF-β as measured by the PAI-1 assay prior to and after heat treatment. Hence, the quantity of heat-activatable TGF-β was significantly diminished in BAL fluid of $NE^{-/-}$ mice as early as seven days following bleomycin treatment. The current studies show that neutrophil elastase activates recombinant LAP-TGF-β in an equipotent manner to plasmin under *in vitro* conditions, but unlike the latter, does not activate latent TGF-β in BAL fluid. This observation is consistent with findings from studies using cultured epithelial and endothelial matrices indicating that greater than 95% of matrix-bound TGF-β released by purified neutrophil elastase is biologically latent and resistant to activation by the same proteinase (Taipale et al., 1995).

More recently, the instillation of porcine pancreatic elastase to induce experimental emphysema has been shown to both liberate latent TGF-β from lung tissue stores as well as activate a minor proportion of it (Buczek-Thomas et al., 2004). At the current time, the ability of neutrophil elastase to directly activate TGF-β *in vivo* has neither been completely proven nor refuted.

Nonetheless, the current data suggest that the predominant action of neutrophil elastase in modulating TGF-β activity in the injured lung is by releasing activatable TGF-β from matrix-bound stores rather than by directly activating latent TGF-β.

6.3.iv TGF-β activation occurs at sites of parenchymal lung damage in fibrosis-susceptible mice

Accurate tissue localisation of TGF-β is made difficult by its production as a latent complex, its susceptibility to different extracellular activation mechanisms and its tendency to bind connective tissue elements. Histological identification of TGF-β in bleomycin-injured lungs has revealed its commonest cellular sources to be inflammatory and resident lung cells, the latter represented mainly by fibroblasts and myofibroblasts, with additional expression by bronchial epithelial cells (Khalil et al., 1989; Zhang et al., 1995). In the current studies, latent TGF-β (LAP-TGF-β) was present in extracellular foci as well as within some alveolar epithelial cells in both bleomycin-treated WT and $NE^{-/-}$ lungs. In the lungs of fibrosis-susceptible WT animals, much of the active TGF-β was appreciated extracellularly with a predilection for compact areas of alveolar damage and increased cellularity, a week following bleomycin administration. It is possible that these areas may represent early sites of fibrogenesis. These changes correlated with measurable increases in active TGF-β in BAL fluid. By comparison, the levels of both active and total TGF-β in BAL fluid of bleomycin-treated $NE^{-/-}$ mice remained significantly decreased, and few pathological changes were seen on staining for active TGF-β in these lungs.

Although descriptive, immunohistologic observations of changes in staining for active and latent TGF-β can provide insights into lung tissue remodelling. Expression of active TGF-β and receptors for TGF-β is increased at sites of bleomycin-induced injury (Zhao and Shah, 2000). Zhang and colleagues have shown that following bleomycin instillation, early (< 3 days) localisation of TGF-β in inflammatory cells contrasts with its later (3 – 14 days) prominence in myofibroblasts and fibroblasts within areas of lung injury and fibrosis (Zhang et al., 1995). The LAP and LC(1-30) antibodies used in these studies were previously shown to specifically localise latent and active TGF-β (Barcellos-Hoff et al., 1994). The same antibodies have been used to indicate histological sites of TGF-β production in studies of murine lung injury (Zhang et al.,

1995; Franko et al., 1997). In the current studies, an increased abundance of active TGF-β in extracellular sites was identified in the lungs of bleomycin-treated WT animals with normal levels of neutrophil elastase. TGF-β immunoreactivity was particularly prominent in areas of hypercellularity, alveolar damage and matrix deposition at day 7. Staining was also evident in bronchiolar epithelium and in subepithelial matrix, consistent with results previously described by others (Khalil et al., 1989).

Attempts have been made to correlate TGF-β staining with increased procollagen production or matrix lung accumulation. TGF-β staining appears to temporally and spatially overlap with procollagen I mRNA expression in pulmonary fibrosis induced by inorganic fibres of silica (Mariani et al., 1996). In adult sheep, endotracheal instillation of asbestos fibres induces lesions of asbestosis (fibrosis) that have abundant matrix-associated but sparse cell-based TGF-β staining (Lee et al., 1997). Franko and colleagues have shown that following exposure to non-ionising radiation, TGF-β-positive fibroblasts congregate on the periphery of fibrotic lung lesions. In contrast, LAP staining is distributed uniformly throughout such lesions (Franko et al., 1997). This observation suggests that the earlier stages of pulmonary fibrosis may involve an association between extracellular matrix-producing fibroblasts and the geographic localisation of TGF-β.

6.3.v Neutrophil elastase activity enhances the release of lung tissue-bound TGF-β following bleomycin-induced lung damage

The current data raised the possibility that decreased TGF-β activity in the lungs of bleomycin-treated $NE^{-/-}$ mice might have resulted from impaired release of latent TGF-β from tissue stores. Processes that target binding interactions between TGF-β and the ECM can potentially influence the biological availability of TGF-β. Latent TGF-β can associate with different elements of the ECM, including permanent structural components (e.g. type IV collagen), as well as proteoglycans that have a higher rate of turnover (e.g. biglycan and decorin) (Hildebrand et al., 1994). Although unproven, mobilisation of matrix-associated latent TGF-β has been suggested as a pathologic mechanism by which increased TGF-β may influence lung matrix remodelling (Buczek-Thomas et al., 2004). *In vitro* studies have shown that the physical association between latent TGF-β and the ECM yields to proteolytic cleavage by neutrophil elastase (Taipale

et al., 1995). Thus, targeted interactions between neutrophil elastase and matrix-bound TGF-β may critically influence the means by which active TGF-β is supplied to areas of lung undergoing fibrotic repair.

The addition of exogenous neutrophil elastase to lung tissue of bleomycin-treated $NE^{-/-}$ mice was followed by the detection of increased amounts of heat-activatable TGF-β, suggesting the possibility that neutrophil elastase can mobilise stored TGF-β. In published studies, neutrophil elastase has been shown to liberate latent TGF-β from extracellular matrices produced by cultured pulmonary fibroblasts, epithelial cells, endothelial cells and bone osteoblasts (Taipale et al., 1995; Dallas et al., 2002). The experiments using cryosections and homogenised lung tissue in this thesis reveal that bleomycin-treated $NE^{-/-}$ lungs contain a small but significantly greater quantity of activatable TGF-β compared to WT controls. While its capacity to release tissue-sequestered TGF-β is at least as potent as that of plasmin, neutrophil elastase appears to be inefficient at completely activating latent TGF-β. Hence, neutrophil elastase-mediated release of matrix-stored TGF-β might represent an important early step in the conversion of latent TGF-β to its biologically active form within the remodelling lung. In this context, the most likely substrate for neutrophil elastase is the high molecular weight LTBP (Taipale et al., 1995).

6.3.vi *In vivo* relevance of neutrophil elastase-mediated TGF-β activation

Historically, it has been difficult to correlate quantitative changes in TGF-β activity to the extent of latent TGF-β activation assessed *in vivo*. The realisation now that the total pool of latent TGF-β is likely to consist of a tissue (matrix) reservoir as well as a soluble component in the form of TGF-β-LAP indicates complex regulation of its activity. Although the signals that sense and stimulate neutrophil elastase-mediated TGF-β release from the pulmonary matrix remain poorly understood, it seems likely that the regulation of neutrophil localisation and activation in the lung are important in this regard.

LTBP plays a role in the correct folding, secretion and targeting of LAP-TGF-β to the extracellular matrix (Miyazono et al., 1991; Nunes et al., 1997). All three TGF-β isoforms have been found in association with LTBP in high molecular weight TGF-β complexes, suggesting that

LTBP may mediate the targeting of all mammalian TGF-β isoforms to the ECM (Olofsson et al., 1992). Physically, LTBP has been shown to associate with fibroblasts and matrix microfibrillar elements, and more patchily with fibronectin and collagen type IV (Taipale et al., 1994). Large latent TGF-β containing LTBP is also known to associate with both interstitial and basement membrane ECM rich in type IV collagen (Paralkar et al., 1991; Roberts and Sporn, 1996). Incidentally, all these structural proteins are proteolytic substrates of neutrophil elastase. *In vivo*, however, the presence of neutrophil elastase and LTBP in the same microenvironment is required to fulfill the minimal caveat that both enzyme and substrate must co-localise for a cleavage reaction to occur. Although concentrations of neutrophil elastase sufficient to digest LTBP are likely to be present in the immediate pericellular vicinity of degranulating neutrophils (Taipale et al., 1995), proof that neutrophil elastase directly cleaves LTBP in the physiological setting is still lacking.

Placing the current data in perspective, it is proposed that neutrophil elastase proteolytically cleaves matrix-bound LTBP associated with LAP-TGF-β to modulate TGF-β activity at sites of bleomycin-induced lung damage. From previous *in vitro* studies, less than 1% of recombinant large latent TGF-β can be activated directly by treatment with purified neutrophil elastase (Taipale et al., 1995). When 1 μM plasmin is substituted for elastase, the amount of large latent TGF-β activated is only in the region of 1 – 2%. These observations are consistent with the concept that the bulk of biologically relevant large latent TGF-β is targeted to the extracellular matrix and not in solution. This means that other mechanisms for activation of soluble TGF-β apart from neutrophil elastase and plasmin are likely to exist.

Although purified plasmin can remove LAP to activate latent TGF-β, large amounts (~ 1 μM) of the proteinase are required (Lyons et al., 1988). To circumvent this, the release of LAP-TGF-β from the matrix could be modified so the latent TGF-β can concentrate at the cell surface in order to maximise its activation. Such a mechanism has been shown to operate in the bleomycin model where LAP-TGF-β first binds thrombospondin (TSP)-1 before engaging with CD36, the TSP-1 cellular receptor, to enhance the proteolytic activity of plasmin (Yehualasehet et al., 1999). Apart from plasmin, cell-surface proteolysis of LAP-TGF-β yielding active TGF-β has also been associated with the action of MMP-9 (Yu and Stamenkovic, 2000). The presence of call-associated staining of active TGF-β in the current experiments may point to a role for such mechanisms in the context of bleomycin-induced lung fibrosis.

Three other potential mechanisms of TGF-β activation also implicate a role for the ECM. Mice lacking αvβ6, an epithelium-restricted integrin, are protected from bleomycin-induced pulmonary fibrosis (Munger et al., 1999). *In vitro*, αvβ6 to RGD sequences on LAP, enabling the β6 cytoplasmic domain to engage cytoskeletal actin elements in the cell. These interactions produce a conformational change in the LAP-TGF-β complex, allowing the mature TGF-β to directly interact with its receptors. The second mechanism involves thrombospondin-1 (TSP-1), an insoluble anti-adhesive molecule derived from platelets, particularly in matrix-associated haemostatic plugs (Bornstein, 1992). In cell-free systems, TSP-1 binds to and activates small and large forms of latent TGF-β in a process that is plasmin-independent (Schultz-Cherry et al., 1994b). Cross-linking studies have shown that TSP-1-TGF-β binding can trigger TGF-β activation without the involvement of proteolysis or cell binding (Schultz-Cherry and Murphy-Ullrich, 1993). This interaction is dependent on a three amino acid sequence known as 'RFK' located between the first two properdin-like repeats in the TSP-1 moleculeas well as sequences in the amino terminal of LAP (Murphy-Ullrich and Poczatek, 2000). Histological similarities between TSP-1 null and TGF-β null mice, particularly in the developing lung, testify to the importance of TSP-1 as a natural activator of latent TGF-β in this particular organ (Crawford et al., 1998). Finally, Teder and colleagues have proposed a role for CD44, the major cell-surface receptor for the non-sulfated glycosaminoglycans hyaluronan, in regulating TGF-β activation (Teder et al., 2002). Increased accumulation of hyaluronan appears to influence recovery from pulmonary inflammation. In the proposed model, CD44-hyaluronan ligation increases the clearance of apoptotic neutrophils, a process that is associated with resolution of parenchymal inflammation and the production of increased levels of active TGF-β. A cell-based version of this mechanism, with an additional requirement for MMP-9 activity, has recently been elucidated *in vitro* (Yu and Stamenkovic, 2004). Thus, one recurring determinant of fibrotic lung matrix remodelling in both humans and animal models appears to be an enhanced local capacity to generate active TGF-β following lung injury.

CHAPTER SEVEN

THESIS SUMMARY

Summary of major findings

7.1 Development of bleomycin-induced pulmonary fibrosis is critically influenced by neutrophil elastase activity in the lung

The studies outlined in this thesis were designed to test the hypothesis that neutrophil elastase activity plays a crucial role in the development of pulmonary fibrosis. The current demonstration that absence of neutrophil elastase, a destructive enzyme, is associated with an increased resistance to pulmonary fibrosis might at first seem paradoxical. However, excessive neutrophil elastase activity has been implicated in lung injury associated with acute respiratory distress syndrome (Downey et al., 1999), hypersensitivity pneumonitis (Pardo et al., 2000) and idiopathic pulmonary fibrosis (Ambrosini et al., 2003) in humans. In all three conditions, pulmonary fibroproliferation is a recognised pathologic complication. In animal studies, proof of concept that neutrophil elastase activity can promote or prolong experimentally induced pulmonary fibrosis has been obtained by inhibiting its activity using exogenous α1-proteinase inhibitor (synonymous with α1-AT), secretory leukocyte proteinase inhibitor or ONO-5046, a synthetic neutrophil elastase antagonist. While these observations strengthen the notion that neutrophil elastase activity can enhance the lung fibrotic response, the mechanism/s by which it operates has yet to emerge.

The current *in vivo* studies demonstrate that mice genetically deficient in neutrophil elastase ($NE^{-/-}$) are protected from bleomycin-induced pulmonary fibrosis. In these animals, lung collagen content failed to increase following intratracheal instillation of bleomycin. In wild type (WT) mice, histologic markers of pulmonary fibrosis were firmly established 30 days following bleomycin administration and persisted for up to 60 days. Crucially, fibrosis temporally correlated with a doubling in total lung collagen. Although a fibrotic response was absent in $NE^{-/-}$ mice, bleomycin treatment did induce DNA damage, inflammation, alveolar leak, focal interstitial thickening and alveolar collapse. These manifestations indicate that $NE^{-/-}$ animals are not immune to the injurious effects of bleomycin. Indeed, these phenomena may even enhance the overall susceptibility of wild type mice to develop bleomycin-induced pulmonary fibrosis.

In preliminary studies, a fibrosis-resistant phenotype was also discovered in α1-AT over-expressing mice exposed to an equivalent dose of bleomycin (see Appendix 1). α1-AT is the

major endogenous inhibitor of neutrophil elastase in the distal airways and pulmonary acini. Although these results do not prove that inhibition of neutrophil elastase activity is responsible for protection against pulmonary fibrosis, the results are consistent with the view that neutrophil elastase contributes to the ability of the lung to accumulate collagen-rich extracellular matrix following bleomycin treatment.

7.2 Resistance of $NE^{-/-}$ mice to bleomycin-induced pulmonary fibrosis is not related to impaired neutrophil influx or abrogation of lung injury

Evidence from animal studies increasingly suggests that neutrophil elastase may be less important in facilitating lung neutrophil infiltration than once thought. The current studies demonstrate that the degradative capacity of neutrophil elastase is not a prerequisite for bleomycin-induced neutrophil influx. In the early stages of bleomycin-induced lung injury, the alveolar inflammatory infiltrate is primarily neutrophil-rich in rats (Thrall et al., 1982) and mice (Janick-Buckner et al., 1989). However, most of these 'classic' cellular changes have only been characterised in BAL fluid; much less is known about lung tissue neutrophil turnover. In one particular study, the administration of ONO-5046, a pharmacologic inhibitor of neutrophil elastase, was associated with reduced neutrophil numbers in murine BAL fluid at 1, 15 and 29 days following bleomycin administration (Taooka et al., 1997). The abundance or persistence of tissue-trapped neutrophils was not specifically assessed.

In contrast, bleomycin-treated WT mice in the present *in vivo* studies did not have an excess of BAL fluid neutrophils compared to similarly treated $NE^{-/-}$ mice over the initial 10 days post-bleomycin. A statistically non-significant reduction in neutrophil numbers in $NE^{-/-}$ mice was observed, however, in pooled BAL fluid collected at the seven-day time point. Nonetheless, total lung tissue neutrophil burden was similar in both bleomycin-treated WT and $NE^{-/-}$ animals. In other words, pulmonary accumulation of neutrophils was not defective in bleomycin-treated $NE^{-/-}$ mice. This finding concurs with previous observations in $NE^{-/-}$ mice in models of pneumonic bacterial infection (Allport et al., 2002; Hirche et al., 2004), thioglycollate-induced peritonitis (Tkalcevic et al., 2000) and zymosan-induced inflammation (Young et al., 2004).

Lung tissue neutrophils all originate from the pulmonary circulation. Curiously, neutrophils in bleomycin-treated $NE^{-/-}$ lungs appeared to be retained longer in perivascular areas before

advancing into neighbouring alveoli. This anomaly would have been missed if total lung neutrophil load had been quantified solely by biochemical means (e.g. quantification of tissue myeloperoxidase activity). This observation suggests that neutrophil elastase activity might impose a rate-limiting effect on neutrophil transmigration in the lung. Shapiro and colleagues have reported that fewer neutrophils egress from the pulmonary vasculature into the parenchyma of $NE^{-/-}$ mice chronically exposed to cigarette smoke (Shapiro et al., 2003). Although neutrophil elastase can cleave a number of structural proteins in both the epithelium and endothelium linings, identification of the precise substrate involved in the transmigration process was not pursued in this thesis. Nevertheless, differences in tissue neutrophil distribution between WT and $NE^{-/-}$ mice due to different rates of alveolar infiltration may genuinely influence the final propensity for fibrotic repair in these animals. In other words, the greater ability of activated neutrophils to sequester within the deeper parenchyma of WT mice may indicate an increased tendency to fibrosis although the mechanisms that dictate this pathway remain uncertain.

Protection of $NE^{-/-}$ mice against bleomycin-induced pulmonary fibrosis was not specifically due to the diminished severity of acute lung injury. Initial responses to bleomycin, in terms of DNA damage, inflammatory intensity and cytotoxicity were similar between WT and $NE^{-/-}$ mice. Histologic indices of acute lung injury were also comparable between two groups of animals. Although neutrophil elastase blockade attenuates the intensity of lung injury due to bacterial endotoxin, organic acids and ischaemia-reperfusion (reviewed in Downey et al., 2001), it is also acknowledged that certain actions of neutrophil elastase may paradoxically downregulate the inflammatory response. For example, neutrophil elastase can degrade the pro-inflammatory cytokines, IL-1β and TNF-α (Owen et al., 1997), release complement receptor 1 (CR1) from the erythrocyte surface to neutralise complement proteins (Sadallah et al., 1999) and cleave CD14, the main cellular receptor for bacterial lipopolysaccharide (Le-Barrilec et al., 1999). These and other observations indicate that lung injury responses induced by an external stimulus may be preserved in circumstances where neutrophil elastase is absent.

7.3 Neutrophil elastase activity potentiates bleomycin-induced alveolar barrier leak

The epithelial lining is generally assumed to be the most selective component of the alveolar-capillary barrier. Compromised epithelial integrity facilitates the movement of macromolecules and cells, including leukocytes and matrix-secreting cells, from the vasculature

into interstitial and alveolar spaces. The subsequent transformation of such exudative material into provisional or permanent connective tissue is a pathologic consequence of alveolar barrier breakdown. In the present studies, changes in alveolar permeability as evaluated by differential Evans blue dye retention, enabled the pathological role of neutrophil elastase in alveolar leak to be assessed. Intratracheal instillation of 0.05U bleomycin initially induced an equivalent degree of alveolar hyper-permeability in both WT and $NE^{-/-}$ lungs. However, alveolar barrier dysfunction was clearly prolonged in bleomycin-injured WT mice. The earlier restoration of barrier integrity in $NE^{-/-}$ mice pointed to a possible way in which neutrophil elastase might potentiate bleomycin-induced alveolar leak. Specifically, the action of this serine proteinase appeared to be more relevant to prolonging alveolar-capillary barrier permeability than for initiating its damage. Hindrance of normal alveolar repair in bleomycin-treated WT mice would promote intra-alveolar accumulation of fibrinous exudates, soluble mediators and mesenchymal cells, thereby enhancing the alveolar potential for uncontrolled fibroproliferation. Although proteolysis of an elastase-sensitive substrate has not been identified as the culprit mechanism in this context, several possibilities are suggested by information from previous studies.

In line with its injurious nature, neutrophil elastase may affect alveolar barrier physiology in myriad ways. Cytolysis and detachment of epithelial cells from the basement membrane (Amitani et al., 1991; Van Wetering et al., 1997) as well as apoptosis of pulmonary vascular cells (Okrent et al., 1990) have been described following exposure of these cells to purified neutrophil elastase *in vitro*. These events, however, would be expected to distinguish between WT and $NE^{-/-}$ alveolar integrity early in the course of bleomycin-induced lung injury. Likewise, neutrophil elastase-dependent dissolution of molecules that mediate intercellular adhesion such as cadherins or degradation of components of the basement membrane such as type IV collagen would also be expected to manifest soon after bleomycin administration. The divergence in alveolar leak between WT and $NE^{-/-}$ mice after seven days of bleomycin treatment raised the possibility that neutrophil elastase might be influencing an intermediary molecule whose activity may be more prominent during the latter phases of lung injury.

In accordance with a growing awareness that TGF-β is an important mediator of acute lung injury, its deleterious effects on alveolar cells may be particularly relevant to the current discussion. Excessive pulmonary TGF-β activity has been linked to the depletion of intra-epithelial glutathione stores and enhanced susceptibility of these cells to oxidants generated during bleomycin-induced lung injury (Pittet et al., 2001). TGF-β also has the capacity to inhibit epithelial

expression of sodium channels that regulate cellular osmotic integrity (Frank et al., 2003). Compromised alveolar sodium and water clearance affects the ability of the alveolar barrier to regulate fluid homeostasis leading to enhanced alveolar leak and the development of pulmonary oedema. TGF-β has also been shown to increase microvascular permeability by inducing the contraction of adjacent endothelial cells forming a common barrier (Hurst et al., 1999). A potential link between neutrophil elastase and TGF-β is suggested by observations that neutrophil elastase can liberate, and perhaps even activate, latent TGF-β in extracellular matrices secreted by cultured fibroblasts and epithelial cells (Taipale et al., 1995). *In vivo*, such actions would increase the prevalence of TGF-β at sites of alveolar-capillary barrier damage.

Equally important but less well known are the inhibitory effects of active TGF-β on pulmonary surfactant expression (Beers et al., 1998) and the enhancement of Fas-mediated apoptosis of pulmonary epithelial cells by active TGF-β (Hagimoto et al., 2002). Chen and colleagues have demonstrated that ligation of FasL (CD95L) itself can stimulate pro-inflammatory cytokine release (Chen et al., 1998). More recently, neutrophil elastase activity has been shown to directly induce alveolar epithelial cell apoptosis by acting via the proteinase-activated receptor, PAR-1 (Suzuki et al., 2005). Cellular apoptosis was accomplished through PAR-1-dependent cleavage of caspase-9 and caspase-3, activation of JNK and alterations in mitochondrial permeability in epithelial cells. These effects, if operative within the alveolar compartment, could exacerbate alveolar epithelial cell injury and diminish the capacity of these cells to restore barrier function. Hence, any role played by neutrophil elastase in modulating alveolar integrity early on could have deleterious and often permanent consequences on lung repair such as the induction of fibrosis.

7.4 Neutrophil elastase activity increases TGF-β activation in bleomycin-injured lung tissue

Under physiological conditions, the concentration of free (active) TGF-β in equilibrium with the small latent TGF-β complex is thought to be negligible (Munger et al., 1997). Since extracellular activation of latent TGF-β is the primary means of generating active TGF-β, this must mean that 'free' TGF-β in the extracellular milieu has a very short half-life. Thus, the ability to store large quantities of activatable TGF-β in tissue matrix might be an adaptive mechanism that would allow concentrated pools of this fibrogenic mediator to be rapidly mobilised when

necessary. In the lung, different downstream mechanisms could subsequently operate to activate the released latent TGF-β. These might include proteolysis, oxidant radical production and cell-based mechanisms such as the plasmin/CD36/thrombospondin complex on macrophages (Yehualaeshet et al., 1999) or the αvβ6 integrin on injured epithelial cells (Munger et al., 1999).

WT and $NE^{-/-}$ mice in these studies constitutively expressed latent TGF-β in the lung. Following bleomycin treatment, TGF-β mRNA expression was similar in both groups of animals. However, unlike WT mice, bleomycin-injured $NE^{-/-}$ animals were distinguished phenotypically by an impaired pulmonary fibrotic response and defective activation of TGF-β. Latent TGF-β was retained within the lung parenchyma and markedly reduced quantities of active TGF-β were present in BAL fluid. Tissue-bound TGF-β was susceptible to proteolytic release by purified neutrophil elastase when evaluated *ex vivo*. Liberation of this pool of TGF-β under pathophysiological conditions would likely have increased the bioavailability of activatable TGF-β at sites of matrix remodelling. Hence, neutrophil elastase-mediated generation of active TGF-β appears to be critically important to the fibrotic predisposition of the bleomycin damaged lung.

Taipale and colleagues found that greater than 95% of TGF-β released by plasmin from cultured matrices is biologically latent (Taipale et al., 1995). However, the amount of active TGF-β recovered following lung tissue incubation with plasmin in the current studies was much greater. In the current studies, at least half of the TGF-β released by plasmin incubation was biologically active. By comparison, a much smaller proportion of neutrophil elastase-released TGF-β was in the active state. However, the overall ability of neutrophil elastase to release tissue-bound TGF-β from the lungs of $NE^{-/-}$ mice was comparable to that of plasmin. In essence, most of the TGF-β released by neutrophil elastase remained biologically latent and required activation before it could be measured by the PAI-1 bioassay. Neutrophil elastase-dependent generation of activatable TGF-β may therefore constitute an important mechanism to increase the abundance of TGF-β in the injured lung.

Potential mechanism of neutrophil elastase-mediated generation of active TGF-β

The molecular basis by which neutrophil elastase can enzymatically release matrix-associated latent TGF-β has been elucidated *in vitro*. The mechanism implicates cleavage of the latent TGF-β binding protein (LTBP) at one or more proteinase-sensitive sites. Neutrophil elastase-mediated digestion of LTBP in large latent TGF-β complexes produces biologically inactive TGF-β that is resistant to further proteolysis but is susceptible to heat or acid-mediated activation (Taipale et al., 1995). In terms of comparative proteolytic potency, neutrophil elastase has been shown to be approximately ten-fold more efficient at digesting LTBP-1 than plasmin (ED_{50} 5 nM compared to ED_{50} 50 nM respectively) (Taipale et al., 1995).

Four isoforms of LTBP (LTBP-1, -2, -3 and -4) have so far been cloned (Koli et al., 2001), including several that are believed to act as local regulators of TGF-β deposition in the ECM. LTBPs are structurally related to other members of the fibrillin family of ECM proteins that share a central backbone of tandemly repeating epidermal growth factor (EGF)-like moieties (Saharinen et al., 1999) (**figure 7.1**). These EGF-like repeats mediate protein-protein interactions and bind cations, such as calcium, that help stabilise the entire LTBP molecule. Within this backbone, a unique and highly conserved pattern of four 'eight-cysteine' (8-Cys) residues is interspersed. Studies of human LTBP-1 have shown that cysteine residues in the third 8-Cys domain (near the C-terminus) form disulfide bonds with LAP via the Cys-33 residue in the LAP molecule (Gleizes et al., 1996; Saharinen and Keski-Oja, 2000, Chen et al., 2005). This interaction describes the primary mechanism by which LTBP-1, -3 and -4 bind LAP-TGF-β to form large latent TGF-β complexes (Koli et al., 2001). In addition, 8-cys domains and in particular, the first 8-cys repeat located near the N-terminus, take part in targeting latent TGF-β to the extracellular matrix.

TGF-β activation in cell co-culture systems can be prevented by the addition of exogenous LTBP-1 free of TGF-β, or of anti-LTBP-1 antibodies directed against either its N- or C-terminal regions (Flaumenhaft et al., 1993; Nunes et al., 1997). The blocking of transglutaminase activity also leads to the inhibition of TGF-β activation in cell culture models (Kojima et al., 1993). Thus, in several *in vitro* models, deposition and crosslinking of large latent TGF-β complexes via LTBP

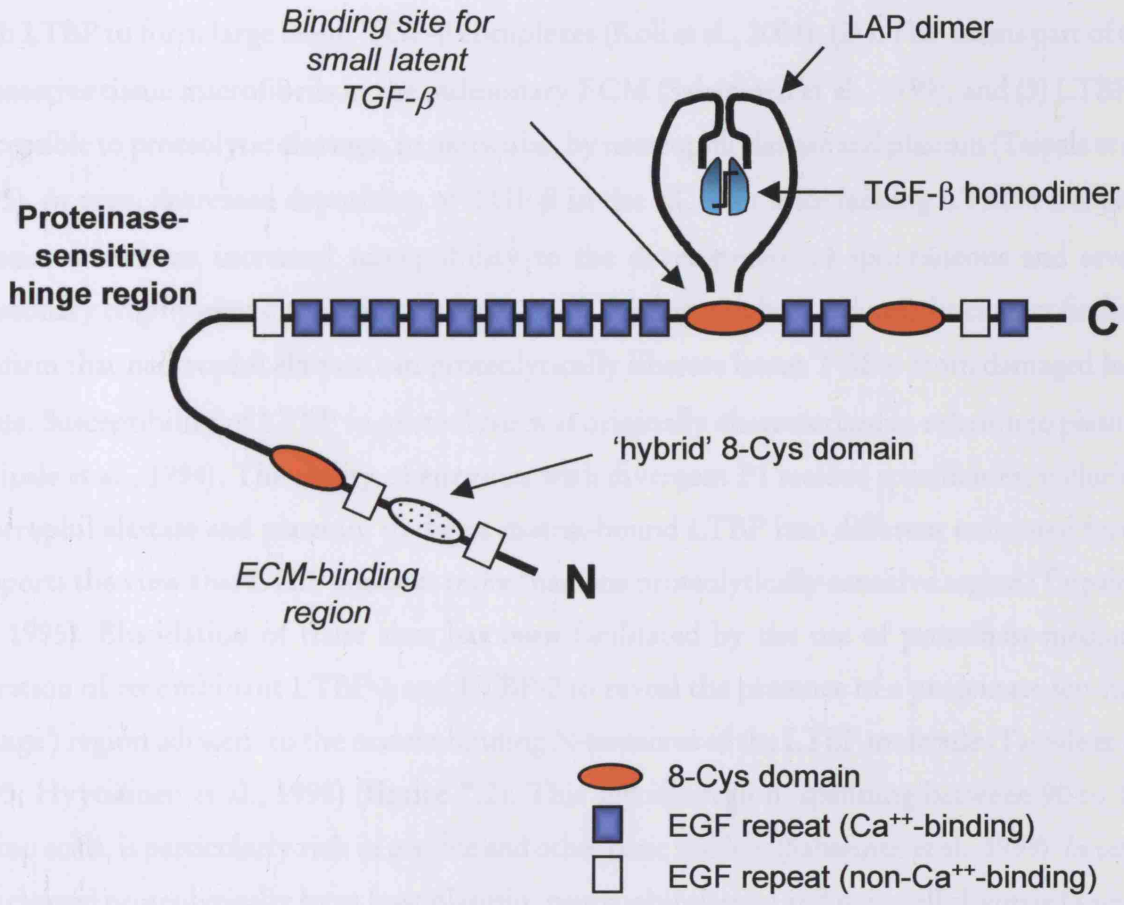

Figure 7.1 Schematic representation of the large latent TGF-β complex comprising the mature TGF-β homodimer, its latency-associated peptide (LAP) and the latent TGF-β binding protein (LTBP).

plays a distinctive role in TGF-β activation. These results suggest that active TGF-β generation may be preceded by the enzymatic/proteolytic release of matrix-associated latent TGF-β. TGF-β activation itself could then be accomplished at or near the cell surface by another proteolytic or non-proteolytic mechanism.

The proposal that LTBP is a principal candidate for the proteolytic modulation of TGF-β activity in the lungs is supported by several lines of evidence: (1) most cell-secreted TGF-β is associated with LTBP to form large latent TGF-β complexes (Koli et al., 2001), (2) LTBP forms part of the connective tissue microfibrils in the pulmonary ECM (Saharinen et al., 1999), and (3) LTBP is susceptible to proteolytic cleavage, in particular, by neutrophil elastase and plasmin (Taipale et al., 1995). *In vivo*, decreased deposition of TGF-β in the ECM in mice lacking LTBP-4 has been associated with an increased susceptibility to the development of spontaneous and severe pulmonary emphysema (Sterner-Kock et al., 2002). Against this background, the current findings confirm that neutrophil elastase can proteolytically liberate latent TGF-β from damaged lung tissue. Susceptibility of LTBP to proteolysis was originally characterised in relation to plasmin (Taipale et al., 1994). The ability of enzymes with divergent P1 residue specificities, including neutrophil elastase and plasmin, to digest matrix-bound LTBP into different truncated forms supports the view that LTBP contains more than one proteolytically-sensitive region (Taipale et al., 1995). Elucidation of these sites has been facilitated by the use of proteinase-mediated digestion of recombinant LTBP-1 and LTBP-2 to reveal the presence of a proteinase-sensitive ('hinge') region adjacent to the matrix-binding N-terminus of the LTBP molecule (Taipale et al., 1995; Hyytiäinen et al., 1998) (**figure 7.2**). This specific region, spanning between 90 to 150 amino acids, is particularly rich in proline and other basic residues (Saharinen et al., 1999). *In vitro*, it is cleaved proteolytically by at least plasmin, neutrophil elastase and mast cell chymase (Taipale et al., 1995). In terms of potency, neutrophil elastase is reportedly ten times more efficient at digesting LTBP-1 than plasmin (ED_{50} 5 nM compared to ED_{50} 50 nM respectively) (Taipale et al., 1995).

Treatment of the large latent TGF-β complex with either plasmin or neutrophil elastase leaves a 120 – 140 kDa proteolysis-resistant core, possibly representing a small latent TGF-β : truncated LTBP molecule (Taipale et al., 1995). Three lines of evidence support the potential existence of such a molecule. Firstly, other serine proteinases such as mast cell chymase and plasmin also degrade LTBP to final reaction products between 85 – 120 kDa in size (Taipale et al., 1994).

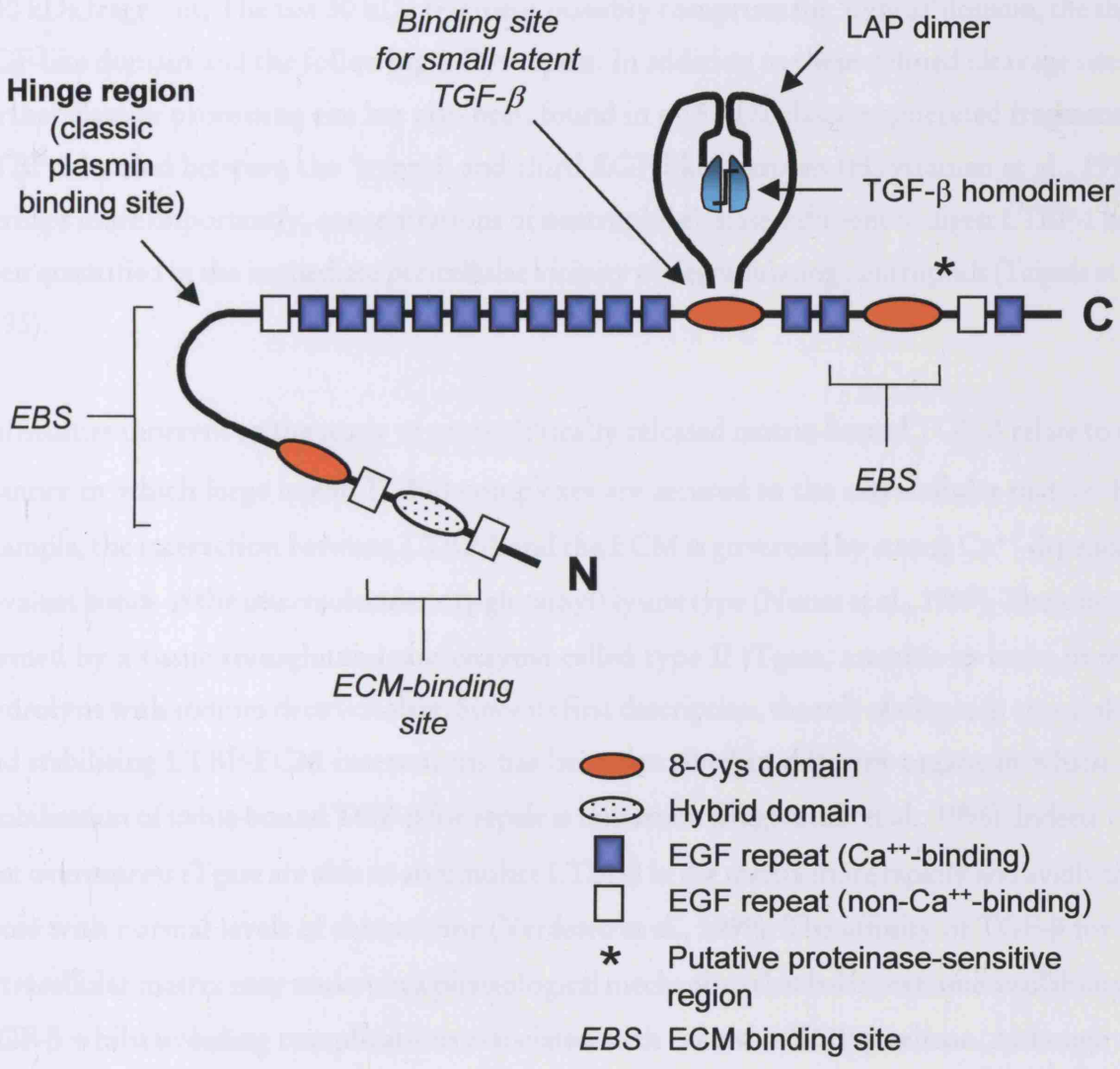

Figure 7.2 Schematic representation of the large latent TGF-β complex showing the hinge region and putative extracellular matrix-binding domains of the latent TGF-β binding protein (LTBP).

Secondly, platelet-derived LTBP molecules (140 kDa) are strongly proteinase-resistant (Taipale et al., 1994). Finally, studies using recombinant LTBP-2 have shown that processing by neutrophil elastase in a dose-dependent manner consistently produces fragments of approximately 120 – 160-kDa in size (Hyytiäinen et al., 1998). The first proteolytic cleavage is believed to release a 160 kDa LTBP-2 fragment from the matrix substratum, with the reaction occurring at a site proximal to the first 8-Cys ('hybrid') domain of the LTBP-2 parent molecule. Subsequent processing by neutrophil elastase generates the major proteinase-resistant 120-kDa fragment and less frequently, a 30 kDa fragment. The last 30 kDa fragment possibly comprises the 'hybrid' domain, the third EGF-like domain and the following 8-Cys repeat. In addition to these defined cleavage sites, a further elastase processing site has also been found in a 15 kDa elastase-generated fragment of LTBP-2 located between the 'hybrid' and third EGF-like domains (Hyytiäinen et al., 1998). Perhaps more importantly, concentrations of neutrophil elastase sufficient to digest LTBP-1 have been quantified in the immediate pericellular vicinity of degranulating neutrophils (Taipale et al., 1995).

Difficulties inherent to the study of proteolytically released matrix-bound TGF-β relate to the manner in which large latent TGF-β complexes are secured to the extracellular matrix. For example, the interaction between LTBP-1 and the ECM is governed by strong Ca^{++}-dependent covalent bonds of the intermolecular ε (γ-glutamyl) lysine type (Nunes et al., 1997). These bonds, formed by a tissue transglutaminase enzyme called type II tTgase, are able to resist *in vitro* hydrolysis with sodium deoxycholate. Since its first description, the role of tTgase in crosslinking and stabilising LTBP-ECM interactions has been described in different organs in which the mobilisation of tissue-bound TGF-β for repair is important (Raghunath et al., 1996). Indeed, cells that overexpress tTgase are able to accumulate LTBP-1 in the matrix more rapidly and avidly than those with normal levels of the enzyme (Verderio et al., 1999). The affinity of TGF-β for the extracellular matrix may underpin a physiological mechanism that balances tissue availability of TGF-β whilst avoiding complications associated with excessive TGF-β release. Although the precise mechanism by which neutrophil elastase modulates TGF-β-matrix cross-linking is still unknown, current evidence suggests that proteolysis of matrix-bound latent TGF-β by this serine proteinase leaves a remnant of the LTBP molecule behind in the ECM.

Concluding remarks

The finding that mice lacking neutrophil elastase are protected from bleomycin-induced pulmonary fibrosis forms the key observation in this thesis. Use of the bleomycin model enabled the temporal pattern of inflammatory cell accumulation, evolution of lung injury and development of a typical bleomycin-induced pulmonary fibrotic response to be delineated in wild type mice. Similar indices were used to characterise a fibrosis-resistant phenotype in neutrophil elastase null mice. Protection against bleomycin-induced pulmonary fibrosis in $NE^{-/-}$ mice correlated with: (1) slower pulmonary (alveolar) neutrophil infiltration following bleomycin-induced injury, (2) earlier restoration of alveolar barrier integrity to macromolecule leak, and (3) impaired generation of active TGF-β, particularly at sites of lung extracellular matrix damage.

Neutrophil elastase appears to play a pathogenetic role in the development of bleomycin-induced pulmonary fibrosis at several levels. During the acute or subacute phases of bleomycin-induced lung injury, the capacity for neutrophils bearing neutrophil elastase to disseminate widely within the lung is likely to increase the total lung damage burden in WT animals. Put another way, it is conceivable that the early curtailment of tissue neutrophil infiltration in $NE^{-/-}$ mice might blunt the vulnerability of *NE* gene-deleted mice to bleomycin-induced pulmonary fibrosis. On top of this, prolongation of alveolar leak in the presence of neutrophil elastase might also be expected to heighten the pulmonary fibroproliferative potential of bleomycin-injured WT mice. One fibrogenic denominator common to both these phenomena (neutrophil chemotaxis and alveolar leak) is transforming growth factor-β.

TGF-β ranks highest within the biological hierarchy of fibrogenic mediators. Its pro-fibrotic activities in the lung are potent and wide-ranging. Apart from the above postulated means of enhancing pulmonary fibrotic potential, one additional mechanism proposes that neutrophil elastase can specifically cleave matrix-anchored latent TGF-β to increase the availability of activatable cytokine for ECM regeneration. The findings in this thesis provide an *in vivo* basis for a previously described *in vitro* mechanism and implicate LTBP as the neutrophil elastase-sensitive substrate (**figure 7.3**). The released latent TGF-β can then be activated by a number of mechanisms that are either engaged on the surface of inflammatory or resident cells, or incorporated within the extracellular matrix.

Figure 7.3 Schematic overview: proposed mechanism of neutrophil elastase-mediated TGF-β activation

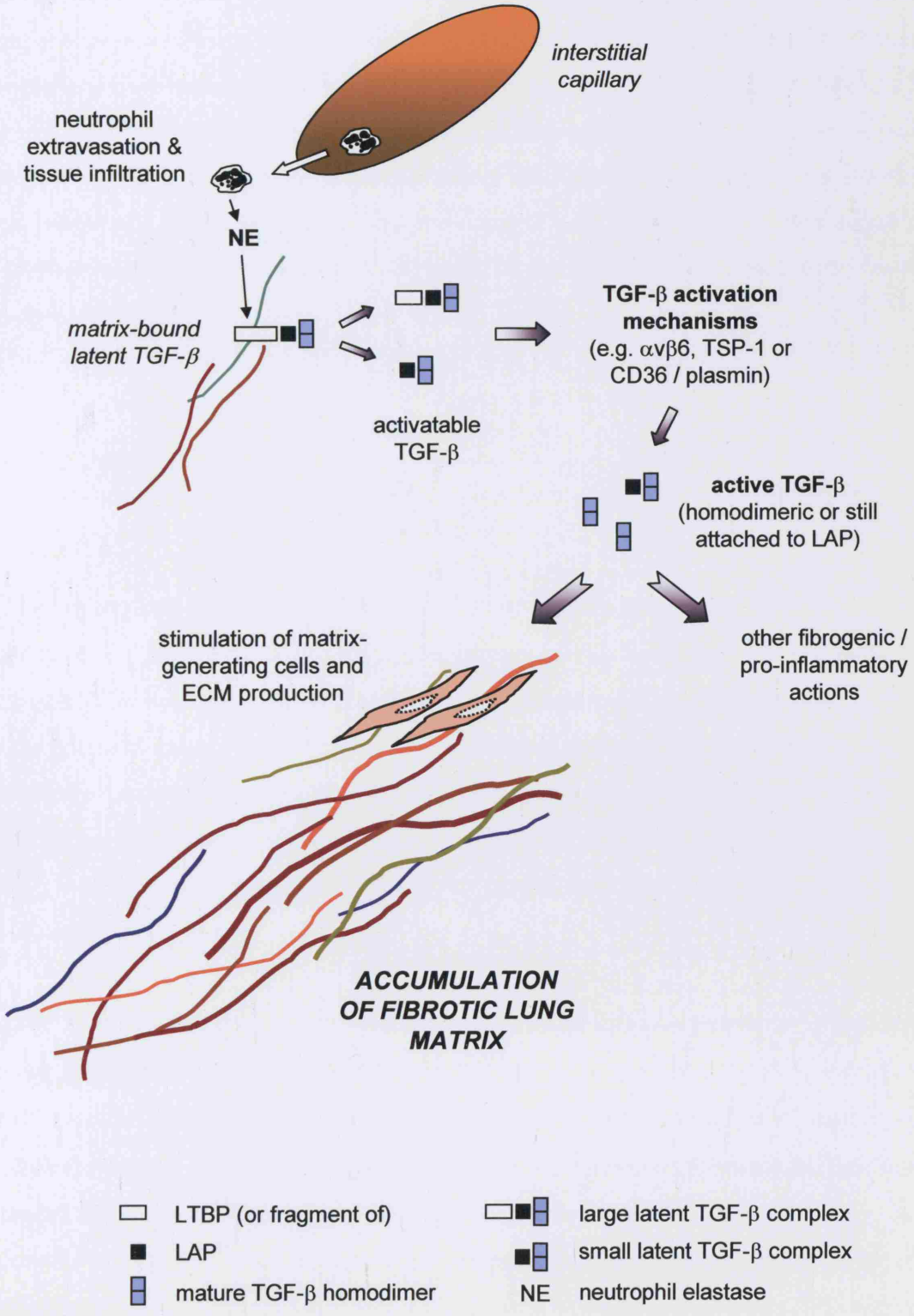

Comprehensive studies in cell culture systems have shown that the LTBP molecule possesses a proteinase-degradable region. Cleavage of this region destabilises the large latent TGF-β complex, and leads to the release of smaller latent complexes. Matrix-sequestered LTBP is thus the most plausible proteolytic substrate for neutrophil elastase in the current model. By focusing neutrophil elastase activity at discrete sites of repairing lung parenchyma, the activation of latent TGF-β and its consequent effects on the formation of fibroproliferative lesions can be spatially enhanced. Aberrant proteolysis exemplified by the degradation of specific matrix molecules is thought to be a vital step in the progression of fibrotic lung injury. The findings contained in this thesis explain how neutrophil elastase can potentiate the early events of bleomycin-induced lung injury as well as subsequent pathologic ECM accumulation, providing a link between these two stages of pulmonary fibrosis. It fulfills this role by proteolytically increasing the local abundance and with it, activation of latent TGF-β.

Therapeutic implications

The finding that neutrophil elastase activity can enhance pulmonary TGF-β activation raises the possibility of manipulating particular aspects of this biological phenomenon for therapeutic gain. To date, scepticism in the clinical utility of neutrophil elastase inhibitors has been related to the potential risks of inhibiting a key antimicrobial molecule and the uncertain efficacy of administering an enzyme inhibitor after the initiation of tissue damage. While the potency of a neutrophil elastase inhibitor is relatively easy to assess by measuring its enzyme inhibition constant (*Ki*), the pharmacodynamics and thus, safety of each individual compound require more detailed scrutiny.s

Over the past two decades, efforts to augment the body's elastase inhibitory capacity by positively manipulating proteinase/antiproteinase defenses, particularly in disease, have been intensified. One approach has involved the use of high molecular weight inhibitors such as α1-antitrypsin, secretory leukoproteinase inhibitor (SLPI), eglin C and elafin (reviewed in Edwards and Bernstein, 1994). Several of these inhibitors have been produced by recombinant technology, and formulations have been developed for aerosolisation or intravenous administration. A second approach has been the development of low molecular weight, non-peptidic neutrophil elastase

inhibitors. This strategy offers several advantages over the first: improved oral absorption, less proteolytic inactivation, greater enzyme selectivity and decreased risk of immunological intolerance.

Pulmonary fibrosis is a poorly understood condition whose late clinical presentation is a key limitation to any therapeutic intervention. However, novel biological targeting, including neutrophil elastase inhibition may help suppress or ameliorate exacerbative episodes of fibrotic lung injury where neutrophilia is pathologically prominent. A similar strategy may be feasible for inhibiting the early fibroproliferation that occurs in the acute respiratory distress syndrome (ARDS). Sivelestat, a synthetic neutrophil elastase inhibitor that combines two related compounds, ONO-5046 and LY544349, has been assessed in a cohort of patients with the systemic inflammatory response syndrome (SIRS) and ARDS. Although the use of sivelestat was initially associated with decreased duration of mechanical ventilation and earlier discharge from intensive care (Tamakuma et al., 1998), neither these observations nor any survival benefit were apparent in a larger international study (Zeiher et al., 2004). This disappointing outcome is unsurprising, given the intensity of lung damage in established ARDS and unpredictability of an approach in a diffuse disease where regional ventilation / perfusion abnormalities may result in increased drug delivery to less severely affected areas of lung and away from more damaged areas. On the other hand, preliminary studies in patients with cystic fibrosis have shown that the epithelial lining fluid anti-elastase inhibitory capacity can be increased following aerosolisation of recombinant SLPI (secretory leukoproteinase inhibitor) (Vogelmeier et al., 1996). And while conclusive benefit that α1-AT replacement therapy in individuals with α1-AT deficiency-related emphysema is lacking, parenteral replacement does appear to augment anti-proteinase levels in bronchoalveolar lavage fluid (Sandhaus, 2004). Thus, if a suitable neutrophil elastase inhibitor did become available and the timing of therapy as well as drug dispersal (including genetic approaches) can be optimised, the potential of such an intervention may yet be realised.

Future work

Many of the findings in this thesis, including the primary observation that neutrophil elastase is required for bleomycin-induced pulmonary fibrosis to develop, have scope for further study. To confirm that the fibrosis-prone phenotype in mice bearing the *NE* gene is robust and

dependent on unopposed neutrophil elastase activity in the ECM, experiments aimed at restoring the fibrotic phenotype to $NE^{-/-}$ mice would be a suitable extension. One approach would involve lethal bone marrow irradiation in these animals, followed by reconstitution with wild type haematopoietic progenitor cells (including $NE^{+/+}$ precursors) and finally, instillation of intratracheal bleomycin. Alternatively, targeted over-expression of active TGF-β could be accomplished using a lung-specific delivery vector in $NE^{-/-}$ mice prior to bleomycin instillation. As control, the vector could contain latent TGF-β. The same system could be further refined to inducibly turn the TGF-β gene 'on' or 'off' in adult $NE^{-/-}$ mice and thus avoid manipulation of TGF-β during crucial periods of lung development. This approach could also be modified to evaluate the role of neutrophil elastase in influencing matrix repair in response to other fibrogenic agents such as asbestos fibers or non-ionising thoracic irradiation. Both of these stimuli have been linked to TGF-β-mediated pulmonary fibrosis.

Molecular co-operation may potentially exist between neutrophil elastase and the αvβ6 integrin. As both $NE^{-/-}$ and $\alpha v\beta 6^{-/-}$ mice are available on the same genetic background (129/Sv), crossbreeding to generate combined NE/αvβ6-null animals is theoretically feasible. These animals could be used to determine whether the absence of both molecules affords greater protection from TGF-β activation and hence, bleomycin-induced lung fibrosis than would be expected from knocking out each gene individually. On the same principle, a similar approach could be taken to assess the impact of combined neutrophil elastase-MMP-9 deficiency on bleomycin-induced lung pathology.

Further characterisation of neutrophil elastase-mediated proteolysis of matrix-bound TGF-β complexes in the lung would also be feasible. In particular, analysis of LTBP solubilisation products in BAL fluid has hitherto not been reported. In the first instance, these could be assayed by Western blot analysis combined with an examination of the abundance of LTBP in lung tissue of bleomycin-injured mice. Such changes could also be correlated to neutrophil elastase activity within the lung matrix by the use specific fluorogenic substrates. Data from such studies would help to conceptualise the spatial relationship between neutrophil elastase release, LTBP cleavage and active TGF-β generation at the tissue level. The possibility of compensatory MMP elastolytic activity in the absence of neutrophil elastase (in $NE^{-/-}$ lungs) is as yet unresolved and could be evaluated using comparative kappa-elastin zymograms in time course experiments using BAL fluid as the starting material.

APPENDIX 1 RESPONSE OF ALPHA-1-ANTITRYPSIN OVEREXPRESSING MICE TO BLEOMYCIN-INDUCED PULMONARY FIBROSIS

Generation of alpha-1-antitrypsin overexpressing mice

Transgenic mice overexpressing human alpha-1-antitrypsin (α1-AT) were generated by Dr. Sue Povey and colleagues at University College London (Kelsey et al., 1987). Mice in these studies were obtained from a colony maintained by Dr. David Flavell at UCL. In brief, a cDNA clone encoding human α1-AT PiM gene was isolated from a human liver cDNA library with a synthetic oligonucleotide using optimised screening conditions. The restriction map of the most intensely hybridising recombinant, α1-ATc1, was established by partial digestion and confirmed to contain the entire α1-AT gene. Following gel-purification, the human insert DNA was microinjected into the pronuclear eggs collected from (C57BL/6 x CBA)F_1 mice and transferred to pseudo-pregnant foster mothers. Forty-nine mice were born following microinjection. Two separate lines (AT16 and AT39) were established from founders that contained 10-20 copies of the α1-AT gene. Extensive preliminary studies have shown that these transgenic mice stably express the human α1-AT gene and that the gene product is processed and secreted by hepatocytes into serum (Kelsey et al., 1986). Mice used in the present study were derived from the AT39 founder line and had been backcrossed onto the C57BL/6 background for four generations. Circulating levels of human a1-AT in these mice are 32 mg/ml (Ali et al., 1994).

Results

Thirty days following the intratracheal instillation of 0.05 U bleomycin, lungs of wild type mice showed evidence of diffuse fibroproliferative changes. At low power, the alveolar architecture appeared grossly abnormal with widespread inflammation, focal areas of interstitial

thickening and increased deposition of loose and dense fibrous matrix (top panel, **figure A.1**). The fibrillar pattern of blue-staining collagen strands was better appreciated at higher power (inset). In contrast, lungs of α1-AT overexpressing mice had small and isolated areas of inflammation and a milder degree of altered matrix deposition (lower panel, **figure A.1**). In these animals, the overall parenchymal architecture appeared well preserved.

The measurement of hydroxyproline concentration was used to assess changes in lung collagen content following bleomycin instillation. The administration of 0.05 U bleomycin induced a 1.5-fold increase in total lung collagen in wild type mice compared to α1-AT overexpressing animals at 30 days (3.57 ± 0.51 vs. 2.4 ± 0.26 mg, $P < 0.05$) (**figure A.2**). In fact, bleomycin instillation did not have an effect on collagen in the α1-AT overexpressor group when compared to its own saline-treated controls.

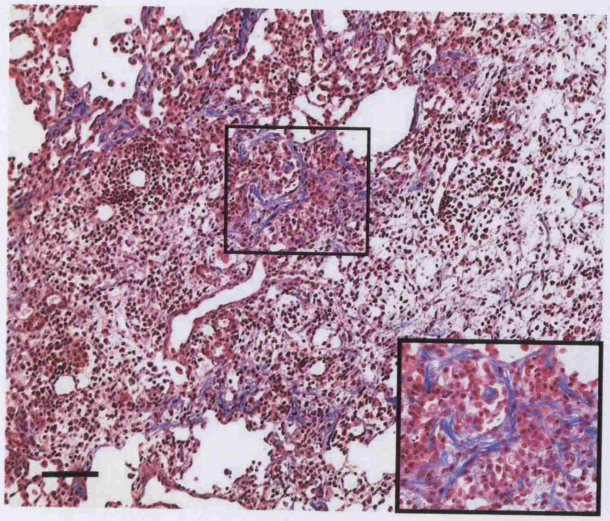

wild type

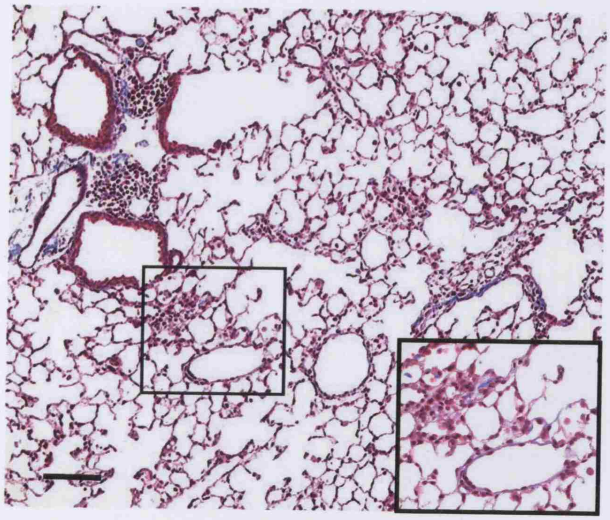

α1-antitrypsin overexpressor

Figure A.1. **Lungs of bleomycin-treated α1-AT overexpressing mice share morphologic similarities to bleomycin-treated $NE^{-/-}$ mice.**

Lungs were harvested from alpha-1-antitrypsin ($\alpha1\text{-}AT^{+/+}$) overexpressing mice (C57BL/6 x CBA progeny backcrossed on to C57BL/6 for at least four generations) 30 days following intratracheal instillation of 0.05 U bleomycin. Extensive fibroproliferative changes were present in the lungs of wild type animals generated on the same genetic background (top panel) in contrast to the minor and isolated changes in lungs from $\alpha1\text{-}AT^{+/+}$ mice (*Bar*, 100 μm).

Masson's trichrome stain

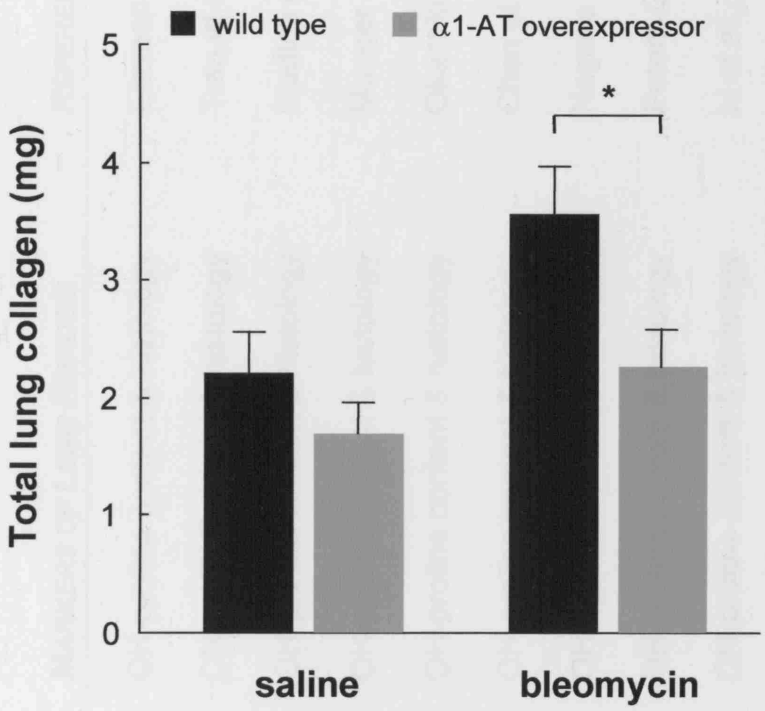

Figure A.2. **Bleomycin-induced changes in lung collagen content in transgenic mice that overexpress human α1-AT.**

Total lung collagen was determined by the measurement of hydroxyproline content 30 days following the instillation of either saline or 0.05 unit bleomycin in wild type and α1-AT overexressing mice. Values are expressed as mean total lung collagen ± SEM (four to six animals per group). * *P < 0.05*

APPENDIX 2 TRANSGENIC STUDIES OF BLEOMYCIN-INDUCED PULMONARY FIBROSIS

LOSS-OF-FUNCTION ('KNOCKOUT') MODELS

MOLECULE	*PHENOTYPE*	*MARKERS OF LUNG FIBROSIS*	*REFERENCE*
PAI-1	decreased fibrosis	OH-proline content & histology	Eitzman et al., 1996
bleomycin RG	decreased fibrosis	OH-proline content & histology	Tran et al., 1997
TGF-α	decreased fibrosis	OH-proline content & histology	Madtes et al., 1999
αVβ6	decreased fibrosis	OH-proline content & histology	Munger et al., 1999
CD28	decreased fibrosis	OH-proline content & histology	Okazaki et al., 2001
interferon-γ	decreased fibrosis	OH-proline content & histology	Chen et al., 2001
cytosolic PA_2	decreased fibrosis	OH-proline content & histology	Nagase et al., 2002
5-lipooxygenase	decreased fibrosis	OH-proline content & histology	Peters-Golden et al., 2002
matrilysin	decreased fibrosis	OH-proline content & histology	Li et al., 2002
L-selectin	decreased fibrosis	OH-proline content & histology	Hamaguchi et al., 2002
ICAM-1	"	"	
L-selectin/ICAM-1 dual knockout	"	"	

LOSS-OF-FUNCTION ('KNOCKOUT') MODELS *(continued)*

MOLECULE	*PHENOTYPE*	*MARKERS OF LUNG FIBROSIS*	*REFERENCE*
SMAD3	decreased fibrosis	OH-proline content & histology	Zhao et al., 2002
CCR2	decreased fibrosis	OH-proline content & histology	Gharaee-Kermani et al., 2003
IL-4	decreased fibrosis	OH-proline content & histology	Huaux et al., 2004
IL-13	decreased fibrosis	OH-proline content & histology	Liu et al., 2004
IL-4 / IL-13 dual	"	"	
p47phox	decreased fibrosis	OH-proline content & histology	Manoury et al., 2005
PAR-1	decreased fibrosis	OH-proline content & histology	Howell et al., 2005
uPA	equivalent to WT	OH-proline content & histology	Swaisgood et al., 2000
uPA receptor	"	"	
tPA	"	"	
plasminogen	"	"	
fibrinogen	equivalent to WT	OH-proline content & histology	Poplis et al., 2000
FAS / FAS-L	equivalent to WT	OH-proline content & histology	Aoshiba et al., 2000
SPARC	equivalent to WT	OH-proline content & histology	Savani et al., 2000

LOSS-OF-FUNCTION ('KNOCKOUT') MODELS *(continued)*

MOLECULE	*PHENOTYPE*	*MARKERS OF LUNG FIBROSIS*	*REFERENCE*
COX-2	equivalent to WT	OH-proline content & histology	Hodges et al., 2004
osteopontin	equivalent to WT	OH-proline content & histology	Berman et al., 2004
EC-SOD	equivalent to WT	OH-proline content & histology	Fattman et al., 2003
GM-CSF	enhanced fibrosis	OH-proline content & histology	Moore et al., 2000
NRF2	enhanced fibrosis	OH-proline content & histology	Cho et al., 2004
IP-10/CXCL10	enhanced fibrosis	OH-proline content & histology	Tager et al., 2004

GAIN-OF-FUNCTION (TRANSGENIC / OVEREXPRESSION) MODELS

MOLECULE	*PHENOTYPE*	*ASSESSMENT OF FIBROSIS*	*REFERENCE*
SMAD7	decreased fibrosis	OH-proline content & collagen mRNA	Nakao et al., 1999
uPA	decreased fibrosis	OH-proline content & histology	Sisson et al., 1999
IL-10	decreased fibrosis	OH-proline content only	Arai et al., 1999

GAIN-OF-FUNCTION (TRANSGENIC / OVEREXPRESSION) MODELS *(continued)*

MOLECULE	*PHENOTYPE*	*ASSESSMENT OF FIBROSIS*	*REFERENCE*
PDGF receptor	decreased fibrosis	OH-proline content & histology	Yoshida et al., 1999
E-selectin	decreased fibrosis	OH-proline content & histology	Azuma et al., 2000
decorin	decreased fibrosis	OH-proline content & histology	Kolb et al., 2001
IL-4	decreased fibrosis	OH-proline content & histology	Izbicki et al., 2002b
TGF-β	enhanced fibrosis	OH-proline content & histology	Sime et al., 1997
TNF-α	enhanced fibrosis	OH-proline content & histology	Sime et al., 1998
endothelin-1	age-related fibrosis	OH-proline content & histology	Hocher et al., 2000
IL-1β	enhanced fibrosis	OH-proline content & histology	Kolb et al., 2001
p53 dominant negative (human)	enhanced fibrosis	OH-proline content & histology	Ghosh et al., 2002
TGF-α (inducible)	enhanced fibrosis	OH-proline content & histology	Hardie et al., 2004
IGF-1A (inducible)	enhanced fibrosis	OH-proline content & histology	Frankel et al., 2004

BIBLIOGRAPHY

Abdelouahed M, Ludlow A, Brunner G and Lawler J. Activation of platelet transforming growth factor-beta1 in the absence of thrombospondin-1. *J Biol Chem* 2000; **275**: 17933-17936.

Abe M, Harpel JG, Metz CN, Nunes I, Loskutoff DJ and Rifkin DB. An assay for transforming growth factor-β using cells transfected with a plasminogen activator inhibitor-1 promoter-luciferase construct. *Analyt Biochem* 1994; **216**: 276-84.

Abe M, Oda N and Sato Y. Cell-associated activation of latent transforming growth factor-β by calpain. *J Cell Physiol* 1998; **174**: 186-193.

Adamson IYR and Prieditis HL. Response of mouse lung to carbon deposition during injury and repair. *Environ Health Perspect* 1995; **103**: 72-76.

Adler KB, Callahan LM and Evans JN. Cellular alterations in the alveolar wall in bleomycin-induced pulmonary fibrosis in rats. An ultrastructural morphometric study. *Am Rev Respir Dis* 1986; **133**: 1043-1048.

Albertine KH. Lung injury and neutrophil density during air embolization in sheep after leukocyte depletion with nitrogen mustard. *Am Rev Respir Dis* 1988; **138**: 1444-1453.

Ali R, Perfumo S, Rocca CD, Amicone L, Pozzi L, McCullagh P, Millward-Sadler H, Edwards Y, Povey S and Tripodi M. Evaluation of a transgenic mouse model for alpha1-antitrypsin (AAT)-related disease. *Ann Hum Genet* 1994; **58**: 305-320.

Allen DH and Tracy PB. Human coagulation factor V is activated to the functional cofactor by elastase and cathepsin G expressed at the monocyte surface. *J Biol Chem* 1995; **270**: 1408-1415.

Allport JR, Lim YC, Shipley JM, Senior RM, Shapiro SD, Matsuyoshi N, Vestweber D and Luscinskas FW. Neutrophils from MMP-9 or neutrophil elastase-deficient mice show no defect in transendothelial migration under flow in vitro. *J Leukoc Biol* 2002; **71**: 821-828.

Ambrosini V, Cancellieri A, Chilosi M, Zompatori M, Trisolini R, Saragoni L and Poletti V. Acute exacerbation of idiopathic pulmonary fibrosis: report of a aseries. *Eur Respir J* 2003; **22**: 821-826.

American Thoracic Society. Guidelines for the approach to the patient with severe hereditary alpha-1-antitrypsin deficiency. *Am Rev Respir Dis* 1989; **140**: 1494-1497.

American Thoracic Society (ATS) and European Respiratory Society (ERS) Joint Statement. Idiopathic pulmonary fibrosis: diagnosis and treatment: International Consensus Statement. *Am J Respir Crit Care Med* 2000; **161**: 646-664.

American Thoracic Society (ATS) and European Respiratory Society (ERS) Joint Statement. International Multidisciplinary Consensus Classification of the Idiopathic Interstitial Pneumonias. *Am J Respir Crit Care Med* 2002; **165**: 277-304.

Amitani R, Wilson R, Rutman A, Read R, Ward C, Burnett D, Stockley RA and Cole PJ. Effect of neutrophil elastase and *Pseudomonas aeruginosa* proteinases on human respiratory epithelium. *Am J Respir Cell Mol Biol* 1991; **4**: 26-32.

Andres JL, Stanly K, Cheifetz S and Massague J. Membrane-anchored and soluble forms of betaglycan, a polymorphic proteoglycans that binds transforming growth factor-β. *J Cell Biol* 1989; **109**: 3137-3145.

Annes JP, Rifkin DB and Munger JS. The integrin alphaVbeta6 binds and activates latent TGF-beta3. *FEBS Lett* 2002; **511**: 65-68.

Anscher MS, Peters WP, Reisenbichler H, Petros WP and Jirtle RL. Transforming growth factor-β as a predictor of liver and lung fibrosis after autologous bone marrow transplantation for advanced breast cancer. *N Engl J Med* 1993; **328**: 1592-1598.

Antonelli-Orlidge A, Saunders KB, Smith SR and D'Amore PA. An activated form of transforming growth factor-β is produced by cocultures of endothelial cells and pericytes. *Proc Natl Acad Sci USA* 1989; **86**: 4544-4548.

Aoshiba K, Yasui S, Tamaoki J and Nagai A. The Fas/Fas-ligand system is not required for bleomycin-induced pulmonary fibrosis in mice. *Am J Respir Crit Care Med* 2000; **162**: 695-700.

Aprikyan AA, Dale DC. Mutations in the neutrophil elastase gene in cyclic and congenital neutropenia. *Curr Opin Immunol* 2001; **5**: 535-538.

Arai T, Abe K, Matsuoka H, Yoshida M, Goya S, Kida H, Nishino K, Osaki T, Tachibana I, Kaneda Y and Hayashi S. Introduction of the interleukin-10 gene into mice inhibited bleomycin-induced lung injury in vivo. *Am J Physiol (Lung Cell Mol Physiol)* 2000; **278**: L915-L922.

Archer SJ, Bax A, Roberts AB, Sporn MB, Ogawa Y, Piez KA, Weatherbee JA, Tsang ML, Lucas R, Zheng BL, et al. Transforming growth factor beta 1: NMR signal assignments of the recombinant protein expressed and isotopically enriched using Chinese hamster ovary cells. *Biochemistry* 1993; **32**: 1152-1163.

Ariel A, Yavin EJ, Hershkoviz R, Franitza S, Avron A, Cahalon L, Fridkin M and Lider O. IL-2 induces T-cell adherence to extracellular matrix: inhibition of adherence and migration by IL-2 peptides generated by leukocyte elastase. *J Immunol* 1998; **161**: 2465-2472.

Arsalane K, Dubois CM, Muanza T, Begin R, Bondreau F, Asselin C and Cantin AM. Transforming growth factor-beta 1 is a potent inhibitor of glutathione synthesis in lung epithelial cell line A549: transcriptional effect on the GSH rate-limiting enzyme gamma-glutamylcysteine synthetase. *Am J Respir Cell Mol Biol* 1997; **17**: 599-607.

Assoian RK, Komoriya A, Meyers CA, Miller DM and Sporn MB. Transforming growth factor-beta in human platelets. Identification of a major storage site, purification and characterization. *J Biol Chem* 1983; **258**: 7155-7160.

Attisano L and Wrana JL. Signal transduction by the TGF-β superfamily. Science 2002; 296: 1646-1647.

Atlas D and Berger A. On the specificity of elastase. Hydrolysis of peptide p-nitrobenzyl esters. *Biochemistry* 1972; **11**: 4719-4123.

Aubert JD, Dadal BI, Bai TR, Roberts CR, Hayashi S and Hogg JC. Transforming growth factor β1 gene expression in human airways. *Thorax* 1994; **49**: 225-232.

Awad MR, El-Gamel A, Hasleton P, Turner DM, Sinnot PJ and Hutchinson IV. Genotypic variation in the transforming growth factor-β1 gene. *Transplantation* 1998; 66: 1014-1020.

Azuma A, Furuta T, Enomoto T, Kashimoto Y, Uematsu K, Nukariya N, Murata A and Kudoh S. Protective effect of erythromycin on experimental bleomycin-induced acute lung injury in rate. *Thorax* 1998; **53**: 186-189.

Azuma A, Takahaski S, Nose M, Araki K, Araki M, Takahashi T, Hirose M, Kawashima H, Miyasaka M and Kudoh S. Role of E-selectin in bleomycin-induced lung fibrosis in mice. *Thorax* 2000; **55**: 147-152.

Azuma A, Li YJ, Abe S, Usuki J, Matsuda K, Henmi S, Miyauchi Y, Ueda K, Izawa A, Sone S, Hashimoto S and Kudoh S. Interferon-β inhibits bleomycin-induced lung fibrosis by decreasing transforming growth factor-beta and thrombospondin. *Am J Respir Cell Mol Biol* 2005; **32**: 93-98.

Baggiolini M and Dewald B. Exocytosis by neutrophils: regulation of leukocyte function. *New York: Plenum Press*; 1984: 221-246.

BAL Cooperative Group Steering Committee. Bronchoalveolar lavage constituents in healthy individuals, idiopathic pulmonary fibrosis and selected comparison groups. *Am Rev Respir Dis* 1990; **141**: 169-202.

Balharry D, Oreffo V and Richards R. Use of toxicogenics for identifying genetic markers of pulmonary oedema. *Toxicol Appl Pharmacol* 2005; **204**: 101-108.

Bank U, Kupper B, Reinhold D, Hoffman T and Ansorge S. Evidence for crucial role of neutrophil-derived serine proteases in the inactivation of interleukin-6 at sites of inflammation. *FEBS Lett* 1999; **461**: 235-240.

Bank U and Ansorge S. More than destructive: neutrophil-derived serine proteases in cytokine bioactivity control. *J Leukoc Biol* 2001; **69**: 201-210.

Barcellos-Hoff MH, Derynck R, Tsang MLS and Weatherbee JA. Transforming growth factor-β activation in irradiated murine mammary gland. *J Clin Invest* 1994; **93**: 892-899.

Barcellos-Hoff MH, Ehrhart EJ, Kalia M, Jirtle R, Flanders K and Tsang MLS. Immunohistochemical detection of active transforming growth fcaor-β in situ using engineered tissue. *Am J Path* 1995; **147**: 1228-1237.

Barth RK, Hanchett LA and Baecher-Allen CM. Mapping susceptibility genes for the induction of pulmonary fibrosis in mice. *Chest* 2002; **121**: 21s.

Basset F, Ferrans VJ, Soler P, Takemura T, Fukuda Y and Crystal RG. Intraluminal fibrosis in interstitial lung disorders. *Am J Pathol* 1986; **122**: 443-461.

Bateman ED, Turner-Warwick M, Haslam PL and Adelmann-Grill BC. Cryptogenic fibrosing alveolitis: prediction of fibrogenic activity from Immunohistochemical studies of collagen types in lung biopsy specimens. *Thorax* 1983: **38**: 93-101.

Bedard M, McClure CD, Schiller NL, Francoeur C, Cantin A and Denis M. Release of interleukin-8, interleukin-6 and colony stimulating factors by upper airway epithelial cells: implications for cystic fibrosis. *Am J Respir Cell Mol Biol* 1993; **9**: 455-462.

Beers MF, Solarin KO, Guttentag SH, Rosenbloom J, Kormilli A, Gonzales LW and Ballard PL. TGF-β1 inhibits surfactant component expression and epithelial cell maturation in cultured human fetal lung. *Am J Physiol (Lung Cell Mol Physiol)* 1998; **275**: L950-L960.

Behzad A, Chu F and Walker DC. Fibroblasts are in a position to provide directional information to migrating neutrophils during pneumonia in rabbit lungs. *Microvas Res* 1996; **51**: 303-316.

Belaaouaj AA, Walsh BC, Jenkins NA, Copeland NG and Shapiro SD. Characterization of the mouse neutrophil elastase gene and localization to Chromosome 10. *Mamm Genome* 1997; **8**: 5-8.

Belaaouaj AA, McCarthy R, Baumann M, Gao Z, Ley TJ, Abraham SN and Shapiro SD. Mice lacking neutrophil elastase reveal impaired host defense against gram negative bacterial sepsis. *Nature Med* 1998; **4**: 615-618.

Belaaouaj AA, Kim KS and Shapiro SD. Degradation of outer membrane protein A in *Escherichia coli* killing by neutrophil elastase. *Science* 2000; **289**: 1185-1187.

Benezra M, Vlodavsky I, Ishai-Michaeli R, Neufeld G, Bar-Shavit R. Thrombin-induced release of active basic fibroblast growth factor-heparan sulfate complexes from subendothelial extracellular matrix. *Blood* 1993; 81: 3324-3331.

Berman JS, Serlin D, Li X, Whitley G, Hayes J, Rishikof DC, Ricupero DA, Liaw L, Goetschkes M and O'Regan AW. Altered bleomycin-induced lung fibrosis in osteopontin-deficient mice. *Am J Physiol (Lung Cell Mol Physiol)* 2004; **286**: L1311-L1318.

Bernstein PR, Edwards PD and Williams JC. In: Ellis GP and Luscombe DK, eds. Inhibitors of human leukocyte elastase. London: Elsevier Science B.V., 1994; **31**: 59-121.

Betsuyaku T, Fukuda Y, Parks WC, Shipley JM and Senior RM. Gelatinase B is required for alveolar bronchiolization after intratracheal bleomycin. *Am J Pathol* 2000; **157**: 525-535.

Bieth JG. Elastases: catalytic and biological properties. In: Mecham R., ed. Regulation of Matrix Accumulation. New York: Academic Press; 1986: 217-230.

Bieth JG. Leukocyte elastase. In: Barrett AJ, Rawlings ND and Woessner JF, eds. Handbook of Proteolytic Enzymes. London: Academic Press; 1998: 54-60.

Bitterman PB, Rennard SI, Keogh BA, Wewers MD, Adelberg S and Crystal RG. Familial idiopathic pulmonary fibrosis. Evidence of lung inflammation in unaffected family members. *N Engl J Med* 1986; **314**: 1343-1347.

Bjoraker JA, Ryu JH, Edwin MK, Myers JL, Tazelaar HD, Schroeder DR and Offord KP. Prognostic significance of histopathologic subsets in idiopathic pulmonary fibrosis. *Am J Respir Crit Care Med* 1998; **157**: 199-203.

Black R, Kronheim S, Sleath P, Greenstreet T, Virca GD, March C and Kupper T. The proteolytic activation of interleukin-1 beta. *Agents Actions (Suppl)* 1991; **35**: 85-89.

Bless NM, Smith D, Charlton J, Czermak BJ, Schmal H, Friedl HP and Ward PA. Protective effects of an aptamer inhibitor of neutrophil elastase in lung inflammatory injury. *Curr Biol* 1997; **7**: 877-880.

Blobe GC, Schiemann WP and Lodish HF. Mechanisms of disease: role of transforming growth factor-β in human disease. *N Engl J Med* 2000; **342**: 1350-1358.

Bode W, Meyer Jr E and Powers JC. Human leukocyte and porcine pancreatic elastase: X-ray crystal structures, mechanism, substrate specificity and mechanism-based inhibitors. *Biochemistry* 1989; **28**: 1951-1963.

Bonewald LF, Wakefield L, Oreffo RO, Escobedo A, Twardzik DR and Mundy GR. Latent forms of transforming growth factor-β derived from bone cultures: identification of a naturally occurring 100-kDa complex with similarity to recombinant latent TGF-β. *Mol Endocr* 1991; **5**: 741-751.

Bonnefoy A and Legrand C. Proteolysis of subendothelial adhesive glycoproteins (fibronectin, thrombospondin and von Willebrand factor) by plasmin, leukocyte cathepsin G and neutrophil elastase. *Thromb Res* 2000; **140**: 323-332.

Bonner JC, Lindroos PM, Rice AB, Moomaw CR and Morgan DL. Induction of PDGF receptor-alpha in rat myofibroblasts during pulmonary fibrogenesis in vivo. *Am J Physiol (Lung Cell Mol Physiol)* 1998; **274**: L72-80.

Border WA and Noble NA. Transforming growth factor-beta in tissue fibrosis. *N Engl J Med* 1994; **331**: 1286-1292.

Bornstein P. Thrombospondins – structure and regulation of expression. *FASEB J* 1992; **6**: 3290-3299.

Bornstein P and Sage H. Structurally distinct collagen types. *Ann Rev Biochem* 1980; **49**: 957-1003.

Borok Z, Trapnell BC and Crystal RG. Neutrophils and the pathogenesis of idiopathic pulmonary fibrosis. In: Pozzi E, ed. Neutrophils, lymphocytes and lung. Milan: Masson, 1990: 11-121.

Borzi RM, Grigolo B, Meliconi R, Fasano L, Sturani C, Fabbri M, Porstmann T and Fancchini A. Elevated serum superoxide dismutase levels correlate with disease severity and neutrophil degranulation in idiopathic pulmonary fibrosis. *Clin Sci Lond* 1993; **85**: 353-359.

Borzone G, Moreno R, Urrea R, Meneses M, Oyarzun M and Lisboa C. Bleomycin-induced chronic lung damage does not resemble human idiopathic pulmonary fibrosis. *Am J Respir Crit Care Med* 2001; **163**: 1648-1653.

Bowden DH. Unravelling pulmonary fibrosis: the bleomycin model. *Lab Invest* 1984; **50**: 487-488.

Bradley KH, McConnell SK and Crystal RG. Lung collagen composition and synthesis.Characterization and changes with age. *J Biol Chem* 1974; **249**: 2674-2683.

Broekelmann TJ, Limper AH, Colby TV and McDonald JA. Transforming growth factor beta 1 is present at sites of extracellular matrix gene expression in human pulmonary fibrosis. *Proc Natl Acad Sci USA* 1991; **88**: 6642-6646.

Brown PD, Wakefield LM, Levinson AD and Sporn MB. Physicochemical activation of recombinant transforming growth factor-betas 1, 2 and 3. *Growth Factors* 1990; **3**: 35-43.

Bruch M and Bieth JG. Influence of elastin on the inhibition of leukocyte elastase by alpha-1-proteinase inhibitor and bronchial inhibitor. Potent inhibitor of elastin-bound elastase by bronchial inhibitor. *Biochem J* 1986; **238**: 269-273.

Buczek-Thomas JA and Nugent MA. Elastase-mediated release of heparan sulfate proteoglycans from pulmonary fibroblast cultures. *J Biol Chem* 1999; **35**: 25167-25172.

Buczek-Thomas JA, Lucey EC, Stone PJ, Chu CL, Rich CB, Carreras I, Goldstein RH, Foster JA and Nugent MA. Elastase mediates the release of growth factors from lung in vivo. *Am J Respir Cell Mol Biol* 2004; **31**: 344-350.

Bugge, T.H., M.J. Flick, C.C. Daugherty, and J.L. Degen. Plasminogen deficiency causes severe thrombosis but is compatible with development and reproduction. *Genes Dev* 1999: **9**: 794–807.

Bunnell E and Pacht ER. Oxidised glutathione is increased in the alveolar fluid of patients with the adult respiratory distress syndrome. *Am Rev Respir Dis* 1993; **148**: 1174-1178.

BUILD-1: Bosentan Use in Interstitial Lung Disease study; www.actelion.com

Burger RM, Peisach J and Horwitz SB. Activated bleomycin. A transient complex of drug, iron and oxygen that degrades DNA. *J Biol Chem* 1981; **256**: 11232-1644.

Burkhardt A. Alveolitis and collapse in the pathogenesis of pulmonary fibrosis. *Am Rev Respir Dis* 1989; **140**: 513-524.

Burns AR, Smith CW and Walker DC. Unique structural features that infuence neutrophil emigration into the lung. *Physiol Rev* 2003; **83**: 309-336.

Busk M, Pytela R and Sheppard D. Characterization of the integrin alpha v beta 6 as a fibronectin-binding protein. J Biol Chem 1992; 267: 5790-5796.

Cai T-Q and Wright SD. Human leukocyte elastase is an endogenous ligand for the integrin CR3 (CD11b/18, Mac-1, $\alpha_M\beta_2$) and modulates polymorphonuclear leukocyte adhesion. *J Exp Med* 1996; **184**: 1213-1223.

Cailes JB, O'Connor C, Pantelidis P, Southcott AM, Fitzgerald MX, Black CM and du Bois RM. Neutrophil activation in fibrosing alveolitis: a comparison of lone cryptogenic fibrosing alveolitis and systemic sclerosis. *Eur Respir J* 1996; **9**: 992-999.

Cambien F, Ricard S, Troesch A, Mallet C, Generenaz L, Evans A, Arvelier D, Luc G, Ruidavets JB and Poirer O. Polymorphisms of transforming growth factor-β1 gene in relation to myocardial infarction and blood pressure: the Etude Cas-Temoin de l'Infarctus du Myocarde (ECTM) Study. *Hypertension* 1996; **28**: 881-887.

Campa JS, McAnulty RJ and Laurent GJ. Application of high-pressure liquid chromatography to studies of collagen production by isolated cells in culture. *Anal Biochem* 1990; **186**: 257-263.

Campbell EJ and Campbell MA. Pericellular proteolysis by neutrophils in the presence of proteinase inhibitors: effects of substrate opsonization. *J Cell Biol* 1988; **106**: 667-676.

Campbell EJ, Silverman EK and Campbell MA. Elastase and cathepsin G of human monocytes. Quantification response to stimuli and heterogeneity in elastase-mediated proteolytic activity. *J Immunol* 1989; **143**: 2961-2968.

Caniggia I, Han R, Liu J, Wang J, Tanswell AK, Post M. Differential expression of collagen-binding receptors in fetal rat lung cells. *Am J Physiol* 1995; **268 (1 Pt 1)**: L136-L143.

Carden D, Xiao F, Moak C, Willis BH, Robinson-Jackson S and Alexander S. Neutrophil elastase promotes lung microvascular injury and proteolysis of endothelial cadherins. *Am J Physiol* 1998; **275**: H385-392.

Carney DF, Jagels MA, Hugli TE, Sands H and Rubin H. Alpha-1-proteinase inhibitor, anti-chymotrypsin and a recombinant hybrid mutant of anti-chymotrypsin (LEX-032) modulate neutrophil adhesion interactions. *J Leukoc Biol* 1998; **68**: 75-82.

Carre PC, King TE Jr, Mortensen R and Riches DW. Cryptogenic organizing pneumonia: increased expression of interleukin-8 and fibronectin genes by alveolar macrophages. *Am J Respir Cell Mol Biol* 1994; **10**: 100-105.

Cavarra E, Martorana PA, de Santi M, Bartalesi B, Cortese S, Gambelli F and Lungarella G. Neutrophil influx into the lungs of beige mice is followed by elastolytic damage and emphysema. *Am J Respir Cell Mol Biol* 1999; **20**: 264-269.

Cavarra E, Martorana PA, Bartalesi B, Fineschi S, Gambelli F, Lucattelli M, Ortiz L and Lungarella G. Genetic deficiency of alpha1-PI in mice influences lung responses to bleomycin. *Eur Respir J* 2001; **17**: 474-480.

Carvalho CRR, Kairala RA and Schettino GP. Acute respiratory failure after interferon-γ therapy in IPF. Letter. *Am J Respir Crit Care Med* 2004; **169**: 543.

Chambers RC and Laurent GJ. Collagens. In: Crystal RG, West JB, Weibel ER and Barnes PJ. The Lung: Scientific Foundations. 2nd Edition. Philadelphia: Lippincott-Raven 1997: 709-727.

Chapman HA. Disorders of lung matrix remodeling. *J Clin Invest* 2004; **113**: 148-157.

Cheifetz S, Bassols A, Stanley K, Ohta M, Greenberger J and Massague J. Heterodimeric transforming growth factor-β. Biological properties and interaction with three types of cell surface receptors. *J Biol Chem* 1988; **263**: 10783-10789.

Chen ES, Greenlee BM, Wills-Karp M and Moller DR. Attenuation of lung inflammation and fibrosis in interferon-gamma-deficient mice after intratracheal bleomycin. *Am J Respir Cell Mol Biol* 2001; **24**: 545-555.

Chen HC, Lin HC, Liu CY, Wang CH, Hwang T, Huang TT, Lin CH and Kuo HP. Neutrophil elastase induces IL-8 synthesis by lung epithelial cells via the mitogen-activated protein kinase pathway. *J Biomed Sci* 2004; **11**: 49-58.

Chen JJ, Sun Y and Nabel GJ. Regulation of the proinflammatory effects of Fas ligand (CD95L). *Science* 1998; **282**: 1714.

Chen R, Ebner R and Derynck R. Inactivation of the type II receptor reveals two receptor pathways for the diverse TGF-beta activities. *Science* 1993; **260**: 1335-1338.

Chen SJ, Yuan W, Lo S, Trojanowska M and Varga J. Interaction of smad3 with a proximal smad-binding element of the human alpha2(I) procollagen gene promoter required for transcriptional activation by TGF-beta. *J Cell Physiol* 2000; **183**: 381-392.

Chen Y, Ali T, Todorovic V, O'Leary JM, Downing AK and Rifkin DB. Amino acid requirements for formation of the TGF-β latent TGF-β binding protein complexes. *J Mol Biol* 2004; **345**: 175-186.

Cheresh DA. Integrins in thrombosis, wound healing and cancer. *Biochem Soc Trans* 1991; **19**: 835-838

Cho HY, Reddy SP, Yamamoto M and Kleeberger SR. The transcription factor NRF2 protects against pulmonary fibrosis. *FASEB J* 2004; **18**: 1258-1260.

Christensen PJ, Goodman RE, Pastoriza L, Moore B and Toews GB. Induction of lung fibrosis in the mouse by intratracheal instillation of fluorescein isothiocyanate is not T-cell-dependent. *Am J Pathol* 1999; **155**: 1773-1779.

Chu TM and Kawinski E. Plasmin, substilisin-like endoproteases, tissue plasminogen activator, and urokinase plasminogen activator are involved in activation of latent TGF-beta 1 in human seminal plasma. *Biochem Biophys Res Commu.* 1998; **253**: 128-134.

Clark JG and Kuhn III C. Bleomycin-induced pulmonary fibrosis in hamsters: effect of neutrophil depletion on lung collagen synthesis. *Am Rev Respir Dis* 1982; **126**: 737-739.

Clark JG, Milberg JA, Steinberg KP and Hudson LD. Type III procollagen peptide in adult respiratory distress syndrome. Association of increased peptide levels in bronchoalveolar lavage with increased risk of death. *Ann Intern Med* 1994; **122**: 17-23.

Coker RK, Laurent GJ, Shahzeidi S, Lympany PA, du Bois RM, Jeffery PK and McAnulty RJ. Transforming growth factors-β1, -β2 and -β3 stimulate fibroblast procollagen production *in vitro* but are differentially expressed during bleomycin-induced pulmonary fibrosis. *Am J Pathol* 1997; **150**: 981-991.

Coker RK, Laurent GJ, Jeffery PK, du Bois RM, Black CM and McAnulty RJ. Localisation of transforming growth factor-β1 and β2 mRNA transcripts in normal and fibrotic human lung. *Thorax* 2001; **56**: 548-556.

Cooper JA Jr. Pulmonary fibrosis: pathways are slowly coming into light. *Am J Respir Cell Mol Biol* 2000; **22**: 520-523.

Corrin B, Butcher D, McAnulty RJ and Laurent GJ. Immunohistochemical localization of transforming growth factor-beta 1 in the lungs of patients with systemic sclerosis, cryptogenic fibrosing alveolitis and other lung disorders. *Histopathology* 1994; **24**: 145-150.

Cosgrove GP, Brown KK, Schiemann WP, Serls AE, Parr JE, Geraci MW, Schwarz MI, Cool CD and Worthen GS. Pigment epithelium-derived factor in idiopathic pulmonary fibrosis: a role in aberrant angiogenesis. *Am J Respir Crit Care Med* 2004; **170**: 242-251.

Coultas DB, Zumwalt RE, Black WC and Sobonya RE. The epidemiology of interstitial lung diseases. *Am J Respir Crit Care Med* 1994; **150**: 967-972.

Crawford SE, Stellmach V, Murphy-Ullrich JE, Ribeiro SMF, Lawler J, Hynes RO, Boivin GP and Bouck N. Thrombospondin-1 is a major activator of TGF-β1 in vivo. *Cell* 1998; **93**: 1159-1170.

Crystal RG. Lung collagen: definition, diversity and development. *Federation Proc* 1974; **33**: 2248-2255.

Crystal RG, Gadek JE, Ferrans VJ, Fulmer JD, Line BR and Hunninghake TW. Interstitial lung disease. Current concepts of pathogenesis, staging and therapy. *Am J Med* 1981; **70**: 542-568.

Crystal RG, Bitterman PB, Mossman B, Schwarz MI, Sheppard D, Almasy L, Chapman HA, Friedman SL, King Jr. TE, Leinwand LA, Liotta L, Martin GR, Schwartz DA, Schultz GS, Wagner CR and Musson RA. Future research directions in idiopathic pulmonary fibrosis. Summary of a National Heart, Lung and Blood Institute working group. *Am J Respir Crit Care Med* 2002; **166**: 236-246.

Cui W, Fowlis DJ, Cousins FM, Duffie E, Bryson S, Balmain A, Akhurst RJ. Concerted action of TGF-β1 and its type II receptor in control of epidermal homeostasis in transgenic mice. *Genes Dev* 1995; **9**: 945-955.

Cutillo AG, Chan PH, Ailion DC,Watanabe S, Rao NV, Hansen CB, Albertine KH, Laicher G and Durney CH. Characterization of bleomycin injury by nuclear magnetic resonance: correlation between NMR relaxation times and lung water collagen content. *Magn Reson Med* 2002; **47**: 246-256.

Cutroneo KR. How is type I procollagen synthesis regulated at the gene level during tissue fibrosis. *J Cell Biochem* 2003; **90**: 1-5.

D'Amours D, Desnoyers S, D'Silva I and Poirier GG. Poly (ADP-ribosyl)ation reactions in the regulation of nuclear functions. *Biochem J* 1999; **342**: 249-268.

Dallal MM and Chang SW. Evans blue dye in the assessment of permeability-surface area product in perfused rat lungs. *J Appl Physiol* 1994; **77**: 1030-1035.

Dallas SL, Park-Snyder S, Miyazono K, Twardzik D, Mundy GR and Bonewald LF. Characterization and autoregulation of latent transforming growth factor-β (TGF-β) complexes in osteoblast-like cell lines. *J Biol Chem* 1994; **269**: 6815-6822.

Dallas SL, Rosser JL, Mundy GR and Bonewald LF. Proteolysis of latent transforming growth factor-beta (TGF-β)-binding protein-1 by osteoclasts. *J Biol Chem* 2002; **277**: 21352-21360.

Das SK and Fanburg DL. TGF-β1 produces a 'pro-oxidant' effect on bovine pulmonary artery endothelial cells in culture. *Am J Physiol (Lung Cell Mol Physiol)* 1991; **262**: L249-L254.

De Crescenzo G, Grothe S, Zwaagstra J, Tsang M and O'Connor-McCourt MD. Real-time monitoring of the interactions of transforming growth factor-β isoforms with latency-associated protein and the ectodomains of the TGF-β type I and II receptors reveals different kinetic models and stoichiometries of binding. *J Biol Chem* 2001; **276**: 29632-29643.

Demedts M, Wells AU, Anto JM, Costabel U, Hubbard R, Cullinan P, Slabbynck H, Rizzato G, Poletti V, Verbeken EK, Thomeer MJ, Kokkarinen J, Dalphin JC and Newman Taylor A. Interstitial lung diseases: an epidemiological overview. *Eur Respir J* 2001; **18** (suppl 32): 2s-16s.

Dennis PA and Rifkin DB. Cellular activation of latent transforming growth factor-β requires binding to the cation-dependnet mannose-6-phosphate/insulin-like growth factor type II receptor. *Proc Natl Acad Sci USA* 1991; **88**: 580-584.

Derynck R, Zhang Y and Feng X-H. Smads: transcriptional activators of TGF-β responses. *Cell* 1998; **95**: 737-740.

Desmouliere A, Geinoz A, Gabbiani F and Gabbiani G. Transforming growth factor-β1 induces α-smooth actin expression in granulation tissue myofibroblasts and in quiescent and growing cultured fibroblasts. *J Cell Biol* 1993; **122**: 103-111.

Dhainaut JF, Charpentier J and Chiche JD. Transforming growth factor-beta: a mediator of cell regulation in acute respiratory distress syndrome. *Crit Care Med* 2003; **31** (4 Suppl): S258-S264.

Doerschuk CM, Winn RK, Coxson HO and Harlan JM. CD18-dependent and -independent mechanisms of neutrophil adherence in the pulmonary and systemic microvasculature of rabbits. *J Immunol* 1990; **114**: 2327-2333.

Doerschuk CM, Tasaka S and Wang Q. CD11/CD18-dependent and -independent neutrophil emigration in the lungs. *Am J Respir Cell Mol Biol* 2000; **23**: 133-136.

Donnelly SC, MacGregor I, Zamani A, et al., Plasma elastase levels and the development of the adult respiratory distress syndrome. *Am J Respir Crit Care Med* 1995; **151**: 1428-1433.

Downey GP, Dong Q, Kruger J, Dedhar S and Cherapanov V. Regulation of neutrophil activation in acute lung injury. *Chest* 1999; **116**: 46S-54S.

Dubois CM, Laprise MH, Blanchette F, Gentry LE and Leduc R. Processing transforming growth factor β1 precursor by human furin convertase. *J Biol Chem* 1995; **270**: 10618-10624.

Duncan MR, Frazier KS, Abramson S, Williams S, Klapper H, Huang X and Grotendorst GR. Connective tissue growth factor mediates transforming growth factor beta-induced collagen synthesis: down-regulation by cAMP. *FASEB J* 1999; **13**: 1774-1786.

Dunsmore SE and Rannels DE. Extracellular matrix biology in the lung. *Am J Physiol (Lung Cell Mol Physiol)* 1996; **270**: L3-27.

Eckle I, Setz R, Egbring R, Kolb G and Havemann K Protein C degradation in vitro by neutrophil elastase. *Biol Chem Hoppe-Seyler* 1991; **372**: 1007-1013.

Edwards CA and O'Brien WD Jr. Modified assay for determination of hydroxyproline in a tissue hydrolyzate. *Clin Chim Acta* 1980; **104**: 161-167.

Edwards PD and Bernstein PR. Synthetic inhibitors of neutrophil elastase. *Med Res Rev* 1994; **14**: 127-194.

Eitzman DT, McCoy RD, Zheng X, Fay WP, Shen T, Ginsburg D and Simon RH. Bleomycin-induced pulmonary fibrosis in transgenic mice that either lack or overexpress the murine plasminogen activator inhibitor-1 gene. *J Clin Invest* 1996; **97**: 232-237.

Ekimoto H, Takada K, Ohnuki T, Takahashi K, Matsuda A, Takita T and Umezawa H. Different sensitivity to bleomycin-induced pulmonary fibrosis among various strains of mice. *J Clin Biochem Nutr* 1987; **2**: 25-31.

El-Gamel A, Awad MR, Hasleton PS, Yonan NA, Hutchinson JA, Campbell CS, Rahman AH, Deiraniya AK, Sinnot PJ and Hutchinson IV. Transforming growth factor-β (TGF-β1) genotype and lung allograft fibrosis. *J Heart Lung Transplant* 1999; 18: 517-523.

Entzian P, Zahringer U, Schlaak M, Gerlach C and Zabel P. Comparative study on effects of pentoxifylline, prednisolone and colchicine in experimental alveolitis. *Int J Immunopharmacol* 1998; **20**: 723-735.

Evans TW, Rogers DF, Aursudkij B, Chung KF and Barnes PJ. Inflammatory mediators involved in antigen-induced airway microvascular leakage in guinea pigs. *Am Rev Respir Dis* 1988; **138**: 395-399.

Fattman CL, Chnag LY, Termin TA, Petersen L, Enghild JJ and Oury TD. Enhanced bleomycin-induced pulmonary damage in mice lacking extracellular superoxide dismutase. *Free Radic Biol Med* 2003; **35**: 763-771.

Filderman AE and Lazo JS. Murine strain differences in pulmonary bleomycin metabolism. *Biochem Pharmacol* 1991; **42**: 195-8.

Flanders KC, Sullivan CD, Fujii M, Sowers A, Anzano MA, Arabshahi A, Major C, Deng C, Russo A, Mitchell JB and Roberts AB. Mice lacking Smad3 are protected against cutaneous injury induced by ionising radiation. *Am J Pathol* 2002; **160**: 1057-1068.

Flaumenhaft R, Abe M, Mignatti P and Rifkin DB. Basic fibroblast growth factor-induced activation of latent TGF-β in endothelial cells: regulation of plasminogen activator activity. *J Cell Biol* 1992; **118**: 901-909.

Fleischmann RW, Baber JR, Thompson GR, Schaeppi UH, Illievsky VR, Coonney DA and Davis RD. Bleomycin-induced interstitial pneumonia in dogs. *Thorax* 1971; **26**: 675-682.

Fletcher DS, Osinga DG, Hand KM, Dellea PS, Ashe BM, Mumford RA, Davies P, Hagmann W, Finke PE, Doherty JB. A comparison of alpha 1-proteinase inhibitor methoxysuccinyl-Ala-Ala-Pro-Val-chloromethylketone and specific beta-lactam inhibitors in an acute model of human polymorphonuclear leukocyte elastase-induced lung hemorrhage in the hamster. *Am Rev Respir Dis* 1990; **141**: 672-677.

Frank J, Roux J, Kawakatsu H, Su G, Dagenais A, Berthiaume Y, Howard M, Canessa CM, Fang X, Sheppard D, Matthay MA and Pittet JF. Transforming growth factor-beta1 decreases expression of the epithelial sodium channel alphaENaC and alveolar epithelial vectorial sodium and fluid transport via an ERK1/2-dependent mechanism. *J Biol Chem* 2003; **278**: 43939-43950.

Frankel SK, Moats-Staats BM, Cool CD, Wynes MW, Stiles AD and Riches DW. Human insulin-like growth factor-IA expression in transgenic mice promotes adenomatous hyperplasia but not pulmonary fibrosis. *Am J Physiol (Lung Cell Mol Physiol)* 2005; **288**: L805-L812.

Franko AJ, Sharplin J, Ghahary A and Barcellos-Hoff MH. Immunohistochemical localization of transforming growth factor-β and tumor necrosis factor-α in the lungs of fibrosis-prone and "non-fibrosing" mice during the latent period and early phase after radiation. *Radiat Res* 1997; **147**: 245-256.

Freitas E and Costa M. Epidemiology of sarcoidosis: outlook. In: Grassi C, Rizzato J and Pozzi E, eds. Sarcoidosis and other granulomatous disorders. Amsterdam: Elsevier Science Publishers, 1988: 329-337.

Freudenstein-Dan A, Gold D, Fishelson Z. Killing of schistosomes by elastase and hydrogen peroxide: implications for leukocyte-mediated schistosome killing. *J Parasitol* 2003; **6**: 1129-1135.

Fuchimukai T, Fujiwara T, Takahashi A and Enhorning G. Artificial pulmonary surfactant inhibited by proteins. *J Appl Physiol* 1987; **62**: 429-437.

Fukuda Y, Ishizaki M, Masuda Y, Kimura G, Kawanami O and Masugi Y. The role of intra-alveolar fibrosis in the process of pulmonary structural remodeling in patients with diffuse alveolar damage. *Am J Pathol* 1987; 126: 171-182.

Gadher SJ, Eyre DR, Duance VC, Wotton SF, Heck LW, Schmid TM and Woolley DE. Susceptibility of cartilage collagens type II, IX, X and XI to human synovial collagenase and neutrophil elastase. *Eur J Biochem* 1988; **175**: 1-7.

Gaidarova S and Jimenez SA. Inhibition of basal and transforming growth factor-beta-induced stimulation of COL1A1 transcription by the DNA intercalators, mitoxantrone and WP631, in cultured human dermal fibroblasts. *J Biol Chem* 2002; 277: 38737-38745.

Gando S, Kameue T, Nanzaki S, Hayakawa T and Nakanishi Y. Increased neutrophil elastase, persistent intravascular coagulation and decreased fibrinolytic activity in patients with post-traumatic acute respiratory distress syndrome. *J Trauma* 1997; **42**: 1068-1072.

Garcia R, Gusmani L, Murgia R, Guarnaccia C, Cinco M and Rottini G. Elastase is the only human neutrophil granule protein that alone is responsible for the in vitro killing of *borrelia burgdoferi*. *Infect Immun* 1998; **66**; 1408-1412.

Gardi C, Calzoni P, Marcolongo P, Cavarra E, Vanni L and Lungarella G. Collagen breakdown products and lung collagen metabolism: an *in vivo* study on fibroblast cultures. *Thorax* 1994; **49**: 312-318.

Gardi C, Pacini A, de Santi MM, Calzoni P, Viti A, Corradeschi F and Lungarella G. Development of interstitial lung fibrosis by long-term treatment with collagen breakdown products in rabbits. *Res Commun Chem Pathol Pharmacol* 1990; **68**: 235-250.

Gauldie J, Kolb M and Sime PJ. A new direction in the pathogenesis of idiopathic pulmonary fibrosis? Commentary. *Respir Res* 2001; **3**: 1-3.

Gautam N, Olofsson AM, Herwald H, Iversen LF, Lundgren-Akerlund E, Hedqvist P, Arfors KE, Flodgaard H, Lindbom L. Heparin-binding protein (HBP/Cap37): a missing link in neutrophil-evolved alteration of vascular permeability in inflammation. *Nature* 2001; **7**: 1123-1127.

Geiser AG, Zeng QQ, Sato M, Helvering LM, Hirano T and Turner CH. Decreased bone mass and bone density in mice lacking the TGF-β1 gene. *Bone* 1998; **23**: 87-93.

Gentry LE, Lioubin MN, Purchio AF and Marquardt H. Molecular events in the processing of recombinant type 1 pre-pro-transforming growth factor-beta to the mature polypeptide. *Mol Cell Biol* 1988; **8**: 4162-4168.

Gewaltig J, Mangasser-Stephan K, Gartung C, Biesterfeld S and Gressner AM. Association of polymorphisms of the transforming growth factor-β1 gene with the rate of progression of HCV-induced liver fibrosis. *Clin Chim Acta* 2002; **316**: 83-94.

Gharaee-Kermani M, McCullum-Smith RE, Charo IF, Kunkel SL and Phan SH. CC-chemokine receptor 2 required for bleomycin-induced pulmonary fibrosis. *Cytokine* 2003; **24**: 266-276.

Ghosh S, Mendoza T, Ortiz LA, Hoyle GW, Fermin CD, Brody AR, Friedman M and Morris GF. Bleomycin sensitivity of mice expressing dominant-negative p53 in the lung epithelium. *Am J Respir Crit Care Med* 2002; **166**: 890-897.

Giloni L, Takeshita M, Johnson F, Iden C and Grollman AP. Bleomycin-induced strand-scission of DNA. Mechanism of deoxyribose cleavage. *J Biol Chem* 1981; **256**: 8608-8615.

Ginzberg HH, Cherapanov V, Dong Q, Cantin A, McCulloch CAG, Shannnon PT and Downey GP. Neutrophil-mediated epithelial injury during transmigration: role of elastase. *Am J Physiol (Gastrointest Liver Physiol)* 2001; **281**: G705-717.

Giri SN, Hyde DM and Hollinger MA. Effect of antibody to transforming growth factor beta on bleomycin-induced accumulation of lung collagen in mice. *Thorax* 1993; **48**: 956-966.

Gleizes PE, Beavis RC, Mazzieri R, Shen B and Rifkin DB. Identification and characterization of an 8 cysteine repeat of the latent transforming growth factor-B binding protein-1 that mediates binding to the latent transforming growth factor-B. *J Biol Chem* 1996; **271**: 29891-19896.

Gleizes PE, Munger JS, Nunes I, Harpel JG, Mazzieri R, Noguera I and Rifkin DB. TGF-β latency: biological significance and mechanisms of action. *Stem Cells* 1997; **15**: 190-197.

Goldman G, Welbourn R, Kobzik L, Valeri CR, Shepro D and Hetchman HB. Reactive oxygen species and elastase mediate lung permeability after acid aspiration. *J Appl Physiol* 1992; **73**: 571-575.

Goodman RB, Strieter RM, Steinberg KP, Milberg JA, Maunder RJ, Kunkel SL, Walz A, Hudson LD and Martin TD. Inflammatory cytokines in patients with persistence of the acute respiratory distress syndrome. *Am J Respir Crit Care Med* 1996; **154**: 602-611.

Gossage JR, Kuratomi Y, Davidson JM, Lefferts PL and Snapper JR. Neutrophil elastase inhibitors, SC-37698 and SC-39026, reduce endotosin-induced lung dysfunction in awake sheep. *Am Rev Respir Dis* 1993; **147**: 1371-1379.

Grainger DJ, Kemp PR, Liu AC, Lawn RM and Metcalfe JC. Activation of transforming growth factor-β is inhibited in transgenic apolipoprotein(a) mice. *Nature* 1994; **370**: 460-462.

Grainger DJ, Heathcote K, Chiano M, Sneider H, Kem PR, Metcalf JC, Carter ND and Spector TD. Genetic control of the circulating concentration of transforming growth factor type β1. *Hum Mol Genet* 1999; 8: 93-97.

Grande NR, Peao MND, de Sa CM and Aguas AP. Lung fibrosis induced by bleomycin: structural changes and overview of recent advances. *Scan Micro* 1998; **12**: 487-494.

Gray AJ, Bishop JE, Reeves JT, Mecham RP and Laurent GJ. Partially degraded fibrin(ogen) stimulates fibroblast proliferation in vitro. *Am J Respir Mol Cell Biol* 1995; **12**: 684-690.

Green TP, Johnson DE, Marchessault RP and Gatto CW. Transvascular flux and tissue accrual of Evans blue: effects of endotoxin and histamine. *J Lab Clin Med* 1988; **111**: 173-183.

Griffiths MJD and Evans TW. Adult Respiratory Distress Syndrome. *In:* Brewis RAL, Corrin B, Geddes DM and Gibson GJ, eds. Respiratory Medicine. London: Balliere Tindall., 1995: 605-629.

Gross TJ and Hunninghake GW. Idiopathic pulmonary fibrosis. *N Engl J Med* 2001; **345**: 517-525.

Grotendorst GR, Smale G and Percev D. Production of transforming growth factor-beta by human peripheral blood monocytes and neutrophils. *J Cell Physiol* 1989; **140**: 396-402.

Grutter MG, Fendrich G, Huber R and Bode W. The 2.5 A X-ray crystal structure of the acid-stable proteinase inhibitor from human mucous secretions analysed in its complex with bovine alpha-chymotrypsin. *EMBO J* 1988; **7**: 345-351.

Guidot DM, Modelska K, Lois M, Jain L, Moss IM, Pittet JF and Brown LA. Ethanol ingestion via glutathione depletion impairs alveolar epithelial barrier function in rats. *Am J Physiol (Lung Cell Mol Physiol)* 2000; **279**: L127-L135.

Gunther A, Schmidt R. Nix F, Yabut-Perez M, Guth C, Rosseau S, Siebert C, Grimminger F, Morr H and Velcovsky HG. Surfactant abnormalities in idiopathic pulmonary fibrosis, hypersensitivity pneumonitis and sarcoidosis. *Eur Respir J* 1999; **14**: 565-573.

Guo M, Mathieu PA, Linebaugh B, Sloane BF and Reiners JJ Jr. Phorbol ester activation of a proteolytic cascade capable of activating latent TGF-a: a process initiated by the exocytosis of cathepsin B. *J Biol Chem* 2002; 277:14829-14837.

Gurujeyalakhsmi G, Hollinger MA and Giri SN. Regulation of transforming growth factor-beta1 mRNA expression by taurine and niacin in the bleomycin hamster model of lung fibrosis. *Am J Respir Cell Mol Biol* 1998; **18**: 334-342.

Gurujeyalakhsmi G and Giri SN. Molecular mechanisms of antifibrotic effect of interferon gamma in bleomycin mouse model of lung fibrosis: downregulatinon of TGF-β and procollagen I and III gene expression. *Exp Lung Res* 1995; **21**: 791-808.

Hagimoto N, Kuwano K, Inoshima I, Yoshimi M, Nakamura N, Fujita M, Maeyama T and Hara N. TGF-β1 as an enhancer of Fas-mediated apoptosis of lung epithelial cells. *J Immunol* 2002; **168**: 6470-6478.

Hagiwara SI, Ishii Y and Kitamura S. Aerosolized administration of N-acetylcysteine attenuates lung fibrosis induced by bleomycin in mice. *Am J Respir Crit Care Med* 2000; **162**: 225-231.

Hamaguchi Y, Nishizawa Y, Yasui M, Hasegawa M, Kaburagi Y, Komura K, Nagaoka T, Saito E, Shimada Y, Takehara K, Kadono T, Steeber DA, Tedder TF and Sato S. Intercellular adhesion molecule-1 and L-selectin regulate bleomycin-induced lung fibrosis. *Am J Pathol* 2002; **161**: 1607-1611.

Hamman L and Rich AR. Acute diffuse interstitial fibrosis of the lungs. *Bull Johns Hopkins Hosp* 1944; **74**: 177.

Hardie WD, Le Cras TD, Jiang K, Tichelaar JW, Azhar M and Korfhagen TR. Conditional expression of transforming growth factor-alpha in adult mouse lung causes pulmonary fibrosis. *Am J Physiol (Lung Cell Mol Physiol)* 2004; **286**: L741-L749.

Harrison JH Jr, Hoyt DG and Lazo JS. Acute pulmonary toxicity of bleomycin: DNA scission and matrix protein mRNA levels in bleomycin-sensitive and -resistant strains of mice. *Mol Pharmacol* 1989; **36**: 231-238.

Hascall VC and Hascall GK. Proteoglycans. In: Hay ED, ed. Cell biology of extracellular matrix. New York: Plenum Press, 1991: 39-63.

Hashimoto N, Jin H, Liu T, Chensue SW, Phan SH. Bone marrow-derived progenitor cells in pulmonary fibrosis. *J Clin Invest* 2004; **113**: 243-252.

Haslett C, Shen AS, Feldsien DC, Allen D, Henson PM and Cherniack RM. ^{111}-Indium-labeled neutrophil migration into the lungs of bleomycin-treated rabbits assessed non-invasively by external scintigraphy. *Am Rev Respir Dis* 1989; **140**: 756-763.

Haston CK and Travis EL. Murine susceptibility to radiation-induced pulmonary fibrosis is influenced by a genetic factor implicated in susceptibility to bleomycin-induced pulmonary fibrosis. *Cancer Res* 1997; **57**: 5286-5291.

Haston CK, Wang M, Dejournett RE, Zhou X, Ni D, Gu X, King TM, Weil MM, Newman RA, Amos CI and Travis EL. Bleomycin hydrolase and a genetic locus within the MHC affect risk for pulmonary fibrosis in mice. *Hum Mol Genet* 2002; **11**: 1855-1863.

Hawgood S. Pulmonary surfactant apoproteins: a review of protein and genomic structure. *Am J Physiol (Lung Cell Mol Physiol)* 1989; **257(2 Pt 1)**: L13-L22.

Hay J, Shahzeidi S and Laurent GJ. Mechanisms of bleomycin-induced lung damage. *Arch Toxicol* 1991; **65**: 81-94.

Hecht SM. DNA strand scission by activated bleomycin group antibiotics. *Fed Proc* 1986; **45**: 2784-2791.

Heck LW, Blackburn WD, Irwin MH and Abrahamson DR. Degradation of basement membrane laminin by human neutrophil elastase and cathepsin G. *Am J Pathol* 1990; **136**: 1267-1274.

Heldion C-H, Miyazono K and ten Dijke P. TGF-β signalling from cell membrane to nucleus through SMAD proteins. *Nature* 1997; **390**: 465-471.

Hernandez-Rodriguez NA, Harrison NK,Chambers RC, Gray AJ, Aotuhcott AM, du Bois RM, Black CM, Scully MF, McAnulty RJ and Laurent GJ. Role of thrombin in pulmonary fibrosis. *Lancet* 1995; **346**: 1071-1073.

Hesterberg TW, Gerriets JE, Reiser KM, Jackson AC, Cross CE and Last JA. Bleomcyin-induced pulmonary fibrosis: correlation of biochemical, physiological and histological changes. *Toxicol Appl Pharmacol* 1981; **60**: 360-367.

Hiemstra PS. Novel roles of protease inhibitors in infection and inflammation. Biochem Soc Trans 2002; 30 (part 2): 116-120.

Hiemstra PS, Maassen RJ, Stolk J, Heinzel-Wieland R, Steffens GJ and Dijkman JH. Antibacterial activity of antileukoprotease. *Infect Immun* 1996; **64**: 4520-4524.

Hildebrand AM, Romaris M, Rasmussen LM, Heinegard D, Twardzik DR, Border WA and Ruoslahti E. Interaction of the small intestinal proteoglycans biglycan, decorin and fibromodulin with TGF-β. *Biochem J* 1994; **302**: 527-534.

Hirche TO, Atkinson JJ, Bahr S and Belaaouaj A. Deficiency in neutrophil elastase does not impair neutrophil recruitment to inflamed sites. *Am J Respir Cell Mol Biol* 2004; **30**: 576-584.

Hocher B, Schwarz A, Fagan KA, Thone-Reineke C, El-Hag K, Kusserow H, Elitok S, Bauer C, Neumayer H-H, Rodman DM and Theuring F. Pulmonary fibrosis and chronic lung inflammation in ET-1 transgenic mice. *Am J Respir Cell Mol Biol* 2000; **23**; 19-26.

Hodges RJ, Jenkins RG, Wheeler-Jones CP, Copeman DM, Bottoms SE, Bellingan GJ, Nanthakumar CB, Laurent GJ, Hart SL, Foster ML and McAnulty RJ. Severity of lung injury in cyclooxygenase-2-deficient mice is dependent on reduced prostaglandin E9") production. *Am J Pathol* 2004; **165**: 1663-1676.

Hodgson U, Laitinrn T and Tukiainen P. Nationwide prevalence of sporadic and familial idiopathic pulmonary fibrosis: evidence of founder effect among multiplex families in Finland. *Thorax* 2002; **57**: 338-342.

Hojo S, Fujita J, Yoshinouchi T, Yamanouchi H, Kamei T, Yamadori I, Otsuki Y, Ueda N, and Takahara J. Hepatocyte growth factor and neutrophil elastase in idiopathic pulmonary fibrosis. *Respiratory Medicine* 1997; **91**: 511-516.

Homma S, Nagaoka I, Abe H, Takahashi K, Seyama K, Nukiwa T, Kira S. Localization of platelet-derived growth factor and insulin-like growth factor I in the fibrotic lung. *Am J Respir Crit Care Med* 1995; **152**: 2084-2989.

Horimoto M, Kato J, Takimoto R, Terui T, Mogi Y and Niitsu Y. Identification of a transforming growth factor-β1 activator derived from a human gastric cancer cell line. *Br J Cancer* 1995; **72**: 676-682.

Howell DC, Johns RH, Lasky JA, Shan B, Scotton CJ, Laurent GJ and Chambers RC. Absence of proteinase-activated receptor-1 signaling affords protection from bleomycin-induced lung inflamamtion and fibrosis. *Am J Pathol* 2005; **166**: 1353-1365.

Hoyt DG and Lazo JS. Alterations in pulmonary mRNA encoding procollagens, fibronectin and transforming growth factor-beta precede bleomycin-induced pulmonary fibrosis in mice. *J Pharmacol Exp Ther* 1988; **246**: 765-771.

Hoyt DG, Rizzo M, Gerritsen ME, Pitt BR and Lazo JS. Integrin activation protects pulmonary endothelial cells from the genotoxic effects of bleomycin. *Am J Physiol (Lung Cell Mol Physiol)* 1997; **273**: L612-617.

Huang X, Wu J, Spong S and Sheppard D. The integrin alphavbeta6 is critical for keratinocyte migration on both its known ligand, fibronectin, and on vitronectin. J Cell Sci 1998; 111: 2189-2195.

Huang M, Sharma S, Zhu LX, Keane MP, Luo J, Zhang L, Burdick MD, Lin YQ, Dohadwala M, Gardner B, Batra RK, Strieter RM and Dubinett SM. IL-7 inhibits fibroblast TGF-beta production and signaling in pulmonary fibrosis. *J Clin Invest* 2002; **109**: 931-937.

Huaux F, Liu T, McGarry B, Ullenbruch M and Phan SH. Dual roles of IL-4 in lung injury and fibrosis. *J Immunol* 2003; **170**: 2083-2092.

Hubbard R, Johnston I, Coultas DB and Britton J. Mortality rates from cryptogenic fibrosing alveolitis in seven countries. *Thorax* 1996; **51**: 711-716.

Huggins RA, Smith EL and Deavers S. Volume distribution of Evans blue dye and iodinated albumin in the dog. *Am J Physiol* 1963; **205**: 351-356.

Hurst V, Goldberg PL, Minnear FL, Heimark RL and Vincent PA. Rearrangement of adherens junctions by TGF-β1: role of contraction. *Am J Physiol (Lung Cell Mol Physiol)* 1999; **276**: L582-L595.

Hussain MZ, Giri SN and Bhatnagar RS. Poly (ADP-ribose) aynthetase activity during bleomycin-induced lung fibrosis in hamsters. *Exp Mol Pathol* 1985; **43**: 162-176.

Hybertson BM, Jepson EK, Allard JD, Cho OJ, Lee YM, Huddleston JR, Weinman JP, Oliva AM and Repine JE. Transforming growth factor-beta contributes to lung leak in rats given interleukin-1 intratracheally. *Exp Lung Res* 2003; **29**: 361-373.

Hyytiäinen M, Taipale J, Heldin, C-H and Keski-Oja. Recombinant latent transforming growth factor-β binding protein 2 assembles to fibroblast extracellular matrix and is susceptible to proteolytic processing and release. *J Biol Chem* 1998; **273**: 20669-20676.

Hyytiäinen M, Penttinen C and Keski-Oja J. Latent TGF-beta binding proteins: extracellular matrix association and roles in TGF-beta activation. *Crit Rev Clin Lab Sci* 2004; **41**: 233-264.

IFEGENIA: Idiopathic Pulmonary Fibrosis International Group Exploring NAC I Annual study; www.zambongroup.com

Ignotz RA and Massague J. Transforming growth factor-β stimulates the expression of fibronectin and collagen and their incorporation into the extracellular matrix. *J Biol Chem* 1986; **261**: 4337-4345.

Isaka Y, Brees DK, Ikegaya K, Kaneda Y, Imai E, Noble NA and Border WA. Gene therapy by skeletal muscle expression of decorin prevents fibrotic disease in rat kidney. *Nat Med* 1996; **2**: 418-423.

Itoh Y and Nagase H. Preferential inactivation of tissue inhibitor of metalloproteinase-1 that is bound to the precursor of matrix metalloproteinase-9 (pro-gelatinase B) by human neutrophil elastase. *J Biol Chem* 1995; **270**: 16518-16521.

IUBMB, International Union of Biochemistry and Molecular Biology. Recommendations on Biochemical and Organic Nomenclature, Symbols and Terminology. Available at http: // www. Chem. Qmw. Ac. Uk / iubmb/.

Iyer SN, Hyde DM and Giri SN. Anti-inflammatory effect of pirfenidone in the bleomycin-hamster model of lung inflammation. *Inflammation* 2000; **24**: 477-491.

Izbicki G, Segel MJ, Christensen TG, Conner MW and Breuer R. Time course of bleomycin-induced lung fibrosis. *Int J Exp Path* 2002a; **83**: 111-119.

Izbicki G, Or R, Christensen TG, Segel MJ, Fine A, Goldstein RH and Breuer R. Bleomycin-induced lung fibrosis in IL-4-overexpressing and knockout mice. *Am J Physiol (Lung Cell Mol Physiol)* 2002b; **283**: L1110-L1116.

Janick-Buckner D, Ranges GE and Hacker MP. Alteration of bronchoalveolar lavage cell populations floowing bleomycin treatment in mice. *Toxicol Appl Pharmacol* 1989; **100**: 465-473.

Janoff A and Scherer J. Mediators of inflammation in leukocyte lysosomes. IX. Elastinolytic activity in granules of human polymorphonuclear leukocytes. *J Exp Med* 1968; 128: 1137-1155.

Jie Z, Cai Y, Yang W, Jin M, Zhu W, Zhu C. Protective effects of alpha 1-antitrypsin on acute lung injury in rabbits induced by endotoxin. *Chin Med J (Engl)* 2003; **116**: 1678-1682.

Jimenez SA, Varga J, Olsen A, Li L, Diaz A, Herhal J and Koch J. Functional analysis of human alpha 1(I) procollagen gene promoter. Differential activity in collagen-producing and -non-producing cells and response to transforming growth factor beta 1. *J Biol Chem* 1994; **269**: 12684-12691.

Jin FY, Nathan C, Radzioch D and Ding A. Secretory leukocyte protease inhibitor: a macrophage product induced by and antagonistic to bacterial lipopolysaccharide. *Cell* 1997; **88**: 417-426.

Johnston CJ, Piedboeuf B, Baggs R, Rubin P and Finkelstein JN. Differences in correlation of mRNA gene expression in mice sensitive and resistant to radiation-induced pulmonary fibrosis. *Radiat Res* 1995; **142**: 197-203.

Johnston I, Britton K, Kinnear W and Logan R. Rising mortality from cryptogenic fibrosing alveolitis. *Brit Med J* 1990; **301**: 1017-1021.

Jones HA, Schofield JB, Krausz T, Boobis AR and Haslett C. Pulmonary fibrosis correlates with duration of tissue neutrophil activation. *Am J Respir Crit Care Med* 1998; **158**: 620-628.

Jordana M, Dolovich M, Irving LB, Tomioka M, Befus D, Gauldie J and Newhouse MT. Solute movement across the alveolar-capillary membrane after intratracheally administered bleomycin in rats. *Am Rev Respir Dis* 1988; **138**: 96-100.

Joslin G, Fallon R, Bullock J, Adams SP and Perlmutter DH. The SEC receptor recognizes a pentapeptide neodomain of alpha 1-antitrypsin-protease complexes. *J Biol Chem* 1991; **266**: 11282-11288.

Kafienah W, Buttle DJ, Burnett D and Hollander AP. Cleavage of native type I collagen by human neutrophil elastase. *Biochem J* 1998; **330**: 897-902.

Kamal AM, Corrigan CJ, Tetlet TD, Alaghband-Zadeh J and Smith SF. Effect of fluticasone on the elastase:antielastase profile of the normal lung. *Eur J Clin Invest* 2002; **32**: 713-719.

Kaminski N, Allard JD, Pittet JF, Zuo F, Griffiths MJD, Morris D, Huang X, Sheppard D and Heller RA. Global analysis of gene expression in pulmonary fibrosis reveals distinct programs regulating lung inflammation and fibrosis. *Proc Natl Acad Sci USA* 2000; **97**: 1778-1783.

Kaneko K, Kudoh I, Hattori S, Yamada H, Ohara M, Wiener-Kronish J and Okumura F. Neutrophil elastase inhibitor, ONO-5046, modulates acid-induced lung and systemic injury in rabbits. *Anesthesiology* 1997; **87**: 635-641.

Kaner RJ, Ladetto JV, Singh R, Fukuda N, Matthay MA, Crystal RG. Lung overexpression of the vascular endothelial growth factor gene induces pulmonary edema. *Am J Respir Cell Mol Biol* 2000; **22**: 657-664.

Kanzaki T, Olofsson A, Moren A, Wernstedt C, Hellman U, Miyazono K, Claesson-Welsh L and Heldin CH. TGF-beta1 binding protein: a component of the large latent complex of TGF-beta 1 with multiple repeat sequences. *Cell* 1990; **61**: 1051-1061.

Katzenstein A-L. Pathogenesis of 'fibrosis' in interstitial pneumonia: an electron microscopic study. *Hum Pathol* 1985; **16**: 1015-1024.

Katzenstein A, Myers JL, Prophet WD, Corley LS and Shin MS. Bronchiolitis obliterans organizing pneumonia. *Am J Surg Pathol* 1986; **10**: 372-381.

Katzenstein A-L and Myers JL. Idiopathic pulmonary fibrosis: clinical relevance of pathologic classification. *Am J Respir Crit Care Med* 1998; **157**: 1301-1315.

Kaufmann E. Lehrbuch der speziellen pathologischen Anatomie für Studierende und Ärzte, Vol I. Berlin-Liepzig: Walter de Gruyter Co., 1922: 275-278.

Kawabata K, Hagio T, Matsumoto S, Nakao S, Orita S, Aze Y and Ohno H. Delayed neutrophil elastase inhibition prevents subsequent progression of acute lung injury induced by endotoxin inhalation in hamsters. *Am J Respir Crit Care Med* 2000; **161**: 2013-2018.

Keane MP and Strieter RM. The importance of balanced pro-inflamamtory and anti-inflamamtory mechanisms in diffuse lung disease. *Respir Res* 2002; **3**: 5-13.

Keeton MR, Curriden SA, van Zonneveld Aj and Loskutoff DJ. Identification of regulatory sequences in the type 1 plasmnogen activator inhibitor gene responsive to transforming growth factor-beta. *J Biol Chem* 1991; **266**: 23048-52.

Kelley J, Fabisiak JP, Hawes K and Absher M. Cytokine signalling in lung: transforming growth factor-beta secretion by lung fibroblasts. *Am J Physiol (Lung Cell Mol Physiol)* 1991; **260**: L123-128.

Kelsey GD, Povey S, Bygrave AE and Lovell-Badge RH. Species- and tissue-specific expression of human α1-antitrypsin in transgenic mice. *Genes Dev* 1987; **1**: 161-171.

Kerr LD, Miller DB and Matrisian LM. TGF-β1 inhibition of transin/stromelysin gene expression is mediated through a Fos binding sequence. *Cell* 1990; **61**: 267-278.

Khalil N. TGF-β: form latent to active. *Microb Infect* 1999; **1**: 1255-1263.

Khalil N, Bereznay O, Sporn M and Greenberg AH. Macrophage production of transforming growth factor-beta and fibroblast collagen synthesis in chronic pulmonary inflammation. *J Exp Med* 1989; **170**: 727-737.

Khalil N, O'Connor RN, Unruh HW, Warren PW, Flanders KC, Kemp A, Bereznay OH and Greenberg AH. Increased production and immunohistochemical localization of transforming growth factor-β in idiopathic pulmonary fibrosis. *Am J Respir Cell Mol Biol* 1991; **5**: 155-162.

Khalil N, Corne S, Whitman C and Yacyshyn H. Plasmin regulates the activation of cell-associated latent TGF-beta 1 secreted by rat alveolar macrophages after in vivo bleomycin injury. *Am J Respir Cell Mol Biol* 1996a; **15**: 252-259.

Khalil N, O'Connor R, Flanders KC and Unruh H. TGF-β1 but not TGF-β2 or TGF-β3 is differentially present in epithelial cells of advanced pulmonary fibrosis: an immunohistochemical study. *Am J Respir Cell Mol Biol* 1996b; **14**: 131-138.

Khalil N, Parekh TV, O'Connor R, Antman N, Kepron W, Yehualaeshet T, Yu YD and Gold LI. Regulation of the effects of TGF-beta 1 and differential expression of TGF-beta receptors (TβR-I and TβR-II) in idiopathic pulmonary fibrosis. *Thorax* 2001; **56**: 907-915.

Kim TA, Cutry AF, Kinniburgh AJ and Wenner CE. Transforming growth factor beta 1-induced delay of cell cycle progression and its association with growth-related gene expression in mouse fibroblasts. *Cancer Lett* 1993; **71**: 125-132.

King Jr TE, Scwarz MI, Brown K, Tooze JA, Colby TV, Waldron JA Jr, Flint A, Thurlbeck W and Cherniack RM. Idiopathic pulmonary fibrosis. Relationship between histopathologic features and mortality. *Am J Respir Crit Care Med* 2001; **164**: 1025-1032.

Kirk JM, Heard BE, Kerr I, Turner-Warwick M and Laurent GJ. Quantitation of types I and III collagen in biopsy lung samples from patients with cryptogenic fibrosing alveolitis. *Coll Relat Res* 1984; **4**: 169-182.

Kittelberger R, Neale TJ, Francky KT, Grennhill NS and Gibson GJ. Cleavage of type VIII collagen by human neutrophil elastase. *Biochim Biophys Acta* 1992; **1139**: 295-299.

Koff A, Ohtsuki M, Polyak K, et al. Negative regulation of G1 in mammalian cells: Inhibition of cyclin E-dependent kinase by TGF-β. *Science* 1993; **260**: 536-539.

Kojima S, Kiyomitsu N and Rifkin DB. Requirement for transglutaminase in the activation of latent transforming growth factor-β in bovine endothelial cells. *J Cell Biol* 1993; **121**: 439-448.

Kolb M, Margetts PJ, Anthony DC, Pitossi F, Gauldie J. Transient expression of IL-1beta induces acute lung injury and chronic repair leading to pulmonary fibrosis. *J Clin Invest* 2001a; **107**: 1529-1536.

Kolb M, Margetts PJ, Galt T, Sime PJ, Xing Z, Schmidt M and Gauldie J. Transient transgene expression of decorin in the lung reduces the fibrotic response to bleomycin. *Am J Respir Crit Care Med* 2001b: **163**: 770-777.

Kolb M, Margetts PJ, Sime PJ and Gauldie J. Proteoglycans decorin and biglycan differentially modulate TGF-beta-mediated fibrotic responses in the lung. *Am J Physiol (Lung Cell Mol Physiol)* 2001; **280**: L1327-1334.

Koli K, Saharinen J, Hyytiainen M, Penttinen C and Keski-Oja J. Latency, activation and binding proteins of TGF-β. *Micros Res Tech* 2001; **52**: 354-362.

Koli K, Saharinen J, Karkkainen M and Keski-Oja J. Novel non-TGF-β-binding splice variant of LTBP-4 in human cells and tissues provides means to decrease TGF-β deposition. *J Cell Sci* 2001; **114**: 2869-2878.

Kuhn III C, Boldt J, King TE, Crouch E, Vartio T and McDonald A. An immunohistochemical study of architectural remodeling and connective tissue synthesis in pulmonary fibrosis. *Am Rev Respir Dis* 1989; **140**: 1693-1703.

Kumar RK, O'Grady R, Maronese SE and Wilson MR. Epithelial cell-derived transforming growth factor-β in bleomycin-induced lung injury. *Int J Exp Path* 1996; **77**: 99-107.

Kuwano K, Kunitake R, Kawasaki M, Nomoto Y, Hagimoto N, Nakanishi Y and Hara N. P21Waf1/Cip1/Sdi1 and p53 expression in association with DNA strand breaks in idiopathic pulmonary fibrosis. *Am J Respir Crit Care Med* 1996; **154**: 477-483.

Kuwano K, Hagimoto N, Kawasaki M, Yatomi T, Nakamura N, Nagata S, Suda T, Kunitake R, Maeyama T, Miyazaki H and Hara N. Essential roles of the Fas-FasL ligand pathway in the development of pulmonary fibrosis. *J Clin Invest* 1999; **104**: 13-19.

Lafrenie RM, Yamada KM. Integrin-dependent signal transduction. *J Cell Biochem* 1996; **61**: 543-553

Last JA, Gllzleichter TR, Pinkerton KE, Walker RM and Witschi H. A new odel of progressive pulmonary fibrosis in rats. *Am Rev Respir Dis* 1993; **148**: 487-494.

Laurell CB and Eriksson S. The lectrophoretic alpha 1-globulin pattern of serum in alpha 1-antitrypsin deficiency. *Scan J Clin Lab Invest* 1963; **15**: 132-140.

Laurent GJ, McAnulty RJ, Corrin B and Cockerill P. Biochemical and histological changes in pulmonary fibrosis induced in rabbits with intratracheal bleomycin. *Eur J Clin Invest* 1981; **11**: 441-448.

Laurent GJ. Rates of collagen synthesis in lung, skin and muscle obtained in vivo by a simplified method using [^{3}H] proline. *Biochem J* 1982; **206**: 535-544.

Laurent GJ and McAnulty RJ. Protein metabolism during bleomycin-induced pulmonary fibrosis in rabbits: in vivo evidence for collagen accumulation because of increased synthesis and decreased degradation of the newly synthesized collagen. *Am Rev Respir Dis* 1983; **128**: 82-88.

Laurent GJ, Harrison NK and McAnulty RJ. The regulation of collagen production in normal lung and during interstitial lung disease. *Postgrad Med J* 1988; **64** (suppl 4): 26-34.

Lawrence DA, Pircher R, Keyceve-Martinerie C and Jullien P. Normal embryo fibroblasts release transforming growth factor-beta in a latent form. *J Cell Physiol* 1984; **121**: 184-188.

Lawrence DA. Identification and activation of latent transforming growth factor-beta. *Methods Enzymol* 1991; **198**: 327-336.

Lawrence DA. Transforming growth factor-β: a general overview. *Eur Cyto Network* 1996; **7**: 363-374.

Lazo JS and Pham ET. Pulmonary fate of [3H]bleomycin A2 in mice. *J Pharmacol Exp Ther* 1984; **228**: 13-18.

Le-Barrilec K, Si-Tahar M, Balloy V and Chignard M. Proteolysis of monocyte CD14 by human leukocyte elastase inhibits lipopolysaccharide-mediate cell activation. *J Clin Invest* 1999; **103**: 1039-1046.

Leask A, Abraham DJ, Finlay DR, Holmes A, Pennington D, Shi-Wen X, Chen Y, Venstrom K, Dou X, Ponticos M, et al., Dysregulation of transforming growth factor-beta signalling in scleroderma: overexpression of endoglin in cutaneous scleroderma fibroblasts. *Arthritis Rheum* 2002; **46**: 1857-1865.

Leavell KJ, Peterson MW and Gross TJ. Human neutrophil elastase abolishes interleukin-8 chemotactic activity. *J Leukol Biol* 1996; **61**: 361-366.

Lee CG, Homer RJ, Zhu Z, Lanone S, Wang X, Koteliansky V, Shipley JM, Gotwals P, Noble P, Chen Q, Senior RM and Elias JA. Interleukin-13 induces tissue fibrosis by selectively stimulating and activating transforming growth factor-beta1. *J Exp Med* 2001; **194**: 809-821.

Lee CT, Fein AM, Lippmann M, Holtzman H, Kimbel P and Weinbaum G. Elastolytic activity in pulmonary lavage fluid from patients with adult respiratory distress syndrome. *N Engl J Med* 1981; **304**: 192-196.

Lee TC, Gold LI, Reibman J, Aston C, Begin R, Rom WN and Jagirdar J. Immunohistochemical localization of transforming growth factor-beta and insulin-like growth factor-I in asbestosis in the sheep model. *Int Arch Occup Environ Health* 1997; **69**: 157-164.

Lee WL and Downey GP. Leukocyte elastase: physiological functions and role in acute lung injury. *Am J Respir Crit Care Med* 2001; **164**: 896-904.

Lemaire I. Silica- and asbestos-induced pulmonary fibrosis. In: Phan SH and Thrall RS, eds. Pulmonary Fibrosis. New York: Marcel Dekker Inc., 1995: 319-362.

Lestienne P and Bieth JG. Activation of human leukocyte elastase activity by excess substrate, ionic strength and hydrophobic solvents. *J Biol Chem* 1980; **255**: 9289-9294.

Letamendia A, Lestres P, Botella LM, Raab U, Langa C, Velasco B, Attisano L and Bernabeu C. Role of endoglin in cellular responses to transforming growth factor-beta. A comparative study with betaglycan. *J Biol Chem* 1998; **273**: 33011-33019.

Levesque JP, Hendy J, Takamatsu Y, Simmons PJ and Bendall LJ. Disruption of the CXCR4/CXCL12 chemotactic interaction during hematopoietic stem cell mobilization induced by GCSF or cyclophosphamide. *J Clin Invest* 2003; **111**: 187-196.

Levesque JP, Liu F, Simmons PJ, Betsuyaku T, Senior RM, Pham C and Link DC. Characterization of hematopoietic progenitor mobilization in protease-deficient mice. Blood 2004; 104: 65-72.

Li Q, Park PW, Wilson CL and Parks WC. Matrilysin shedding of syndecan-1 regulates chemokine mobilization and transepithelial efflux of neutrophils in acute lung injury. *Cell* 2002; **111**: 635-646.

Liebow AA and Carrington CB. The interstitial pneumonias. In: Simon M, Potchen EJ, Lemay M, editors. Frontiers of pulmonary radiology, 1st edition. New York: Grune and Stratton; 1969: 102-141.

Liou TG and Campbell FJ. Non-isotropic enzyme-inhibitor interactions: a novel non-oxidative mechanism for quantum proteolysis by human neutrophils. *Biochemistry* 1995; **34**: 16171-16177.

Lioubin N, Madisen L, Roth RA and Purchio AF. Characterization of latent transforming growth factor-beta2 from monkey kidney cells. Endocrinology 1991; 128: 2291-2296.

Liu JY, Sime PJ, Wu T, Warshamana S, Pociask D, Tsai S-Y and Brody AR. Transforming growth factor-β1 overexpression in tumor necrosis factor-α receptor knockout mice induces fibroproliferative lung disease. *Am J Respir Cell Mol Biol* 2001; **25**: 3-7.

Liu T, Jin H, Ullenbruch M, Hu B, Hashimoto N, Moore B, McKenzie A, Lukacs NW and Phan SH. Regulation of found in inflammatory zone 1 expression in bleomycin-induced lung fibrosis: role of IL-4/IL-13 and mediation via STAT-6. *J Immunol* 2004; **173**: 3425-3431.

Liu Z, Shapiro SD, Zhou X, Twining SS, Senior RM, Giudice GJ, Fairley JA and Diaz LA. A critical role for neutrophil elastase in experimental bullous pemphigoid. *J Clin Invest* 2000a; **105**: 113-123.

Liu Z, Zhou X, Shapiro SD, Shipley JM, Twining SS, Diaz LA, Senior RM and Werb Z. The serpin alpha-1-proteinase inhibitor is a critical substrate for gelatinase B/MMP-9 in vivo. *Cell* 2000b; **102**: 647-655.

Logan A, Baird A and Berry M. Decorin attenuates gliotic scar formation in the rat cerebral hemisphere. *Exp Neurol* 1999; **159**: 504-510.

Lomas DA, Evans DL, Finch JT and Carrell RW. The mechanism of Z alpha 1-antitrypsin accumulation in the liver. *Nature* 1992; **357**: 605-7.

Lomas DA and Parfrey H. α1-antitrypsin deficiency. Molecular pathophysiology. *Thorax* 2004; **59**:529-535.

Ludbrook SB, Barry ST, Delves CJ and Horgan CM. The integrin αvβ3 is a receptor for the latency-associated peptides of transforming growth factors β1 and β3. *Biochem J* 2003; **369**: 311-318.

Luisetti M and Travis J. Bioengineering: alpha-1-proteinase inhibitor site-specific mutagenesis. The prospect for improving the inhibitor. *Chest* 1996; 110: 278s-283s.

Lyman S, Ujjani B, Renner K, Antholine W, Pertering DH, Whetstone JW and Knight JM. Properties of the initial reaction of bleomycin and several of its metal complexes with Ehrlich cells. *Cancer Res* 1986; **46**: 4472-4478.

Lyons RM, Keski-Oja and Moses HL. Proteolytic activation of latent transforming growth factor-beta from fibroblast-conditioned medium. *J Cell Biol* 1988; **106**: 1659-1665.

Lyons RM, Gentry LE, Purchio AF and Moses HL. Mechanism of activation of latent recombinant transforming growth factor beta 1 by plasmin. *J Biol Chem* 1990; **110**: 1361-1367.

Madri JA and Furthmayr H. Collagen polymorphism in the lung. An immunochemical study of pulmonary fibrosis. *Hum Pathol* 1980; **11**: 353-366.

Madtes DK, Elston AL, Hackman RC, Dunn AR and Clark JG. Transforming growth factor-α deficiency reduces pulmonary fibrosis in transgenic mice. *Am J Respir Cell Mol Biol* 1999; **20**:924-934.

Maeda A, Ishioka S. Taooka Y, et al. Expression of growth factor-beta1 and tumor necrosis factor-alpha in bronchoalveolar lavage cells in murine pulmonary fibrosis after intraperitoneal administration of bleomycin. *Respirology* 1999; **4**: 359-363.

Mahadeva R and Lomas DA. Genetics and respiratory disease. 2. Alpha 1-antitrypsin deficiency, cirrhosis and emphysema. *Thorax* 1998; **53**: 501-5.

Manoury B, Nenan S, Leclerc O, Guenon I, Boichot E, Planquois JM, Bertrand CP and Lagente V. The absence of reactive oxygen species production protects mice against bleomycin-induced pulmonary fibrosis. *Respir Res* 2005; **6**: 11.

Mariani TJ, Roby JD, Mecham RP, Parks WC, Crouch E and Pierce RA. Localization of type I procollagen gene expression in silica-induced granulomatous lung disease and implication of transforming growth factor-beta as a mediator of fibrosis. *Am J Pathol* 1996; **148**: 151-164.

Marshall RP, Bellingan G, Webb S, Puddicombe A, Goldsack NR, McAnulty RJ and Laurent GJ. Fibroproliferation occurs early in the acute respiratory distress syndrome and impacts on outcome. *Am J Respir Crit Care Med* 2000; **162**: 1783-1788.

Mason RJ, Schwarz MI, Hunninghake GW and Musson RA. Pharmacological therapy for idiopathic pulmonary fibrosis: past, present and future. NHLBI Workshop Summary. *Am J Respir Crit Care Med* 1999; **160**: 1771-1777.

Massague J. The transforming growth factor-beta family. *Ann Rev Cell Biol* 1990; **6**: 597-641.

Massague J. TGF-β signal transduction. *Annu Rev Biochem* 1998; **67**: 753-791.

Matthay MA. Fibrosing alveolitis in the adult respiratory distress syndrome. *Ann Intern Med* 1995; **122**: 65-66.

Mays C and Rosenberry TL. Characterization of pepsin-resistant collagen-like tail subunit fragments of 18S and 14S acetylcholinesterases from *Electrophorus electricus*. *Biochemistry* 1981; **20**: 2810-2817.

Mays PK, McAnulty RJ, Campa JS and Laurent GJ. Age-related changes in collagen synthesis and degradation in rat tissues. *Biochem J* 1991; **276**: 307-313.

McAnulty RJ and Laurent GJ. Collagen and its regulation in pulmonary fibrosis. In: Phan SM and Thrall RS, eds. Pulmonary Fibrosis. New York: Marcel Dekker Inc., 1995: 135-171.

McGowan SE, Jackson SK, Olson PJ, Parekh T and Gold LI. Exogenous and endogenous transforming growth factor-beta influence elastin gene expression in cultured lung fibroblasts. *Am J Respir Cell Mol Biol* 1997; **17**: 25-35.

McHugh LG, Milberg JA, Whitcomb ME, Schoene RB, Maunder RJ and Hudson LD. Recovery of functiuon in survivors of the acute respiratory distress syndrome. *Am J Resp Crit Care Med* 1994; **150**: 90-94.

McMahon GA, Dignam JD, Gentry LE. Structural characterization of the latent complex between transforming growth factor beta 1 and beta 1-latency-associated peptide. *Biochem J* 1996; **313**: 343-351.

Miller LA, Barnett NL, Sheppard D and Hyde DM. Expression of the β6 integrin subunit is associated with sites of neutrophil influx in lung epithelium. *J Histochem Cytochem* 2001; **49**: 41-47.

Mitsuhashi H, Asano S, Nonaka T, Hamamura I, Masuda K-I and Kiyoki M. Administration of truncated secretory leukoprotease inhibitor ameliorates bleomycin-induced pulmonary fibrosis in hamsters. *Am J Respir Crit Care Med* 1996; **153**: 369-374.

Mittl PR, Priestle JP, Cox DA, McMaster G, Cerletti N, Grutter MG. The crystal structure of TGF-beta 3 and comparison to TGF-beta 2: implications for receptor binding. *Protein Sci* 1996; **5**: 1261-1271.

Miyazaki Y, Inoue T, Kyi M, Sawada M, Miyake S and Yoshizawa Y. Effects of a neutrophil elastase inhibitor (ONO-5046) on acute pulmonary injury induced by tumor necrosis factor-alpha (TNF-alpha) and activated neutrophils in isolated perfused rabbit lungs. *Am J Respir Crit Care Med* 1998; **157**: 89-94.

Miyazono K, Olofsson A, Colosetti P and Heldin C-H. A role of the latent TGF-beta 1-binding protein in the assembly and secretion of TGF-beta 1. *EMBO* J 1991; **10**: 1091-1101.

Moore BB, Coffey MJ, Christensen P, Sitterding S, Ngan R, Wilke CA, McDonald R, Phare SM, Peters-Golden M, Paine R 3rd, Toews GB. GM-CSF regulates bleomycin-induced pulmonary fibrosis via a prostaglandin-dependent mechanism. *J Immunol* 2000; **165**: 4032-4039.

Mordelet-Dambrine M, Lafuma C, Stanislas-Leguern G, Robert L, Chretien J and Hornebeck W. Elastase activity of bronchoalveolar lavage cells in advanced pulmonary sarcoidosis. *Eur Respir J* 1988; 1:748-757.

Moren A, Olofsson A, Stenman G, Sahlin P, Kanzaki T, Claesson-Welsh L, ten Dijke P, Miyazono K and Heldin CH. Identification and characterization of LTBP-2, a novel latent transforming growth factor-β-binding protain. *J Biol Chem* 1994; **269**: 32469-32478.

Morris DG, Li Y and Sheppard D. Differential murine susceptibility to bleomycin-induced mortality and pulmonary fibrosis. *Am J Respir Crit Care Med* 2002; **165**: A169.

Morris SM, Stone PJ and Snider GL. Electron microscopic study of human lung tissue after in vitro exposure to elastase. *J Histochem Cytochem* 1993; **41**: 851-866.

Morrison HM, Welhus HG, Stockley RA, Burnett D and Campbell EJ. Inhibition of human leukocyte elastase bound to elastin: relative ineffectiveness and two mechanisms of inhibitory activity. *Am J Respir Mol Biol* 1990; **2**: 263-269.

Moses HL, Branum EL, Proper JA and Robinson RA. Transforming growth factor production by chemically transformed cells. *Cancer Res* 1981; **41**: 2842-2848.

Mu D, Cambier S, Fjellbirkeland L, Baron JL, Munger JS, Kawakatsu H, Shepaprd D, Broaddus VC and Nishimura SL. The integrin αvβ8 mediates epithelial homeostasis through MT1-MMP-dependent activation of TGF-β1. *J Cell Biol* 2002; **157**: 493-507.

Mulder KM. Role of Ras and MAPKs in TGF-beta signalling. *Cytokine Growth Factor Rev* 2000; **11**: 23-35.

Muller NL and Colby TV. Idiopathic interstitial pneumonias: high-resolution CT and histologic findings. *Radiographics* 1997; **17**: 1016-1022.

Mulligan MS, Desrochers PE, Chinnaiyan AM, Gibbs DF, Varani J, Johnson KJ and Weiss SJ. In vivo suppression of immune complex-induced alveolitis by secretory leukoproteinase inhibitor and tissue inhibitor of metalloproteinases 2. *Proc Natl Acad Sci USA* 1993; **90**: 11523-11527.

Mummery CL. Transforming growth factor-β and mouse development. *Microsc Res Tech* 2001; **52**: 374-386.

Munger JS, Harpel JG, Giancotti FG and Rifkin DB. Interactions between growth factors and integrins: latent forms of transforming growth factor-beta are ligands for the integrin alpha v beta 1. Mol Biol Cell 1998; 9: 2627-2638.

Munger J, Huang X, Kawakatsu H, Griffiths MJ, Dalton SL, Wu J, Pittet JF, Kaminski N, Garat C, Matthay MA, Rifkin DB and Sheppard D. The integrin alpha v beta 6 binds and activates latent TGF beta 1: a mechanism for regulating pulmonary inflammation and fibrosis. *Cell* 1999; **96**: 319-328.

Murphy-Ullrich JE and Poczatek M. Activation of latent TGF-beta by thrombospondin-1: mechanisms and physiology. *Cytokine Growth Factor Rev* 2000; **11**: 59-69.

Nagai A, Aoshiba K, Ishihara Y, Inano H, Sakamoto K, Yamaguchi E, Kagawa J and Takizawa T. Administration of α_1-proteinase inhibitor ameliorates bleomycin-induced pulmonary fibrosis in hamsters. *Am J Respir Crit Care Med* 1992; **145**: 651-656.

Nagase T, Oozumi N, Ishii S, Kita Y, Yamamoto H, Ohga E, Ouchi Y and Shimizu T. A pivotal role of cytosolic phospholipase A(2) in bleomycin-induced pulmonary fibrosis. *Nat Med* 2002; **8**: 480-484.

Nakajima K and Powers JC. Mapping the extended substrate binding site of cathepsin G and human leukocyte elastase. *J Biol Chem* 1979; **254**: 4027-4032.

Nakao A, Fujii M, Matsumura R, Kumano K, Saito Y, Miyazono K and Iwamoto I. Transient gene transfer and expression of Smad7 prevents bleomycin-induced lung fibrosis in mice. *J Clin Invest* 1999; **104**: 5-11.

Narayanan AS, Whitney J, Souza A and Raghu G. Effect of gamma-interferon on collagen synthesis by normal and fibrotic human lung fibroblasts. *Chest* 1992; **101**: 1326-1331.

Navia MA, McKeever BM, Springer JP, Lin TY, Williams HR, Fluder EM, Dorn CP and Hoogsteen K. Structure of human neutrophil elastase in complex with a peptide chloromethyl ketone inhibitor at 1.84-Å resolution. *Proc Natl Acad Sci USA* 1989; **86**: 7-11.

NCBI BLAST® website: **www.ncbi.nlm.nih.gov/blast/bl2seq/wblast2.cgi** (accessed January 2004)

Nunes I, Shapiro RL and Rifkin DB. Characterization of latent TGF-β activation by murine peritoneal macrophages. *J Immunol* 1995; **155**: 1450-1459.

Nunes I, Gleizes PE, Metz CN and Rifkin DB. Latent transforming growth factor-β binding protein domains involved in actiation and transglutaminase dependent crosslinking of latent transforming growth factor-β. *J Cell Biol* 1997; **136**: 1151-1163.

Nusrat A, Parkos CA, Liang TW, Carnes DK and Madara JL. Neutrophil migration across model intestinal epithelia: monolayer disruption and subsequent events in epithelial repair. *Gastroenterology* 1997; **113**: 1489-1500.

Obayashi Y, Yamadori I, Fujita J, Yoshinouchi T, Ueda N and Takahara J. The role of neutrophils in the pathogenesis of idiopathic pulmonary fibrosis. *Chest* 1997; **112**: 1338-1343.

O'Connor-McCourt M and Wakefield LM. Latent transforming growth-beta in serum. A specific complex with alpha 2-macroglobulin. *J Biol Chem* 1987; **262**: 14090-14099.

Okazaki T, Nakao A, Nakano H, Takahashi F, Takahashi K, Shimozato O, Takeda K, Yagita H and Okumura K. Impairment of bleomycin-induced lung fibrosis in CD28-deficient mice. *J Immunol* 2001; **167**: 1977-1981.

Okrent DG, Lichtenstein AK and Ganz T. Direct cytotoxicity of polymorphonuclear leukocyte granule proteins to human lung-derived cells and endothelial cells. *Am Rev Respir Dis* 1990; **141**: 179-185.

Olman MA, White KE, Ware LB, Simmons WL, Benveniste EN, Zhu S, Pugin J and Mattahy MA. Pulmonary edema fluid from patients with early lung injury stimulates fibroblast proliferation through IL-1 beta-induced IL-6 expression. *J Immunol* 2004; **172**: 2668-2677.

Oloffson A, Miyazono K, Kanzaki T, Colosetti P, Engstrom U and Heldin C-H. Transforming growth factor-beta 1, -beta 2 and -beta 3 secreted by a human glioblastoma cell line. Identification of small and different forms of large latent complexes. *J Biol Chem* 1992; **267**: 19482-19488.

Oloffson A, Ichijo H, Moren A, ten Dijke P, Miyazono K and Heldin CH. Efficient association of an amino-terminally extended form of human latent TGF-β binding protein with the extracellular matrix. *J Biol Chem* 1995; **270**: 31294-31297.

Omer FM, de Souza JB, Corran PH, Sultan AA, Riley EM. Activation of transforming growth factor beta by malaria parasite-derived metalloproteinases and a thrombospondin-like molecule. *J Exp Med* 2003; **198**: 1817-1827.

Orian A and Eisenmann RN. TGF-beta flips the Myc switch. *Science STKE* 2001; **88**: PE1.

Ortiz LA, Lasky J, Hamilton RF Jr., Holian A, Hoyle GW, Banks W, Peschon JJ, Brody AR, Lungarella G and Friedman M. Expression of TNF-α and the necessity of TNF receptors in bleomycin-induced lung injury in mice. *Exp Lung Res* 1998; **24**: 721-743.

Owen CA, Campbell MA, Sannes PL, Boukedes SS and Campbell EJ. Cell surface-bound elastase and cathepsin G on human neutrophils. A novel, non-oxidative mechanism by which neutrophils focus and preserve catalytic activity of serine proteinases. *J Cell Biol* 1995; **131**: 775-789.

Owen CA, Campbell MA, Boukedes SS and Campbell EJ. Cytokines regulate membrane-bound leukocyte elastase on neutrophils: a novel mechanism for effector activity. *Am J Physiol (Lung Cell Mol Physiol)* 1997; **272**: L385-393.

Owen CA and Campbell EJ. The cell biology of leukocyte-mediated proteolysis. *J Leukol Biol* 1999; **65**: 137-150.

Pacini A, Gardi C, Corradeschi F, Viti A, Belli C, Calzoni P and Lungarella G. *In vivo* stimulation of lung collagen synthesis by collagen-derived peptides. *Res Commun Chem Pathol Pharmacol* 1990; **68**: 89-101

Pan T, Nielsen CD, Allen MJ, Shannon KM, Shannon JM, Selman M and Mason RJ. Serum SP-D is a marker of lung injury in rats. *Am J Physiol Cell Mol Physiol* 2002; **282**: L824-832.

Papakonstantinou E, Aletras AJ, Roth M, Tamm M and Karakiulakis G. Hypoxia modulates the effects of transforming growth factor-β isoforms on matrix formation by primary lung fibroblasts. *Cytokine* 2003; **24**: 25-35.

Paralkar VM, Vukicavic S and Reddi AH. Transforming growth factor-beta type 1 binds to collagen type IV of basement membrane matrix: implications for development. *Dev Biol* 1991; **143**: 303-308.

Pardo A, Barrios R, Gaxiola M, Segura-Valdez L, Carrillo G, Estrada A, Mejia M, Selman M. Increase of lung neutrophils in hypersensitivity pneumonitis is associated with lung fibrosis. *Am J Respir Crit Care Med* 2000; **161**: 1698-1704.

Paterson T and Moore S. The expression and characterization of five recombinant murine alpha(1)-protease inhibitor proteins. *Biochem Biophys Res Comm* 1996; **219**: 64-69.

Pedrozo HA, Schwartz Z, Robinson M, Gomez R, Dean DD, Bonewald LF, and Boyan BD. Potential mechanisms for the plasmin-mediated release and activation of latent transforming growth factor-β1 from the extracellular matrix of growth plate chondrocytes. *Endocrinology* 1999; **140**: 5806-5816.

Pelton RW, Johnson MD, Perkett EA, Gold LI and Moses HL. Expression of transforming growth fator-β1, -β2 and -β3 mRNA and protein in the murine lung. *Am J Respir Cell Mol Biol* 1991; **5**: 522-530.

Penttinen RP, Kobayashi S and Bornstein P. Transforming growth factor β increases mRNA for matrix proteins both in the presence and in the absence of changes in mRNA stability. *Proc Natl Acad Sci USA* 1988; **85**: 1105-1108.

Perlman R, Schiemann WP, Brooks MW, Lodish HF, Weinberg RA. TGF-β-induced apoptosis is mediated by the adaptor protein Daxx that facilitates JNK activation. *Nat Cell Biol* 2001; **3**: 708-714.

Perlmutter DH, Cole FS, Kilbridge P, Rossing TH and Colten HR. Expression of the alpha 1-proteinase inhibitor gene in human monocytes and macrophages. *Proc Natl Acad Sci U S A*. 1985; **82**: 795-9.

Perlmutter DH and Punsal PI. Distinct and additive effects of elastase and endotoxin on expression of alpha 1 proteinase inhibitor in mononuclear phagocytes. *J Biol Chem* 1988; **263**: 16499-16503.

Perrey C, Pravica V, Sinnott PJ and Hutchinson IV. Genotyping for polymorphisms in interferon-gamma, interleukin-10, transforming growth factor-beta 1 and tumour necrosis factor-alpha genes: a technical report. *Transpl Immunol* 1998; **6**: 193-197.

Peters-Golden M , Mailie M, Marshall T, Wilke C, Phan SH, Toews GB and Moore BB. Protection from pulmonary fibrosis in leukotriene-deficient mice. *Am J Respir Crit Care Med* 2002; **165**: 229-235.

Pfundt R, van Ruissen F, Vlijmen-Willems IM, Alkemade HA, Zeeuwen PL, Jap PH, Dijkman H, Fransen J, Croes H, ven Erp PE and Schalkwijk J. Title. Elafin paper. *J Clin Invest* 1996; **98**: 1389-1399.

Phan SH. The myofibroblast in pulmonary fibrosis. *Chest* 2002; **122** (Suppl): 286S-289S.

Phan SH and Kunkel SL. Lung cytokine production in bleomycin-induced pulmonary fibrosis. *Exp Lung Res* 1992; **18**: 29-43.

Phan SH, Schrier D, McGarry B and Duque RE. Effect of the beige mutation on bleomycin-induced pulmonary fibrosis in mice. *Am Rev Respir Dis* 1983; **127**: 456-459.

Phillips RJ, Burdick MD, Hong K, Lutz MA, Murray LA, Xue YY, Belperio JA, Keane MP and Strieter RM. Circulating fibrocytes traffic to the lungs in response to CXCL12 and mediate fibrosis. *J Clin Invest* 2004; **114**: 438-446.

Pickrell JA and Abdel-Mageed AB. Radiation-induced pulmonary fibrosis. In: Phan SH and Thrall RS, eds. Pulmonary Fibrosis. New York: Marcel Dekker Inc., 1995: 363-381.

Pittet J-P, Griffiths MJD, Geiser T, Kaminski N, Dalton SL, Huang X, Brown LAS, Gotwals PJ, Koteliansky VE, Matthay MA and Sheppard D. TGF-β is a critical mediator of acute lung injury. *J Clin Invest* 2001; **107**: 1537-1544.

Poncelet AC and Schnaper HW. Sp1 and Smad proteins cooperate to mediate transforming growth factor-beta 1-induced alpha 2(I) collagen expression in human glomerular mesangial cells. *J Biol Chem* 2001; **276**: 6983-6992.

Poplis VA, Wilberding J, McLennan L, Liang Z, Cornelissen I, DeFord ME, Rosen ED and Castellino FJ. A total fibrinogen deficiency is compatible with the development of pulmonary fibrosis in mice. *Am J Pathol* 2000; **157**: 703-708.

Postlethwaite AE, Keski-Oja J, Moses HL and Kang AH. Stimulation of the chemotactic migration of human fibroblasts by transforming growth factor-β. *J Exp Med* 1987; **165**: 251-256.

Powell DW, Mifflin RC, Valentich JD, Crowe SE, Saada JI and West AB. Myofibroblasts. I. Paracrine cells important in health and disease. *Am J Physiol (Cell and Mol Physiol)*; **277**: C1-C19.

Powers JC and Harper JW. Inhibitors of serine proteinases. *In*: Barrett AJ and Salvesen G, eds. Proteinase. Amsterdam: Elsevier Science Publishers, 1986: 55-152.

Prieto AL, Edelman GM and Crossin GL. Multiple integrins mediate cell attachment to cytotactin/tenascin. Proc Natl Acad Sci USA 1993; 90: 10154-10158.

Protin, U., T. Schweighoffer, W. Jochum, and F. Hilberg. CD44-deficient mice develop normally with changes in subpopulations and recirculation of lymphocyte subsets. *J Immunol* 1999; **163**: 4917–4923.

Quinones F and Crouch E. Biosynthesis of interstitial and basement membrane collagens in pulmonary fibrosis. *Am Rev Respir Dis* 1986; **134**: 1163-1171.

Raghow R, Irish P and Kang AH. Coordinate regulation of TGF-β gene expression and cell proliferation in hamster lung undergoing bleomycin-induced pulmonary fibrosis. *J Clin Invest* 1989; **84**: 1836-1842.

Raghu G, Striker LJ, Hudson LD and Striker GE. Extracellular matrix in normal and fibrotic human lungs. *Am Rev Respir Dis* 1985; **131**: 281-289.

Raghu G, Brown KK, Bradford WZ, Starko K, Noble PW, Schwartz DA and King TE Jr. A placebo-controlled trial of interferon gamma-1b in patients with idiopathic pulmonary fibrosis. *N Engl J Med* 2004; **350**: 125-133.

Raghunath M, Unsold C, Kubitscheck U, Bruckner-Tuderman L, Peters R and Meuli M. The cutaneous microfibrillar appararus contains latent transforming growth factor-β binding protein-1 (LTBP-1) and is a repository for latent TGF-β1. *J Invest Dermatol* 1998; **111**: 559-564.

Randall RA, Germain S, Inman GS, Bates PA and Hill CS. Different Smad-2 partners bind a common hydrophobic pocket in Smad-2 via a defined proline-rich motif. *EMBO J* 2002; **21**: 145-146.

Reed MJ, Iruela-Arispe L, O'Brien ER, Truong T, LaBell T, Bornstein P and Sage SH. Expressions of thrombospondins by endothelial cells. Injury is correlated with TSP-1. *Am J Pathol* 1995; **147**: 1068-1080.

Reid KB. Complete amino acid sequences of the three collagen-like regions present in the subcomponent C1q of the first component of human complement. *Biochem J* 1979; **179**: 367-371.

Reiser KM, Hasetek WM, Hesterberg TW and Last JA. Experimental silicosis. II. Long-term effects of intratracheally instilled quartz on collagen metabolism and morphologic characteristics of rat lungs. *Am J Pathol* 1983; **110**: 30-41.

Ribeiro SM, Poczatek M, Schultz-Cherry S, Villain M and Murphy-Ullrich JE. The activation sequence of thrombospondin-1 interacts with the latency-associated peptide to regulate activation of latent transforming growth factor-beta. *J Biol Chem* 1999; **274**: 13586-15393.

Roberts AB, Anzaro MA, Lamb LC, Smith JM and Sporn MB. New class of transforming growth factors potentiated by epidermal growth factor: isolation from non-beoplastic tissues. *Proc Natl Acad Sci USA* 1981; **78**: 5339-5343.

Roberts CJ, Birkenmeier TM, McQuillan JJ, Akiyama SK, Yamada SS, Chen WT, Yamada KM and McDonald JA. Transforming growth factor-beta stimulates the expression of fibronectin and both subunits of the human fibronectin receptor by cultured human lung fibroblasts. *J Biol Chem* 1988; **263**: 4586-4592.

Roberts AB and Sporn MB. Transforming growth factor-β. *In:* Clark RF, ed. The Molecular and Cellular Biology of Wound Repair. New York: Plenum, 1996: 275-308.

Roes J and Rajewsky K. Immunoglobulin D (IgD)-deficient mice reveal an auxillary receptor funvtion for IgD in antigen-mediated recruitment of B cells. *J Exp Med* 1993; **177**: 45-55.

Rojkind M and Gonzalez E. An improved method for determination of hydroxyproline in a tissue hydrolyzate. *Clin Chim Acta* 1980; **104**: 161-167.

Roman J. Extracellular matrix and lung inflammation. *Immunol Res* 1996; **15**: 163-167.

Rosenbloom J. Elastin: an overview. In: Cunningham LW, ed. Methods in Enzymology. New York: Raven; 1987.

Rube CE, Uthe D, Schmid KW, Richter KD, Wessel J, Schuck A, Willich N and Rube C. Dose-dependent induction of transforming growth factor-β in the lung tissue of firbosis-prone mice after thoracic irradiation. *Int J Radiat Oncol Biol Phys* 2000; **47**: 1003-1042.

Rudd RM, Haslam PL and Turner-Warwick M. Cryptogenic fibrosing alveolitis. Relationships of pulmonary physiology and bronchoalveolar lavage to response to treatment and prognosis. *Am Rev Respir Dis* 1981; **124**: 1-8.

Ruoslahti E. Structure and biology of proteoglycans. *Annu Rev Cell Biol* 1988; **4**: 229-255.

Ruoslahti E, Yamaguchi Y, Hildebrand A and Border WA. Extracellular matrix/growth factor interactions. *Cold Spring Harbor Symp Quant Biol* 1992; **57**: 309-315.

Sadallah S, Hess C, Miot S, Spertini O, Lutz H and Schifferli J-A. Elastase and metalloproteinase activities regulate soluble complement receptor 1 release. *Eur J Immnol* 1999; **29**: 3754-3761.

Saharinen J and Keski-Oja J. Specific sequence motif of 8-cys repeats of TGF-β binding proteins, LTBPs, creates a hydrophobic interaction surface for binding of small latent TGF-β. *Mol Biol Cell* 2000; **11**: 2691-2704.

Sakamaki F, Ishizaka A, Urano T, Sayama K, Nakamura H, Terashima T, Waki Y, Tasaka S, Hasegawa N, Sato K, Nakagawa N, Obata T and Kanazawa M. Effect of a specific neutrophil elastase inhibitor, ONO-5046, on endotoxin-induced acute lung injury. *Am J Respir Crit Care Med* 1996; **153**: 391-397.

Saldeen T, Ahn C and Glass M. The effect of the neutrophil elastase inhibitor ICI-200,355 on development of pulmonary edema in the rat thrombosis model of ARDS (abstract). *Am Rev Respir Dis* 1991; **143**: A581.

Salez F, Gosset P, Copin MC, et al. Transforming growth factor-β1 in sarcoidosis. *Eur Respir J* 1998; **12**: 913-999.

Sallenave J-M, Donnelly SC, Grant IS, Robertson C, Gauldie J and Haslett C. Secretory leukocyte proteinase inhibitor is preferentially increased in patients with acute respiratory distress syndrome. *Eur Respir J* 1999; **13**: 1029-1036.

Sallenave J-M. The role of secretory leukocyte proteinase inhibitor and elafin (elastase-specific inhibitor/skin-derived antikeu0koprotease) as alarm antiproteinases in inflammatory lung disease. *Respir Res* 2000; **1**: 87-92.

Sallenave J-M, Silva A. Characterization and gene sequence of the precursor of elafin, an elastase-specific inhibitor in bronchial secretions. *Am J Respir Cell Mol Biol* 1993; **8**: 439-445.

Sandhaus RA. α1-Antitrypsin deficiency: new and emerging treatments for α1-antitrypsin deficiency. *Thorax* 2004; **59**: 904-909.

Santana A, Saxena B, Noble NA, Gold LI and Marshall BC. Increased expression of transforming growth factor-β isoforms (β1, β2, β3) in bleomycin-induced pulmonary fibrosis. *Am J Respir Cell Mol Biol* 1995; **13**: 34-44.

Sasaki H, Sato T, Yamauchi N, Okamoto T, Kobayashi D, Iyama S, Kato J, Matsunaga G, Takimoto R, Takayama T, Kogawa K, Watanabe N and Niitsu Y. Induction of heat shock protein 47 synthesis by TGF-beta and IL-1 beta via enhancement of the heat shock element binding activity of heat shock transcription factor 1. *J Immunol* 2002; 168: 5178-5183.

Sato Y, Tsuboi R, Lyons R, Moses H and Rifkin DB. Characterization of the activation of latent TGF-β by co-cultures of endothelial cells and pericytes or smooth muscle cells: a self-regulating system. *J Cell Biol* 1990; **111**: 757-763.

Savani RC, Zhou Z, Arguri E, Wang S, Vu D, Howe CC and DeLisser HM. Bleomycin-induced pulmonary injury in mice deficient in SPARC. *Am J Physiol (Lung Cell Mol Physiol)* 2000; **279**: L743-750.

Savov JD, Whitehead GS, Wang J, Liao G, Usuka J, peltz G, Foster WM and Schwartz DA. Ozone-induced acute pulmonary injury in inbred mouse strains. *Am J Respir Cell Mol Biol* 2004; **31**: 69-77.

Scadding JG. Diffuse pulmonary alveolar fibrosis. *Thorax* 1974; **29**: 271-281.

Schalkwijk J, Wiedow O and Hirose S. The trappin gene family: proteins defined by an N-terminal transglutaminase substrate domain and a C-terminal four-disulphide core. *Biochem J* 1999; **340**: 569-577.

Schnabl B, Kweon YO, Frederick JP, Wang XF, Rippe RA and Brenner DA. The role of Smad3 in mediating mouse hepatic stellate cell activation. *Hepatology* 2001; **34**: 89-100.

Schneider T and Issekutz AC. Quantitation of eosinophil and neutrophil infiltration into rat lung by specific assays for eosinophil peroxidase and myeloperoxidase. Application in a Brown Norway rat model of allergic pulmonary inflammation. *J Immunol Meth* 1996; **198**: 1-14.

Schoenberger CI, Rennard SI, Bitterman PB, Fukuda Y, Ferrans VJ and Crystal RG. Paraquat-induced pulmonary fibrosis. Role of the alveolitis in modulating the development of fibrosis. *Am Rev Respir Dis* 1984; **129**: 168-173.

Schrier DJ, Kunkel RG and Phan SM. The role of strain variation in murine bleomycin-induced pulmonary fibrosis. *Am Rev Respir Dis* 1983; **127**: 63-66.

Schultz-Cherry S and Murphy-Ullrich JE. Thrombospondin causes activation of latent transforming growth factor-B secreted by endothelial cells by a novel mechanism. *J Cell Biol* 1993; **122**: 923-932.

Schultz-Cherry S, Lawler J, Murphy-Ullrich JE. The type 1 repeats of thrombospondin 1 activate latent transforming growth factor-beta. *J Biol Chem* 1994a; **269**: 26783-26788.

Schultz-Cherry S, Ribeiro S, Gentry L and Murphy-Ullrich JE. Thrombospondin binds and activates the small and large forms of latent transforming growth factor-β in a chemically defined system. *J Biol Chem* 1994b; **269**: 26775-26782.

Schultz-Cherry S, Chen H, Moser D, Misenheimer TM, Krutzsch HC, Roberts DD and Murphy-Ullrich JE. Regulation of transforming growth factor-β activation by discrete sequence of thrombospondin-1. *J Biol Chem* 1995; **270**: 7304-7310.

Schultz-Cherry S and Henshaw DS. Influenza virus neuraminidase activates latent transforming growth factor-beta. *J Virol* 1996; **70**: 8624-8629.

Schwartz DA, van Fossen DS, Davis CS, Helmers RA, Dayton CS, Burmeister LF and Hunninghake GW. Determinants of progression in idiopathic pulmonary fibrosis. *Am J Respir Crit Care Med* 1994; **149**: 444-449.

Schwarz MI and Brown KK. Fibroproliferation: a new therapeutic target for idiopathic pulmonary fibrosis. *Pneumon* 2002; **1(15)**: 16-18.

Scott J, Johnston I and Britton J. What causes cryptogenic fibrosing alveolitis? A case-control study of environmental exposure to dust. *BMJ* 1990; **301**: 1015-1017.

Scuderi P, Nez PA, Duerr ML, Wong BJ and Valdez CM. Cathepsin G and leukocyte elastase inactivate human tumor necrosis factor and lymphotoxin. *Cell Immunol* 1991; **135**: 299-313.

Sear H, Allen TH and Gregersen MI. Simultaneous measurement in dogs of plasma volume with I^{131} human albumin and T-1824 with comparisons of their long-term disappearance from the plasma. *Am J Physiol* 1953; **179**: 240-242.

Seeger W, Elssner A, Gunther A, Kramer HJ and Kalinowski HO. Lung surfactant phospholipids associate with polymerizing fibrin: loss of surface activity. *Am J Respir Cell Mol Biol* 1993; **9**: 213-220.

Selman M, Montano M, Ramos C and Chapela R. Concentration, biosynthesis and degradation of collagen in idiopathic pulmonary fibrosis. *Thorax* 1986; **41**: 355-359.

Selman M, Ruiz V, Cabrera S, Segura L, Ramirez R, Barrios R and Pardo A. TIMP-1, -2, -3 and –4 in idiopathic pulmonary fibrosis: a prevailing non-degradative microenvironment? *Am J Physiol (Lung Cell Mol Physiol)* 2000; **279**: L562-574.

Senior RM, Tegner H, Kuhn C, Ohlsson K, Starcher BC and Pierce JA. Induction of pulmonary emphysema with human leukocyte elastase. *Am Rev Respir Dis* 1977; **116**: 469-475.

Seoane J, Pouponnot C, Staller P, Schader M, Eilers M and Massague J. TGF-beta influences Myc, Miz-1 and Smad to control the CDK inhibitor p15INK4b. *Nat Cell Biol* 2001; **3**: 400-408.

Serrano-Mollar A, Closa D, Cortijo J, Morcillo EJ, Prats N, Gironella M, Panes J, Rosello-Catafau J and Bulbena O. P-selectin upregulation in bleomycin-induced lung injury in rats: effect of N-acetyl-L-cysteine. *Thorax* 2002; **57**: 629-634.

Seyer JM, Hutcheson T and Kang AH. Collagen polymorphism in idiopathic chronic pulmonary fibrosis. *J Clin Invest* 1976; **57**: 1498-1507.

Shahzeidi S, Jeffrey PK, Laurent GJ and McAnulty RJ. Increaesd type I procollagen mRNA transcripts in the lungs of mice during the development of bleomycin-induced fibrosis. *Eur Respir J* 1994; **7**: 1938-1943.

Shapiro SD, Endicott SK, Province MA, Pierce JA and Campbell EJ. Marked longevity of human lung parenchymal elastic fibers deduced from prevalence of D-aspartate and nuclear weapons-related radiocarbon. *J Clin Invest* 1991; **87**: 1828-1834.

Shapiro SD. Proteinases in chronic obstructive pulmonary disease. *Biochem Soc Trans* 2002; **30**: 98-102.

Shapiro SD, Goldstein NM, Houghton AM, Kobayashi DK, Kelley D and Belaaouaj A. Neutrophil elastase contributes to cigarette smoke-induced emphysema in mice. *Am J Pathol* 2003; **163**: 2329-2335.

Shen AS, Haslett C, Feldsien DC, Henson PM and Cherniack RM. The intensity of chronic lung inflammation and fibrosis after bleomycin is directly related to the severity of acute injury. *Am Rev Respir Dis* 1988; **137**: 564-571.

Shi DL, Savona C, Gagnon J, Cochet C, Chambaz EM and Feige JJ. Transfoming growth factor-beta stimulates the expression of alpha2-macroglobulin by cultured bovine adrenocortical cells. *J Biol Chem* 1990; **265**: 2881-2887.

Shi YG and Massague J. Mechanisms of TGF-β signaling from cell membrane to the nucleus. *Cell* 2003; 113: 685-700.

Shotton D and Watson H. Three-dimensional structure of tosyl-elastase. *Nature* 1970; **225**: 811-816.

Shotton D and Hartley B. Evidence for the amino acid sequence of porcine pancreatic elastase. *Biochem J* 1973; **131**: 643-675.

Sibille Y, Martinot JB, Staquet P, Delaunois L, Chatelain B and Delacroix DL. Antiproteases are increased in bronchoalveolar lavage in interstitial lung disease. *Eur Resp J* 1988; **1**: 498-504.

Sie P, Dupouy D, Dol F and Boeu B. Inactivation of heparin cofactor II by polymorphonuclear leukocytes. *Thromb Res* 1987; **47**: 657-664.

Sikic BI, Young DM, Mimnaugh EG and Gram TE. Quantification of bleomycin pulmonary toxicity in mice by changes in lung hydroxyproline content and morphometric histopathology. *Cancer Res* 1978; **38**: 787-792.

Sime PJ, Xing Z, Graham FL, Csaky KG and Gauldie J. Adenovector-mediated gene transfer of active transforming growth factor-β1 induces prolonged severe fibrosis in rat lung. *J Clin Invest* 1997; **100**: 768-776.

Sime PJ, Marr RA, Gauldie D, Xing Z, Hewlett BR, Graham FL and Gauldie J. Transfer of tumor necrosis factor-alpha to rat lung induces severe pulmonary inflammation and patchy interstitial fibrogenesis with induction of transforming growth factor-beta1 and myofibroblasts. *Am J Pathol* 1998; **153**: 825-32.

Simpson AJ, Maxwell AI, Govan JRW, Haslett C and Sallenave J-M. Elafin (elastase-specific inhibitor) has anti-microbial activity against Gram-positive and Gram-negative respiratory pathogens. *FEBS Lett* 1999; **452**: 309-313.

Sinha S, Watorek W, Karr S, Giles J, Bode W and Travis J. Primary structure of human neutrophil elastase. *Proc Natl Acad Sci* 1987; **84**: 2228-2232.

Sisson TH, Hattori N, Xu Y and Simon RH. Treatment of bleomycin-induced pulmonary fibrosis by transfer of urokinase-type plasminogen activator genes. *Hum Gene Ther* 1999; **10**: 2315-2323.

Skold CM, Liu X, Umino T, Zhu Y, Ohkuni Y, Romberger DJ, Spurzem JR, Heires Aj and Rennard SI. Human neutrophil elastase augments fibroblast-mediated contraction of released collagen gels. *Am J Respir Crit Care Med* 1999; **159**: 1138-1146.

Snider GL, Celli BR, Goldstein RH, O'Brien JJ and Lucey EC. Chronic interstitial pulmonary fibrosis produced in hamsters by endotracheal bleomycin. *Am Rev Respir Dis* 1978; **117**: 289-297.

Sommerhoff CP, Nadel JA, Basbaum CB and Caughey GH. Neutrophil elastase and cathepsin G stimulate secretion from cultured bovine airway gland serous cells. *J Clin Invest* 1990; **85**: 682-689.

Spanswick VJ, Hartley JM, Ward TH and Hartley JA. Measurement of drug-induced DNA interstrand crosslinking using the single cell gel electrophoresis (Comet) assay. *In*: Brown B and Boger-Brown U, eds. Methods in Molecular Medicine: Cytotoxic Drug Resistance Mechanisms. Vol 28. Totowa, NJ: Humana Press, 1999: 143-154.

Specks U, Nerlich A, Colby TV, Wiest I and Timpl R. Increased expression of type VI collagen in lung fibrosis. *Am J Respir Crit Care Med* 1995; **151**: 1956-1964.

Starcher BC and Galione MJ. Purification and comparison of elastins from different animal species. *Anal Biochem* 1976; **74**: 441-447.

Starcher B, Peterson B, The kinetics of elastolysis: elastin catabolism during experimentally induced fibrosis. *Exp Lung Res* 1999; **25**: 407-424.

Sterner-Kock A, Thorey IS, Koli K, Wempe F, Otte J, Bangsow T, Kuhlmeier K, Kirchner T, Jin S, Keski-Oja J and von Melchner H. Disruption of the gene encoding the latent transforming growth factor-beta binding protein 4 (LTBP-4) causes abnormal lung development, cardiomyopathy and colorectal cancer. *Genes Dev* 2002; **16**: 2264-2273.

Suzuki H, Nagai K, Yamaki H and Umezawa H. On the mechanism of action of bleomycin scission of DNA strand in vitro and in vivo. *J Antibiot* 1969; **22**: 446-448.

Suzuki T, Moraes TJ, Vachon E, Ginzberg HH, Huang TT, Matthay MA, Hollenberg MD, Marshall J, McCulloch CA, Herrera Abreu MT, Chow CW and Downey GP. Proteinase activated receptor-1 mediates elastase-induced apoptosis of human lung epithelial cells. *Am J Respir Cell Mol Biol* 2005; **12**: 231-247.

Swaisgood CM, French EL, Noga C, Simon RH and Poplis VA. The development of bleomycin-induced pulmonary fibrosis in mice deficient for components of the fibrinolytic system. Am J Pathol 2000; 157: 177-187.

Taconic website. http://www.taconic.com/addinfo/129SVE_phenotyping.htm

Tager AM, Kradin RL, LaCamera P, Bercury SD, Campanella GS, Leary CP, Polosukhin V, Zhao LH, Sakamoto H, Blackwell TS and Luster AD. Inhibition of pulmonary fibrosis by the chemokine IP-10/CXCL10. *Am J Respir Cell Mol Biol* 2004; **31**: 395-404.

Taipale J, Koli K and Keski-Oja J. Release of latent transforming growth factor-beta 1 from the pericellular matrix of cultured fibroblasts and fibrosarcoma cells by plasmin and thrombin. *J Biol Chem* 1992; **267**: 25378-25384.

Taipale J, Miyazono K, Heldin CH and Keski-Oja J. Latent transforming growth factor-beta 1 associates to fibroblast extracellular matrix via latent TGF-beta binding protein. *J Cell Biol* 1994; **124**: 171-181.

Taipale J, Lohi J, Saarinen J, Kovanen PT and Keski-Oja J. Human mast cell chymase and leukocyte elastase release latent transforming growth factor-beta 1 from the extracellular matrix of cultured human epithelial and endothelial cells. *J Biol Chem* 1995; **270**: 4689-4696.

Taipale J, Saharinen J, Hedman K and Keski-Oja J. Latent transforming growth factor-β1 and its binding protein are components of extracellular matrix microfibrils. *J Histochem Cytochem* 1996; **44**: 875-889.

Taipale J and Keski-Oja J. Growth factors in the extracellular matrix. *Faseb J* 1997; **11**: 51-59.

Takahashi H, Nukiwa T, Yoshimura K, Quick CD, States DJ, Holmes MD, Whang-Peng J, Knutsen T and Crystal RG. Structure of the human neutrophil elastase gene. *J Biol Chem* 1988; **263**: 14739-14747.

Takeyama K, Agusti C, Ueki I, Lausier J, Cardell LO and Nadel JA. Neutrophil-dependent goblet cell degranulation: role of membrane-bound elastase and adhesion molecules. *Am J Physiol (Lung Cell Mol Physiol)* 1998; **275**: L294-302.

Tamakuma S, Ogawa M, Aikawa N, Kubota T, Hirasawa H, Ishizaka A, Taenaka N, Hamada C, Matsuoka S and Abiru T. Relationship between neutrophil elastase and acute lung injury in humans. *Pulm Pharmacol Ther* 2004; **17**: 271-279.

Taooka Y, Maeda A, Hiyama K, Ishioka S and Yamakido M. Effects of neutrophil elastase inhibitor on bleomycin-induced pulmonary fibrosis in mice. *Am J Respir Crit Care Med* 1997; **156**: 260-265.

Teder P, Vandivier RW, Jiang D, Liang J, Cohn L, Pure E, Henson PM and Noble PW. Resolution of lung inflammation by CD44. *Science* 2002; **296**: 155-158.

Tetley TD. Neutrophil and mactophage-derived proteinases in chronic obstructive pulmonary disease and acute respiratory distress syndrome. *In*: Bellingan GJ and Laurent GJ, eds. Acute Lung Injury: From inflammation to repair. Amsterdam: IOS Press, 2000: 129-142.

Theodorescu D, Bergsma D, Man MS, ElShourbagy N, Sheehan C, Rieman D and Kerbel RS. Cloning and over-expression of TGF-β1 cDNA in a aprimary adenocarcinoma: in vitro and in vivo effects. *Growth Factors* 1991; **5**: 305-316.

Thomas GJ, Hart IR, Speight PM and Marshall JF. Binding of TGF-β1 latency-associated peptide (LAP) to αvβ6 integrin modulates behaviour of squamous carcinoma cells. *Br J Cancer* 2002; **87**: 859-867.

Thomeer MJ, Costabel U, Rizzato G, Poletti V and Demedts M. Comparison of registries of interstitial lung diseases in three European countries. *Eur Respir J* 2001; **18 Suppl 32**: 114s-188s.

Thrall RS, McCormick JR, Jack RM, McReynolds RA and Ward PA. Bleomycin-induced pulmonary fibrosis in the rat. *Am J Pathol* 1979; **95**: 117-130.

Thrall RS, Phan SM, McCormick JR and Ward PA. The development of bleomycin-induced pulmonary fibrosis in neutrophil-depleted and complement-depleted rats. *Am J Pathol* 1981; **105**: 76-81.

Thrall RS, Barton RW, D'Amato DA and Sulavik SB. Differential cellular analysis of bronchoalveolar lavage fluid obtained at various stages during the development of bleomycin-induced pulmonary fibrosis in the rat. *Am Rev Respir Dis* 1982; **126**: 488-492.

Thrall RS and Scalise PJ. Bleomycin. *In*: Thrall RS and Phan SM, eds. Pulmonary Fibrosis. New York: Marcel Dekker Inc., 1995: 230-292.

Tkalcevic J, Novelli M, Phylactides M, Iredale JP, Segal AW and Roes J. Impaired immunity and enhanced resistance to endotoxin in the absence of neutrophil elastase and cathepsin G. *Immunity* 2000; **12**: 201-210.

Torry DJ, Richards CD, Podor TJ and Gauldie J. Anchorage-independent colony growth of pulmonary fibroblasts derived from fibrotic human lung tissue. *J Clin Invest* 1994; **93**: 1525-1532.

Tran PL, Weinbacj J, Opolon P, Linares-Cruz G, Reynes JP, Gregoire A, Kremer E, Durand H and Perricaudet M. Prevention of bleomycin-induced pulmonary fibrosis after adenovirus-mediated transfer of the bacterial bleomycin resistance gene. *J Clin Invest* 1997; **99**: 608-617.

Travis J. Structure, function and control of neutrophil proteinases. *Am J Med* 1988; **84** (suppl 6A): 37-42.

Travis J, Dubin A, Potempa J, Watorek W and Kurdowska A. Neutrophil proteinases: caution signs in designing inhibitors against enzymes with possible multiple functions. *Ann NY Acad Sci* 1991; **624**: 81-86.

Tripodi M, Perfumo S, Ali R, Amicone L, Abbott C and Cortese R. Generation of small mutation in large genomic fragments by homologous recombination: description of the technique and examples of its use. *Nucl Acids Res* 1990; **18**: 6247-6251.

Tsukazaki T, Chiang TA, Davison AF, Attisano L and Wrana JL. SARA, a FYVE domain protein that recruits Smad-2 to the TGF-β receptor. *Cell* 1998; 95: 779-791.

Tucker RF, Branum EL, Shipley GD, Ryan RJ and Moses HL. Specific binding to cultured cells of 125I-labeled transforming growth factor-beta from human platelets. *Proc Natl Acad Sci USA* 1984; **81**: 6757-6761.

Tucker R, Shipley G, Moses HL and Holley R. Growth inhibitor from BSC-1 cells closely related to platelet type-β transforming growth factor. *Science* **226**: 705-707.

Umezawa H, Maeda K and Takeuchi T. New antibiotics: bleomycin A and B. *Cancer* 1966; **19**: 201-209.

Unsold C, Hyytiainen M, Bruckner-Tuderman L and Keski-Oja J. Latent TGF-β binding protein LTBP-1 contains three potential extracellular matrix interacting domains. *J Cell Sci* 2000; **114**: 187-197.

Unsold C, Hyytiainen M, Bruckner-Tuderman L and Keski-Oja J. Interaction of latent TGF-β binding protein with human fibroblast extracellualr matrix invloves multiple domains. *J Cell Sci* 2001; **114**: 187-197.

Usuki K and Fukuda Y. Evolution of three patterns of intra-alveolar fibrosis produced by bleomycin in rats. *Pathol Int* 1995; **45**: 552-564.

Van Hoozen BE, Grimmer KL, Marelich GP, Armstrong LC and Last JA. Early phase collagen synthesis in lungs of rats exposed to bleomycin. *Toxicology* 2000; **147**: 1-13.

Venge P. The monitoring of inflammation by specific cellular markers. *Scand J Clin Lab Invest Suppl* 1994; **219**: 47-54.

Venkatesan N, Ebihara T, Roughley PJ, Ludwig MS. Alterations in large and small proteoglycans in bleomycin-induced pulmonary fibrosis in rats. *Am J Respir Crit Care Med* 2000; **161**: 2066-2073.

Verderio E, Gaudry C, Gross S, Smith C, Downes S and Griffin M. Regulation of cell surface tissue transglutaminase: effects on matrix storage of latent transforming growth factor-β binding protein-1. *J Histochem Cytochem* 1999; **47**: 1417-1432.

Voynow JA, Young LR, Wang Y, Horger T, Rose MC and Fischer BM. Neutrophil elastase increases MUC5AC mRNA and protein expression in respiratory epithelial cells. *Am J Physiol (Lung Cell Mol Physiol)* 1999; **276**: L835-843.

Wakefield LM, Smith DM, Flanders KC and Sporn MB. Latent transforming growth factor-beta from human platelets. A high molecular weight complex containing precursor sequences. *J Biol Chem* 1988; **263**: 7646-7654.

Wallace WA, Ramage EA, Lamb D, Howie SE. A type 2 (Th2-like) pattern of immune response predominates in the pulmonary interstitium of patients with cryptogenic fibrosing alveolitis (CFA). *Clin Exp Immunol* 1995; **101**: 436-41.

Walsh DE, Greene CM, Carroll TP, Taggart CC, Gallagher PM, O'Neill SJ and McElvaney NG. Interleukin-8 up-regulation by neutrophil elastase is mediated by MyD88/IRAK/TRAF-6 in human bronchial epithelium. *J Biol Chem* 2001; **276**: 35494-35499.

Wang S, Souza RF, Kong D, Yin J, Smolinski KN, Zou TT, Frank T, Young J, Flanders KC and Sugimura H. Deficient transforming growth factor-β1 activation and excessive insulin-like growth factor II (IGFII) expression in IGFII receptor mutant tumors. *Cancer Res* 1997; **57**: 2543-2546.

Wang HG, Shibamoto T, Miyahara T, Haniu H, Tanaka S, Fujimoto K, Honda T, Kubo K and Koyama S. Effect of ONO-5046, a specific neutrophil elastase inhibitor, on the phorbol myristate-induced injury in isolated dog lung. *Exp Lung Res* 1999; **25**: 55-67.

Wang Q, Wang Y, Hyde DM, Gotwals PJ, Koteliansky VE, Ryan ST and Giri SN. Reduction of bleomycin-induced lung fibrosis by TGF-β soluble receptor in hamsters. *Thorax* 1999; **54**: 805-812.

Ware LB and Matthay MA. Alveolar fluid clearance is impaired in the majority of patients with acute lung injury and the acute respiratory distress syndrome. *Am J Respir Crit Care Med* 2001; **163**: 1376-1383.

Watanabe H, Hattori S, Katsuda S, Nakanishi I and Nagai Y. Human neutrophil elastase: degradation of basement membrane components and immunolocalization in the tissue. *J Biochem* 1990; **108**: 753-759.

Weinacker A, Ferrando R, Elliott M, Hogg J, Balmes J and Sheppard D. Distribution of integrins alpha v beta 6 and alpha 1 beta 1 and their known ligands, fibronectin and tenascin, in human airways. *Am J Respir Cell Mol Biol* 1995; **12**: 547-556.

Weinrauch Y, Drujan D, Shapiro SD, Weiss J and Zychlinsky A. Nautrophil elastase targets virulence factors of enterobacteria. *Nature* 2002; **417**: 91-94.

Wells AU. Lung disease in association with connective tissue diseases. *European Respiratory Society Monograph* 2000; **5(14)**: 137-164.

Westergren-Thorsson G, Hernnas J, Sarnstrand B, Oldberg A, Heinegard D and Malmstrom A. Altered expression of small proteoglycans, collagen and transforming growth factor-β1 in developing bleomycin-induced pulmonary fibrosis in rats. *J Clin Invest* 1993; **92**: 632-637.

Wewers M. Pathogenesis of emphysema. Assessment of basic science concepts through clinical investigation. *Chest* 1989; **95**: 190-195.

Wahl SM, Allen JB, Weeks BS, Wong HL and Klotman PE. Transforming growth factor beta enhances integrin expression and type IV collagenase secretion in human monocytes. *Proc Natl Acad Sci U S A* 1993; **90**: 4577-4581.

Williams AO, Flanders KC and Saffiotti U. Immunohistochemical localization of transforming growth factor-beta 1 in rats with experimental silicosis, alveolar type II hyperplasia and lung cancer. *Am J Pathol* 1993; **142**: 1831-1840.

Wright DG. Human neutrophil degranulation. *Methods Enzymol* 1988; **162**: 538-551.

Xaubet A, Marin-Arguedas A, Lario S, Anochea J, Moreel F, Ruiz-Manzano J, Rodriguez-Arias JM, Inigo P, Sanz S, et al. TGF-β1 gene polymorphisms are associated with disease progression in idiopathic pulmonary fibrosis. *Am J Respir Crit Care Med* 2003; **168**: 431-435.

Xing Z, Tremblay GM, Sime PJ, Gauldie J. Overexpression of granulocyte-macrophage colony-stimulating factor induces pulmonary granulation tissue formation and fibrosis by induction of transforming growth factor-β1 and myofibroblast accumulation. *Am J Pathol* 1997; **150**: 59-66.

Xing Z, Jordana M, Gauldie J and Wang J. Cytokines and pulmonary inflammatory and immune diseases. *Histol Histopathol* 1999; **14**: 185-201.

Xu YD, Hua J, Mui A, O'Connor R, Grotendorst G and Khalil N. Release of biologically active TGF-β1 by alveolar epithelial cells results in pulmonary fibrosis. *Am J Physiol (Lung Cell Mol Physiol)* 2003; **285**: L527-539.

Yamane K, Ihn H, Kubo M and Tamaki K. Increased transcriptional activities of transforming growth factor beta receptors in scleroderma fibroblasts. *Arthritis Rheum* 2002; **46**: 2421-2428.

Yamanouchi H, Fujita J, Hojo S, Yoshinouchi T, Kamei T, Yamadori I, Ohtsuki Y, Ueda N and Takahara J. Neutrophil elastase: alpha-1-proteinase inhibitor complex ins serum and bronchoalveolar lavage fluid in patients with pulmonary fibrosis. *Eur Respir J* 1998; **11**: 120-125.

Yamazaki T, Ooshima H, Usui A, Watanabe T and Yasuura K. Protective effects of ONO-5046-Na, a specific neutrophil elastase inhibitor, on post-perfusion lung injury. *Ann Thoracic Surg* 1999; **68**: 2141-2146.

Yang JJ, Kettritz R, Falk RJ, Jenette JC and Gaido ML. Apoptosis of endothelial cells induced by the neutrophil serine proteinases proteinase 3 and elastase. *Am J Pathol* 1996; **149**: 1617-1626.

Yasui, H, Gabazza EC, Tamaki S, Kobayashi T, Hataji O, Yuda H, Shimizu S, Suzuki K, Adachi Y and Taguchi O. Intratrcaheal administration of activated protein C inhibits bleomycin-induced pulmonary fibrosis in the mouse. *Am J Respir Crit Care Med* 2001; **163**: 1660-1668.

Yasutake A and Powers JC. Reactivity of human leukocyte elastase and porcine elastase toward peptide 4-nitroanilides containing model desmosine residues. Evidence that human leukocyte elastase is selective for cross-linked regions of elastin. *Biochemistry* 1981; **20**: 3675-3679.

Yee JA, Yan L, Dominguez JC, Allan EH and Martin TJ. Plasminogen-dependent acyivation of latent transforming growth factor-beta (TGF-β) by growing cultures of osteoblast-like cells. *J Cell Physiol* 1993; **157**: 528-534.

Yehualaeshet T, O'Connor R, Green-Johnson J, Mai S, Silverstein R, Murphy-Ullrich JE and Khalil N. Activation of rat macrophage-derived L-TGF-β1 by plasmin requires interaction with TSP-1 and the TSP-1 cell surface receptor, CD36. *Am J Pathol* 1999; **155**: 841-855.

Yi ES, Bedoya A, Lee H, Chin E, Sanders W, Kim SJ, Danielpour D, Remick DG, Yin S and Uich TR. Radiation-induced lung injury *in vivo*: expression of transforming growth factor-β precedes fibrosis. *Inflammation* 1996; **20**: 339-352

Yi ES, Salgado M, Williams S, Kim SJ, Masliah E, Yin S, Ulich TR. Keratinocyte growth factor decreases pulmonary edema, transforming growth factor-beta and platelet-derived growth factor-BB expression, and alveolar type II cell loss in bleomycin-induced lung injury. *Inflammation* 1998; **22**: 315-325

Young RE, Thompson RD, Karbi KY, La Mylinh, Roberts CE, Shapiro SD, Peretti M and Nourshargh S. Neutrophil elastase-deficient mice demonstrate a non-redundant role for NE in neutrophil migration, generation of proinflammatory mediators and phagocytosis in response to zymosan particles in vivo. *J Immunol* 2004; **172**: 4493-4502.

Yoshida M, Sakuma-Mochizuki J, Abe K, Arai T, Mori M, Goya S, Matsuoka H, Hayashi S, Kaneda Y and Kishimoto T. In vivo gene transfer of an extracellular domain of platelet-derived growth factor beta receptor by the HVJ-liposome method ameliorates bleomycin-induced pulmonary fibrosis. *Biochem Biophys Res Commun* 1999; **265**: 503-508.

Yu Q and Stamenkovic I. Cell surface-localized matrix metalloproteinase-9 proteolytically activates TGF-β and promotes tumor invasion and angiogenesis. *Genes Dev* 2000; **14**: 163-176.

Yu Q and Stamenkovic I. Transforming growth factor-beta facilitates breast carcinoma metastasis by promoting tumor cell survival. *Clin Exp Metastasis* 2004; **21**: 235-242.

Zawel L, Dai JL, Buckhaults P, Zhou S, Kinzler KW, Vogelstein B and Kern SE. Human Smad3 and Smad4 are sequence-specific transcription activators. *Mol Cell* 1998; **1**: 611-617.

Zeiher NG, Artigas A, Vincent JL, Dmitrienko A, Jackson A, Thompson BT and Bernard G. Neutrophil elastase inhibition in acute lung injury: results of the STRIVE study. *Crit Care Med* 2004; **32**: 1695-1670.

Zhang H and Phan SH. Inhibition of myofibroblast apoptosis by transforming growth factor-β1. *Am J Respir Cell Mol Biol* 1999; **21**: 658-665.

Zhang K and Phan SH. Cytokines and pulmonary fibrosis. *Biol Signals* 1996; **5**: 232-239.

Zhang K, Rekhter MD, Gordon D and Phan SH. Myofibroblasts and their role in lung collagen gene expression during pulmonary fibrosis: a combined immunohistochemical and *in situ* hybridization study. *Am J Pathol* 1994; **145**: 114-125.

Zhang K, Flanders KC and Phan SH. Cellular localization of transforming growth factor-beta expression in bleomycin-induced pulmonary fibrosis. *Am J Pathol* 1995; **147**: 352-361.

Zhao J, Shi W, Wang Y-L, Chen H, Bringas Jr P, Datto MB, Frederick JP, Wang X-F and Warburton D. Smad3 deficiency attenuates bleomycin-induced pulmonary fibrosis in mice. *Am J Physiol (Lung Cell Mol Physiol)* 2002; **282**: L585-593.

Zhao Y and Shah DU. Expression of transforming growth factor-β type I and type II receptors is altered in rat lungs undergoing bleomycin-induced pulmonary fibrosis. *Exp Mol Pathol* 2000; **69**: 67-78.

Zhu Y, Liu X, Skold CM, Wang H, Kohyama T, Wen FQ, Ertl RF and Rennard SI. Collaborative interactions between neutrophil elastase and metalloproteinases in extracellular matrix degradation in three-dimensional collagen gels. *Respir Res* 2001; **2**: 300-305.

Zia DS, Hyde DM and Giri SN. Development of a bleomycin hamster model of subchronic lung fibrosis. *Pathology* 1992; **24**: 155-163.

Ziesche R, Hofbauer E, Wittmann K, Petkov V and Block LH. A preliminary study of long-term treatment with interferon gamma-1b and low-dose prednisolone in patients with pulmonary fibrosis. *N Engl J Med* 1999; **341**: 1264-1269.

Zimmer M, Medcalf RL, Fink TM, Mattmann C, Lichter P and Jenne DE. Three human elastase-like genes coordinately expressed in the myelomonocyte lineage are organized as a single genetic locus on 19pter. *Proc Natl Acad Sci USA* 1992; **89**: 8215-8219.

Ziesche R, Hofbauer E, Wittman K, Petkov V and Block LH. A preliminary study of long-term treatment with interferon gamma-1b and low-dose prednisolone in patients with idiopathic pulmonary fibrosis. *N Engl J Med* 1999; **341**: 1264-1269.

Zitnik RJ, Zhang J, Kashem MA, Kohno T, Lyons DE, Wright CD, Rosen E, Goldberg I and Hayday AC. The cloning and characterization of a murine secretory leukocyte protease inhbitor cDNA. *Biochem Ciophys Res Com* 1997; **232**: 687-697.

Zuo F, Kaminski N, Eugui E, Allard J, Yakhini Z, Ben-Dor A, Lollini L, Morris D, Kim Y, DeLustro B, Sheppard D, Pardo A and Selman M. Gene expression analysis reveals matrilysin as a key regulator of pulmonary fibrosis in mice and humans. *Proc Nat Acad Sci USA* 2002; **99**: 6292-6297.

PUBLICATIONS

Papers in submission

Chua F, Dunsmore SE, Clingen P, Mutsaers SM, Shapiro SD, Segal AW, Roes J and Laurent GJ. Mice lacking neutrophil elastase are resistant to bleomycin-induced pulmonary fibrosis. *Submitted to Am J Path*

Published papers

Dunsmore SE, Roes J, Chua F, Segal AW, Mutsaers SE and Laurent GJ. Evidence that neutrophil elastase-deficient mice are resistant to bleomycin-induced fibrosis. *Chest* 2001; **120**: 35S-36S.

Original articles, reviews and book chapters in the field of pulmonary fibrosis published during the tenure of the Fellowship

Chua F, Gauldie J and Laurent GJ. Pulmonary Fibrosis: Searching for Model Answers. *Am J Resp Cell Mol Biol* 2005; **33**: 9-13.

Chua F, Sly PD and Laurent GJ. State-of-the-art review: Pediatric Lung Diseases: From Proteinases to Pulmonary Fibrosis. *Ped Pulmonol* 2005; **39**: 392-401.

Chua F, Atzori L, Dunsmore SE, Willis D, Barbarisi M, McAnulty RJ and Laurent GJ. Attenuation of bleomycin-induced pulmonary fibrosis using the heme oxygenase inhibitor Zn-deuteroporphyrin IX-2,4-bisethylene glycol. *Thorax* 2004; **59**: 217-223.

Chua F and Bellingan GJ. Acute Respiratory Distress Syndrome: Fibrosis Fast and Furious. *Clin Intens Care* 2002; **13**: 65-72.

Chua F and Laurent GJ. Fibroblasts. *In*: Encyclopedia of Pulmonary Medicine. Laurent GJ and Shapiro SD, eds. London: Elsevier Science, 2006. *Proofing stage*

Published abstracts

Chua F, Dunsmore SE, Clingen P, Segal AW, Roes J, Laurent GJ. Transforming growth factor-β activation is diminished in alveolar tissue of bleomycin-injured neutrophil elastase-deficient mice. *Am J Respir Crit Care Med* 2003; 167: A346.

Chua F, Dunsmore SE, Segal AW, Roes J, Laurent GJ. TGF-β activation is diminished following bleomycin-induced lung injury in mice lacking neutrophil elastase. *Thorax* 2002; 57: iii1.

Chua F, Dunsmore SE, Segal AW, Roes J, Laurent GJ. Neutrophil elastase participates in transforming growth factor-beta activation during bleomycin-induced pulmonary fibrosis. *Am J Respir Crit Care Med* 2002; 165: A91.

Chua F, Dunsmore SE, Segal AW, Roes J, Laurent GJ. Neutrophil elastase potentiates bleomycin-induced alveolar leak. *Am J Respir Crit Care Med* 2002; 165: A374.

Chua F, Dunsmore SE, Segal AW, Roes J, Laurent GJ. Latent transforming growth factor-beta is associated with the extracellular matrix in bleomycin-treated neutrophil elastase 'knockout' mice. *Am J Respir Crit Care Med* 2002; 165: B25.

Atzori L, Chua F, Barbarisi M, Dunsmore SE, Willis D and Laurent GJ. Heme oxygenase activity is required for bleomycin-induced fibrosis. *Am J Respir Crit Care Med* 2002; 165: A56.

Collins RA, Turner DJ, Dunsmore SE, Chua F, Roes J, Laurent GJ and Sly PD. Initial characterization of lung function in mice deficient in neutrophil proteinases. *Am J Respir Crit Care Med* 2002; 165: A56.

Chua F, Dunsmore SE, Segal AW, Roes J, Laurent GJ. Alveolar-capillary leak is attenuated in neutrophil elastase 'knockout' mice with bleomycin-induced lung injury. *Thorax* 2001; 56: iii5.

Chua F, Thomas R, Dunsmore SE, Segal A, Roes J, Laurent GJ. Neutrophil elastase is necessary for increases in active transforming growth factor-beta in bleomycin-induced pulmonary fibrosis. *Eur Respir J* 2001; 18 :181s.

Chua F, Dunsmore SE, Segal A, Roes J, Laurent GJ. Lung inflammation and alveolar function are altered in neutrophil elastase-deficient mice. *Eur Respir J* 18 (suppl 33): 197S, 2001.

Dunsmore SE, Chua F, Segal A, Roes J, Laurent GJ. Evidence that cathepsin G modifies the antifibrotic effects of neutrophil elastase. *Eur Respir J* 2001; 18: 199S.

Chua F, Dunsmore SE, Mutsaers S, Segal AW, Roes J, Laurent GJ. Characterization of the response of mice deficient in neutrophil elastase and cathepsin G to bleomycin. *Am J Respir Crit Care Med* 2001; 163: A231.

Chua F, Dunsmore SE, Segal AW, Roes J, Laurent GJ. Bleomycin-induced pulmonary fibrosis is attenuated in neutrophil elastase-deficient mice. *Thorax* 2000; 55: A14.

Dunsmore SE, Chua F, Roes J, Segal AW, Laurent GJ. Collagen deposition in neutrophil elastase-deficient mice is not increased in response to bleomycin. *Eur Respir J* 2000; 16: 355S.

PUBLICATIONS

Papers in submission

Chua F, Dunsmore SE, Clingen P, Mutsaers SM, Shapiro SD, Segal AW, Roes J and Laurent GJ. Mice lacking neutrophil elastase are resistant to bleomycin-induced pulmonary fibrosis. *Submitted to Am J Path*

Published papers

Dunsmore SE, Roes J, Chua F, Segal AW, Mutsaers SE and Laurent GJ. Evidence that neutrophil elastase-deficient mice are resistant to bleomycin-induced fibrosis. *Chest* 2001; **120**: 35S-36S.

Original articles, reviews and book chapters in the field of pulmonary fibrosis published during the tenure of the Fellowship

Chua F, Gauldie J and Laurent GJ. Pulmonary Fibrosis: Searching for Model Answers. *Am J Resp Cell Mol Biol* 2005; **33**: 9-13.

Chua F, Sly PD and Laurent GJ. State-of-the-art review: Pediatric Lung Diseases: From Proteinases to Pulmonary Fibrosis. *Ped Pulmonol* 2005; **39**: 392-401.

Chua F, Atzori L, Dunsmore SE, Willis D, Barbarisi M, McAnulty RJ and Laurent GJ. Attenuation of bleomycin-induced pulmonary fibrosis using the heme oxygenase inhibitor Zn-deuteroporphyrin IX-2,4-bisethylene glycol. *Thorax* 2004; **59**: 217-223.

Chua F and Bellingan GJ. Acute Respiratory Distress Syndrome: Fibrosis Fast and Furious. *Clin Intens Care* 2002; **13**: 65-72.

Chua F and Laurent GJ. Fibroblasts. *In*: Encyclopedia of Pulmonary Medicine. Laurent GJ and Shapiro SD, eds. London: Elsevier Science, 2006. *Proofing stage*

Published abstracts

Chua F, Dunsmore SE, Clingen P, Segal AW, Roes J, Laurent GJ. Transforming growth factor-β activation is diminished in alveolar tissue of bleomycin-injured neutrophil elastase-deficient mice. *Am J Respir Crit Care Med* 2003; 167: A346.

Chua F, Dunsmore SE, Segal AW, Roes J, Laurent GJ. TGF-β activation is diminished following bleomycin-induced lung injury in mice lacking neutrophil elastase. *Thorax* 2002; 57: iii1.

Chua F, Dunsmore SE, Segal AW, Roes J, Laurent GJ. Neutrophil elastase participates in transforming growth factor-beta activation during bleomycin-induced pulmonary fibrosis. *Am J Respir Crit Care Med* 2002; 165: A91.

Chua F, Dunsmore SE, Segal AW, Roes J, Laurent GJ. Neutrophil elastase potentiates bleomycin-induced alveolar leak. *Am J Respir Crit Care Med* 2002; 165: A374.

Chua F, Dunsmore SE, Segal AW, Roes J, Laurent GJ. Latent transforming growth factor-beta is associated with the extracellular matrix in bleomycin-treated neutrophil elastase 'knockout' mice. *Am J Respir Crit Care Med* 2002; 165: B25.

Atzori L, Chua F, Barbarisi M, Dunsmore SE, Willis D and Laurent GJ. Heme oxygenase activity is required for bleomycin-induced fibrosis. *Am J Respir Crit Care Med* 2002; 165: A56.

Collins RA, Turner DJ, Dunsmore SE, Chua F, Roes J, Laurent GJ and Sly PD. Initial characterization of lung function in mice deficient in neutrophil proteinases. *Am J Respir Crit Care Med* 2002; 165: A56.

Chua F, Dunsmore SE, Segal AW, Roes J, Laurent GJ. Alveolar-capillary leak is attenuated in neutrophil elastase 'knockout' mice with bleomycin-induced lung injury. *Thorax* 2001; 56: iii5.

Chua F, Thomas R, Dunsmore SE, Segal A, Roes J, Laurent GJ. Neutrophil elastase is necessary for increases in active transforming growth factor-beta in bleomycin-induced pulmonary fibrosis. *Eur Respir J* 2001; 18 :181s.

Chua F, Dunsmore SE, Segal A, Roes J, Laurent GJ. Lung inflammation and alveolar function are altered in neutrophil elastase-deficient mice. *Eur Respir J* 18 (suppl 33): 197S, 2001.

Dunsmore SE, Chua F, Segal A, Roes J, Laurent GJ. Evidence that cathepsin G modifies the antifibrotic effects of neutrophil elastase. *Eur Respir J* 2001; 18: 199S.

Chua F, Dunsmore SE, Mutsaers S, Segal AW, Roes J, Laurent GJ. Characterization of the response of mice deficient in neutrophil elastase and cathepsin G to bleomycin. *Am J Respir Crit Care Med* 2001; 163: A231.

Chua F, Dunsmore SE, Segal AW, Roes J, Laurent GJ. Bleomycin-induced pulmonary fibrosis is attenuated in neutrophil elastase-deficient mice. *Thorax* 2000; 55: A14.

Dunsmore SE, Chua F, Roes J, Segal AW, Laurent GJ. Collagen deposition in neutrophil elastase-deficient mice is not increased in response to bleomycin. *Eur Respir J* 2000; 16: 355S.